ZSoil
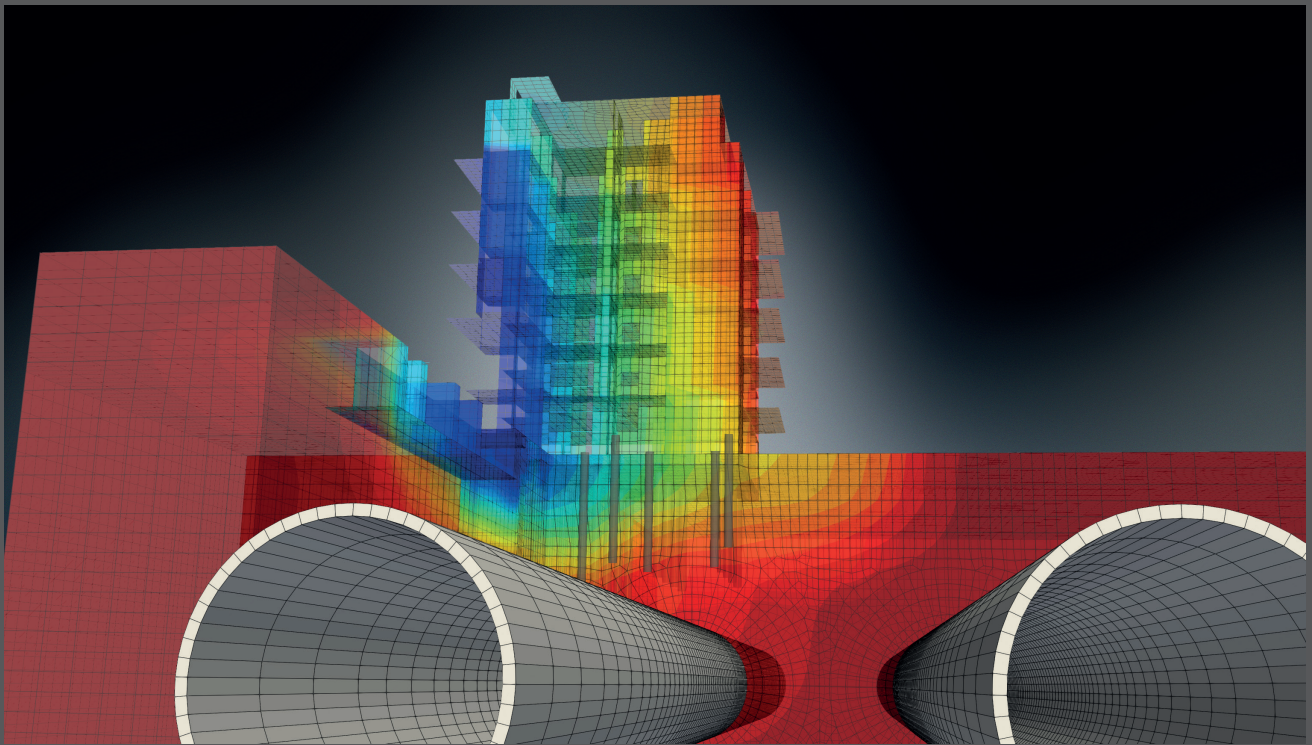
for geotechnics & structures

User manual
THEORETICAL MANUAL

Soil, rock and structural mechanics in dry or partially saturated media

ZSoil

for geotechnics & structures

THEORY
User manual
ZSoil®2023

A. Truty Th. Zimmermann K. Podleś R. Obrzud
with contribution by A. Urbański and S. Commend

WARNING

ZSoil is regularly updated for minor changes. We recommend that you send us your e-mail, as ZSoil owner, so that we can inform you of latest changes. Otherwise, consult our site regularly and download free upgrades to your version.

Latest updates to the manual are always included in the online help, so that slight differences with your printed manual will appear with time; always refer to the online manual for latest version, in case of doubt.

ZSoil 2023 manual:
1. Data preparation
2. Tutorials and benchmarks
3. Theory

END-USER LICENSE AGREEMENT FOR GeoDev's ZSoil® SOFTWARE

Applicable to all V2023 versions: professional & academic, single user & networks, under Windows 10, 11.

Read carefully this document, it is a binding agreement between you and GeoDev Sarl (GeoDev) for the software product identified above. By installing, copying, or otherwise using the software product identified above, you agree to be bound by the terms of this agreement. If you do not agree to the terms of this agreement, promptly return the unused software product to the place from which you obtained it for full refund of price paid. GEODEV SARL OFFERS A 60 DAYS MONEY-BACK GUARANTEE ON ZSOIL.

ZSOIL (the Software & associated hotline services when applicable) SOFTWARE PRODUCT LICENSE:

ZSOIL Software is protected by copyright laws and international copyright treaties, as well as other intellectual property laws and treaties. The **ZSOIL** software product is licensed, not sold.

1. GRANT OF LICENSE

   A: **GeoDev Sarl** grants you, the customer, a non-exclusive license to use N_{bought} (= the number of licenses bought) copies of **ZSOIL**. You may install copies of **ZSOIL** on an unlimited number of computers, provided that you use only N_{bought} copies at the time.

   B: You may make an unlimited number of copies of documents accompanying **ZSOIL**, provided that such copies shall be used only for internal purposes and are not republished or distributed to any third party.

   C: Duration of the agreement may be limited or unlimited, depending on license purchased. Installation of time unlimited licenses of ZSOIL V2023 will be supported for a period of 3 years starting from date of purchase. This support is limited to ZSOIL V2023 upgrades, under Windows 10 and 11.

2. COPYRIGHT

   All title and copyrights in and to **the Software** product (including but not limited to images, photographs, text, applets, etc.), the accompanying materials, and any copies of **ZSOIL** are owned by **GeoDev Sarl**. **ZSOIL** is protected by copyright laws and international treaties provisions. Therefore, you must treat **ZSOIL** like any other copyrighted material except that you may make copies of the software for backup or archival purposes or install the software as stipulated under section 1 above.

3. OTHER RIGHTS AND LIMITATIONS

   A: Limitations on Reverse Engineering, Decompilation, Disassembly. You may not reverse engineer, decompile, or disassemble **the Software**.

   B: No separation of components. **ZSOIL** is licensed as a single product and neither **the Software's** components, nor any upgrade may be separated for use by more than N_{bought} user(s) at the time.

   C: Rental. You may not lend, rent or lease the software product.

   D: Software transfer. You may permanently transfer all of your rights under this agreement and within the territory (country of purchase and delivery), provided you do not retain any copies, and the recipient agrees to all the terms of this agreement.

   E: Termination. Without prejudice to any other rights, **GeoDev Sarl** may terminate this agreement if you fail to comply with the conditions of this agreement. In such event, you must destroy all copies of **the Software**.

WARRANTIES & LIMITATIONS TO WARRANTIES

1. DISCLAIMER

   ZSOIL, developed by **GeoDev Sarl** is a finite element program for the analysis of above- and underground structures in which soil/rock & structural models are used to simulate the soil, rock and/or structural behaviour. The **ZSOIL** code and its soil/rock & structural models have been developed with great care. Although systematic testing and validation have been performed, it cannot be guaranteed that the **ZSOIL** code is free of errors. Moreover, the simulation of geotechnical and/or structural problems by means of the finite element method implicitly involves some inevitable numerical and modelling errors. **ZSOIL** is a tool intended to be used by trained professionals only and is not a substitute for the user's professional judgment or independent testing. The accuracy at which reality is approximated depends highly on the expertise of the user regarding the modelling of the problem, the understanding of the soil and structural models and their limitations, the selection of model parameters, and the ability to judge the reliability of the computational results. Hence, **ZSOIL** may only be used by professionals that possess the aforementioned expertise. The user must be aware of his/her responsibility when he/she uses the computational results for geotechnical design purposes. **GeoDev Sarl** cannot be held responsible or liable for design errors that are based on the output of **ZSOIL** calculations. The user is solely responsible for establishing the adequacy of independent procedures for testing the reliability, accuracy and completeness of any output of **ZSOIL** calculations.

2. LIMITED WARRANTY

   GeoDev Sarl warrants that **ZSOIL** will a) perform substantially in accordance with the accompanying written material for a period of 90 days from the date of receipt, and b) any hardware accompanying the product will be free from defects in materials and workmanship under normal use and service for a period of one year, from the date of receipt.

3. CUSTOMER REMEDIES

   GeoDev Sarl entire liability and your exclusive remedy shall be at **GeoDev's** option, either a) return of the price paid, or b) repair or replacement of the software or hardware component which does not meet **GeoDev**'s limited warranty, and which is returned to **GeoDev Sarl**, with a copy of proof of payment. This limited warranty is void if failure of **the Software** or hardware component has resulted from accident, abuse, or misapplication. Any replacement of software or hardware will be warranted for the remainder of the original warranty period or 30 days, whichever is longer.

NO OTHER WARRANTIES.

YOU ACKNOWLEDGE AND AGREE THAT **ZSOIL** IS PROVIDED ON AN "AS IS" AND "AS AVAILABLE" BASIS AND THAT YOUR USE OF OR RELIANCE UPON **ZSOIL** AND ANY THIRD PARTY CONTENT AND SERVICES ACCESSED THEREBY IS AT YOUR SOLE RISK AND DISCRETION. **GeoDev Sarl** AND ITS AFFILIATES, PARTNERS, SUPPLIERS AND LICENSORS HEREBY DISCLAIM ANY AND ALL REPRESENTATIONS, WARRANTIES AND GUARANTIES REGARDING **ZSOIL** AND THIRD PARTY CONTENT AND SERVICES, WHETHER EXPRESS,IMPLIED OR STATUTORY. TO THE MAXIMUM EXTENT PERMITTED BY APPLICABLE LAW, **GeoDev Sarl** DISCLAIMS ALL OTHER WARRANTIES, EITHER EXPRESS OR IMPLIED, INCLUDING, BUT NOT LIMITED TO, IMPLIED WARRANTIES OF MERCHANTABILITY AND FITNESS FOR A PARTICULAR PURPOSE, WITH REGARD TO THE SOFTWARE PRODUCT, AND ANY ACCOMPANYING HARDWARE.

NO LIABILITY FOR CONSEQUENTIAL DAMAGES.

TO THE MAXIMUM EXTENT PERMITTED BY LAW, IN NO EVENT SHALL **GeoDev Sarl** HAVE ANY LIABILITY (DIRECTLY OR INDIRECTLY) FOR ANY SPECIAL INCIDENTAL, INDIRECT, OR CONSEQUENTIAL DAMAGES WHATSOEVER (INCLUDING, WITHOUT LIMITATION, DAMAGES FOR LOSS OF BUSINESS, PROFITS, BUSINESS INTERRUPTION, LOSS OF BUSINESS INFORMATION, OR ANY OTHER PECUNIARY LOSS) ARISING OUT OF THE USE OF OR INABILITY TO USE ZSOIL, EVEN IF **GeoDev Sarl** HAS BEEN ADVISED OF THE POSSIBILITY OF SUCH DAMAGES.

OTHER PROVISIONS.

SUPPORT: If included in license price, assistance will be provided by **GeoDev Sarl**, by e-mail exclusively, during the first year following purchase. This service excludes all forms of consulting on actual projects. Installation support is limited to initially supported OS and a four year duration.

PROFESSIONAL VERSIONS of **ZSOIL** are meant to be used in practice & in research centers.

ACADEMIC VERSIONS of **ZSOIL** are meant to be used exclusively for teaching and research in academic institutions.

ACADEMIC WITH CONSULTING VERSIONS of **ZSOIL** are meant to be used exclusively for teaching, research and consulting in academic institutions.

The terms of this agreement may be amended in the future, by **GeoDev Sarl**, when necessary. In such cases the revised agreement will be resubmitted for user approval on the software's front screen.

APPLICABLE LAW AND JURISDICTION THIS AGREEMENT IS GOVERNED BY THE (SUBSTANTIVE) LAWS OF SWITZERLAND, ALL DISPUTES ARISING OUT OF OR IN CONNECTION WITH THIS AGREEMENT OR THE USE OF ZSOIL SHALL EXCLUSIVELY BE SETTLED BY THE ORDINARY COURTS OF CANTON DE VAUD (ARRONDISSEMENT DE LAUSANNE)

LAUSANNE 1.11.2022

Contents of Theoretical Manual

Preface

Document *THEORY MANUAL* presents the constitutive model and the finite element implementation. The discussion is limited to features which are actually used in the program. No attempt is made to give a general overview of numerical methods in soil mechanics.

The proposed models include elasticity, various plasticity models, time dependent behavior resulting from consolidation, and actual creep.

Sign convention are different in continuum and soil mechanics. Both sign conventions are used in this text; variables which are positive in compression are underlined, in order to avoid possible confusion.

INTRODUCTION

PROBLEM STATEMENT

MATERIAL MODELS

NUMERICAL IMPLEMENTATION

STRUCTURES

INTERFACE

GEOTECHNICAL ASPECTS

Chapter 1

INTRODUCTION

The following sections present the constitutive model and the finite element implementation. The discussion is limited to features which are actually used in the program. No attempt is made to give a general overview of numerical methods in soil mechanics.

The proposed models include elasticity, various plasticity models, time dependent behavior resulting from consolidation, and creep.

Sign convention are different in continuum and soil mechanics. Both sign conventions are used in this text; variables which are positive in compression are underlined, in order to avoid possible confusion.

1.1   NOTATION

General rules

- underlined variables (like stress $\underline{\sigma}$, pressure $\underline{p}$, etc.) are positive in compression

- overbarred symbols mean the parameters with prescribed (known) value ($\bar{p}$, $\bar{u}$)

- abbreviations in sub/superscripts

cr	creep
e	elastic part
e	element
eq	equilibrium
Ext	external
F	fluid
L	liquid
m	mean
max	maximum
min	minimum
n	normal direction
p	plastic part
tot	total
0	reference state
∞	infinity

Symbols

Latin symbol	SI units	Meaning
b_i, $\mathbf{b}$	N/m^3	body force vector
C_{ijkl}, $\mathbf{C}$	N/m^2	compliance constitutive tensor
D_{ijkl}, $\mathbf{D}$	N/m^2	stiffness
G	N/m^2	Kirchhoff modulus
g	m/s^2	earth acceleration
E	N/m^2	Young modulus
e	–	void ratio
e_{ij}	–	strain deviator
k_{ij}, $\mathbf{k}$	m/s	permeability tensor
K	N/m^2	bulk modulus (solid)
n_i, $\mathbf{n}$	–	normal vector
n	–	porosity
u_i, $\mathbf{u}$	m	displacement vector
p	N/m^2	pressure
Q	kg/(s m^2)	mass source
V_i, $\mathbf{v}$	m/s	relative fluid velocity
R^{MC}	N/m^2	radius of the Mohr–Coulomb circle
S	–	saturation coefficient
S_r	–	residual saturation coefficient
s_{ij}	N/m^2	stress deviator

Greek symbol	SI units	Meaning
$\varepsilon_{ij}, \boldsymbol{\varepsilon}$	–	strain tensor
η	Ns/m^2	fluid viscosity
γ	N/m^3	specific weight
$\Gamma = \partial\Omega$	m	boundary of the domain Ω
Γ_p	m	boundary with imposed pressure conditions
Γ_q	m	boundary with imposed flow conditions
Γ_s	m	boundary with imposed seepage (i.e. pressure dependent) flow conditions
Γ_t	m	boundary with imposed traction conditions
Γ_u	m	boundary with imposed displacement conditions
λ	N/m^2	Lame constant
ν	–	Poisson coefficient
ρ	kg/m^3	mass density
$\sigma_{ij}, \boldsymbol{\sigma}$	N/m^2	stress tensor
$\sigma'_{ij}, \boldsymbol{\sigma}'$	N/m^2	effective stress tensor
$\tau_{ij}, \boldsymbol{\sigma}$	N/m^2	shear stress tensor

1.2   SOME IMPORTANT FORMULAE IN TENSOR ALGEBRA AND ANALYSIS

In mechanics several tensorial variables of different rank are used. Examples are:

scalar (zeroth rank tensor) — density ρ, temperature T, energy W, ...

vector (first rank tensor)— displacement vector $\mathbf{u}$, velocity vector $\mathbf{v}$, ...

dyad (second rank tensor) — stress tensor $\boldsymbol{\sigma}$, deformation tensor $\boldsymbol{\varepsilon}$, ...

— fourth, sixth and higher rank tensor — material tensor ...

Some rules of calculations with tensors in the three-dimensional Euclidean space are presented in this section. The direct (symbolic) and the component notation of tensor quantities are used. For shorter writing we introduce the Einstein's summation convention (repeated index in some term in the expression requires summation)

$$\ldots + a_i b_i + \ldots = \cdots + \sum_{i=1}^{3} a_i b_i + \ldots = \ldots + a_1 b_1 + a_2 b_2 + a_3 b_3 + \ldots$$

i is a dummy index.

Window 1-1: Scalars, vectors and tensors

SCALAR

Scalars are variables, which are fully independent on the choice of coordinate system (invariant variables) because they have no orientation.

VECTOR

Vectors can be written as

$$\mathbf{a} = a_1\mathbf{e}_1 + a_2\mathbf{e}_2 + a_3\mathbf{e}_3, \qquad \mathbf{a} = (a_1, a_2, a_3), \qquad \mathbf{a} = (a_i), \ i = 1, 2, 3.$$

The a_i are the coordinates of the vector, which are related to the vector basis $\mathbf{e}_i$ with respect to the given coordinate system. This vector basis is assumed to be an orthonormal basis

$$|\mathbf{e}_i| = 1, \quad \mathbf{e}_i \cdot \mathbf{e}_j = \begin{cases} 1 & i = j \\ 0 & i \neq j \end{cases}$$

The scalar product (inner product, dot product) of two vectors $\mathbf{a}$ and $\mathbf{b}$ is defined as

$$\mathbf{a} \cdot \mathbf{b} = a_i\mathbf{e}_i \cdot b_j\mathbf{e}_j = a_ib_j\mathbf{e}_i \cdot \mathbf{e}_j = a_ib_j\delta_{ij} = a_ib_i = \alpha; \quad \delta_{ij} = \begin{cases} 1 & i = j \\ 0 & i \neq j \end{cases}$$

The dyadic product of two vectors $\mathbf{a}$ and $\mathbf{b}$

$$\mathbf{ab} = a_i\mathbf{e}_i b_j\mathbf{e}_j = a_ib_j\mathbf{e}_i\mathbf{e}_j = T_{ij}\mathbf{e}_i\mathbf{e}_j = \mathbf{T}.$$

In some textbooks for this product the following designation is used

$$\mathbf{a} \otimes \mathbf{b} \equiv \mathbf{ab}.$$

SECOND RANK TENSOR With the help of the dyadic product the second rank tensor $\mathbf{T}$ can be introduced

$$\mathbf{T} = \mathbf{ab} = a_ib_j\mathbf{e}_i\mathbf{e}_j = T_{ij}\mathbf{e}_i\mathbf{e}_j.$$

For the second rank tensors $\mathbf{T}$ and $\mathbf{S}$ we define the following products:

Scalar product e.g. tensor product with the contraction

$$\mathbf{T} : \mathbf{S} = T_{ij}\mathbf{e}_i\mathbf{e}_j : S_{kl}\mathbf{e}_k\mathbf{e}_l = T_{ij}S_{kl}\mathbf{e}_i\delta_{jk}\mathbf{e}_l = T_{ij}S_{jl}\mathbf{e}_i\mathbf{e}_l = M_{il}\mathbf{e}_i\mathbf{e}_l,$$

which leads to a second rank tensor.

Double scalar product e.g. tensor product with the double contraction

$$\mathbf{T} :: \mathbf{S} = T_{ij}\mathbf{e}_i\mathbf{e}_j :: S_{kl}\mathbf{e}_k\mathbf{e}_l = T_{ij}S_{kl}\delta_{jk}\delta_{il} = T_{ij}S_{ji} = \alpha,$$

resulting in a scalar.

HIGHER RANK TENSOR

In a similar way (by dyadic product) we can define tensors of higher ranks:

the 4th rank tensor $\quad ^{(4)}\mathbf{A} = \mathbf{abcd} = a_ib_jc_kd_l\mathbf{e}_i\mathbf{e}_j\mathbf{e}_k\mathbf{e}_l = \mathbf{TS} =$
$$T_{ij}S_{kl}\mathbf{e}_i\mathbf{e}_j\mathbf{e}_k\mathbf{e}_l = A_{ijkl}\mathbf{e}_i\mathbf{e}_j\mathbf{e}_k\mathbf{e}_l$$

the 6th rank tensor $\quad ^{(6)}\mathbf{B} = \mathbf{abcdgh} = \mathbf{TSP} =$
$$T_{ij}S_{kl}P_{mn}\mathbf{e}_i\mathbf{e}_j\mathbf{e}_k\mathbf{e}_l\mathbf{e}_m\mathbf{e}_n = B_{ijklmn}\mathbf{e}_i\mathbf{e}_j\mathbf{e}_k\mathbf{e}_l\mathbf{e}_m\mathbf{e}_n.$$

Also tensor products (from uni- to multi- scalar) can be defined.

| | Window 1-1 |

| **Window 1-2: Special for second rank tensors** |

Unit tensor (identity tensor) $\mathbf{I}$

$$\mathbf{I} = \delta_{ij}\mathbf{e}_i\mathbf{e}_j$$

Transposed tensor $\mathbf{T}^\mathrm{T}$

$$\mathbf{T} = \mathbf{ab} \implies \mathbf{T}^\mathrm{T} = \mathbf{ba}\,,$$
$$\mathbf{T} = T_{ij}\mathbf{e}_i\mathbf{e}_j \implies \mathbf{T}^\mathrm{T} = T_{ij}\mathbf{e}_j\mathbf{e}_i = T_{ji}\mathbf{e}_i\mathbf{e}j\,,$$

Symmetric tensor

If $\mathbf{T} = \mathbf{T}^\mathrm{T}$ ($T_{ij} = T_{ji}$) then tensor $\mathbf{T}$ is symmetric

Antisymmetric tensor

If $\mathbf{T} = -\mathbf{T}^\mathrm{T}$ ($T_{ij} = -T_{ji}$) then tensor $\mathbf{T}$ is antisymmetric

Trace of the tensor

$$\mathrm{tr}\mathbf{T} = \mathbf{I} :: \mathbf{T} = T_{ii} = T_{11} + T_{22} + T_{33}.$$

Tensor decomposition

The tensor $\mathbf{T}$ may be decomposed into two parts: axiator and deviator defined as follow:

Axiator (spherical tensor); denoted $\mathbf{A}_\mathrm{T}$ or $\mathbf{T}^\mathrm{A}$

$$\mathbf{A}_\mathrm{T} = \frac{1}{3}(\mathbf{I} :: \mathbf{T})\mathbf{I} = \frac{1}{3}T_{kk}\delta_{ij}\mathbf{e}_i\mathbf{I}_j$$

Deviator denoted $\mathbf{D}_\mathrm{T}$ or $\mathbf{T}^\mathrm{D}$

$$\mathbf{D}_\mathrm{T} = \mathbf{T} - \mathbf{A}_\mathrm{T} = (T_{ij} - \frac{1}{3}T_{kk}\delta_{ij})\mathbf{e}_i\mathbf{e}_j$$

so

$$\mathbf{T} = \mathbf{A}_\mathrm{T} + \mathbf{D}_\mathrm{T}$$

| Window 1-2 |

Window 1-3: Transformation rules for tensors

The rules of transformation from one coordinate system to a rotated system (marked with ')
for tensors of the rank 2, 4 or 6 are (all indices range from 1 to 3)

$$
\begin{aligned}
a'_{ij} &= \alpha_{mi}\alpha_{nj}a_{mn}, \\
b'_{ijkl} &= \alpha_{mi}\alpha_{nj}\alpha_{sk}\alpha_{tl}b_{mnst}, \\
c'_{ijklop} &= \alpha_{mi}\alpha_{nj}\alpha_{sk}\alpha_{tl}\alpha_{uo}\alpha_{vp}c_{mnstuv}.
\end{aligned}
$$

The α_{ij} are the elements of the transformation matrix (direction cosines):

$$
\alpha_{ij} = \cos(\mathbf{e}'_i, \mathbf{e}_j).
$$

Window 1-3

Window 1-4: Eigenvalue problem for a second rank tensor

The eigenvalues λ and the eigenvectors (eigendirections) $\mathbf{n}$ for a second rank tensor $\mathbf{T}$ can
be obtained from the solution of the following equations

$$
(\mathbf{T} - \lambda\mathbf{I}) \cdot \mathbf{n} = \mathbf{0}, \quad (T_{ij} - \lambda\delta_{ij})n_j = 0
$$

The eigenvalues follow from the condition that nontrivial solutions are existing, which leads
to the characteristic equation:

$$
\det(\mathbf{T} - \lambda\mathbf{I}) = 0; \quad \det(T_{ij} - \lambda\delta_{ij}) = 0. \tag{1}
$$

The roots of this equation $\lambda_{(\alpha)}, \alpha = 1, 2, 3$ sort in the ascending order (e.g. $\lambda_1 \geq \lambda_2 \geq \lambda_3$)
are called the principal values. It can be shown that in the case of symmetric second rank
tensors all principle values are real.

For each root we get the eigenvector (eigendirections, principal directions) $n_j^{(\alpha)}, \alpha = 1, 2, 3$
from the system

$$
\begin{aligned}
(T_{11} - \lambda)n_1 + T_{12}n_2 + T_{13}n_3 &= 0, \\
T_{21}n_1 + (T_{22} - \lambda)n_2 + T_{23}n_3 &= 0, \\
T_{31}n_1 + T_{32}n_2 + (T_{33} - \lambda)n_3 &= 0, \\
n_1^2 + n_2^2 + n_3^2 &= 1.
\end{aligned}
$$

Window 1-4

Window 1-5: Invariants of a second rank tensor

Invariant terms are independent on the choice of the coordinate system. Such a system of invariants can be related to the coefficients of the characteristic equation (1) rewrite in the form:

$$\det(\mathbf{T} - \lambda\mathbf{I}) = \lambda^3 - I_1(\mathbf{T})\lambda^2 + I_2(\mathbf{T})\lambda - I_3(\mathbf{T}) = 0. \tag{1}$$

The I_i are called principal invariants, defined as:

Linear principal invariant

$$I_1(\mathbf{T}) = \mathrm{tr}\mathbf{T} \equiv \mathbf{T} :: \mathbf{I} \equiv T_{ii},$$

Quadratic principal invariant

$$I_2(\mathbf{T}) = \frac{1}{2}\left[J_1^2(\mathbf{T}) - J_1(\mathbf{T}^2)\right] = \frac{1}{2}(T_{ii}T_{jj} - T_{ij}T_{ji}),$$

Cubic principal invariant

$$\begin{aligned}
I_3(\mathbf{T}) &= \frac{1}{3}\left[J_1(\mathbf{T}^3) + 3J_1(\mathbf{T})J_2(\mathbf{T}) - J_1^3(\mathbf{T})\right] \\
&= \frac{1}{3}J_1(\mathbf{T}^3) - \frac{1}{2}J_1(\mathbf{T}^2)J_1(\mathbf{T}) + \frac{1}{6}J_1^3(\mathbf{T}) \\
&= \det(T_{ij}).
\end{aligned}$$

In the stress space very often we use invariants of the stress deviator $\mathbf{D}^\sigma = s_{ij}$:

$$\begin{aligned}
J_1 &= 0 \\
J_2 &= \frac{1}{2}s_{ij}s_{ji} \\
J_3 &= \frac{1}{3}s_{ij}s_{jk}s_{ki}
\end{aligned}$$

Cylindrical invariants of stress tensor (Haigh and Westergaard):

$$\begin{aligned}
\xi &= \frac{1}{\sqrt{3}}I_1 \\
\cos 3\theta &= \frac{3\sqrt{3}}{2}J_3 J_2^{-3/2} \\
\rho &= \sqrt{2J_2}
\end{aligned}$$

Invariants commonly used in geotechnical material models are:

$$\begin{aligned}
p &= -\frac{1}{3}I_1 \\
q &= \sqrt{3J_2}
\end{aligned}$$

Window 1-5

Window 1-6: Cayley-Hamilton theorem

The second rank tensor satisfies characteristic equation

$$\mathbf{T}^3 - I_1(\mathbf{T})\mathbf{T}^2 + I_2(\mathbf{T})\mathbf{T} - I_3(\mathbf{T})\mathbf{I} = 0,$$

which enables the representation of $\mathbf{T}^n$ ($n \geq 3$) as a linear function of $\mathbf{T}^2, \mathbf{T}, \mathbf{T}^0 = \mathbf{I}$, e.g.,

$$\mathbf{T}^3 = I_1(\mathbf{T})\mathbf{T}^2 - I_2(\mathbf{T})\mathbf{T} + I_3(\mathbf{T})\mathbf{I}.$$

Window 1-6

Window 1-7: Derivatives of the invariants of a second rank tensor

A scalar-valued function of a second rank tensor can be represented by

$$\psi = \psi(\mathbf{T}) = \psi(T_{11}, T_{22}, \ldots, T_{31}).$$

Then we can calculate the derivative by the following equation

$$\psi_{,\mathbf{T}} = \frac{\partial \psi}{\partial \mathbf{T}} = \frac{\partial \psi}{\partial T_{kl}}\mathbf{e}_k\mathbf{e}_l.$$

On the other hand the derivatives of the invariants are

$$\begin{aligned}
J_1(\mathbf{T})_{,\mathbf{T}} &= \mathbf{I}, \quad J_1(\mathbf{T}^2)_{,\mathbf{T}} = 2\mathbf{T}^{\mathrm{T}}, \quad J_1(\mathbf{T}^3)_{,\mathbf{T}} = 3\mathbf{T}^{2\,\mathrm{T}}, \\
J_2(\mathbf{T})_{,\mathbf{T}} &= J_1(\mathbf{T})\mathbf{I} - \mathbf{T}^{\mathrm{T}}, \\
J_3(\mathbf{T})_{,\mathbf{T}} &= \mathbf{T}^{2\,\mathrm{T}} - J_1(\mathbf{T})\mathbf{T}^{\mathrm{T}} + J_2(\mathbf{T})\mathbf{I} = J_3(\mathbf{T})(\mathbf{T}^{\mathrm{T}})^{-1}.
\end{aligned}$$

So, we finally get

$$\psi[J_1, J_2, J_3]_{,\mathbf{T}} = \left(\frac{\partial \psi}{\partial J_1} + J_1\frac{\partial \psi}{\partial J_2} + J_2\frac{\partial \psi}{\partial J_3}\right)\mathbf{I} - \left(\frac{\partial \psi}{\partial J_2} + J_1\frac{\partial \psi}{\partial J_3}\right)\mathbf{T}^{\mathrm{T}} + \frac{\partial \psi}{\partial J_3}\mathbf{T}^{2\,\mathrm{T}}.$$

These calculations can be helpful for the use of the representation theorem of an isotropic function

$$\mathbf{P} = \mathbf{F}(\mathbf{T}) = \nu_0\mathbf{I} + \nu_1\mathbf{T} + \nu_2\mathbf{T}^2.$$

The coefficients ν_i itself are functions of the invariants

$$\nu_i = \nu_i\left[J_1(\mathbf{T}), J_2(\mathbf{T}), J_3(\mathbf{T})\right]. \tag{1}$$

Window 1-7

Window 1-8: Transition from tensorial to matrix notation

It is assumed that stress/strain components are ordered in column vectors as follows:

$$\boldsymbol{\sigma} = \left\{ \begin{array}{cccccc} \sigma_{xx} & \sigma_{yy} & \tau_{xy} & \sigma_{zz} & \tau_{xz} & \tau_{yz} \end{array} \right\}^{\mathsf{T}}$$

$$\boldsymbol{\varepsilon} = \left\{ \begin{array}{cccccc} \varepsilon_{xx} & \varepsilon_{yy} & \gamma_{xy} & \varepsilon_{zz} & \gamma_{xz} & \gamma_{yz} \end{array} \right\}^{\mathsf{T}}$$

The following table is used to extract vector components from appropriate tensorial objects:

I/J	i/k	j/l
1	1	1
2	2	2
3	1	2
4	3	3
5	1	3
6	2	3

With the above table we can set:

- I-th component of stress vector $\boldsymbol{\sigma}$: $\sigma_I = \sigma_{i(I)j(I)}$

- I-th component of strain vector $\boldsymbol{\varepsilon}$: $\varepsilon_I = \varepsilon_{i(I)j(I)}$ (shear terms have to doubled)

- I-th, J-th component of stiffness matrix $\mathbf{D}$: $D_{IJ} = D_{i(I)j(I)k(J)l(J)}$

| Window 1-8 |

Window 1-9: Example: 2nd rank tensor in 2D space

Transformation rule

The (u, v) coordinates system is rotated from (x, y) one by φ angle

$$
t_{uu} = t_{xx} \cos^2 \varphi + t_{yy} \sin^2 \varphi + 2 t_{xy} \sin \varphi \cos \varphi = \frac{t_{xx} + t_{yy}}{2} + \frac{t_{xx} - t_{yy}}{2} \cos 2\varphi + t_{xy} \sin 2\varphi
$$

$$
t_{vv} = t_{xx} \sin^2 \varphi + t_{yy} \cos^2 \varphi - 2 t_{xy} \sin \varphi \cos \varphi = \frac{t_{xx} + t_{yy}}{2} - \frac{t_{xx} - t_{yy}}{2} \cos 2\varphi - t_{xy} \sin 2\varphi
$$

$$
t_{uv} = -(t_{xx} - t_{yy}) \sin \varphi \cos \varphi + t_{xy} \left(\cos^2 \varphi - \sin^2 \varphi \right) = \frac{t_{xx} - t_{yy}}{2} \sin 2\varphi - t_{xy} \cos 2\varphi
$$

Principal coordinate system $(\varphi \to \theta)$
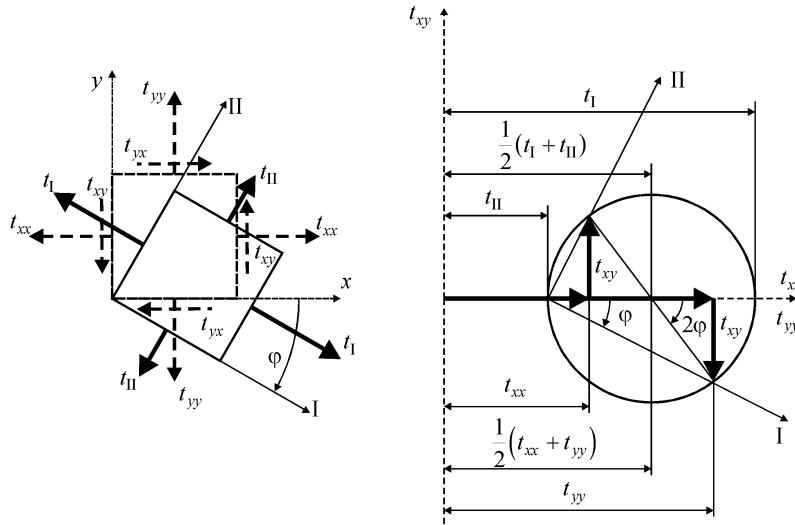
$$
t_{12} = t_{21} \stackrel{\text{def}}{=} 0 \Leftrightarrow \theta = \frac{1}{2} \arctan \left(\frac{2 t_{xy}}{t_{xx} - t_{yy}} \right)
$$

Diagonal, principal (max/min) components

$$
t_{1,2} = t_{\max,\min} = \frac{t_{xx} + t_{yy}}{2} \pm \sqrt{ \left(\frac{t_{xx} - t_{yy}}{2} \right)^2 + t_{xy}^2 }
$$

Maximal out–of diagonal component

Position of the coordinate system:

$$
t_{12} \to \max \Leftrightarrow \varphi = \frac{1}{2} \arctan \left(\frac{t_{yy} - t_{xx}}{2 t_{xy}} \right)
$$

e.g. such system is rotated from principal one by $45°$

Maximal value of out-of diagonal component

$$
t_{uv}^{\max} = \frac{t_1 - t_2}{2}
$$

Window 1-9

Chapter 2

PROBLEM STATEMENT

In following sections formulations of problems available to be solved are given. In particular:

SINGLE PHASE
TWO PHASE
TRANSIENT FLOW
HEAT TRANSFER
HUMIDITY TRANSFER

They contain governing differential equations and boundary conditions (strong formulation). Despite this, for each problem variational formulations (weak form) are given which are the basis for numerical solution.

2.1   SINGLE PHASE, SOLID MEDIUM

Window 2-1: Strong form of the boundary value problem
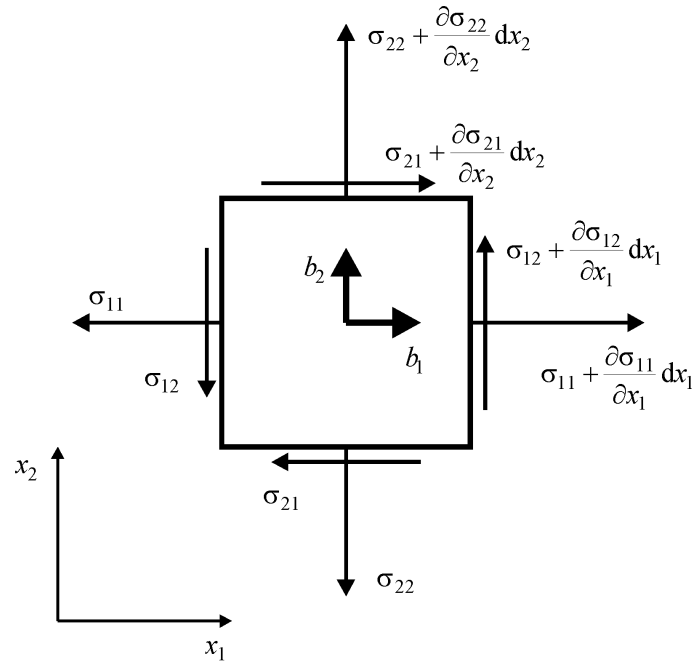
Equilibrium of the single phase medium

Equilibrium equation:

$$\sigma_{ij,j} + b_i = 0, \quad \text{in } \Omega$$

Boundary conditions (BC):

$$
\begin{aligned}
\text{traction BC:} \quad & \sigma_{ij} n_j = \bar{t}_i, \quad \text{on} \quad \Gamma_t \\
\text{displacement BC:} \quad & u_i = \bar{u}_i, \quad \text{on} \quad \Gamma_u \\
& \Gamma = \Gamma_t \cup \Gamma_u
\end{aligned}
$$

Strain–displacement relation (analysis of the small strain tensor and the linear relation is assumed):

$$\varepsilon_{ij} = \frac{1}{2}\left(u_{i,j} + u_{j,i}\right)$$

Constitutive equation (incremental form e.g. $\dot{\boldsymbol{\sigma}}$ means a stress increment $\Delta\boldsymbol{\sigma}$)

$$\dot{\sigma}_{ij} = C_{ijkl}\dot{\varepsilon}_{kl}$$

where C_{ijkl} is the 4th rank constitutive tensor

Window 2-1

Related Topics

- *THEORY MANUAL: TWO-PHASE MEDIA*

- *THEORY MANUAL: WEAK FORM*

2.2 TWO-PHASE PARTIALLY SATURATED MEDIUM

The simulation of a two–phase medium is necessary in order to account for time-dependent behaviour resulting from consolidation and/or transient flow. Actual creep will be discussed later on.

The boundary–value–problem to be solved requires the coupled solution of conservation of mass and momentum in both the solid and the liquid phases, together with boundary and initial conditions. The general transient case is considered here.

The Windows in section present:

Two phase medium model – Window 2-2

Equilibrium of two phase medium – Window 2-3

Strong form of BVP for two phase partially saturated medium – Window 2-4

Strong form of BVP for two phase fully saturated medium – Window 2-5

Window 2-2: Two–phase medium model
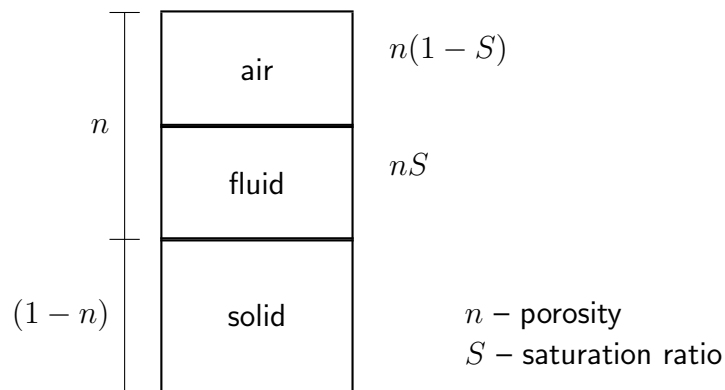
The two-phase medium is in fact an approximation of a three-phase medium where it is assumed that the air bubbles are trapped in the liquid phase so that the mixture (fluid + air) forms a compressible fluid obeying Darcy's law.

Window 2-2

Window 2-3: Equilibrium of two–phase medium
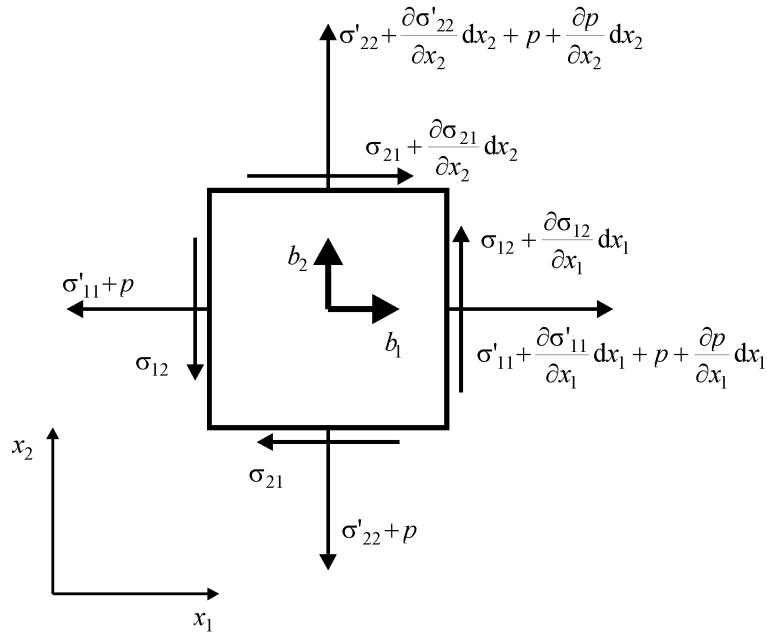
b_i denote body force, p is the fluid pressure (positive in tension). σ'_{ij} is used here for the effective stresses (positive in tension) – see problem statement for:

Partially saturated medium – Window 2-4

Fully saturated medium – Window 2-5

Equilibrium equation:
$$\sigma_{ij,j} + b_i = 0 \quad \text{on} \quad \Omega \times T$$

Strain–displacement relation (analysis of the small strain tensor and the linear relation is assumed):
$$\varepsilon_{ij} = \frac{1}{2}\left(u_{i,j} + u_{j,i}\right)$$

Constitutive equation (incremental form e.g. $\dot{\boldsymbol{\sigma}}$ means a stress increment $\Delta\boldsymbol{\sigma}$)
$$\dot{\sigma}_{ij} = C_{ijkl}\dot{\varepsilon}_{kl}$$

where C_{ijkl} is the 4th rank constitutive tensor

Window 2-3

Window 2-4: Strong form of BVP for 2–phase partially saturated medium problem
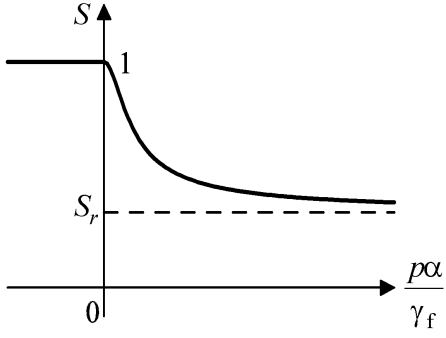
Effective stresses σ'_{ij}:

$$\sigma'_{ij} = \sigma_{ij} - \tilde{\alpha}\tilde{S}p\delta_{ij},$$

where $\tilde{\alpha}$ is the elastic Biot coefficient, $\tilde{S}$ can be selected as a saturation coefficient S[1] or as a corrected effective saturation $\tilde{S}_e$ defined as follows

$$S = S(p) = \begin{cases} S_r + \dfrac{1 - S_r}{\left[1 + \left(\alpha\dfrac{p}{\gamma_{\mathsf{F}}}\right)^n\right]^m} & \text{if } p > 0 \\ 1 & \text{if } p \le 0 \end{cases}$$

$$\tilde{S}_e = S_e^{\frac{1}{nm}} = \underbrace{\left(\frac{S - S_r}{1 - S_r}\right)^{1/nm}}_{S_e}$$

$$\tilde{\alpha} = 1 - \frac{K_t}{K_s} \qquad m = 1 - \frac{1}{n}$$

γ_{F} stands for the unit weight of fluid, S_r is the residual saturation ratio, α, n and m are the soil water retention curve (SWRC) parameters, for van Genuchten's model, while K_t and K_s are elastic solid and solid grains bulk moduli respectively. The assumed form of the $\tilde{S}_e$ enforces monotonic and asymptotic behavior of the $\tilde{S}p$ when suction p tends to infinity. For any n parameter value, $\tilde{S}p \to \gamma_w/\alpha$ for $p \to \infty$. In this way, the resulting apparent cohesion can be controlled in order to avoid unrealistic excessive values. Parameters α, n and S_r can be optimized for the coarse grained and fine grained soils through the best fit to the Modified Kovacs model that can easily be identified using basic geotechnical data ie. e_0, d_{60} and d_{10} for coarse grained soils or e_0 and LL (liquid limit) for undeformed fine grained soils [2],[3].

Flow equation (the Darcy law – Window 3-4)

$$q_i = -k^*_{ij}\left(-\frac{p}{\gamma_{\mathsf{F}}} + z\right)_{,j}$$

The permeability tensor k^*_{ij} is obtained by scaling the k_{ij} tensor for fully saturated medium by scalar valued function k_r which depends the saturation ratio S.

$$k^*_{ij} = k_r(S)k_{ij}$$

$k_r = S_e^3$ (Irmay)
or
$$k_r = S_e^{1/2}\left(1 - \left(1 - S_e^{\frac{1}{m}}\right)^m\right)^2$$
(Mualem)

---
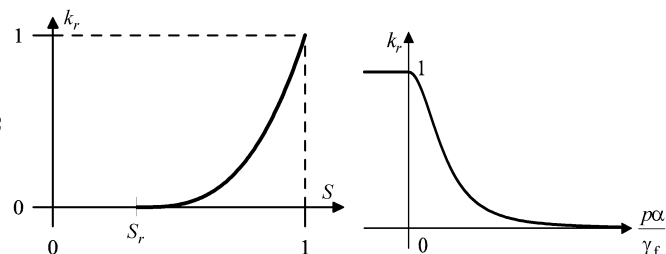
[1]Van Genuchten (1980) A closed form of the equation for predicting the hydraulic conductivity of unsaturated soils. Soil Sciences Am. Soc., 44, 892–898.

[2]M. Aubertin, M. Mbonimpa, B. Bussière, and R.P. Chapuis. A model to predict the water retention curve from basic geotechnical properties. Can. Geotech. J. 40: 1104–1122 (2003)

[3]M. Mbonimpa, M. Aubertin, A. Maqsoud and B. Bussière. Predictive Model for the Water Retention Curve of Deformable Clayey Soils. Journal of Geotechnical and Geoenvironmental Engineering, Vol. 132, No. 9, September 1, 2006

November 6, 2023   QuickHelp DataPrep Benchmarks Tutorials

Mass balance:

$$\rho = nS\rho_w + (1-n)\rho_s$$

where n is the porosity defined by the void ratio e

$$n = \frac{e}{1+e}, \qquad e = \frac{\texttt{void volume}}{\texttt{solid volume}}$$

Continuity equation:

$$\tilde{\alpha} S \dot{\varepsilon}_{kk} + q_{k,k} = c\dot{p}$$

with c the specific storage coefficient[4]

$$c = c(p) = n\left(\frac{S}{K_{\mathrm{w}}} - \frac{\mathrm{d}S}{\mathrm{d}p}\right) + \frac{\tilde{\alpha} - n}{K_s}S\left(S - \frac{\mathrm{d}S}{\mathrm{d}p}p\right)$$

K_{w} is the water-air mixture bulk modulus defined as

$$\frac{1}{K_w} = \frac{S}{K_f} + \frac{1-S}{K_a}$$

K_f is the fluid bulk modulus and K_a is the air bulk modulus at the atmospheric pressure ($K_a = 100$ kPa).

Boundary conditions:

on solid phase	on fluid phase
$\sigma_{ij}n_j = \bar{t}_i$ on Γ_t	$q_j n_j = \bar{q}$ on Γ_q
$u_i = \bar{u}_i$ on Γ_u,	$q_j n_j = \bar{q}_s$ on Γ_s
	$p = \bar{p}$ on Γ_p
$\Gamma = \Gamma_u + \Gamma_t$	$\Gamma = \Gamma_p + \Gamma_q + \Gamma_s$

The seepage surface requires a special treatment as the applicable boundary condition is unknown *a priori*. Boundary condition on Γ_s:

$$\bar{p} = 0 \quad \text{on} \quad \Gamma_s \text{ if } S = 1$$
$$\bar{p} = \bar{p}_{\mathsf{Ext}} \quad \text{on} \quad \Gamma_s \text{ if } S = 1 \text{ and } \bar{p}_{\mathsf{Ext}} \text{ imposed}$$
$$\bar{q} = 0 \quad \text{on} \quad \Gamma_s \text{ if } S < 1$$

This boundary condition is satisfied through penalization imposing

$$\bar{q} = 0 \quad \text{if} \quad p \geq 0 \text{ in the domain and } p_{\mathsf{Ext}} = 0$$
$$\bar{q} = -k_v p \quad \text{if} \quad p < 0 \text{ in the domain and } p_{\mathsf{Ext}} = 0$$
$$\bar{q} = -k_v(p - p_{\mathsf{Ext}}) \quad \forall p \text{ in the domain and } p_{\mathsf{Ext}} \neq 0$$

with k_v, a fictitious permeability (penalty parameter) and p_{Ext} the pressure on the external face of Γ_s; $p_{\mathsf{Ext}} = 0$ corresponds to atmospheric pressure.

Initial conditions

$$u_i(t = t_0) = u_{i0} \quad \text{on} \quad \Omega$$
$$p(t = t_0) = p_0 \quad \text{on} \quad \Omega$$

Window 2-4

---

[4]R. W. Lewis, B. A. Schrefler (1998). The finite element method in the static and dynamic deformation and consolidation of porous media. John Wiley & Sons. Second edition.
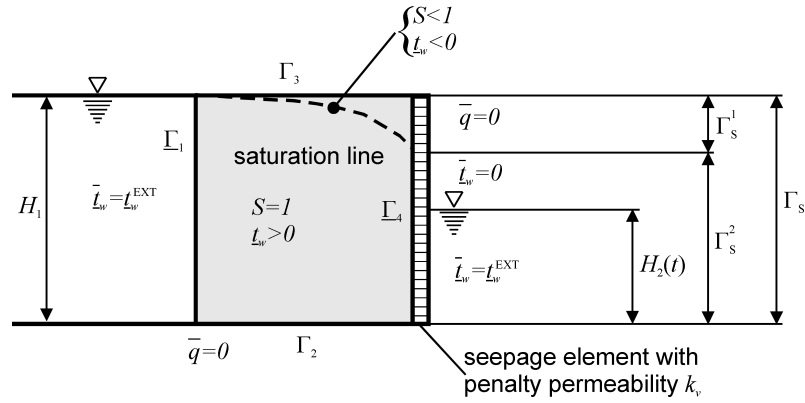
Boundary conditions for typical flow problem (damping)

| **Window 2-5: Strong form of BVP for 2–phase fully saturated medium problem** |

It can be treated as the particular case of partially saturated medium for which $S_r \to 1$ e.g. $S \equiv 1$ and $S_e \equiv 1$.

Effective stresses σ'_{ij}:

$$\sigma'_{ij} = \sigma_{ij} - \tilde{\alpha} p \delta_{ij}$$

Continuity equation:

$$\tilde{\alpha}\dot{\varepsilon}_{kk} + q_{k,k} - \left(\frac{n}{K_f} + \frac{\tilde{\alpha} - n}{K_s}\right)\dot{p} = 0 \quad \text{in} \quad \Omega \times T$$

Flow equation (the Darcy law – Window 3-4)

$$q_i = -k_{ij}\Phi_{,j} = -k_{ij}\left(\Phi = -\frac{p}{\gamma_{\mathsf{F}}} + z\right)_{,j}$$

k_{ij} is the permeability tensor and γ_{F} stands for proper weight of fluid.

Boundary conditions:

$$
\begin{array}{cc}
\text{on solid phase} & \text{on fluid phase} \\
\sigma_{ij}n_j = \bar{t}_i \quad \text{on} \quad \Gamma_t & q_j n_j = \bar{q} \quad \text{on} \quad \Gamma_q \\
u_i = \bar{u}_i \quad \text{on} \quad \Gamma_u, & q_j n_j = \bar{q}_s \quad \text{on} \quad \Gamma_s \\
\Gamma = \Gamma_u + \Gamma_t & \Gamma = +\Gamma_q + \Gamma_s
\end{array}
$$

Initial conditions

$$u_i(t = t_0) = u_{i0} \quad \text{on} \quad \Omega$$
$$p(t = t_0) = p_0 \quad \text{on} \quad \Omega$$

| Window 2-5 |

| **Window 2-6: Strong form of BVP for 2–phase undrained problem** |

Modeling undrained behavior is meaningful for fully saturated low permeable media. However, formulation shown below is formulated for the general case of fully/partially saturated medium. As the undrained driver can be run after the initial state analysis (hence the pore pressure field at steady state is nonzero) we will distinguish between the pore pressure generated by two-phase drivers (uncoupled or coupled) denoted by p and excess pore pressure (produced exclusively by the undrained drivers) denoted by Δp

Effective stresses σ'_{ij}:

$$\sigma'_{ij} = \sigma_{ij} - \tilde{\alpha}\tilde{S}(p)(p + \Delta p)\delta_{ij}$$

Suction pore pressure cut-off condition:

$$\tilde{S}(p)(p + \Delta p) \leq p_{cut-off} \quad if(p + \Delta p) \geq 0$$

Reduced continuity equation:

$$\dot{\varepsilon}_{kk} - \frac{1}{\xi\,E}\dot{p} = 0 \quad \text{in} \quad \Omega \times T$$

E – solid elastic Young's modulus
ξ – penalty factor $(10^6 \div 10^8)$

Boundary conditions: To be set as for single-phase problems

| Window 2-6 |

Related Topics

- THEORY MANUAL: TRANSIENT FLOW

- THEORY MANUAL: SINGLE PHASE, SOLID MEDIUM

- THEORY MANUAL: TWO–PHASE MEDIA. APPROXIMATION AND MATRIX FORM

- THEORY MANUAL: TWO–PHASE MEDIA. WEAK FORM

2.3   TRANSIENT FLOW

Transient flow problem formulation may be derived from two–phase media formulation, see section 2.2. The only primary state variable is pore pressures p. In continuity equation, term resulting from skeleton volume changes $\dot{\varepsilon}_{kk}$ should be neglected. Constitutive relation for the flow (generalized Darcy law will take identical form). Also boundary conditions for fluid phase are identical as in the case of two–phase media.

2.4 HEAT TRANSFER

Following section gives steady state/transient heat transfer formulation for the isotropic case of 2/3D continuum, including differential equation, boundary and initial conditions.

Window 2-7: Heat transfer formulation in strong form

- **Fourier equation:**

$$(\lambda\, T_{,i})_{,i} + \frac{\partial H}{\partial t} = c^* \frac{\partial T}{\partial t} \qquad \text{on } \Omega$$

- **Boundary conditions:**

  ⋆ Temperature BC , with prescribed temperature $\overline{T}$:
  $$T = \overline{T} \ \text{ on } \ \Gamma_T$$

  ⋆ Heat flow BC , with prescribed heat flux $\overline{q}$:
  $$\lambda\frac{\partial T}{\partial n} = -\overline{q} \qquad \text{on } \ \Gamma_q$$

  ⋆ Convective BC , with prescribed ambient temperature T_e:
  $$\lambda\frac{\partial T}{\partial n} = -h(T - T_e) \ \text{on } \Gamma_c$$
  Note: $(\Gamma_q \cup \Gamma_c) \cup \Gamma_T = \Gamma; \quad \text{but } \ (\Gamma_q \cup \Gamma_c) \cap \Gamma_T = \varnothing$

- **Initial condition:**

  Known temperature field T_0 at time $t = 0$: $T(\mathbf{x},0) = T_0(\mathbf{x}) \qquad \text{on } \Omega$

where :

T	temperature,	[°K]
t	time,	[day]
λ	heat conductivity,	[kN/(°K day)]
$c^* = c\rho$	heat capacity,	[kN/(m^2 °K)]
c	specific heat,	[kN m/(kg °K)]
ρ	mass density,	[kg/m^3]
$\overline{q}$	external heat flux,	[kN/(m day)]
T_e	ambient temperature,	[°K]
h	heat convection coefficient,	[kN/(m °K day)]
H	heat source	[kN/m^2]

Window 2-7

Note: $(\Gamma_q \cup \Gamma_c) \cup \Gamma_T = \Gamma$; but $(\Gamma_q \cup \Gamma_c) \cap \Gamma_T = \varnothing$ which means that setting **temperature** B.C. exclude other boundary conditions at given part Γ_T, while **heat flow** B.C. and **convective** B.C. may coexist on a common part of the boundary i.e. mixed condition may be set on $\Gamma_q \cap \Gamma_c$ as: $\lambda\frac{\partial T}{\partial n} + h(T - T_e) + \overline{q} = 0$. Leaving a part of the boundary with no B.C. specified explicitly, corresponds to setting no heat flow, i.e. adiabatic condition $\frac{\partial T}{\partial n} = 0$ on it.

Steady state problem described by Laplace equation

$$(\lambda\, T_{,i})_{,i} = 0$$

can be formulated. Physically, it describes continuum at thermal equilibrium state, while mathematically it corresponds to a limit of the transient problem at time $t \rightarrow \infty$ with all state variables independent from time.

It is possible to define $\lambda(T)$ and $c^*(T)$ as explicit functions of temperature.

The source term H adopted in the formulation is related to the phenomena of heat emission during concrete hydration process and is described by the following set of equations:

Window 2-8: Concrete hydration heat source

- heat source as a function of maturity M :

$$H(t,T) = H_\infty \frac{(aM)^b}{1 + (aM)^b}$$

- maturity M as a function of absolute temperature T and time t:

$$M(t,T) = \int\limits_{t_d}^{t} \exp\left[\frac{Q}{R}\left(\frac{1}{T_f} - \frac{1}{T} \right) \right] \mathrm{d}t$$

where:

H_∞	total value of concrete hydration heat per unit volume	[kJ/m³],
a	heat source parameter	[1/day]
b	heat source parameter	[-]
Q/R	activation energy/universal gas constant	[°K]
T_f	reference temperature, normally $20°\text{C} = 293°\text{K}$	[°K]
t_d	dormant period	[day]

Window 2-8

2.5 HUMIDITY TRANSFER

Following section gives steady state/transient humidity transfer formulation for the isotropic case of 2/3D continuum, including differential equation, boundary and initial conditions.

Window 2-9: Humidity transfer formulation in strong form

- **Fickś equation:**

$$(D(W)W_{,i})_{,i} = \frac{\partial W}{\partial t} \qquad \text{on} \ \ \Omega$$

- **Boundary conditions:**

  ★ Humidity BC, with prescribed relative humidity
  $$W = \overline{W} \ \ \text{on} \ \ \Gamma_W$$

  ★ Perfect isolation, with humidity flux $\overline{q}_W = 0$:
  $$-\overline{q}_W = \frac{\partial(DW)}{\partial n} = 0 \qquad \text{on} \ \ \Gamma_q$$

  ★ Note: $\ \ \Gamma_q \cup \Gamma_W = \Gamma; \ \ \text{but} \ \ \Gamma_q \cap \Gamma_W = \varnothing$

- **Initial condition:**

  Known relative humidity field W_0 at time $t = 0$: $\qquad W(\mathbf{x},0) = W_0(\mathbf{x}) \qquad \text{on} \ \Omega$

with :

W	moisture potential, i.e. relative humidity	[–]
t	time,	[day]
$D(W)$	diffusion coeffcient as a function of W,	[m²/day]

$$D(W) = D_1 \left(a + \frac{1 - a}{1 + \left(\frac{1-W}{1-W_1}\right)^4} \right) \qquad \text{where:}$$

D_1	diffusion coefficient for a moisture potential of $W = 1$,	[m²/day]
W_1	moisture potential at which $D(W) = \frac{1}{2}D_1(1 + a)$	[–]
a	factor, to define diffusion at low relative humidity	[–]

Window 2-9

Note: $\Gamma_q \cup \Gamma_W = \Gamma; \ \ \text{but} \ \ \Gamma_q \cap \Gamma_W = \varnothing$ which means that setting **humidity** B.C. exclude **perfect isolation** BC at given part Γ_W. Leaving a part of the boundary with no B.C. specified explicitly (default), corresponds to setting no **humidity** flux, i.e. perfect isolation condition $\frac{\partial(DW)}{\partial n} = 0$ on it.

Steady state problem described by Laplace equation

$$(D\,W_{,i})_{,i} = 0$$

can be formulated. Physically, it describes continuum at diffusion equilibrium state, while mathematically it corresponds to a limit of the transient problem at time $t \to \infty$ with all state variables independent from time.

Chapter 3

MATERIAL MODELS

ELASTICITY

CREEP

CONSOLIDATION

PLASTICITY

SWELLING

AGING CONCRETE

APPENDICES

3.1 ELASTICITY

Hooke's law is used as the basis of the model. In the subsequent windows a review of formulae from general to some particular cases is presented:

Hooke's law

Plane Strain

Axisymmetric Analysis

To simplify the writing, different sets of material constant are introduced. The relations between Lame's constant λ and μ, the coefficient of compressibility K, Young's modulus E and Poisson's ratio ν are given in Table 3.1:

<div align="center">

Table 3.1: Elastic constants

</div>

	λ	$G = \mu$	E	ν	K
λ, μ	λ	μ	$\dfrac{\mu(3\lambda + 2\mu)}{\lambda + \mu}$	$\dfrac{\lambda}{2(\lambda + \mu)}$	$\dfrac{3\lambda + 2\mu}{3}$
E, ν	$\dfrac{\nu E}{(1 + \nu)(1 - 2\nu)}$	$\dfrac{E}{2(1 + \nu)}$	E	ν	$\dfrac{E}{3(1 - 2\nu)}$
K, μ	$\dfrac{3K - 2\mu}{3}$	μ	$\dfrac{9K\mu}{3K + \mu}$	$\dfrac{3K - 2\mu}{2(3K + \mu)}$	K

Window 3-1: Hooke's law

Generalized constitutive equation

$$\sigma_{ij} = D_{ijkl}\varepsilon_{kl} \tag{1}$$

where D_{ijkl} is the modulus tensor with 36 independent components

Orthotropic case – 9 independent material constants

$$
\begin{aligned}
\varepsilon_{11} &= \frac{1}{E_1}\sigma_{11} - \frac{\nu_{21}}{E_2}\sigma_{22} - \frac{\nu_{31}}{E_3}\sigma_{33} \\
\varepsilon_{22} &= -\frac{\nu_{12}}{E_1}\sigma_{11} - \frac{1}{E_2}\sigma_{22} - \frac{\nu_{32}}{E_3}\sigma_{33} \\
\varepsilon_{33} &= -\frac{\nu_{13}}{E_1}\sigma_{11} - \frac{\nu_{23}}{E_2}\sigma_{22} - \frac{1}{E_3}\sigma_{33} \\
\gamma_{12} &= \frac{1}{\mu_{12}}\sigma_{12}, \qquad \gamma_{13} = \frac{1}{\mu_{13}}\sigma_{13}, \qquad \gamma_{23} = \frac{1}{\mu_{23}}\sigma_{23}
\end{aligned}
\tag{2}
$$

Isotropic case – 2 independent material constants

Isotropy conditions:

$$
\begin{aligned}
\nu &= \nu_{12} = \nu_{21} = \nu_{31} = \nu_{13} = \nu_{23} = \nu_{32} \\
E &= E_1 = E_2 = E_3 \\
\mu &= \mu_{12} = \mu_{13} = \mu_{23}
\end{aligned}
\tag{3}
$$

one obtains:

$$
\begin{aligned}
\varepsilon_{11} &= \frac{1}{E}(\sigma_{11} - \nu\sigma_{22} - \nu\sigma_{33}) \\
\varepsilon_{22} &= \frac{1}{E}(-\nu\sigma_{11} + \sigma_{22} - \nu\sigma_{33}) \\
\varepsilon_{33} &= \frac{1}{E}(-\nu\sigma_{11} - \nu\sigma_{22} + \sigma_{33}) \\
\gamma_{ij} &= \frac{1}{\mu}\sigma_{ij}, \qquad i \neq j
\end{aligned}
\tag{4}
$$

Isotropic case: tensor notation

Strain vs stress

$$\varepsilon_{ij} = \frac{1}{E}\left[(1+\nu)\sigma_{ij} - \nu\sigma_{kk}\delta_{ij}\right] \tag{5}$$

Stress vs strain

$$\sigma_{ij} = \lambda\varepsilon_{kk}\delta_{ij} + 2\mu\varepsilon_{ij} \tag{6}$$

Isotropic case: volumetric–deviatoric split

$$
\begin{aligned}
\sigma_{kk} &= 3K\varepsilon_{kk} \tag{7} \\
s_{ij} &= 2\mu e_{ij} \tag{8}
\end{aligned}
$$

s_{ij}, e_{ij} denote the components of stress and strain deviators respectively

Window 3-1

Window 3-2: Plane Strain

Plane Strain assumptions:

$$\varepsilon_{33} = \varepsilon_{13} = \varepsilon_{23} \equiv 0$$

Under the above assumptions from Eqs (4) (Win.(3-1)), one obtains:

$$\sigma_{33} = \nu(\sigma_{11} + \sigma_{22}) \tag{1}$$

and

$$
\begin{bmatrix} \sigma_{11} \\ \sigma_{22} \\ \sigma_{12} \end{bmatrix}
= \frac{E(1-\nu)}{(1+\nu)(1-2\nu)}
\begin{bmatrix} 1 & \dfrac{\nu}{1-\nu} & 0 \\[2mm] \dfrac{\nu}{1-\nu} & 1 & 0 \\[2mm] 0 & 0 & \dfrac{1-2\nu}{2(1-\nu)} \end{bmatrix}
\begin{bmatrix} \varepsilon_{11} \\ \varepsilon_{22} \\ \gamma_{12} \end{bmatrix}
\tag{2}
$$

or,

$$
\begin{bmatrix} \sigma_{11} \\ \sigma_{22} \\ \sigma_{12} \end{bmatrix}
=
\begin{bmatrix} 1 & \lambda & 0 \\ \lambda & \lambda + 2\mu & 0 \\ 0 & 0 & \mu \end{bmatrix}
\begin{bmatrix} \varepsilon_{11} \\ \varepsilon_{22} \\ \gamma_{12} \end{bmatrix}
$$

Window 3-2

Window 3-3: Axisymmetric Analysis

In an axisymmetric analysis, the following notation for coordinates and components of displacements, in the cylindrical coordinates system, are used:

$x_1 = r$ – the radial coordinate $\qquad$ $u_1 = u_r$ – the radial displacement

$x_2 = y$ – the axial coordinate $\qquad$ $u_2 = u_y$ – the axial displacement

$x_3 = \theta$ – the circumferential coordinates $\qquad$ $u_3 = u_\theta$ – the circumferential displacement

Analysis of axisymmetric body is assumed as well as that all state variables are independent of θ i.e. they are dependent on r and y only. Hence three dimensional problems can be reduced to 2–dimensional ones.

In the axisymmetric torsionless case it is additionally assumed:

$$u_\theta = 0$$

which results in

$$\varepsilon_{r\theta} = \varepsilon_{y\theta} = 0$$
$$\sigma_{r\theta} = 0 \quad \text{and} \quad \sigma_{y\theta} = 0$$

Rewriting the constitutive equations in vector form, one gets:

$$\begin{bmatrix} \varepsilon_{11} \\ \varepsilon_{22} \\ \gamma_{12} \\ \varepsilon_{33} \end{bmatrix} = \frac{1}{E} \begin{bmatrix} 1 & -\nu & 0 & -\nu \\ -\nu & 1 & 0 & -\nu \\ 0 & 0 & \dfrac{E}{\mu} & 0 \\ -\nu & -\nu & 0 & 1 \end{bmatrix} \begin{bmatrix} \sigma_{11} \\ \sigma_{22} \\ \tau_{12} \\ \sigma_{33} \end{bmatrix}. \tag{1}$$

First inverting the above stress–strain relations, one obtains:

$$\begin{bmatrix} \sigma_{11} \\ \sigma_{22} \\ \tau_{12} \\ \sigma_{33} \end{bmatrix} = \begin{bmatrix} \lambda + 2\mu & \lambda & 0 & \lambda \\ \lambda & \lambda + 2\mu & 0 & \lambda \\ 0 & 0 & \mu & 0 \\ \lambda & \lambda & 0 & \lambda + 2\mu \end{bmatrix} \begin{bmatrix} \varepsilon_{11} \\ \varepsilon_{22} \\ \gamma_{12} \\ \varepsilon_{33} \end{bmatrix}.$$

Remark:

Below matrix consists of the equivalent plane–strain matrix plus a fourth row and column. Hence plane–strain conditions can be obtained from the axisymmetric case by ignoring the fourth row and column, and setting $\sigma_{33} = \nu(\sigma_{11} + \sigma_{22})$.

Window 3-3

3.2   CONSOLIDATION

Primary consolidation is discussed in this section.

It results from the coupling of load–induced Darcy flow with the motion of a quasi–saturated medium.

DARCY LAW

FLUID MOTION

Related Topics

- THEORY: TWO PHASE MEDIA

- NUMERICAL IMPLEMENTATION: CONSOLIDATION

- GEOTECHNICAL ASPECTS: TWO PHASE MEDIA

3.2.1   GENERALIZED DARCY LAW

The generalized Darcy law is summarized in Window 3-4

$\boxed{\textbf{Window 3-4: Darcy flow}}$

Darcy's flow velocity[1]:

$$q = -\frac{K}{\eta} i_p = -k\ i \tag{1}$$

where:

$$q = nv_\mathsf{F} \quad - \quad \text{relative fluid velocity [m/s]}$$
$$v_\mathsf{F} \quad - \quad \text{average velocity through holes [m/s]}$$
$$n \quad - \quad \text{porosity}$$
$$K \quad - \quad \text{permeability [m}^2\text{] (function of porosity,}$$
$$\text{independent of fluid properties)}$$
$$k = K\frac{\gamma_\mathsf{F}}{\eta} = \rho_\mathsf{F} g\frac{K}{\eta} \quad - \quad \text{permeability coefficient [m/s]}$$
$$\rho_\mathsf{F} \quad - \quad \text{fluid mass density [kg/m}^3\text{]}$$
$$g \quad - \quad \text{earth acceleration [m/s}^2\text{]}$$
$$\eta \quad - \quad \text{fluid viscosity [N s/m}^2\text{]}$$
$$i_p = \gamma i \quad - \quad \text{pressure gradient [N/m}^3\text{]}$$
$$\gamma_\mathsf{F} = \rho_\mathsf{F} g \quad - \quad \text{specific weight [N/m}^3\text{]}$$
$$i \quad - \quad \text{hydraulic gradient [nondim.]}$$

Three–dimensional extension (with appropriate sign convention),

$$\mathbf{q} = -\mathbf{k} : \mathbf{grad}\Phi = -\mathbf{k} : \mathbf{grad}(-p_\mathsf{F}/\gamma_\mathsf{F} + z) \tag{2}$$

and in indicial notation

$$q_i = -k_{ij}\left(-\frac{p_\mathsf{F}}{\gamma_\mathsf{F}} + z\right)_{,j} \tag{3}$$

$\boxed{\text{Window 3-4}}$

---

[1]See K. Terzaghi (1943) Theoretical Soil Mechanics, Wiley.

3.2.2   FLUID MOTION

Conservation of mass in the liquid phase is expressed by Eq. (1) in the following Window. The time variation of apparent specific mass splits into two terms as shown in Eq. (2). The variation of porosity can in turn be related to the volumetric strain, Eq. (3). The fluid density change is related to the fluid's volumetric strain by Eq. (4). Assuming a slightly compressible fluid, Eq. (5), replacing then in the mass conservation equation (Eq. (1), using Eq. (1)) and with $Q = 0$, Eq. (6) is obtained.

The convective contribution can be neglected for small strain and Darcy flow, $(\mathbf{v}\,\mathbf{grad}\rho_\mathsf{F})$ is small, this leads to equation (7) after division by ρ_F.

If fluid compressibility is negligible, then the term in t can be ignored. If consolidation effects are negligible then the square brackets in (6) and (7) is ignored.

Window 3-5: Stress induced fluid motion in fully saturated porous medium

Conservation of mass

$$\frac{\partial \rho^\mathsf{F}}{\partial t} + \mathrm{div}\left(\rho^\mathsf{F} v^\mathsf{F}\right) = Q \tag{1}$$

where:

$$\rho^\mathsf{F} = n\rho_\mathsf{F} \quad - \quad \text{apparent specific mass}$$
$$\rho_\mathsf{F} \quad - \quad \text{specific mass of fluid phase}$$
$$q = nv^\mathsf{F} \quad - \quad \text{velocity}$$
$$Q \quad - \quad \text{mass source term (zero if no source)}$$
$$n \quad - \quad \text{porosity}$$

Further,

$$\frac{\partial \rho^\mathsf{F}}{\partial t} = \frac{\partial n}{\partial t}\rho_\mathsf{F} + \frac{\partial \rho_\mathsf{F}}{\partial t}n \tag{2}$$

with

$$\frac{\partial n}{\partial t} = \frac{\partial \varepsilon_{kk}}{\partial t} \tag{3}$$

$$\frac{\partial \rho_\mathsf{F}}{\partial t} = -\rho_\mathsf{F}\frac{\partial \varepsilon^\mathsf{F}_{kk}}{\partial t} \tag{4}$$

$$\frac{\partial p}{\partial t} = K_\mathsf{F}\frac{\partial \varepsilon^\mathsf{F}_{kk}}{\partial t} \tag{5}$$

results in

$$\rho_\mathsf{F}\left[\frac{\partial \varepsilon_{kk}}{\partial t} - \frac{n}{K_\mathsf{F}}\frac{\partial p}{\partial t}\right] + \mathrm{div}\left(\rho_\mathsf{F}q\right) = 0. \tag{6}$$

Finally

$$\dot{\varepsilon}_{kk} - \frac{n}{K_\mathsf{F}}\dot{p} + q_{k,k} = 0 \tag{7}$$

with K_F − the fluid bulk modulus.

Window 3-5

3.3   PLASTICITY

SKETCH OF PLASTICITY APPROACH

MOHR–COULOMB CRITERION

DRUCKER–PRAGER CRITERION

CAP MODEL

CAM-CLAY MODEL

3.3.1   SKETCH OF THE PLASTICITY APPROACH

Plasticity is a nonlinear constitutive theory and leads to a nonlinear system of equations, which is solved iteratively for Δd, the displacement increment, using a tangent (local) stiffness. Once the displacement increment is known the corresponding strain increment results from the usual strain–displacement relations. From the strain increment a trial stress can be deduced which, if it lies outside of the yield criterion, must be returned onto the criterion using a flow rule. This flow rule defines the direction of the stress return. The amplitude of the return results from the consistency condition, which requires the new state–of–stress to lie on the yield criterion. The objective, in this section, is to define precisely the new keywords introduced for plasticity theory. The basic ingredients of the elasto–plasticity theory are as follows:

Strain decomposition

Assume that the total strain increment (or rate) is the sum of an elastic $\dot{\varepsilon}^e$ and a plastic $\dot{\varepsilon}^p$ contribution:

$$\dot{\varepsilon} = \dot{\varepsilon}^e + \dot{\varepsilon}^p$$

and that the following constitutive equation holds:

$$\dot{\boldsymbol{\sigma}} = \mathbf{D^e}(\dot{\varepsilon} - \dot{\varepsilon}^p)$$

with $\mathbf{D^e}$ the elastic constitutive tensor.

Flow rule

The flow rule defines the direction of the plastic flow by:

$$\dot{\varepsilon}^p = \mathrm{d}\lambda\ \mathbf{r}(\boldsymbol{\sigma}, \mathbf{q})$$

where $\mathrm{d}\lambda$ is a positive scalar which defines the amplitude of the plastic flow and $\mathbf{r}$ (in general a function of the stress state $\boldsymbol{\sigma}$ and set of a hardening parameters $\mathbf{q}$) defines the direction in space. The calculation of $\mathrm{d}\lambda$ will be described later on.

For associative plasticity the direction of the flow $\mathbf{r}$ coincides with that of the normal $\mathbf{a}$ to the yield surface:

$$\mathbf{a} = \mathbf{r} = \frac{\partial F}{\partial \boldsymbol{\sigma}}$$

while for non–associative plasticity, we assume the existence of a plastic potential surface Q such that:

$$\mathbf{r} = \frac{\partial Q}{\partial \boldsymbol{\sigma}}$$

Hardening law

The most general form of hardening law can be expressed in rate form as follows:

$$\dot{\mathbf{q}} = \mathrm{d}\lambda\ \mathbf{h}(\boldsymbol{\sigma}, \mathbf{q})$$

where $\mathbf{h}$ (in general a function of the stress state $\boldsymbol{\sigma}$ and of a set of hardening parameters $\mathbf{q}$) is called hardening function.

The amplitude of the plastic flow

The amplitude of plastic flow can be derived from the consistency condition, which expresses that the stress point remains on the yield surface during plastic flow:

$$
\begin{aligned}
\dot{F} &= \frac{\partial F}{\partial \boldsymbol{\sigma}} : \dot{\boldsymbol{\sigma}} + \frac{\partial F}{\partial \mathbf{q}} : \dot{\mathbf{q}} = \mathbf{a} : \mathbf{D^e} : (\dot{\boldsymbol{\varepsilon}} - \dot{\boldsymbol{\varepsilon}}^p) + \frac{\partial F}{\partial \mathbf{q}} : \dot{\mathbf{q}} \\
&= \mathbf{a} : \mathbf{D^e} : (\dot{\boldsymbol{\varepsilon}} - \mathrm{d}\lambda \, \mathbf{r}) + \frac{\partial F}{\partial \mathbf{q}} : \mathrm{d}\lambda \, \mathbf{h} = 0.
\end{aligned}
$$

From the above equation, in which the flow rule and the hardening rule have been applied, the amplitude $\mathrm{d}\lambda$ can be evaluated:

$$
\mathrm{d}\lambda = \frac{(\mathbf{a} : \mathbf{D^e} : \dot{\boldsymbol{\varepsilon}})}{(\mathbf{a} : \mathbf{D^e} : \mathbf{r}) - \dfrac{\partial F}{\partial \mathbf{q}} : \mathbf{h}}
$$

Derivation of the elasto–plastic tangent matrix

Applying the amplitude $\mathrm{d}\lambda$ to the general constitutive equation the tangent elasto–plastic constitutive matrix is defined in the following way:

$$
\begin{aligned}
\dot{\boldsymbol{\sigma}} &= \mathbf{D^e} : (\dot{\boldsymbol{\varepsilon}} - \dot{\boldsymbol{\varepsilon}}^p) = \mathbf{D^e} : (\dot{\boldsymbol{\varepsilon}} - \mathrm{d}\lambda \, \mathbf{r}) = \mathbf{D^e} : \left[\dot{\boldsymbol{\varepsilon}} - \mathbf{r} \frac{(\mathbf{a} : \mathbf{D^e} : \dot{\boldsymbol{\varepsilon}})}{(\mathbf{a} : \mathbf{D^e} : \mathbf{r}) - \dfrac{\partial F}{\partial \mathbf{q}} : \mathbf{h}} \right] \\
&= \left[\mathbf{D^e} - \frac{\mathbf{D^e} : \mathbf{r} : \mathbf{a} : \mathbf{D^e}}{(\mathbf{a} : \mathbf{D^e} : \mathbf{r}) - \dfrac{\partial F}{\partial \mathbf{q}} : \mathbf{h}} \right] \dot{\boldsymbol{\varepsilon}} = \mathbf{D^{ep}} \dot{\boldsymbol{\varepsilon}}
\end{aligned}
$$

In case of perfect elasto–plasticity (no hardening is introduced) the definition of the tangent matrix reduces to:

$$
\mathbf{D^{ep}} = \mathbf{D^e} - \frac{\mathbf{D^e} : \mathbf{r} : \mathbf{a} : \mathbf{D^e}}{(\mathbf{a} : \mathbf{D^e} : \mathbf{r})}.
$$

For a nonassociative plastic flow rule the resulting tangent matrix is nonsymmetric.

3.3.2   MOHR–COULOMB CRITERION

The Mohr–Coulomb (M–C) criterion is more common in soil mechanics. Traditionally, a soil is described by its cohesion C and its angle of friction ϕ. The M–C criterion then states that the shear stress required for yielding depends on the cohesion, the friction angle and the pressure normal to the slip surface.

Window 3-6: Mohr-Coulomb yield criterion
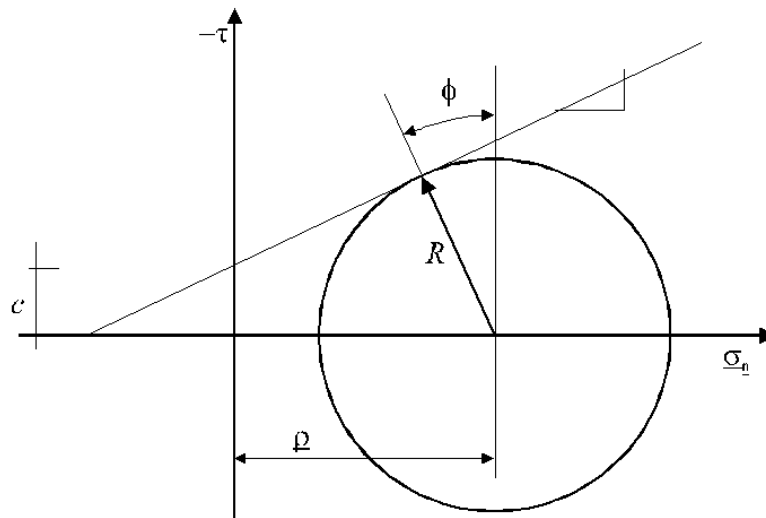
Mohr-Coulomb yield criterion

$$| \tau | = c + \underline{\sigma}_n \tan \phi \tag{1}$$

where

$$\underline{\rho} = \frac{\sigma_{11} + \sigma_{22}}{2} \tag{2}$$

and,

$$R^{\mathsf{MC}} = c \cos \phi + \underline{\rho} \sin \phi \tag{3}$$

is the maximum shear stress equal to radius of the Mohr circle at failure, i.e.:

$$R^{\mathsf{MC}} = \sqrt{\frac{(\sigma_{11} - \sigma_{22})^2}{4} + \tau_{12}^2} \tag{4}$$

Window 3-6

3.3.3 DRUCKER-PRAGER CRITERION

The Drucker–Prager (D–P) yield criterion is, mathematically speaking, the most convenient choice and often numerically the most efficient. The D–P criterion is defined in stress space, by the following equation:

$$F(\boldsymbol{\sigma}) = a_\phi I_1 + \sqrt{J_2} - k = 0$$

where the invariants I_1 and J_2 are defined in Section 1.2 and a_ϕ and k are positive material properties. For $a_\phi = 0$, Huber–Mises criterion results.

Flow rule

Associative plasticity: the direction of the flow $\mathbf{r}$ coincides with that of the normal $\mathbf{a}$ to the yield surface:

$$\mathbf{a} = \mathbf{r} = \frac{\partial F}{\partial \boldsymbol{\sigma}} = a_\phi \delta_{ij} + \frac{1}{2\sqrt{J_2}} s_{ij}$$

Non–associative plasticity: the existence of a plastic potential surface Q of Drucker–Prager type is assumed:

$$r_{ij} = \frac{\partial Q}{\partial \sigma_{ij}} = a_\psi \delta_{ij} + \frac{1}{2\sqrt{J_2}} s_{ij}$$

Notice that the corresponding flow is associative in the deviatoric component and non–associative in the volumetric components, as $a_\psi = a_\phi$.

Cut-off condition

The following tensile cutt–off plasticity condition can be activated in conjunction with the Drucker–Prager plasticity criterion:

$$F(\boldsymbol{\sigma}) = \frac{1}{\sqrt{3}} I_1 + \sqrt{J_2} - \frac{1}{\sqrt{3}} I'_{1T} = 0.$$

It has two basic features, first that maximum first stress invariant I_1 is limited to the value I'_{1T} for zero deviatoric stress s and the second that the maximum stress ratio defined as:

$$\frac{q}{p} = -\frac{3\sqrt{3J_2}}{I_1} \leq 3$$

is limited to the value which can be reached in the uniaxial compression test.

The flow rule has been assumed as fully associated so the plastic flow vector $\mathbf{r}$ is:

$$r_{ij} = \frac{\partial F}{\partial \sigma_{ij}} = \frac{1}{\sqrt{3}} \delta_{ij} + \frac{1}{2\sqrt{J_2}} s_{ij}.$$

Matching of Drucker–Prager criterion

Drucker–Prager constants could be derived directly from experiments, instead of calculated from cohesion and friction angle. Assuming that the material is properly identified by a Mohr–Coulomb criterion, the matching with the Drucker–Prager criterion can be done for various stress states.

Three dimensional matching

Collapse load matching

Elastic domains matching

Window 3-7: D–P criterion: Three dimensional matching

Both criteria are represented in the deviatoric plane along with three–dimensional matching coefficients.
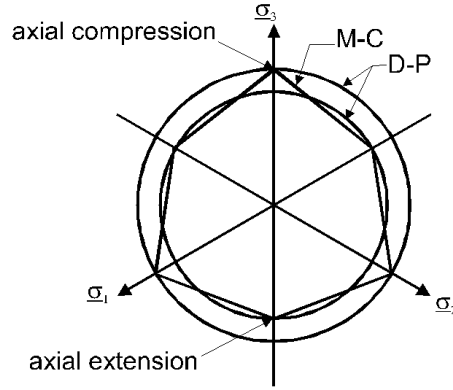
Deviatoric sections of Mohr–Coulomb (M–C) and Drucker–Prager (D–P) criteria

External apices of the M–C criterion yields (axial compression):

$$a_\phi = \frac{2\sin\phi}{\sqrt{3}(3-\sin\phi)} \qquad k = \frac{6c\cos\phi}{\sqrt{3}(3-\sin\phi)} \qquad (1)$$

Internal apices:

$$a_\phi = \frac{2\sin\phi}{\sqrt{3}(3+\sin\phi)} \qquad k = \frac{6c\cos\phi}{\sqrt{3}(3+\sin\phi)} \qquad (2)$$

Window 3-7

Window 3-8: Matching of collapse load (plane strain conditions)

Matching collapse load of D–P and M-C criteria under plane strain conditions is the default adjustment adopted in the program when plane strain is activated.

Assumptions:

$$\text{perfect plasticity:} \quad \varepsilon^{\mathsf{e}} \ll \varepsilon^{\mathsf{p}} \Rightarrow \varepsilon^{\mathsf{e}} = 0; \ \dot{\boldsymbol{\varepsilon}} = \dot{\boldsymbol{\varepsilon}}^{\mathsf{p}} \tag{1}$$

$$\text{plane strain:} \quad \dot{\varepsilon}^{p}_{33} = \dot{\varepsilon}^{p}_{13} = \dot{\varepsilon}^{p}_{23} = 0 \tag{2}$$

$$\text{flow rule :} \quad \dot{\varepsilon}^{p}_{ij} = \mathsf{d}\lambda \ r_{ij} = \mathsf{d}\lambda \left(a_{\psi} \delta_{ij} + \frac{1}{2\sqrt{J_2}} s_{ij} \right), \tag{3}$$

$$r_{ij} = \frac{\partial Q}{\partial \sigma_{ij}}$$

From (3)

$$s_{33} = -2a_{\psi}\sqrt{J_2}; \qquad s_{13} = s_{23} = 0$$

and invariants

$$I_1 = \frac{3}{2}(\sigma_{11} + \sigma_{22}) - 3a_{\psi}\sqrt{J_2}\,; \qquad J_2 = \frac{\left\{ \left[(\sigma_{11} - \sigma_{22})/2 \right]^2 + \sigma_{12}^2 \right\}}{(1 - 3a_{\psi}^2)} = \frac{(R^{\mathsf{MC}})^2}{(1 - 3a_{\psi}^2)}$$

From D–P criterion $\left(F(\boldsymbol{\sigma}) = a_{\phi}I_1 + \sqrt{J_2} - k = 0 \right)$:

$$\frac{3}{2}a_{\phi}(\sigma_{11} + \sigma_{22}) + \frac{R^{\mathsf{MC}}(1 - 3a_{\phi}a_{\psi})}{\sqrt{(1 - 3a_{\psi}^2)}} - k = 0 \tag{4}$$

one obtains

$$R^{\mathsf{MC}} = \frac{\sqrt{(1 - 3a_{\psi}^2)}}{(1 - 3a_{\phi}a_{\psi})} \left[\frac{-3a_{\phi}(\sigma_{11} + \sigma_{22})}{2} + k \right] \tag{5}$$

Identification with Mohr–Coulomb criterion, Eq. 4

$$\sin\phi = 3a_{\phi}\frac{\sqrt{(1 - 3a_{\psi}^2)}}{(1 - 3a_{\phi}a_{\psi})}, \qquad c\cos\phi = k\frac{\sqrt{(1 - 3a_{\psi}^2)}}{(1 - 3a_{\phi}a_{\psi})} \tag{6}$$

Associated flow $a_{\psi} = a_{\phi}$

$$a_{\phi} = \frac{\tan\phi}{\sqrt{9 + 12\tan^2\phi}}, \qquad k = \frac{3c}{\sqrt{9 + 12\tan^2\phi}} \tag{7}$$

Deviatoric flow $a_{\psi} = 0$

$$a_{\phi} = \frac{\sin\phi}{3}, \qquad k = c\cos\phi \tag{8}$$

a_{ψ} specified:

$$a_{\phi} = \frac{\sin\phi}{3}\left(a_{\psi}\sin\phi + \sqrt{1 - 3a_{\psi}^2} \right)^{-1}, \quad k = c\cos\phi\left(a_{\psi}\sin\phi + \sqrt{1 - 3a_{\psi}^2} \right)^{-1} \tag{9}$$

Window 3-8

Window 3-9: Matching of elastic domain

Plane strain conditions are assumed.

D–P criterion (square form of $F(\boldsymbol{\sigma}) = a_\phi I_1 + \sqrt{J_2} - k = 0$):

$$a_\phi^2 I_1^2 - 2a_\phi I_1 k + k^2 = J_2 \tag{1}$$

and invariants:

$$
\begin{aligned}
I_1 &= (\sigma_{11} + \sigma_{22})(1 + \nu) \\
J_2 &= \frac{1}{3}\left[(\sigma_{11} - \sigma_{22})^2 (1 - \nu + \nu^2) + \sigma_{11}\sigma_{22}(1 - 2\nu)^2\right] + \sigma_{12}^2
\end{aligned}
$$

$$
\begin{aligned}
\text{(D–P)}: \quad \left(\frac{\sigma_{11} - \sigma_{22}}{2}\right)^2 + \sigma_{12}^2 &= k^2 - 2a_\phi k(1 + \nu)(\sigma_{11} + \sigma_{22}) \\
&\quad + (\sigma_{11} + \sigma_{22})^2\left[a_\phi^2(1+\nu)^2 - \frac{1}{12}(1 - 2\nu)^2\right] \\
\text{(M–C)}: \quad \left(\frac{\sigma_{11} - \sigma_{22}}{2}\right)^2 + \sigma_{12}^2 &= c^2\cos^2\phi - 2\frac{\sigma_{11} + \sigma_{22}}{2}\sin\phi\, c\,\cos\phi \\
&\quad + \left(\frac{\sigma_{11} + \sigma_{22}}{2}\right)^2\sin^2\phi
\end{aligned}
$$

Matching the constant, linear and quadratic terms $(\sigma_{11} + \sigma_{22})$ yields:

$$
\begin{aligned}
a_\phi &= \frac{\sin\phi}{2(1 + \nu)} \\
k &= c\cos\phi \\
\nu &= 0.5
\end{aligned}
$$

i.e. stress–state–independent matching is possible for arbitrary c and ϕ only when $\nu = 0.5$. Alternatively, when $c = 0$, matching is possible for arbitrary ϕ for a specified ν.

Window 3-9

3.3.4   CAP MODEL

While the constitutive models described previously could be applied to any kind of material, the following one is more specific to soils.

Model is describe in the subsequent windows:

Yield surface

It combines the Drucker–Prager criterion with an ellipsoidal cap closure analogous to the CAM–CLAY ellipse and the tensile cutt–off defined in Section 3.3.3 (if needed). Multisurface plasticity algorithms require the cap definition to be extended to the zone which is covered by the D–P criterion (that is for $\underline{p} < \underline{p}_{cs}$) where it takes the form of a cylinder. $\underline{p}_c$ denotes the preconsolidation pressure defines the current cap size.

Flow rule

Associative flow is assumed on the cap; the corresponding flow vector is derived in Win.(3-10).

Hardening law

The hardening law defines the evolution of the size of the cap yield surface. This requires the evolution law for $\underline{p}_c$ as a function of plastic strain. The corresponding derivation is given in Window 3-11, where Eqs (2) and (3) define respectively the total and the elastic contributions in (4); Eq.(5) results which relates the hardening parameter $\underline{p}_c$ to the volumetric plastic strain

Remark:

Underlined variables are positive in compression.

Window 3-10: Cap model: Yield surface and plastic flow vectors
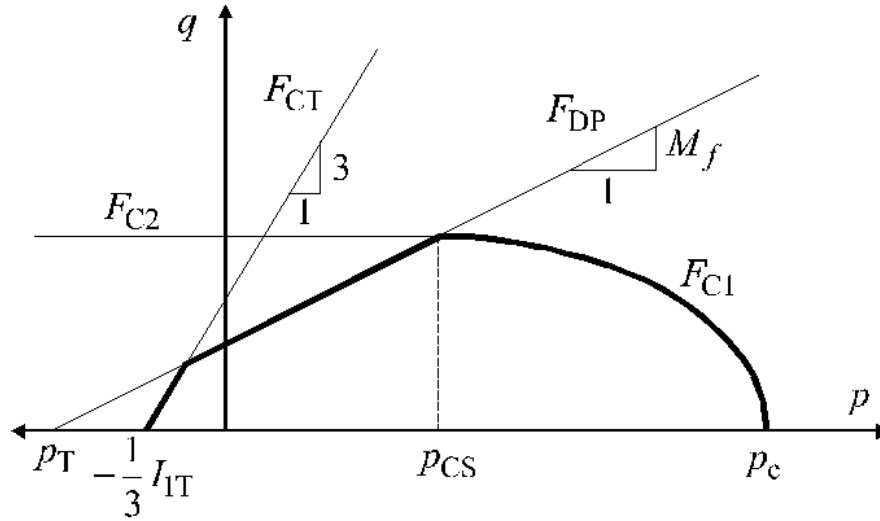
Yield function criterion

Drucker–Prager criterion:

$$F_{\mathsf{DP}} = a_\phi I_1 + \sqrt{J_2} - k = 0$$

Cap:

$$F_{\mathsf{C1}} = q^2 + \frac{M^2}{(R-1)^2}(\underline{p} - \underline{p}_{\mathsf{c}})(\underline{p} + \underline{p}_{\mathsf{c}} - 2\underline{p}_{\mathsf{cs}}) = 0 \quad \text{if} \quad \underline{p} \geq \underline{p}_{\mathsf{cs}}$$

$$F_{\mathsf{C2}} = q^2 + \frac{M^2}{(R-1)^2}(\underline{p}_{\mathsf{cs}} - \underline{p}_{\mathsf{c}})(\underline{p}_{\mathsf{c}} - \underline{p}_{\mathsf{cs}}) = 0 \quad \text{if} \quad \underline{p} < \underline{p}_{\mathsf{cs}}$$

Tensile cut–off:

$$F_{\mathsf{CT}} = \frac{1}{\sqrt{3}}I_1 + \sqrt{J_2} - \frac{1}{\sqrt{3}}I'_{1\mathsf{T}} = 0$$

with

$$
\begin{aligned}
q &= \sqrt{3J_2}, & J_2 &= \frac{1}{2}s_{ij}s_{ij} \\
\underline{p} &= -\frac{I_1}{3}, & \underline{p}_{\mathsf{cs}} &= \frac{\underline{p}_{\mathsf{c}} + (1-R)p_{\mathsf{T}}}{R} \\
M &= 3\sqrt{3}a_\phi, & p_{\mathsf{T}} &= \frac{k}{3a_\phi}
\end{aligned}
$$

Flow vectors

Defined in reduced stress space $\tilde{\sigma} = \{q, \underline{p}\}$ are as follows:

(D–P): generally non–associated flow defined by a_ψ

$$\mathbf{r}_{\text{DP}} = \begin{pmatrix} 1/\sqrt{3} \\ -3a_\psi \end{pmatrix}$$

CAP: associated flow rule is used for both segments of CAP surface

$$\mathbf{r}_{\text{C1}} = \begin{bmatrix} 2q \\ \left(\dfrac{M}{R-1}\right)^2 (2\underline{p} - 2\underline{p}_{\text{cs}}) \end{bmatrix} \quad \text{if} \quad \underline{p} \geq \underline{p}_{\text{cs}}$$

$$\mathbf{r}_{\text{C2}} = \begin{bmatrix} 2q \\ 0 \end{bmatrix} \quad \text{if} \quad \underline{p} < \underline{p}_{\text{cs}}$$

Cut–Off: associated flow rule is used

$$\mathbf{r}_{\text{CT}} = \begin{pmatrix} 1/\sqrt{3} \\ -3/\sqrt{3} \end{pmatrix}$$

Window 3-10

Window 3-11: Cap hardening

Recall:

– relation between volumetric strain rate and void ratio rate

$$\mathrm{d}\varepsilon_{kk} = \frac{\mathrm{d}e}{1 + e_0} \tag{1}$$

– void ratio evolution : derived from the logarithmic $(e - \ln p)$ approximation of the virgin consolidation path

$$\mathrm{d}e = -\frac{\lambda}{\underline{p}_c}\mathrm{d}\underline{p}_c \tag{2}$$

– void ratio variation for elastic unloading path

$$\mathrm{d}e_s = (1 + e_0)\mathrm{d}\varepsilon_{kk} = -(1 + e_0)\frac{\mathrm{d}\underline{p}_c}{K} \tag{3}$$

Evolution law for p_c

– elasto-plastic volumetric strain increment

$$\dot{\varepsilon}_{kk}^{\mathsf{tot}} = \dot{\varepsilon}_{kk}^{\mathsf{e}} + \dot{\varepsilon}_{kk}^{\mathsf{p}} \tag{4}$$

From (1–3) the hardening law for $\underline{p}_\mathsf{c}$ is derived

$$\mathrm{d}\varepsilon_{kk}^{\mathsf{p}} = -\left(\frac{\lambda}{1 + e_0}\frac{1}{\underline{p}_\mathsf{c}} - \frac{1}{K}\right)\mathrm{d}\underline{p}_\mathsf{c}$$

Evolution law for cap shape R parameter

$$R = R_{\mathsf{IN}} - (R_{\mathsf{IN}} - R_0)\frac{\underline{p}_\mathsf{c} - \underline{p}_{\mathsf{c0}}}{a + \underline{p}_\mathsf{c} - \underline{p}_{\mathsf{c0}}} \tag{5}$$

parameters R_{IN} and a are set automatically by the numerical procedure to preserve approximately the same dilatancy $d = \dfrac{\partial Q/\partial p}{\partial Q/\partial q}$ for stress paths with stress ratio $\dfrac{q}{p} = \dfrac{M}{2}$. These depend on initial preconsolidation pressure $\underline{p}_{\mathsf{c0}}$ and on p_T. R_0 is given by the user. This parameter enables proper modelling of the K_0 coefficient for normally consolidated state $(R_0 > 1)$.

Window 3-11

Window 3-12: Evaluation of $\underline{p}_{co}, R_o$ from oedometer test

The initial preconsolidation stress p_{co} and cap shape parameter R_o can be set based on oedometer test once $\underline{\sigma}_{\mathsf{VM}}$ (vertical stress at which transition from secondary to primary consolidation path occurs) and K_o^{NC} (K_o coefficient at state of normal consolidation) values are given (see Window 3-13).

In the oedometer test the following relation holds (assuming that plastic strains are large compared to elastic ones):

$$d\underline{\varepsilon}_V^p = \frac{3}{2} d\varepsilon_D^p$$

where: $d\varepsilon_D^p = \sqrt{\dfrac{2}{3} de_{ij}^p de_{ij}^p}, d\underline{\varepsilon}_V^p = -d\varepsilon_{ii}^p.$

This equation can be rewritten in the form (using plastic flow rule and effect of hardening):

$$\frac{1}{H} n_p^2 \, d\underline{p} + \frac{1}{H} n_p n_q \, dq = \frac{3}{2} \left(\frac{1}{H} n_q n_q \, dq + \frac{1}{H} n_q n_p \, d\underline{p} \right)$$

where: $\qquad n_p = \dfrac{\partial Q_{C1}}{\partial \underline{p}} (Q_{C1} = F_{C1} -$ elliptic cap surface$)$

$n_q = \dfrac{\partial Q_{C1}}{\partial q}$

$dq/dp = \eta^{K_o}$ (along K_o path)

$H = -\dfrac{\partial F_{C1}}{\partial \underline{p}_c} \dfrac{\partial \underline{p}_c}{\partial \underline{\varepsilon}_V^p} n_p$ (plastic modulus for constant shape ratio parameter R)

$\eta^{K_o} = \dfrac{3 (1 - K_o^{\mathsf{NC}})}{2 K_o^{\mathsf{NC}} + 1}$

Window 3-12

Window 3-13: Procedure of evaluation of $\underline{p}_{co}, R_o$ from oedometer test

Given material properties: $e_o, E, \nu, \lambda, \phi$, DP-size adjustment (a_k, a_ϕ)

$\qquad \sigma_{\mathsf{VM}}$ (vertical stress at the transition point from secondary to primary consolidation line), $K_o^{\mathsf{NC}}(K_o$ at state of normal consolidation$)$

Find: $\underline{p}_{co}, R_o$

- initialize:
$$i = 0: \ p_T = \frac{a_k}{3a_\phi}, \ M = 3\sqrt{3} a_\phi \ p_{co}^{(i=0)} = \frac{2 K_o^{\mathsf{NC}} + 1}{3} \ \underline{\sigma}_{\mathsf{VM}}$$
- next iteration: $\ i = i + 1$
- find R_o (see Window 3-14) (for $p_T = 0$)
- find modified shape ratio parameter R_{IN} for real value of p_T and $\underline{p}_{co}^{(i)}$ (see Window 3-15)
- find corrected $\underline{p}_{co}^{(i+1)}$ value (see Window 3-16)
- iterate until $| \underline{p}_{co}^{(i+1)} - \underline{p}_{co}^{(i)} | > 10^{-8}$

Window 3-13

Window 3-14: R_o **evaluation**

Given: M, $\underline{p}_{co}$, $\eta^{K_o} = q/\underline{p}$ (at K_o path) $= \dfrac{3\,(1 - K_o^{\mathsf{NC}})}{2\,K_o^{\mathsf{NC}} + 1}$

Find: R_o (using bisection method)

- Initialize $i = 0$:

    $R_o^{(i=0)} = 1.01;\ \Delta R = 10^{-3}$

- Step $i = i + 1$:

    $R_o^{(i)} = R_o^{(i-1)} + \Delta R$

    for given: M, $R_o^{(i)}$, $\underline{p}_{co}$, η^{K_o} compute mean stress $\underline{p}$ at the intersection point of elliptic cap surface F_{C1} and K_o line

    compute corresponding deviatoric stress: $q = \eta^{K_o}\underline{p}$ and n_p, n_q, $\dfrac{\partial F_{C1}}{\partial \underline{p}_c}$

    compute residuum of the governing equation for oedometer test: $f_{K_o} = n_p/n_q - \dfrac{3}{2}$;

- if $i > 1$ then

    if $f_{K_o}^{last} * f_{K_o} \leq 0$ then

        set: $R_o^{(i+1)} = (R_o^{(i)} - \Delta R_o/2)$ and EXIT

    else

        save: $f_{K_o}^{last} = f_{K_o}$ and go to next iteration

    end if

  end if

Window 3-14

Window 3-15: R_{IN} evaluation

Given:　　$\underline{p}_{co}$

Find:　　modified shape ratio parameter R_{IN} such that dilatancy parameter $d = n_p/n_q$ is the same along trial stress path $\eta^M = M/2$ (some arbitrary path) both for elliptic cap with $p_T = 0$ and cap surface with real p_T value.

- Initialize $i = 0$:

  Compute dilatancy parameter $d_o = n_p/n_q$ for given: $\underline{p}_{co}$, $p_T = 0$, η^M and shape ratio parameter R_o

  set: $\Delta R_{IN} = 0.01$

  set: $R^{last} = R_o$

- Step $i = i + 1$

  $R_{IN}^{(i)} = R_{IN}^{(i-1)} + \Delta R$

  for given $M, \underline{p}_{co}, p_T, \eta^M$ and shape ratio parameter $R = R_{IN}^{(i)}$ compute compute mean stress $\underline{p}$ at the intersection point of elliptic cap surface F_{C1} and stress path line $q/p = \eta^M$

  compute corresponding deviatoric stress: $q = \eta^{K_o}\underline{p}$ and n_p, n_q

  compute dilatancy parameter $d = n_p/n_q$

- if　$i > 1$　then

  if　$d_o > d^{last}$　AND　$d_o < d$　OR　$d_o > d$　AND　$d_o < d^{last}$　then

  set: $R_{IN}^{(i+1)} = R_{IN}^{(i)} + \dfrac{d^{last} - d_o}{d^{last} - d}\Delta R_{IN}$ and EXIT

  else

  set: $d^{last} = d$ and go to next iteration

  end if

  end if

Window 3-15

Window 3-16: Evaluation of corrected $\underline{p}_{co}^{(i+1)}$ value

---

Given: $M, R_{IN}, p_T, \nu, \underline{\sigma}_{\mathsf{VM}}$

Find: $p_{co}^{(i+1)}$

- Set: $K_o^{el} = \dfrac{\nu}{1 - \nu}$, $\eta_{el}^{K_o} = \dfrac{3(1 - K_o^{el})}{1 + 2K_o^{el}}$, $\underline{p} = \dfrac{(1 + 2K_o^{el})\underline{\sigma}_{\mathsf{VM}}}{3}$, $q = \eta_{el}^{K_o}\underline{p}$

- For $\underline{p}, q, p_T, M$ solve quadratic equation (elliptic cap equation) $F_{C1} = 0$ for unknown $p_{co}^{(i+1)}$ value

---

Window 3-16

3.3.5   MOHR-COULOMB (M-W)

●**Yield surface** The original M–C criterion (see Window 3-6) which leads to a non–smooth multisurface plasticity problem, is substituted by its smooth, single–surface approximation, being a particular case of a general 3–parameter criterion developed recently by Mentrey (see Menétrey, Willam: A triaxial failure criterion for concrete and its generalization. ACI Structural Journal 92(3) p.311–318). This criterion takes the form described in Window 3-17.

Window 3-17: Menetrey criterion

.

$$F(\xi, \rho, \theta) = (A_f \rho)^2 + m_f \left[B_f \; \rho \; r_f(\theta, e) + C_f \; \xi \right] - D_f = 0 \tag{1}$$

where ξ, ρ, θ are Haigh-Westergaard stress coordinates equal to:

$$\xi = \frac{1}{\sqrt{3}} I_1 \tag{2}$$

$$\cos 3\theta = \frac{3\sqrt{3}}{2} J_3 J_2^{-\frac{3}{2}} \tag{3}$$

$$\rho = \sqrt{2 J_2} \tag{4}$$

with I_1, J_2, J_3 being the usual stress invariants (1-5)

Function $r_f = r_f(\theta, e), \; 0.5 < e \le 1$, describes the shape of the surface in deviatoric section

$$r_f(\theta, e) = \frac{4 \left(1 - e^2\right) \cos^2 \theta + (2e - 1)^2}{2 \left(1 - e^2\right) \cos \theta + (2e - 1) \left[4 \left(1 - e^2\right) \cos^2 \theta + (2e - 1)^2 - \left(1 - e^2\right) \right]^{1/2}} \tag{5}$$

Window 3-17

The eccentricity parameter e can be calibrated to fit exactly the Mohr–Coulomb surface on both extension and compression meridians which leads to the smooth Mohr–Coulomb surface. All other parameters of the generalized criterion are also expressed in terms of the Mohr–Coulomb friction angle ϕ and cohesion c as shown in Window 3-18.

Window 3-18: Mohr–Coulomb yield criterion by Menetrey criterion

Given:

    ϕ – friction angle, $0° < \phi < 90°$

    c – cohesion $c \geq 0$

$$e = \frac{3 - \sin\phi}{3 + \sin\phi} \tag{1}$$

$$A_f = 0 \tag{2}$$

$$B_f = \frac{3 - \sin\phi}{\sqrt{24}\, c \cos\phi} \tag{3}$$

$$C_f = \frac{1}{\sqrt{3}\, c} \tan\phi \tag{4}$$

$$m_f = 1 \tag{5}$$

$$D_f = 1 \tag{6}$$

— smooth Mohr-Coulomb
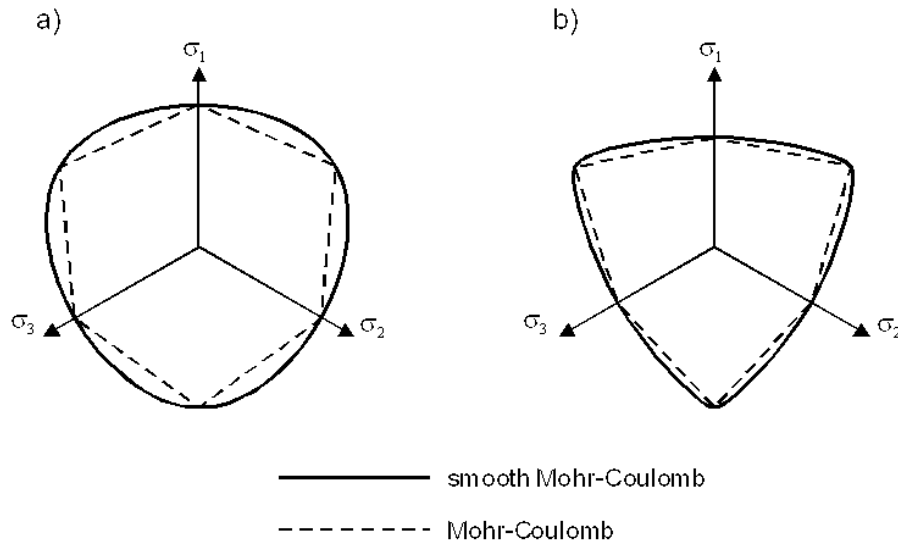
- - - - - - - Mohr-Coulomb

Deviatoric sections of the smooth Mohr-Coulomb yield surface: a) $\varphi = 10°$, $e=0.89$, b) $\varphi = 50°$, $e=0.59$

Window 3-18

• **Flow rule**

The flow rule which defines the direction of the plastic flow is given in a standard form:

$$\dot{\boldsymbol{\varepsilon}}^p = \dot{\lambda}\frac{\partial Q}{\partial \boldsymbol{\sigma}}$$

The flow potential adopted here takes a form similar to the yield surface, but with assumption that r is independent of Lode's angle

$$Q(\xi, \rho) = (A_q\rho)^2 + m_q\left(B_q\rho r_q + C_q\xi\right)$$

radius r_q is taken as the radius r_f for the extension meridian.

Other parameters of flow potential A_q, B_q, C_q, m_q are evaluated in a manner analogous to yield parameters A_f, B_f, C_f, m_f by formulae of Window 3-18, but using the dilatancy angle ψ instead of the friction angle ϕ.

The recommended form of the flow potential is identical with the Drucker–Prager flow potential. It leads to non associated plasticity even in case when $\phi = \psi$ due to the different forms of r_q and r_f. Alternative forms proposed here are tabulated below.

<div align="center">

Plastic flow parameters

</div>

Flow type	A_q	B_q	C_q	Ψ
Drucker–Prager $0 \le a_\psi \le a_\phi$	0	$\dfrac{1}{\sqrt{2}k_\psi}$	$\dfrac{\sqrt{3}a_\psi}{k_\psi}$	
k_ψ and a_ψ are computed from ψ, c using tensile meridian adjustment (putting ψ instead of into formula for k one gets k_ψ value)				
Axisymmetric Hoek–Brown (Hoek–Brown or concrete models only)	1	$\dfrac{2\left(\sqrt{2}\tan\Psi_c f_c - f_t\right)}{\sqrt{3}\left(\dfrac{1}{\sqrt{2}} - \tan\Psi_c\right)}$	$\dfrac{1}{\sqrt{2}}B_q + \dfrac{2}{\sqrt{3}}f_t$	$4° < \Psi_c < 35.3°$
Ψ_c- dilatancy angle for uniaxial compression $\left(\xi = -\dfrac{f_c}{\sqrt{3}}, \quad \rho = \sqrt{\dfrac{2}{3}}f_c, \quad \theta = \dfrac{\pi}{3}\right)$				

•**Matching the smooth Mohr–Coulomb criterion with Mohr–Coulomb criterion**

The proposed smooth Mohr–Coulomb criterion reduces to a von–Misès criterion through external vertices when the excentricity factor e tends towards 1, i.e when ϕ tends to zero. A size adjustment must therefore be activated i.o. to achieve the proper stability results. This consists in replacing the user defined cohesion c and friction angle ϕ by adjusted values which can be derived following the same reasoning as for the Drucker–Prager criterion; this is done in **Window 3.3.3-3**.

Window 3-19: Matching of collapse load (plane–strain conditions)

$$\dot{\varepsilon}^p_{ij} = \mathsf{d}\lambda \; r_{ij} = \mathsf{d}\lambda \left(a_\psi \delta_{ij} + \frac{1}{2\sqrt{J_2}} s_{ij} \right) \tag{1}$$

(plane strain, $\varepsilon^{\mathsf{e}} <<$)

$$\dot{\varepsilon}^p_{33} = \dot{\varepsilon}^p_{13} = \dot{\varepsilon}^p_{23} = 0 \tag{2}$$

from (1)

$$s_{33} = -2a_\psi \sqrt{J_2}; \qquad s_{13} = s_{23} = 0 \tag{3}$$

$$I_1 = \frac{3}{2}(\sigma_{11} + \sigma_{22}) - 3a_\psi \sqrt{J_2} = \sqrt{3}\xi \tag{4}$$

$$J_2 = \frac{\left\{\left[(\sigma_{11} - \sigma_{22})/2\right]^2 + \sigma_{12}^2\right\}}{(1 - 3a_\psi^2)} \tag{5}$$

$$J_2 = \frac{R^2}{(1 - 3a_\psi^2)} = \frac{\rho^2}{2} \tag{6}$$

replacing in Eq. (1) one gets, after some transformations

$$R = \frac{\sqrt{6}}{A} c_f \cos \phi_f - \frac{\sqrt{6}}{2A} \sin \phi_f (\sigma_{11} + \sigma_{22}); \tag{7}$$

index f is added on c and $\sin \phi$, $\cos \phi$ to avoid confusion in Eq. (10) below:

$$A = \frac{\sqrt{2}\left(3 - \sin \phi_f\right) r(e, \theta) - 2\sqrt{6}a_\psi \sin \phi_f}{2\sqrt{1 - 3a_\psi^2}}. \tag{8}$$

Identifying with the Mohr–Coulomb criterion of Window 3-17

$$c \cos \phi = \frac{\sqrt{6}}{A} c_f \cos \phi_f \tag{9}$$

$$\sin \phi = \frac{\sqrt{6}}{A} \sin \phi_f \tag{10}$$

and alternatively

$$\frac{c}{c_f} = \frac{\tan \phi}{\tan \phi_f}. \tag{11}$$

Special cases:

− arbitrary flow

$$\sin \phi_f = \frac{r(e, \theta)(3 - \sin \phi_f) - 2\sqrt{3}a_\psi \sin \phi_f}{2\sqrt{3}\sqrt{1 - 3a_\psi^2}} \sin \phi \tag{12}$$

θ results from

$$\cos 3\theta = \frac{3\sqrt{3}}{2} a_\psi \frac{J_3}{J_2^{3/2}} \tag{13}$$

which for plane strain failure and $\dot{\varepsilon}^e$ neglected yields:

− deviatoric flow yields

$$a_\psi = 0 \qquad \text{yields} \qquad \theta = 30° \tag{14}$$

$$\sin \phi_f = \frac{r(e, \theta)(3 - \sin \phi_f)}{2\sqrt{3}} \sin \phi \tag{15}$$

if in addition $\phi = 0$, then $c_f = 0.866c$

| Window 3-19 |

3.3.6   HOEK–BROWN CRITERION (SMOOTH)

The empirical strength criterion proposed by Hoek and Brown for rock masses is:

$$f(\sigma_1, \sigma_2) = \left(\frac{\sigma_1 - \sigma_3}{f_c}\right)^2 + \phi_{hb}\frac{\sigma_1}{f_c} - c_{hb} = 0$$

where σ_1, σ_3 the material parameters c_{hb} and ϕ_{hb} are measures of cohesive and frictional strength, and f_c designates for uniaxial compressive strength. This yield surface is generated with the general yield surface presented in Window 3-20 by identification of the adjustment parameters as presented next.

Window 3-20: Smooth Hoek-Brown criterion

Given f_c, f_t and e , the uniaxial compressive, tensile strength, and the surface eccentricity. $0.5 < e \leq 1$ and the following eccentricity value is recommended $0.5 < e \leq 0.6$.

$$A_f = \frac{\sqrt{1.5}}{f_c}, \qquad B_f = \frac{1}{\sqrt{6}\,f_c}, \qquad C_f = \frac{1}{\sqrt{3}\,f_c}, \qquad m_f = \frac{3\,(f_c^2 - f_t^2)}{f_c f_t}\frac{e}{1+e}, \qquad c = 1$$

It has to be emphasized that for given f_c, f_t, f_b (f_b-biaxial compressive strength) one may compute the eccentricity ratio using the following formula:

$$e = \frac{f_b\,(f_c^2 - f_t^2) + f_t\,(f_b^2 - f_c^2)}{2\,f_b\,(f_c^2 - f_t^2) - f_t\,(f_b^2 - f_c^2)}$$
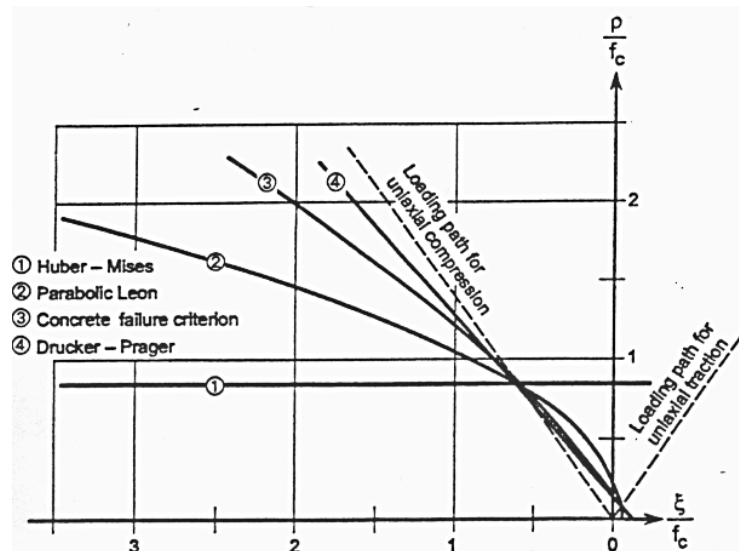
Calibration of the generalized criterion to: 1) Huber–Mises, 2) parabolic Leon, 3) smooth Hoek–Brown

---

Window 3-20

Remark:: The same flow rules as for the Mohr-Coulomb criterion applies.

3.3.7   CUT-OFF CONDITION AND TREATMENT OF THE APEX

As an additional feature of most criteria a tensile Cut–off condition of the following form may be attached if required

$$I_{1_{\max}}^{+} \leq I_{1_t}$$

The presence of the Cut–off condition places the problem into the class of multi–surface plasticity problems as the cut–off may be formally treated as additional stress constraint.
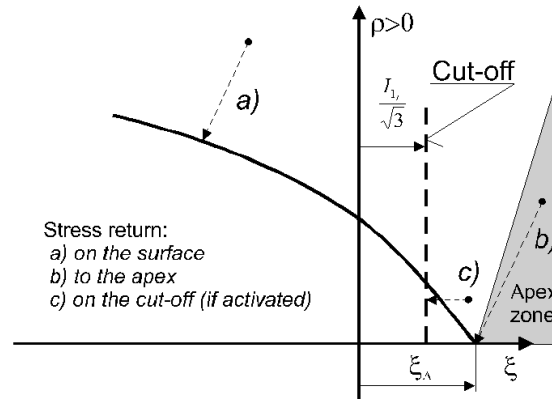
Treatment of the apex

The flow potential accompanying the Cut–off surface has an associative form:

$$Q(\sigma) = I_1.$$

If the Cut–off is disregarded the surface possesses an apex located at the stress point

$$\sigma^A = \left[\begin{array}{ccccccc} \dfrac{\sqrt{3}}{3}\xi^A, & \dfrac{\sqrt{3}}{3}\xi^A, & 0, & \dfrac{\sqrt{3}}{3}\xi^A \,|, & 0, & 0 \\ & & & \quad\quad |, & 3D \end{array} \right]$$

with

$$\xi^A = \frac{D_f}{m_f C_f}$$

If the trial stress state is located inside of the apex cone which means it fulfills condition:

$$\rho^{tr} < (\xi^{tr} - \xi^A)\frac{GB_f r_q}{KC_q}$$

it would return to the apex.

In the case of an active Cut–off condition, limiting value I_{1_t} should be compatible with the position of the surface apex, i.e.

$$\xi_t < (1-\varepsilon)\,\xi^A \qquad \text{with} \qquad \xi_t = \frac{I_{1_t}}{\sqrt{3}} \qquad \text{and} \qquad \varepsilon = 10^{-2}$$

If the above condition is not met, then the maximum possible cut–off position is set automatically as:

$$I_{1_t} = \sqrt{3}\,(1-\varepsilon)\,\xi^A.$$

3.3.8   MULTILAMINATE MODEL

In this model the existence of up to $ML_{\max} = 3$ weakness planes characterizing anisotropy of the material behaviour is assumed. On each plane separately, Mohr–Coulomb plasticity condition and a tension cut–off condition must be fullfilled.

| Window 3-21: Weakness plane plasticity conditions |
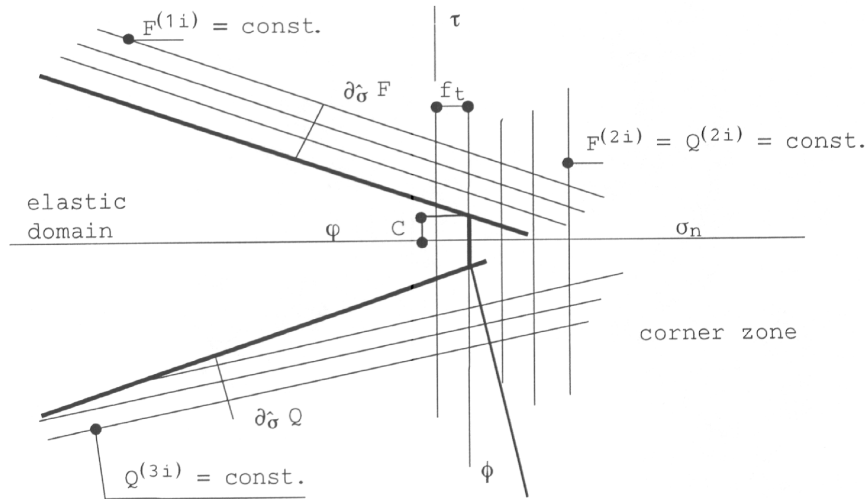
Yield function and flow potential isolines

$$F^{(1i)} = \tau + \sigma_n \tan \phi^i - c^i \qquad \partial_{\widehat{\sigma}} F^{(1i)} = \left\{ \tan \phi^i, 1 \right\}^{\mathrm{T}} \qquad (1)$$

$$Q^{(1i)} = \tau + \sigma_n \tan \psi^i \qquad \partial_{\widehat{\sigma}} Q^{(1i)} = \left\{ \tan \psi^i, 1 \right\}^{\mathrm{T}} \qquad (2)$$

$$F^{(2i)} = -\tau + \sigma_n \tan \phi^i - c^i \qquad \partial_{\widehat{\sigma}} F^{(2i)} = \left\{ \tan \phi^i, -1 \right\}^{\mathrm{T}} \qquad (3)$$

$$Q^{(2i)} = -\tau + \sigma_n \tan \psi^i \qquad \partial_{\widehat{\sigma}} Q^{(2i)} = \left\{ \tan \psi^i, -1 \right\}^{\mathrm{T}} \qquad (4)$$

$$F^{(3i)} = \sigma_n - f_t \qquad \partial_{\widehat{\sigma}} F^{(3i)} = \{1, 0\}^{\mathrm{T}} \qquad (5)$$

$$Q^{(3i)} = \sigma_n \qquad \partial_{\widehat{\sigma}} Q^{(3i)} = \{1, 0\}^{\mathrm{T}} \qquad (6)$$

Note:

$$\partial_{\widehat{\sigma}\widehat{\sigma}}^2 = 0.$$

| Window 3-21 |

This leads to a multisurface plasticity problem which require that a set of up to 3*ML$_{\max}$ plasticity conditions must be simultaneously fullfiled by any stress state in the multilaminate material, i.e

$$F^{\alpha}\left(\widehat{\sigma}^{(i)} \right) \leq 0; \quad \alpha \in J; \quad J : \{1, \ldots, 3ML\}$$

$T^{(i)}, T$ are linear transformation matrices describing transition between $(\sigma_{xx}, \sigma_{yy}, \tau_{xy}, \sigma_{zz})$,

global coordinate system stress components and the i-th weakness plane components $\{\sigma_n, \tau\}^{\mathrm{T}}$
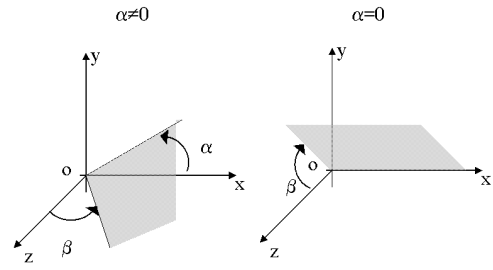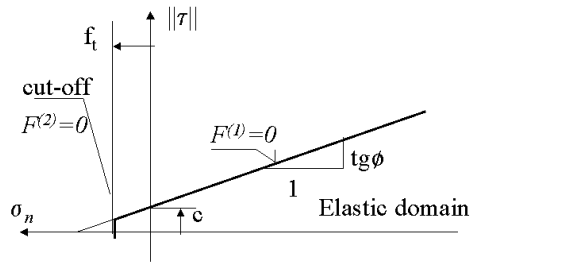
$$\widehat{\sigma}^{(i)} = \left\{ \begin{array}{c} \sigma_n \\ \tau \end{array} \right\}^{(i)} = T^{(i)} \left\{ \begin{array}{c} \sigma_x \\ \sigma_y \\ \tau_{xy} \end{array} \right\}, \qquad T^{(i)} = \left[\begin{array}{ccc} s^2 & c^2 & -2sc \\ -sc & sc & c^2 - s^2 \end{array} \right]$$

where :

$$\begin{aligned} s &= \sin \alpha^{(i)} \\ c &= \cos \alpha^{(i)}. \end{aligned}$$

Window 3-22: Multilaminate model (3D, Generalized Plane Strain analysis type case)

For $i = 1, ML$ $(ML < 3)$

Weakness plane setting:	i–th weakness plane plasticity conditions:
Weakness plane unit normal $\mathbf{n}$: if $\alpha \neq 0$: $$\mathbf{n} = \left[\frac{\sin \alpha \cos \alpha}{a}, \ -\frac{\cos \alpha \cos \beta}{a}, \ -\frac{\sin \alpha \sin \beta}{a} \right]^{\mathrm{T}}$$ where: $$a = \sqrt{\cos^2 \beta + \sin^2 \alpha \sin^2 \beta};$$ if $\alpha = 0$: $$\mathbf{n} = [0, \ \cos \beta, \ \sin \beta]^{\mathrm{T}}.$$	Yield function expressed in terms of σ_n, τ : $$F^{(1i)}(\sigma_n, \tau) = \|\boldsymbol{\tau}\| + \tan \phi \sigma_n - c$$ $$F^{(1i)}(\sigma_n, \tau) = \sigma_n - f_t.$$ Flow potential expressed in terns of σ_n, τ : $$Q^{(1i)}(\sigma_n, \tau) = \|\boldsymbol{\tau}\| + \tan \psi \sigma_n - c$$ $$Q^{(1i)}(\sigma_n, \tau) = \sigma_n - f_t.$$

Expressions of $F^{(ki)}, q^{(ki)}$ by full stress vector $\boldsymbol{\sigma} = \left[\ \sigma_{xx}, \ \ \sigma_{yy}, \ \ \sigma_{xy}, \ \ \sigma_{zz}, \ \ \sigma_{xz}, \ \ \sigma_{yz} \ \right]^{\mathrm{T}}$
normal stress:

$$\sigma_n = \mathbf{n}^{\mathrm{T}} \left(\underline{\underline{\sigma}} \mathbf{n} \right) = \mathbf{v}^{\mathrm{T}} \boldsymbol{\sigma}, \quad \text{where } \mathbf{v} = \left[\ n_x^2, \ \ n_y^2, \ \ 2n_x n_y, \ \ n_z^2, \ \ 2n_x n_z, \ \ 2n_y n_z \ \right]^{\mathrm{T}},$$

tangent stress vector:

$$\boldsymbol{\tau} = \left[\ \tau_x, \ \ \tau_y, \ \ \tau_z \ \right]^{\mathrm{T}} = \underline{\underline{\sigma}} \mathbf{n} - \sigma_n \mathbf{n} = \mathbf{A} \boldsymbol{\sigma}$$

where

$$\mathbf{A} = \left[\begin{array}{cccccc} n_z(1 - n_x^2) & -n_x n_y^2 & n_y(1 - 2n_x^2) & -n_x n_z^2 & n_z(1 - 2n_x^2) & -2n_x n_y n_z \\ -n_y n_x^2 & n_y(1 - n_y^2) & n_z(1 - 2n_y^2) & -n_y n_z^2 & -2n_x n_y^2 & n_z(1 - 2n_y^2) \\ -n_z n_x^2 & -n_z n_y^2 & -2n_x n_y n_z & n_z(1 - n_z^2) & n_x(1 - 2n_y n_z) & n_y(1 - 2n_z^2) \end{array} \right]$$

thus:

$$
\begin{aligned}
F^{(1i)}\left(\boldsymbol{\sigma}\right) &= \sqrt{\boldsymbol{\sigma}^{\mathrm{T}}\left(\mathbf{A}^{\mathrm{T}}\mathbf{A}\right)\boldsymbol{\sigma}} + \tan\phi\,\mathbf{v}^{\mathrm{T}}\boldsymbol{\sigma} - c \\
F^{(2i)}\left(\boldsymbol{\sigma}\right) &= \mathbf{v}^{\mathrm{T}}\boldsymbol{\sigma} - f_t \\
Q^{(1i)}\left(\boldsymbol{\sigma}\right) &= \sqrt{\boldsymbol{\sigma}^{\mathrm{T}}\left(\mathbf{A}^{\mathrm{T}}\mathbf{A}\right)\boldsymbol{\sigma}} + \tan\psi\,\mathbf{v}^{\mathrm{T}}\boldsymbol{\sigma} - c \\
Q^{(2i)}\left(\boldsymbol{\sigma}\right) &= \mathbf{v}^{\mathrm{T}}\boldsymbol{\sigma} - f_t.
\end{aligned}
$$

Gradients required by multi–surface plasticity closest point projection algorithm:

$$
\begin{aligned}
\partial_\sigma F^{(1i)} &= \frac{1}{\|\boldsymbol{\tau}\|}\left(\mathbf{A}^{\mathrm{T}}\mathbf{A}\right)\boldsymbol{\sigma} + \tan\phi\,\mathbf{v} \\
\partial_\sigma F^{(2i)} &= \mathbf{v} \\
\partial_\sigma Q^{(1i)} &= \frac{1}{\|\boldsymbol{\tau}\|}\left(\mathbf{A}^{\mathrm{T}}\mathbf{A}\right)\boldsymbol{\sigma} + \tan\psi\,\mathbf{v} \\
\partial_\sigma Q^{(2i)} &= \mathbf{v} \\
\partial_{\sigma\sigma} Q^{(2i)} &= \frac{1}{\|\boldsymbol{\tau}\|}\left[\mathbf{A}^{\mathrm{T}}\mathbf{A} - \left(\mathbf{A}^{\mathrm{T}}\frac{\boldsymbol{\tau}}{\|\boldsymbol{\tau}\|}\right)\left(\mathbf{A}^{\mathrm{T}}\frac{\boldsymbol{\tau}}{\|\boldsymbol{\tau}\|}\right)^{\mathrm{T}}\right].
\end{aligned}
$$

Window 3-22

This leads to a multi–surface plasticity problem which require that a set of up to $3\times ML\_Max$ plasticity conditions must be simultaneously fulfilled by any stress state in the multilaminate material, i.e.:

$$
F^{(\alpha)}\left(\boldsymbol{\sigma}\right) \leq 0; \quad \alpha \in J; \ J:\left\{\ 1, \ \ldots, \ 3ML\ \right\}.
$$

Plastic strains emerge due to violation of any of those conditions by the trial elastic stress. The total plastic strain is the sum of each plane's contribution.

$$
\begin{aligned}
\dot{\varepsilon}^{p\alpha} &= \dot{\gamma}^{\alpha}\partial_{\hat{\sigma}}Q^{\alpha} \\
\dot{\varepsilon}^{p} &= \sum_{\alpha}\dot{\varepsilon}^{p\alpha}
\end{aligned}
$$

NB : A perfectly elasto–plastic behaviour (no hardening) is assumed.

The flow rule is governed by a flow potential Q, the form of which is analogous to the form of corresponding yield function F. As the dilatancy angle ψ^i specified for each weakness plane may in general differ from the corresponding friction angle, the flow rule adopted is nonassociative $(Q^{\alpha} \neq F^{\alpha})$.

The model requires the data of ML, the number of assumed weakness planes $(ML \leq 3)$.

For each i-th plane , $(i = 1, .., 3ML)$ the following data should be specified:

$\alpha^{(i)}$ — inclination angle of i–th weakness plane (± 90 degrees, positive counterclockwise)

$\phi^{(i)}$ — friction angle

$\psi^{(i)}$ — dilatancy angle

$c^{(i)}$ — cohesion.

The following constitutive model is derived.

Window 3-23: Physical origin of flow potential Q

During plastic slip ($\tau = \tan\phi\,\sigma_n + c$):
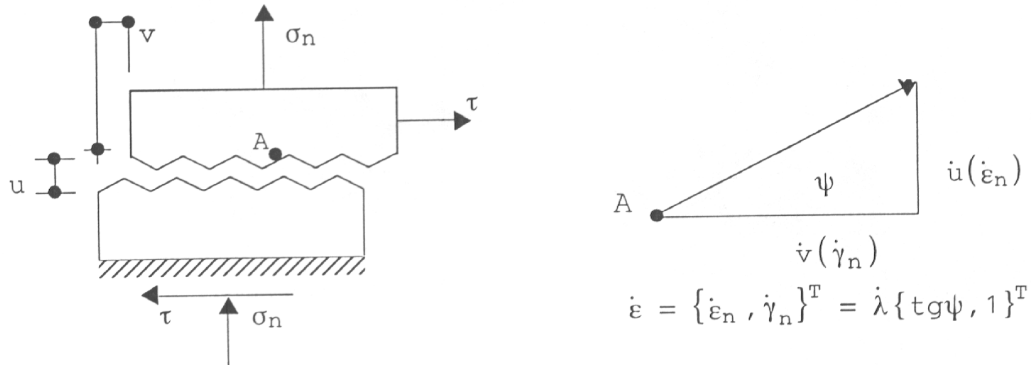
Frictional slide model to explain physical origin of flow potential

ψ — dilatancy angle, $\psi \neq \phi$

if $\psi = \phi$ — associativity is preserved.

Window 3-23

Window 3-24: Constitutive equations of multilaminate model

$$\boldsymbol{\sigma} = \mathbf{D} : (\boldsymbol{\varepsilon} - \boldsymbol{\varepsilon}^p) \tag{1}$$

$$\dot{\boldsymbol{\varepsilon}}^p = \sum_{\alpha} \dot{\gamma}^{\alpha} \partial_{\hat{\sigma}} Q^{\alpha} \tag{2}$$

with yield and loading/unloading conditions for $\alpha \in \{1, 2, ...3ML\}$

$$\dot{\gamma}^{\alpha} \geq 0 \tag{3}$$

$$F^{\alpha}(\boldsymbol{\sigma}) \leq 0 \tag{4}$$

$$\dot{\gamma}^{\alpha} F^{\alpha}(\boldsymbol{\sigma}) = 0 \tag{5}$$

$$\dot{\gamma}^{\alpha} \dot{F}^{\alpha}(\boldsymbol{\sigma}) = 0. \tag{6}$$

In expanded form

if $F^{\alpha}(\boldsymbol{\sigma}) \leq 0$ or $F^{\alpha}(\boldsymbol{\sigma}) = 0$ and $\dot{F}^{\alpha}(\boldsymbol{\sigma}) < 0 \Rightarrow \dot{\gamma}^{\alpha} = 0$

if $F^{\alpha}(\boldsymbol{\sigma}) = 0$ and $\dot{F}^{\alpha}(\boldsymbol{\sigma}) = 0 \Rightarrow \dot{\gamma}^{\alpha} = 0$

($\alpha - - -$ constraint is active).

Window 3-24

3.3.9 MODIFIED CAM CLAY MODEL

Window 3-25: Yield and flow potential surface

The elliptical yield surface (and flow potential as well) is described by the equation (see Fig. below)

$$F(\boldsymbol{\sigma}, p_c) = q^2 + M_c^2\, r^2(\theta)\, p\, (p - p_c) = 0$$

Modified-Cam Clay yield surface
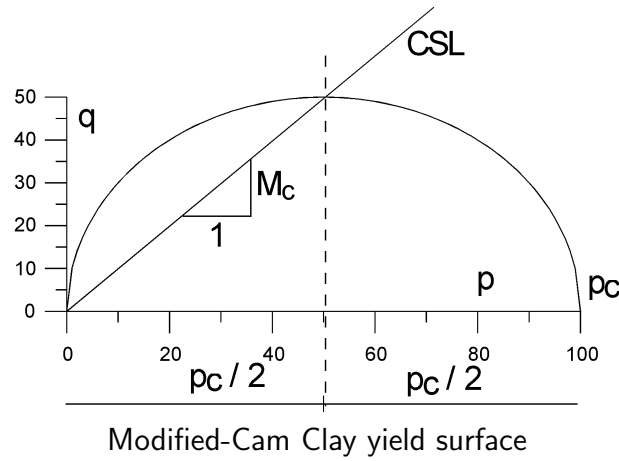
The M_c parameter is the slope of the critical state line along compression meridian, p_c is a preconsolidation pressure adjusted along p axis and $r(\theta)$ is a function of Lode parameter θ describing shape of the yield surface in the deviatoric plane. The $r(\theta)$ function is taken after van Ekelen.

$$r(\theta) = \left(\frac{1 - \alpha\,\sin(3\theta)}{1 - \alpha}\right)^n \qquad sin(3\theta) = -\frac{3\sqrt{3}}{2}\frac{J_3}{J_2^{\frac{3}{2}}} \qquad n = -0.229 \qquad \alpha \le 0.7925$$

The relation between $k = M_E/M_C$ (M_E is the slope of critical state line for the tension meridian) and parameter α is as follows

$$\alpha = \frac{k^{\frac{1}{n}} - 1}{k^{\frac{1}{n}} + 1}$$

and the default setting for the parameter k can be set as

$$k = \frac{3}{3 + M_c}$$

Remark:

The applied $r(\theta)$ function is applicable for friction angles up to 46.55^o.

Window 3-25

Window 3-26: Nonlinear elastic behavior within yield surface

The reversible part of the deformation is governed via nonlinear elasticity assuming that $K = K(p)$, $G/K =$const. and the well-known formula for bulk modulus is applied

$$K = \frac{1 + e_o}{\kappa} \, p$$

where e_o is an initial void ratio, κ is the slope of secondary compression line in $e - ln(p)$ axes.

Remarks

- Shear modulus G is a linear function of p

- Poisson's coefficient ν is a constant

- Mean stress may reach a zero value for infinitely large tensile volumetric strains

- Any calculation carried out with Cam Clay model requires explicit setting of the initial stresses

Window 3-26

Window 3-27: Hardening/softening law

The evolution of the hardening parameter is defined through the following equation

$$\mathrm{d}p_c = \frac{1 + e_o}{\lambda - \kappa} \, p_c \; (-\mathrm{d}\varepsilon_{kk}^p)$$

where λ is a slope of a primary compression line in $e - \ln(p)$ system (see Fig. given below).

Isotropic compression test
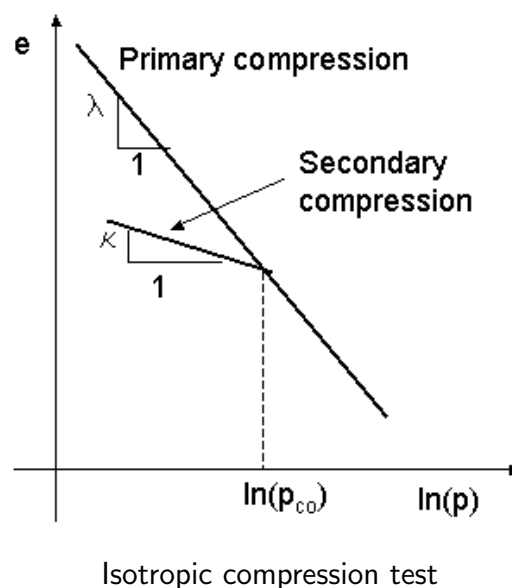
Window 3-27

Window 3-28: Modeling normally consolidated soils with modified C-C model

The Modified Cam-Clay model can describe basic macroscopic phenomena observed for normally consolidated cohesive soils. The model behavior is well represented if we consider a standard triaxial compression test. In that case ($OCR = 1$), as shown in Fig. below, the yield surface follows the current stress state.
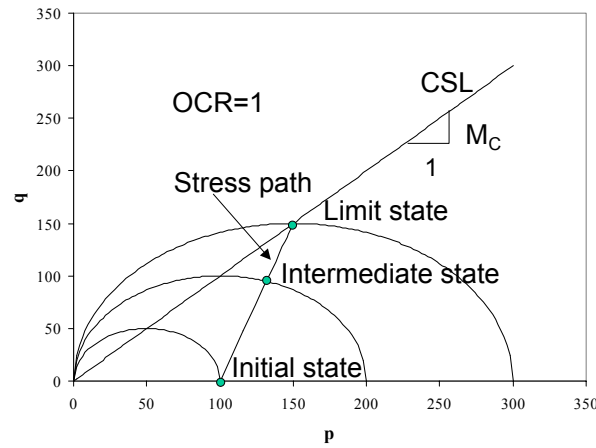
Drained triaxial compression test ($OCR = 1$)

During the application of an axial strain to the specimen the compressive volumetric strain is produced while deviatoric stress grows monotonically up to the value $q = M_c p$ (see Fig. below).
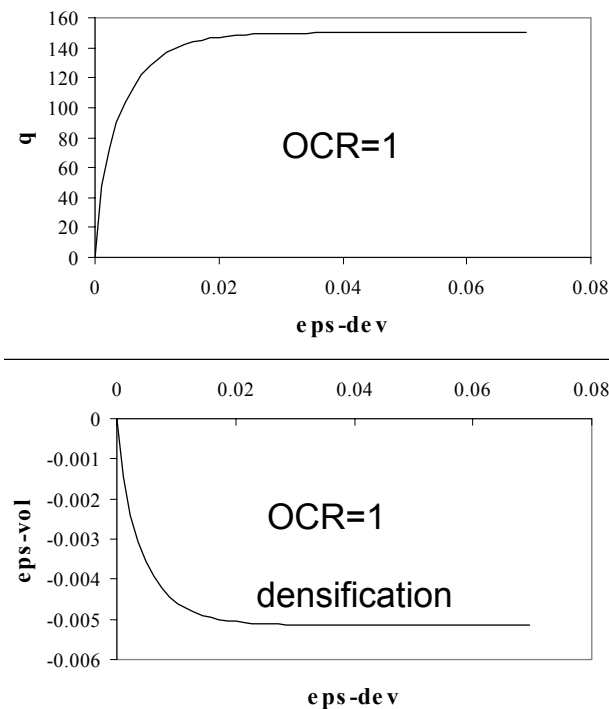
Stress/strain characteristics ($OCR = 1$)

Window 3-28

Window 3-29: Modeling overconsolidated soils with modified Cam-Clay model

The Modified Cam-Clay model describes also some macroscopic phenomena observed for overconsolidated cohesive soils. A typical model behavior, analyzed for a drained triaxial compression test (for $OCR = 5$) is shown in figures given below. In that case the effective stress path passes the critical state line until the current yield surface is met and then goes down until critical state is achieved. This effect corresponds to strain softening.
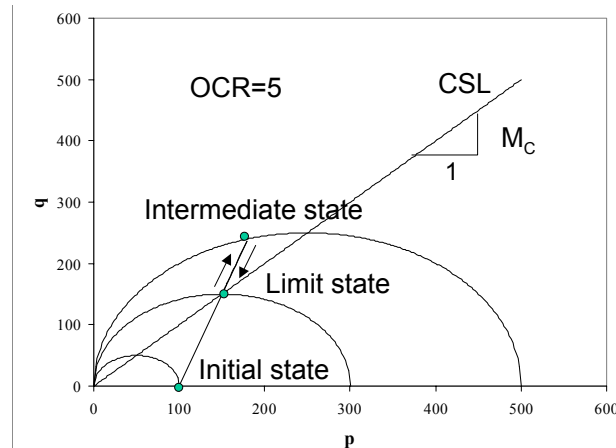
Drained triaxial compression test ($OCR = 5$)

During the application of the axial strain to the specimen the compressive elastic volumetric strain is produced first. Once the yield surface is met a dilatant volumetric strain is growing up tending to an asymptote at the critical state. The deviatoric stress does not grow monotonically exhibiting peak and residual values.
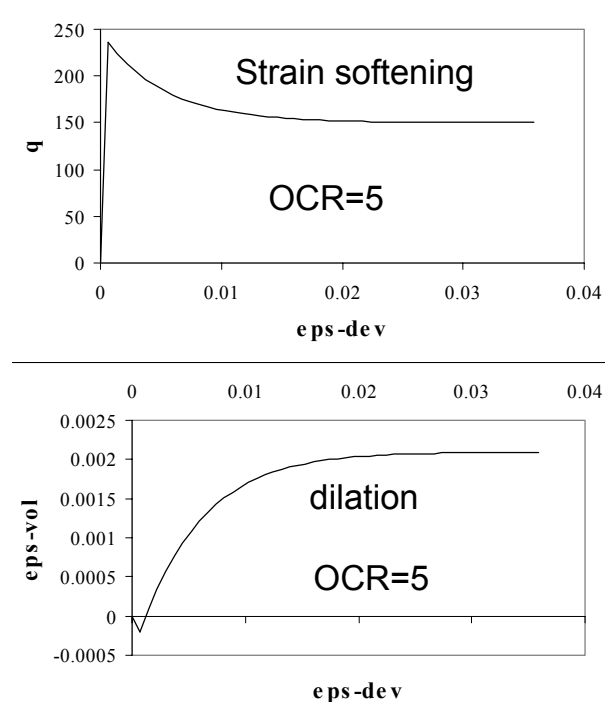
Stress/strain characteristics ($OCR = 5$)

Window 3-29

3.3.10   HS-small MODEL

The detailed description of the model is given in the dedicated report.

3.3.11 Hoek-Brown (true) MODEL

The detailed description of the model is given in the dedicated report.

3.3.12　Plastic damage MODEL for concrete

A detailed description of the model is given in the dedicated report.

3.4   CREEP

Creep is a time–dependent deformation under maintained stress. It is assumed that the stress can be split into volumetric and deviatoric components and the corresponding time–dependent strain components are the volumetric and the deviatoric creep. The following formulation is adopted for one–dimensional creep :

$$\varepsilon^{cr} = \varepsilon_{\text{inst}}^{e} f(t) = \sigma C(t)$$

Creep is considered to be proportional to the instantaneous <u>elastic</u> deformation. $C(t)$ is the creep law corresponding to a unit stress.

The three-dimensional creep law is then:

$$\boldsymbol{\varepsilon}^{cr} = E\mathbf{D}^{-1}\boldsymbol{\sigma}C(t) = \mathbf{D}_{o}^{-1}\boldsymbol{\sigma}C(t)$$

and $C(t)$ is assumed to be e.g. of the form

$$C(t) = A(t - t_0)^m$$

where A and m are material parameters.

In most situations the same creep law will be adopted for both the volumetric and the deviatoric components. Different parameters can however be chosen for the volumetric and deviatoric creep components. Great care has to be taken in that case because this may generate a Poisson coefficient which varies in time.

CREEP UNDER VARIABLE STRESS

CREEP PARAMETER IDENTIFICATION FROM EXPERIMENT

3.4.1   CREEP UNDER VARIABLE STRESS

Creep under variable stress requires a principle of superposition. The adopted power law does not lend itself easily to such in principle. It is therefore replaced, in the implementation, by a series of Kelvin elements. This is described next in **Windows** 3-31 and 3-30.

The automatic adjustment of the Kelvin element parameters to the prescribed power law is derived in **Window** .3-32

Window 3-30: Kelvin element under constant unit stress

Constitutive equation

$$q = G\varepsilon + \eta\dot{\varepsilon}$$

Creep strain increment, due to

$$q = H(t - t_0)$$

where: H — Heaviside unit step function

$$\varepsilon^{cr} = \frac{1}{G}\left\{1 - \exp\left[-\frac{G}{\eta}(t - t_0)\right]\right\} = A\left\{1 - \exp\left[-\frac{1}{B}(t - t_0)\right]\right\} =$$

$$= \sigma C(t - t_0) \quad \text{with} \quad \sigma = 1$$

N.B.:

$$\varepsilon^{cr} = 0 \quad \text{at} \quad t = t_0$$

$$\varepsilon^{cr} = \frac{q}{G} \quad \text{at} \quad t = \infty$$
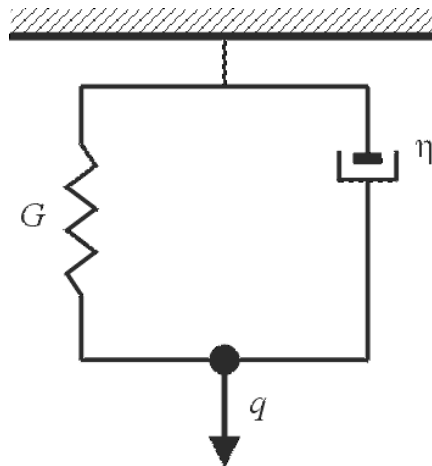
Kelvin mechanical model

	Window 3-30

Window 3-31: Creep under variable stress

Let the creep strain under variable stress be

$$\varepsilon^{cr}(t) = D_0^{-1} \left\{ -\int_{\tau_0}^{t} [\sigma(t) - \sigma(\tau_0)] \frac{\partial C(t-\tau)}{\partial \tau} d\tau \right\}$$

with $D_0 = E^{-1}D$.

For unit stress and a single Kelvin element

$$C(t,\tau) = A \left\{ 1 - \exp\left[-\frac{1}{B}(t-\tau) \right] \right\}$$
$$\frac{\partial C}{\partial \tau} = -\frac{A}{B} \exp\left(-\frac{t-\tau}{B} \right)$$

For a chain of N Kelvin elements in series, and introducing the volumetric-deviatoric split

$$C_v(t,\tau) = \sum_{i=1}^{N} A_i^v \left\{ 1 - \exp\left[-\frac{1}{B_i^v}(t-\tau) \right] \right\}$$

$$C_d(t,\tau) = \sum_{i=1}^{N} A_i^d \left\{ 1 - \exp\left[-\frac{1}{B_i^d}(t-\tau) \right] \right\}$$

$$\varepsilon_m^{cr}(t) = \left(D_{0_v}^v \right)^{-1} \left\{ -\int_{\tau_0}^{t} [\sigma_m(t) - \sigma_m(\tau_0)] \frac{\partial C_v}{\partial \tau} d\tau \right\}$$

$$\mathbf{e}^{cr}(t) = \left(\mathbf{D}_0^d \right)^{-1} \left\{ -\int_{\tau_0}^{t} [\mathbf{s}(t) - \mathbf{s}(\tau_0)] \frac{\partial C_d}{\partial \tau} d\tau \right\}$$

The creep strain increment, required by the general nonlinear incremental scheme, as described in section FULL/MODIFIED NEWTON-RAPHSON ALGORITHM (Section 4.6.1) can be derived by recurrence

$$\Delta \varepsilon^{cr} = \varepsilon_{n+1}^{cr} - \varepsilon_n^{cr} = \mathbf{D}_0^{-1} \sum_{i=1}^{N} \Delta \widetilde{\varepsilon}_i^{cr}$$

and

$$(\Delta\varepsilon_i)_{n+1}^{cr} = [\sigma_n + \theta\Delta\sigma_{n+1} - \sigma(\tau_0)] A_i \left[1 - \exp\left(-\frac{\Delta t_{n+1}}{B_i} \right) \right] + \left[\exp\left(-\frac{\Delta t_{n+1}}{B_i} \right) - 1 \right] (\widetilde{\varepsilon}_i)_n^{cr}$$

$$(\widetilde{\varepsilon}_i)_{n+1}^{cr} = (\widetilde{\varepsilon}_i)_n^{cr} + \Delta\varepsilon_i^{cr}$$

In the case of nonlinear creep the above recurrence formula is modifed by an additional term scaling the amplitude of the creep strain A_i in the following manner

$$(\Delta\varepsilon_i)_{n+1}^{cr} = [\sigma_n + \theta\Delta\sigma_{n+1} - \sigma(\tau_0)] (C_{1\,n} + \theta\Delta C_{1\,n+1}) \times$$
$$A_i \left[1 - \exp\left(-\frac{\Delta t_{n+1}}{B_i} \right) \right] + \left[\exp\left(-\frac{\Delta t_{n+1}}{B_i} \right) - 1 \right] (\widetilde{\varepsilon}_i)_n^{cr}$$

The nonlinear term $C_1(\boldsymbol{\sigma})$ is expressed by the equation

$$C_1(\boldsymbol{\sigma}) = 1 + a\,SL^b$$

where a $(0 \leq a \leq 10)$ and b $(1 \leq b \leq 10)$ are material parameters and SL is a stress level expressing the relative distance of the stress state from the yield surface.

The recurrence formula apply for volumetric and deviatoric creep components when σ, ε, D_0, A_i, B_i are specialized appropriately.

$$\left(D_0^v\right)^{-1} = \frac{E}{3K} = 1 - 2\nu$$

and $\left(\mathbf{D}_0^d\right)^{-1}$ is a (4×4) matrix with the following diagonal

$$\operatorname{diag}\left(\mathbf{D}_0^d\right)^{-1} = \left[\ (1+\nu),\ \ (1+\nu),\ \ 2\,(1+\nu),\ \ (1+\nu)\ \right]$$

which is valid for axisymmetry and for plane strain.

Window 3-31

Window 3-32: Approximation of the creep law
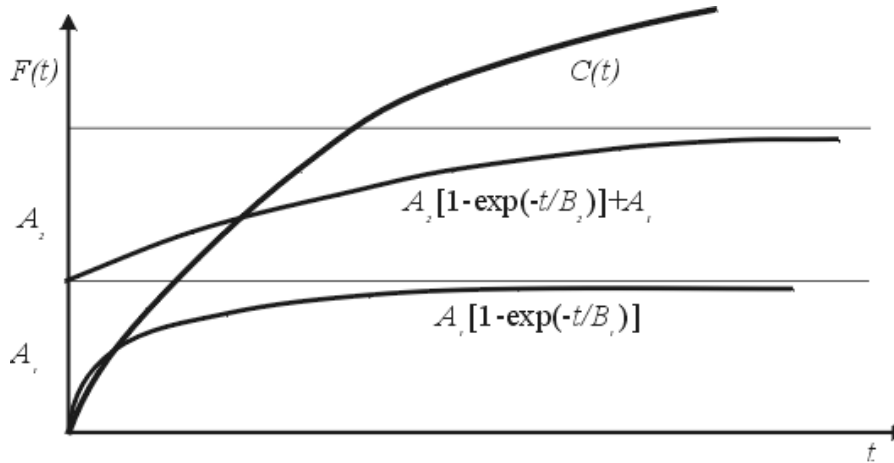
Creep function identification

Parameter identification procedure

•**Initial approximation**

1. Select

$$\left[\ B_1,\ \ B_2,\ \ \ldots,\ \ B_j\ \right] = \left[\ 10^{-4},\ \ 10^{-3},\ \ \ldots\ \right]$$

   N.B.: Six components $[10^{-4}, \ldots, 10]$ seem to be appropriate, less may be sufficient

2. Define $\left[\ t_1,\ \ t_2,\ \ \ldots\ \ t_j\ \right]$ such that

$$\alpha A_j = A_j\left[1 - \exp\left(\frac{t_j}{B_j}\right)\right]$$

   Select $\alpha : 0.5$ e.g., then

$$t_j = -B_j \ln(0.5)$$

3. Define such that for $j = 1$ to J

$$C(t_j) = \sum_{k=1}^{j-1} A_k + A_j \left[1 - \exp\left(-\frac{t_j}{B_j} \right) \right]$$

hence

$$A_j = \left[1 - \exp\left(-\frac{t_j}{B_j} \right) \right]^{-1} \left[C(t_j) - \sum_{k=1}^{j-1} A_k \right]$$

•**2nd approximation**

$$A^{(2)} = \left[1 - \exp\left(-\frac{t_j}{B_j} \right) \right]^{-1} \left[C(t_j) - \sum_{k=1}^{j-1} F_k(t_j) \right]$$

$$F_k(t_j) = A_k^{(1)} \left[1 - \exp\left(-\frac{t_j}{B_j} \right) \right].$$

•**Iterative scheme**

$$A_j^{(0)} = \left[1 - \exp\left(-\frac{t_j}{B_j} \right) \right]^{-1} \left[C(t_j) - \sum_{k=1}^{j-1} A_k^{(0)} \right]$$

•i-**th approximation**

$$A_j^{(i)} = \left[1 - \exp\left(-\frac{t_j}{B_j} \right) \right]^{-1} \left[C(t_j) - \sum_{k \neq j} F_k(t_j) \right]$$

$$F_k(t_j) = A_k^{(i-1)} \left[1 - \exp\left(-\frac{t_j}{B_k} \right) \right].$$

$$t_j = -B_j \ln(0.5)$$
$$B_j = 10^{j-4} \quad \text{[days]} \quad 1 < j < 6.$$

Convergence test

$$\max \left[A_j^{(i)} - \frac{A_j^{(i-1)}}{A_j^{(i)}} \right] < 10^{-2}$$

Window 3-32

3.4.2 CREEP PARAMETER IDENTIFICATION FROM EXPERIMENTS

The easiest way to adjust creep parameters A and m for $C(t, t_0) = A(t - t_0)^m$ from an experimental curve $f(t, t_0)$ is to pick two points situated at $(t - t_0) = 1$ for the adjustment of A and then at a large value of $(t - t_0)$ for the adjustment of m.

Depending on the available test the procedure differs only slightly. Four typical experiments are analyzed next; additional situations can easily be extrapoled using $\mathbf{D}_0^{-1}$ with

$$
\mathbf{D}_0^{-1} = \begin{bmatrix} 1 & -\nu & 0 & -\nu \\ -\nu & 1 & 0 & -\nu \\ 0 & 0 & 2(1+\nu) & 0 \\ -\nu & -\nu & 0 & 1 \end{bmatrix}.
$$

If volumetric and deviatoric creep are different i.e.

$$
C_v(t, t_0) = A_v(t - t_0)^{m_v} \neq C_d(t, t_0) = A_d(t - t_0)^{m_d}
$$

then

$$
(D_0^v)^{-1} = \frac{E}{3K} = 1 - 2\nu
$$

and

$$
\left(\mathbf{D}_0^d\right)^{-1} = \begin{bmatrix} 1+\nu & 0 & 0 & 0 \\ 0 & 1+\nu & 0 & 0 \\ 0 & 0 & 2(1+\nu) & 0 \\ 0 & 0 & 0 & 1+\nu \end{bmatrix}.
$$

Window 3-33: Uniaxial test

$$
\boldsymbol{\varepsilon}_c = \mathbf{D}_0^{-1} \boldsymbol{\sigma} C(t - t_0)
$$

$$
\begin{Bmatrix} \varepsilon_1^c \\ \varepsilon_2^c \\ 0 \\ \varepsilon_3^c \end{Bmatrix} = \begin{bmatrix} 1 & -\nu & 0 & -\nu \\ -\nu & 1 & 0 & -\nu \\ 0 & 0 & 2(1+\nu) & 0 \\ -\nu & -\nu & 0 & 1 \end{bmatrix} \begin{Bmatrix} \sigma_1 \\ 0 \\ 0 \\ 0 \end{Bmatrix} C(t - t_0)
$$

hence with

$$
C(t - t_0) = A(t - t_0)^m
$$
$$
\varepsilon_1^c = \sigma_1 A(t - t_0)^m.
$$

Window 3-33

Window 3-34: Triaxial test

Assuming ε_v^c is measured in the experiment:

$$
\begin{Bmatrix} \varepsilon_1^c \\ \varepsilon_2^c \\ \gamma_{12}^c \\ \varepsilon_3^c \end{Bmatrix} = \begin{bmatrix} 1 & -\nu & 0 & -\nu \\ -\nu & 1 & 0 & -\nu \\ 0 & 0 & 2(1+\nu) & 0 \\ -\nu & -\nu & 0 & 1 \end{bmatrix} \begin{Bmatrix} \sigma_1 \\ \sigma_2 \\ 0 \\ \sigma_3 \end{Bmatrix} C(t - t_0)
$$

hence, with

$$
C(t - t_0) = A(t - t_0)^m
$$
$$
\varepsilon_v^c = 3\,(1 - 2\nu)\,\sigma_m A(t - t_0)^m.
$$

Window 3-34

Window 3-35: Triaxial deviatoric test

Assuming $\varepsilon_2^c - \varepsilon_2^c = \gamma^c$ is measured for a unit $q = (\sigma_1 - \sigma_2)$

$$
\varepsilon_d^c = D_0^{-1} \begin{Bmatrix} \sigma_1 \\ \sigma_2 \\ 0 \\ \sigma_3 \end{Bmatrix} \quad \text{and} \quad \sigma_3 = \sigma_1
$$

then

$$
\varepsilon_2^c = (\sigma_2 - 2\nu\sigma_1)\,C\,(t, t_0)
$$
$$
\varepsilon_1^c = [\sigma_1 - \nu\,(\sigma_2 + \sigma_1)]\,C\,(t, t_0)
$$
$$
\gamma^c = (1 + \nu)\,qC\,(t - t_0)\,.
$$

Window 3-35

Window 3-36: Oedometer test

$$
\varepsilon^c = D_0^{-1} \begin{Bmatrix} K_0\sigma_2 \\ \sigma_2 \\ 0 \\ K_0\sigma_2 \end{Bmatrix} C\,(t, t_0)
$$

then

$$
\varepsilon_2^c = (1 - 2\nu K_0)\,\sigma_2 C\,(t, t_0)\,.
$$

Window 3-36

3.5   SWELLING

A nonlinear creep approach has been adopted here to model swelling phenomena. Creep seems to be the simplest phenomenological approach which can reproduce macroscopic behaviour of swelling soils/rocks both quantitatively and qualitatively without considering all the microscale effects.

Oedometric swelling test

Memorizing of in situ stress σ_0

Correction of σ_{os} with respect to σ_o state

Three-dimensional generalization

Window 3-37: Oedometric swelling test

An oedometric swelling test is taken as the basis for further three-dimensional generalization according to the suggestion of Wittke and Kiehl [2].

A typical relation between swelling strain and vertical stress (after Huder and Amberg) obtained from oedometer test is shown in figure below.
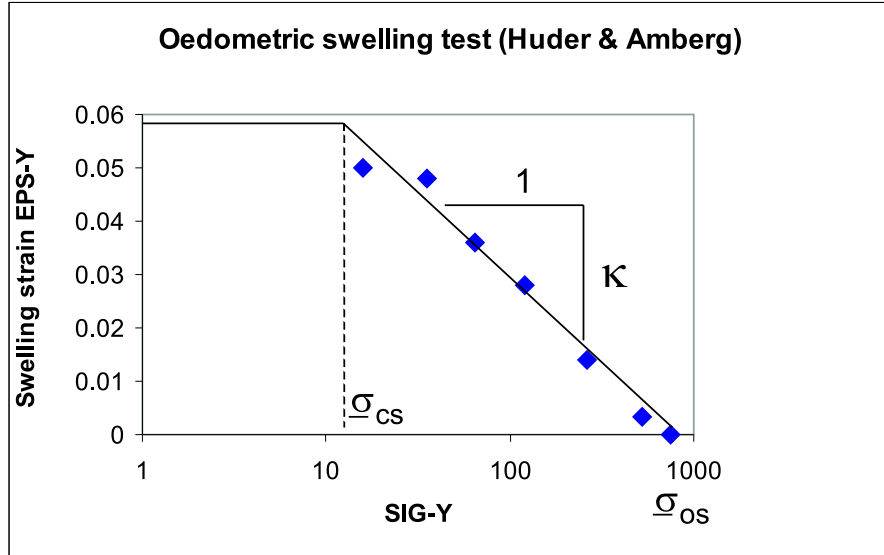
Five basic parameters are needed to calibrate swelling: $\underline{\sigma}_{os}$, $\underline{\sigma}_{cs}$, κ, B_o, and α_s.

Parameter $\underline{\sigma}_{os}$ defines a minimum vertical stress value which stops swelling evolution while $\underline{\sigma}_{cs}$ bounds the excessive increase of the swelling for small or even tensile stress state.

Parameter κ defines the slope of the line $\varepsilon_y^s - \sigma_y$ for stress range $\underline{\sigma}_{cs} \leq \underline{\sigma}_y \leq \underline{\sigma}_{os}$ in semi-logarithmic system. A parameter B_o, the time to reach the steady state for a sudden total unloading, is introduced, which defines maximum swelling evolution rate while α_s reduces or increases swelling evolution rate according to the formula:

$$B(\xi) = \frac{B_o}{1 - \exp(-\alpha_s \xi)}$$

$$\xi = \mathrm{MIN}\left(1, \frac{\|\boldsymbol{\sigma} - \boldsymbol{\sigma}_0\|}{\|\boldsymbol{\sigma}_{os}^{\mathrm{REF}} - \boldsymbol{\sigma}_{cs}^{\mathrm{REF}}\|}\right)$$

where the current effective stress is denoted by $\boldsymbol{\sigma}$, in situ stress is denoted by $\boldsymbol{\sigma}_0$ and appropriate reference stress states $\boldsymbol{\sigma}_{os}^{\mathrm{REF}}$, $\boldsymbol{\sigma}_{cs}^{\mathrm{REF}}$ are defined in the following windows.

Window 3-37

---

[2]W.Wittke.   Stability Analysis of Tunnels.Fundamentals.Verlag Glueckauf Essen, 2000. J.R.Kiehl.Interpretation der Ergebnisse von Grossquellversuchen in situ durch dreidimensionale numerische Berechnungen, Proc. 7th.ISRM Congress, Aachen 1991,pp.1534-1538)

Window 3-38: Memorizing of in situ stress $\boldsymbol{\sigma}_0$

The reference stress $\boldsymbol{\sigma}_0$ is required for evaluation of swelling rate function $B(\xi)$ and has to be memorized during computation. As the computation scenario can be very complex the following recipe is used to set up $\boldsymbol{\sigma}_0$ reference state:

If the initial state analysis is run then for all active (at time $t = 0$) materials $\boldsymbol{\sigma}_0$ is taken as the result of the last step of the initial state.

If the initial state is not specified in list of drivers but swelling is activated for some materials then $\boldsymbol{\sigma}_0$ is taken as the stress state at first converged step since material activation. NB. In such case swelling strain increment will not be generated in the first time step (since material activation).

$\hfill$ Window 3-38

Window 3-39: Correction of $\underline{\sigma}_{\mathsf{os}}$ parameter with respect to σ_0 state

If K_{o} axes do not coincide with global x-y-z system axes

$\qquad$ transform $\boldsymbol{\sigma}_0^* = \mathsf{T}^{\mathsf{G}\to\mathsf{L}} \, \boldsymbol{\sigma}_0$

else

$\qquad \boldsymbol{\sigma}_0^* = \boldsymbol{\sigma}_0$

IF $\underline{\sigma}_{0_\mathsf{y}}^* < \underline{\sigma}_{\mathsf{os}}$ modify parameter $\underline{\sigma}_{\mathsf{os}}$: $\underline{\sigma}_{\mathsf{os}} = \underline{\sigma}_{0_\mathsf{y}}^*$.

$\hfill$ Window 3-39

Window 3-40: Three-dimensional generalization

We assume that the generalized reference stress state $\boldsymbol{\sigma}_{\mathsf{os}}^{\mathsf{REF}}$ and $\boldsymbol{\sigma}_{\mathsf{cs}}^{\mathsf{REF}}$, in xyz system, can be defined as follows:

$$\boldsymbol{\sigma}_{\mathsf{os,xyz}}^{\mathsf{REF}} = \left\{ \begin{array}{cccccc} -K_{ox}\,\sigma_o & -\sigma_o & 0 & -K_{oz}\,\sigma_o & 0 & 0 \end{array} \right\}^{\mathsf{T}}$$
$$\boldsymbol{\sigma}_{\mathsf{cs,xyz}}^{\mathsf{REF}} = \left\{ \begin{array}{cccccc} -K_{ox}\,\sigma_c & -\sigma_c & 0 & -K_{oz}\,\sigma_c & 0 & 0 \end{array} \right\}^{\mathsf{T}}$$

where $K_{ox} = K_{oz} = \dfrac{v}{1-v}$ (if not explicitly defined)

It is possible to set up the in situ K_o coefficients K_{ox}, K_{oz} in local coordinate system $x\prime y\prime z\prime$ rotated with respect to xyz system. In such a case the reference stress states are defined as

$$\boldsymbol{\sigma}_{\mathsf{os},\, x'y'z'}^{\mathsf{REF}} = \left\{ \begin{array}{cccccc} -K_{ox}\sigma_o & -\sigma_o & 0 & -K_{oz}\sigma_o & 0 & 0 \end{array} \right\}^{\mathrm{T}}$$
$$\boldsymbol{\sigma}_{\mathsf{cs},\, x'y'z'}^{\mathsf{REF}} = \left\{ \begin{array}{cccccc} -K_{ox}\sigma_c & -\sigma_c & 0 & -K_{oz}\sigma_c & 0 & 0 \end{array} \right\}^{\mathrm{T}}$$

and the following transformation takes place to set them up in xyz system:

$$\boldsymbol{\sigma}_{\mathsf{os},\, xyz}^{\mathsf{REF}} = \mathbf{T}^{\mathsf{L}\to\mathsf{G}}\boldsymbol{\sigma}_{\mathsf{os},\, x'y'z'}^{\mathsf{REF}}$$
$$\boldsymbol{\sigma}_{\mathsf{cs},\, xyz}^{\mathsf{REF}} = \mathbf{T}^{\mathsf{L}\to\mathsf{G}}\boldsymbol{\sigma}_{\mathsf{cs},\, x'y'z'}^{\mathsf{REF}}$$

where $\mathbf{T}^{\mathsf{L}\to\mathsf{G}}$ is a transformation matrix from local to global system.

The increment of creep strain (swelling strain) is computed using following recurrence formula:

$$\Delta\boldsymbol{\varepsilon}^{\mathsf{CR}} = \frac{\Delta t}{B(\xi)}\, \Delta\boldsymbol{\varepsilon}^{\mathsf{CR}(*)}$$

The following approach is used to compute $\Delta\boldsymbol{\varepsilon}^{\mathsf{CR}(*)}$ for given effective stress state $\boldsymbol{\sigma}$:

- find eigenvalues σ_i and eigendirections $\mathbf{d}_i$ of $\boldsymbol{\sigma}$
- transform $\boldsymbol{\sigma}^{\mathsf{REF}}_{\mathsf{os,xyz}}$, $\boldsymbol{\sigma}^{\mathsf{REF}}_{\mathsf{cs,xyz}}$ to principal directions of $\boldsymbol{\sigma} \rightarrow \boldsymbol{\sigma}^{\mathsf{REF}(*)}_{\mathsf{os,xyz}}$, $\boldsymbol{\sigma}^{\mathsf{REF}(*)}_{\mathsf{cs,xyz}}$
- transform accumulated creep strain $\boldsymbol{\varepsilon}^{\mathsf{ac\text{-}CR}}$ to principal directions of $\boldsymbol{\sigma} \rightarrow \boldsymbol{\varepsilon}^{\mathsf{ac\text{-}CR}(*)}$
- compute predicted swelling strain components in principal directions of $\boldsymbol{\sigma}$ using following formula:

$$\varepsilon_i^{\mathsf{CR}} = \left\{ \begin{array}{ccc} -\kappa\, \ln\dfrac{\sigma_i}{\sigma^{\mathsf{REF}(*)}_{o_{ii}}} & \text{if} & \sigma^{\mathsf{REF}(*)}_{c_{ii}} \geq \sigma_i \geq \sigma^{\mathsf{REF}(*)}_{o_{ii}} \\[2ex] 0 & \text{if} & \sigma_i \leq \sigma^{\mathsf{REF}(*)}_{o_{ii}} \\[2ex] -\kappa\, \ln\dfrac{\sigma^{\mathsf{REF}(*)}_{c_{ii}}}{\sigma^{\mathsf{REF}(*)}_{o_{ii}}} & \text{if} & \sigma_i \geq \sigma^{\mathsf{REF}(*)}_{c_{ii}} \end{array} \right\}$$

- compute $\Delta\boldsymbol{\varepsilon}^{\mathsf{CR}(*)}$ based on $\varepsilon_i^{\mathsf{CR}}$, $\mathbf{d}_i$ and $\boldsymbol{\varepsilon}^{\mathsf{ac\text{-}CR}(*)}$

$$\Delta\boldsymbol{\varepsilon}^{\mathsf{CR}(*)} = \left(\mathsf{MAX}(\varepsilon_i^{\mathsf{CR}}, \varepsilon_{ii}^{\mathsf{ac\text{-}CR}(*)}) - \varepsilon_{ii}^{\mathsf{ac\text{-}CR}(*)} \right)\, \mathbf{d}_i\mathbf{d}_i^{\mathsf{T}}$$

Remarks:

An explicit integration scheme has been adopted here and thus the maximum time step value is limited and should satisfy the condition:

$$0 < \Delta t < \frac{2B\,\underline{\sigma}_{\mathsf{MIN}}}{\kappa\, E_{\mathsf{oed}}}$$

where $\underline{\sigma}_{\mathsf{MIN}}$ is the principal normal stress which yields the largest swelling strain.

	Window 3-40

3.6   AGING CONCRETE

[3] The aging concrete model represent time dependent mechanical properties as well as rheological behavior of concrete in early age.

It consists of a set of parallel Maxwell units, as shown in the Window 3-41. Each unit is described by a maturity dependent Young modulus $E_k(M) = W_k(M)E$, and retardation time $\tau_k = \dfrac{E_k}{\eta_k}$. The contribution of each unit depends on maturity measure M (expressed in time units), by the set of weighting factors W_k, $(\sum_k W_k = 1)$, given for specified time instants t_i .

| **Window 3-41: Aging concrete model** |

Maxwell chain model for aging concrete
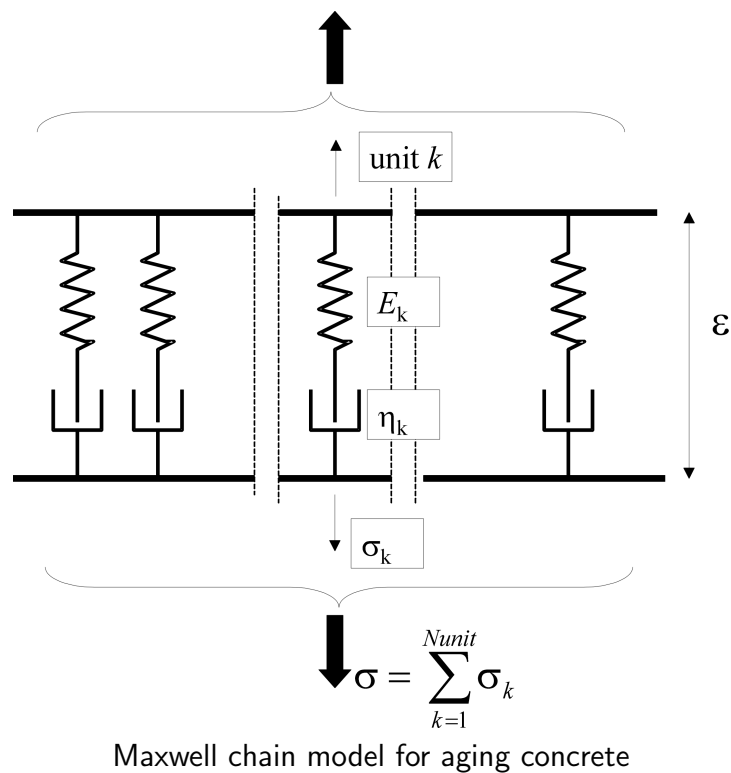
| Window 3-41 |

Remarks:

For details of the numerical implementation see:

AGING CONCRETE MODEL - IMPLEMENTATION SCHEME

---

[3]concerns versions: **ACADEMIC, PROFESSIONAL, EXPERT** only

3.7 AGING AND CREEP DEDICATED TO PLASTIC DAMAGE MODEL FOR CONCRETE

[4]

A creep module following the EC2 standard (including aging phenomenon) is fully described in the report on plastic damage model for concrete. This module can exclusively be used with the mentioned constitutive model. Please refer to that document for comprehensive overview.

---

[4]concerns versions: **ACADEMIC, PROFESSIONAL, EXPERT** only

3.8   APPENDICES

SAFETY FACTORS AND STRESS LEVELS

3.8.1 SAFETY FACTORS AND STRESS LEVELS

The following definitions are used in ZSoil®; of course these definitions are not unique.

Window 3-42: Stress level (SL)

I. for axisymmetric criteria

$$SL = \frac{q}{q_{\text{failure}}} \quad \text{with } q = \sqrt{3J_2}$$

II. for Lode's angle dependent criteria

$$SL = \frac{1}{\lambda} \quad \text{with } \sigma_{\text{failure}} = \sigma_m \delta + \lambda s$$

Remarks:

1. I is a subset of II

2. obviously λ will be different for each material point.

Window 3-42

Window 3-43: Safety factor (SF)

I. Let SF_1 be the multiplier which can be applied uniformly to each deviatoric stress in the structure, such that failure occurs when

$$\sigma' = \sigma_m \delta + SF_1 s$$

II. For two–parameter criteria (C, ϕ) an alternative definition is available which is

$$SF_2 = \left| \frac{\int_\Gamma \tau_{\text{failure}} d\Gamma}{\int_\Gamma \tau \, d\Gamma} \right|$$

where Γ is the failure surface and can, as shown elsewhere, be obtained numerically by a progressive reduction of C and $\tan \phi$ using:

$$c' = \frac{c}{SF_2}$$

$$(\tan \phi)' = \frac{\tan \phi}{SF_2}.$$

In the general Mentrey–Willam definition this amounts to replace the parameters of the criterion by

$$A'_f = SF_1 \, A_f$$
$$B'_f = SF_1 \, B_f$$

Window 3-43

Chapter 4

NUMERICAL IMPLEMENTATION

WEAK FORMULATION

ELEMENTS

INCOMPRESSIBLE AND DILATANT MEDIA

FAR FIELD

OVERLAID MESHES

ALGORITHMS

4.1   WEAK FORM AND MATRIX FORMS OF THE PROBLEM

SINGLE PHASE MEDIUM, TIME INDEPENDENT LOADING

TWO–PHASE MEDIUM, RHEOLOGICAL BEHAVIOUR

HEAT TRANSFER

In the subsequent sections the following Hughes notations is used:

$$w_{(i,j)} = \frac{1}{2}\left(w_{i,j} + w_{j,i}\right)$$

4.1.1 SINGLE PHASE MEDIUM, TIME INDEPENDENT LOADING

In the finite element solution procedure one does not solve the strong form of the boundary value problem but an equivalent weak (variational or virtual work) form which is usually discretized following a Galerkin technique. The equivalence of the strong or differential form of the problem statement and the weak form is discussed in texts concerning finite element implementation (see [Hughes, 1987]).

Window 4-1: Weak and matrix form of single phase medium

Weak form:

$$\int_\Omega w_{(i,j)}\sigma_{ij}\,\mathrm{d}\Omega = \int_\Omega w_i f_i\,\mathrm{d}\Omega + \int_{\Gamma_t} w_i \bar{t}_i\,\mathrm{d}\Gamma \tag{1}$$

$$u_i = \bar{u}_i \quad \text{on } \Gamma_u$$

where Γ_t and Γ_u are boundaries with prescribed tractions and displacements, respectively, and

$$\partial\Omega = \Gamma = \Gamma_u + \Gamma_t.$$

Approximation functions for $\mathbf{w}$ and $\mathbf{u}$

$$w_i = N_a\,w_{ia} \tag{2}$$
$$u_i = N_a\,u_{ia}$$

Index a identifies the element node number.

Matrix form

The matrix form results from the introduction of the appropriate derivatives of these approximations into the weak form and invoking the arbitrariness of the weighting functions $\mathbf{w}$

$$\mathbf{K}\,\mathbf{u} = \mathbf{F} \tag{3}$$
$$u_{ia} = \bar{u}_{ia} \quad \text{on } \Gamma_u$$

where:

$$\mathbf{K} = \mathcal{A}_{e=1,N}\left(\mathbf{K}^e\right), \qquad \mathcal{A} - \text{the assembly of elemental stiffness contributions}$$

and $\mathbf{K}^e$ is the elemental stiffness contribution

$$\mathbf{K}^e = \int_{\Omega^e} \mathbf{B}^T\,\mathbf{D}\,\mathbf{B}\,\mathrm{d}\Omega^e \tag{4}$$

will be established when elements are discussed.

Internal force: term $\mathbf{Ku}$

It can alternatively be written as

$$\mathbf{K}\,\mathbf{u} = \mathcal{A}_{e=1,N}\int_{\Omega^e} \mathbf{B}^T\,\boldsymbol{\sigma}\,\mathrm{d}\Omega^e \tag{5}$$

which will be needed later.

Window 4-1

4.1.2   TWO-PHASE MEDIUM, RHEOLOGICAL BEHAVIOUR

Two–phase medium. Weak form

Integration in time domain

Choice of shape functions

The strong statement of the two–phase boundary value problem was given in Section 2.2. The corresponding weak statement and matrix form are shown in Window 4-2.

Window 4-2 describes the weak form of the overall equilibrium equation (expressed in terms of total stresses according to extended Bishop's effective stress principle) and weak form of the fluid flow continuity equation with associated boundary conditions. The problem is formulated in terms of nodal displacements $\mathbf{u}$ and pore pressures $\mathbf{p}^{\mathsf{F}}$.

The actual implementation of the seepage boundary conditions is done using a two–sided surface element (see Window 2-4) in which boundary conditions are imposed on the external face by the user.

Window 4-2: Two–phase medium. Weak form

Equilibrium equations

$$\underbrace{\int_{\Omega} w_{(i,j)}\sigma_{ij}^{\mathsf{tot}}\,\mathrm{d}\Omega}_{\text{(total internal force)}} = \underbrace{\int_{\Omega} w_i b_i\,\mathrm{d}\Omega}_{\text{(body load)}} + \underbrace{\int_{\Gamma_t} w_i \bar{t}_i\,\mathrm{d}\Gamma}_{\text{(surface traction)}}$$

$$\underbrace{\int_{\Omega} w^{\mathsf{F}}\tilde{\alpha}S\varepsilon_{kk}\,\mathrm{d}\Omega}_{\text{(skeleton def. rate)}} - \underbrace{\int_{\Omega} w_{,k}^{\mathsf{F}} v_{,k}^{\mathsf{F}}\,\mathrm{d}\Omega}_{\text{(internal flux)}} - \underbrace{\int_{\Omega} w^{\mathsf{F}} c\left(p^{\mathsf{F}}\right)\overset{\circ}{\mathbf{p}}{}^{\mathsf{F}}\,\mathrm{d}\Omega}_{\text{(storage)}} + \underbrace{\int_{\Gamma_q} w^{\mathsf{F}}\bar{q}\,\mathrm{d}\Gamma}_{\text{(surface flux)}} - \underbrace{\int_{\Gamma_s} w^{\mathsf{F}} k_v(p^{\mathsf{F}} - p^{\mathsf{F\,ext}})\,\mathrm{d}\Gamma}_{\text{(seepage penalty term)}} = 0$$

Solid boundary conditions

$$u_i = \bar{u}_i \qquad \text{on} \quad \Gamma_u \times T$$
$$\sigma_{ij}^{\mathsf{tot}} n_j = \bar{t}_i \qquad \text{on} \quad \Gamma_t \times T$$

Fluid boundary conditions

$$p^{\mathsf{F}} = \bar{p}^{\mathsf{F}} \qquad \text{on} \quad \left(\Gamma_p + \Gamma_s^2\right) \times T$$
$$v_i^{\mathsf{F}} n_i = \bar{q} \qquad \text{on} \quad \left(\Gamma_q + \Gamma_s^1\right) \times T$$

Initial conditions

$$u_i\left(t_0\right) = u_{i0} \qquad \text{on} \quad \Omega$$
$$p^{\mathsf{F}}\left(t_0\right) = p_0^{\mathsf{F}} \qquad \text{on} \quad \Omega$$

Window 4-2

The matrix form of the problem results from the specific choice of shape functions for interpolation of displacements and pore pressure fields within the element. The application of the implicit integration scheme in time permits an elimination of time derivatives from set of linearized equations which is finally solved for $\Delta \mathbf{u}$ the increment of displacement $\mathbf{u}$ and $\Delta \mathbf{p}^\mathsf{F}$ the increment of pore pressure $\mathbf{p}^\mathsf{F}$. Iterations are needed if the constitutive law of the solid skeleton is nonlinear.

Window 4-3: Integration in time domain

The following predictor-corrector scheme has been adopted for integration of the displacements and pore pressures in time.

$$u_{i_{N+1}} = u_{i_N} + (1-\theta)\,\Delta t\,\dot{u}_{i_N} + \theta\,\Delta t\,\dot{u}_{i_{N+1}} = \underbrace{u_{i_N} + \Delta t\,\dot{u}_{i_N}}_{u_{i_N}^{\text{predictor}}} + \theta\,\Delta t\,\underbrace{\Delta\dot{u}_{i_{N+1}}}_{\dot{u}_{i_{N+1}} - \dot{u}_{i_N}}$$

$$p_{N+1} = p_N + (1-\theta)\,\Delta t\,\dot{p}_N + \theta\,\Delta t\,\dot{p}_{N+1} = \underbrace{p_N + \Delta t\,\dot{p}_N}_{p_{N+1}^{\text{predictor}}} + \theta\,\Delta t\,\underbrace{\Delta\dot{p}_{N+1}}_{\dot{p}_{N+1} - \dot{p}_N}$$

The integration coefficient θ has been assumed to satisfy the sufficient condition for stability $\theta \geq \dfrac{1}{2}$.

Window 4-3

Window 4-4: Choice of shape functions

Let us introduce the following finite element interpolation functions for approximated field(s), i.e. displacements $\mathbf{u}^h$ and pore pressure p^h, within a finite element

$$\mathbf{u}^h = \mathbf{N}^u \mathbf{u}^e \qquad \mathbf{w}^h = \mathbf{N}^u \mathbf{w}^e \qquad p^h = \mathbf{N}^p \mathbf{p}^e \qquad q^h = \mathbf{N}^p \mathbf{q}^e$$

With these definitions the strain-displacement relation is expressed in the standard form

$$\varepsilon\left(\mathbf{u}^h\right) = \mathbf{B}\,\mathbf{u}^e$$

Window 4-4

4.1.3   HEAT TRANSFER

Following section describe the solution algorithm for transient and steady state **heat transfer problem** formulated in section 2.4. In particular hints on

Weak and matrix form of heat transfer analysis

Time marching algorithm for transient analysis

Heat source term

are given.

Notation

T	-temperature field	t	-time
T_E	-external (ambient) temperature	$\overset{\circ}{X}$	-time derivative of X
H	-heat source	Δ	-time increment
q_T	-heat flux	∇	-gradient
c^*	-heat capacity	$\mathbf{X}$	-matrix/vector representation of X
λ	-heat conductivity	$\mathbf{X_e}$	−element contribution of $\mathbf{X}$
M	-maturity		

Weak form and matrix formulation

Window 4-5: Weak and matrix form of heat transfer analysis ————————————

Approximation for temperature field $T(\mathbf{x},t)$

$$T(\mathbf{x},t) = \mathbf{N}(\mathbf{x})\mathbf{T} \tag{1}$$

where $\mathbf{N}$ are shape functions and $\mathbf{T}$ are nodal temperatures.

Matrix form of governing differential equation for transient heat transfer analysis

$$\mathbf{C}\overset{\circ}{\mathbf{T}} + (\mathbf{K} + \mathbf{K}_b)\mathbf{T} = \overset{\circ}{\mathbf{H}} +\ \mathbf{K}_b\mathbf{T} \tag{2}$$

As ZSoil® system is generally based on incremental approach, equations have to be linearized which finally leads to following **linearized form:**

$$\mathbf{C}\Delta\overset{\circ}{\mathbf{T}} + (\mathbf{K} + \mathbf{K}_b + \mathbf{H}^*)\Delta\mathbf{T} = \Delta\mathbf{Q} \tag{3}$$

where :

$$\Delta\mathbf{Q} = \mathbf{Q} + \overset{\circ}{\mathbf{H}} + \mathbf{K}_b\mathbf{T}_E - \mathbf{C}\overset{\circ}{\mathbf{T}} - (\mathbf{K} + \mathbf{K}_b)\mathbf{T} \tag{4}$$

For each matrix $\mathbf{X} = \underset{e=1,N}{\mathcal{A}}(\mathbf{X^e})$, where symbol $\underset{e=1,N}{\mathcal{A}}$ represents the assembly of element

contributions $\mathbf{X}^e$, as listed below.

$$\mathbf{K}^e = \lambda \int_{\Omega^e} \nabla \mathbf{N}^T \nabla \mathbf{N}\, d\Omega^e$$

$$\mathbf{C}^e = c^* \int_{\Omega^e} \mathbf{N}^T \mathbf{N}\, d\Omega^e$$

$$\mathbf{K}_b^e = h_T \int_{\Gamma^e} \mathbf{N}^T \mathbf{N}\, d\Gamma^e$$

$$\mathbf{Q}^e = - \int_{\Gamma^e} \mathbf{N}^T q_T\, d\Gamma^e$$

$$\overset{\circ}{\mathbf{H}}{}^e = \int_{\Omega^e} \mathbf{N}^T \overset{\circ}{H} \Omega^e$$

$$\mathbf{H}^{*e} = - \left(\frac{\partial \overset{\circ}{\mathbf{H}}}{\partial M} \frac{\partial M}{\partial \mathbf{T}} + \frac{\partial \overset{\circ}{\mathbf{H}}}{\partial \mathbf{T}} \right) = - \left(\frac{\partial \overset{\circ}{H}}{\partial M} \frac{\partial M}{\partial T} + \frac{\partial \overset{\circ}{H}}{\partial T} \right) \int_{\Omega^e} \mathbf{N}^T\, \mathbf{N}\, d\Omega^e$$

All those matrices are evaluated using Gauss quadratures.

$$\boxed{\text{Window 4-5}}$$

The general system can be reduced to steady state conditions which is expressed by the set of equations:

$$(\mathbf{K} + \mathbf{K}_b)\Delta\mathbf{T} = \mathbf{Q} + \mathbf{K}_b \mathbf{T}_E - (\mathbf{K} + \mathbf{K}_b)\mathbf{T} \tag{4.1}$$

Window 4-6: Time marching algorithm for transient analysis

Applying finite differences in time domain , with $\theta \in (0,1)$:

$$T_{n+1} = T_n + (1-\theta)\Delta t \overset{\circ}{T}_n + \theta \Delta t \overset{\circ}{T}_{n+1} = \underbrace{\left(T_n + \Delta t \overset{\circ}{T}_n \right)}_{\text{predictor}} + \theta \Delta t \cdot \Delta \overset{\circ}{T}_{n+1} \tag{1}$$

thus:

$$\Delta \overset{\circ}{T}_{n+1} = \frac{\Delta T_{n+1}}{\theta \Delta t} \tag{2}$$

Introducing above into the **linearized form** 3, the following set of incremental equations is obtained:

$$\left[\mathbf{C} + \theta \Delta t \cdot (\mathbf{K} + \mathbf{K}_b + \mathbf{H}^*) \right] \Delta \mathbf{T} = \theta \Delta t \cdot \Delta \mathbf{Q} \tag{3}$$

$$\boxed{\text{Window 4-6}}$$

Handling of concrete hydration heat source term.

In the case of heat source term related to concrete hydration (1), which appear in definition of matrices $\mathbf{H}, \overset{\circ}{\mathbf{H}}$, integration of both heat source term H and maturity factor derivative with respect to temperature $\dfrac{\partial M}{\partial T}$ via Eqn. (2), in each integration point in an element are required. Even with assumption that in given time increment the temperature varies linearly, the integrals (2) can not be evaluated using elementary functions, so it has to be integrated numerically as follows:

Window 4-7: Heat source term

heat source:

$$H = H_\infty \frac{aM}{1 + aM} \tag{1}$$

maturity factor:

$$M = \int\limits_{t_d}^{t} \exp\left(\frac{Q}{R}(\frac{1}{T_{ref}} - \frac{1}{T})\right) \, \mathrm{d}t \tag{2}$$

numerical integration shema:

$$M_{n+1} = M_n + \exp\left[\frac{Q}{R}\left(\frac{1}{T_{ref}} - \frac{1}{T^\theta}\right))\right] \Delta t_{n+1} \quad \text{if} \quad t_{n+1} > t_{BEG} + t_d$$

$$\left(\frac{\partial M}{\partial T}\right)_{n+1} = \left(\frac{\partial M}{\partial T}\right)_n +$$

$$\frac{Q}{R}\left(\frac{1}{T^\theta_{n+1}}\right)^2 \exp\left[\frac{Q}{R}\left(\frac{1}{T_{ref}} - \frac{1}{T^\theta_{n+1}}\right)\right] \cdot \Delta t_{n+1} \quad \text{if} \quad t_{n+1} > t_{BEG} + t_d$$

$$M_{n+1} = 0 \quad \text{if} \quad t_{n+1} \le t_{BEG} + t_d$$

$$\left(\frac{\partial M}{\partial T}\right)_{n+1} = 0 \quad \text{if} \quad t_{n+1} \le t_{BEG} + t_d$$

where:

$$T^\theta_{n+1} = T_n(1 - \theta) + \theta T_{n+1}$$

Window 4-7

The first existence time of an element to which the integration point belongs is denoted by t_{BEG}. In the above scheme in case when $\Delta t_{n+1} < t_{n+1} - t_{BEG} - t_d$ the value Δt_{n+1} should be replaced by appropriate value.

4.2   ELEMENTS

FINITE ELEMENTS FOR 2D/3D CONTINUUM PROBLEMS

NUMERICAL INTEGRATION

STRAINS

STIFFNESS

BODY FORCES

INITIAL STRESSES

4.2.1   FINITE ELEMENTS FOR 2D/3D CONTINUUM PROBLEMS

A family of 2/3D isoparametric elements with 1–st order interpolation function is implemented in the program, see Appendix 4.7.1.

In case of single phase analysis the nodal displacements (active for given analysis type) are the basic unknowns. Derivatives of shape function are necessary for strains analysis and then for stresses calculation. Basic features are summarized in the following table:

Finite elements for 2/3D continuum problems

Analysis type	Plane Strain	Axisymmetry, $r = x$	3D
Ndim	2	2	3
Elementary volume $\mathrm{d}V$	$\mathrm{d}x\ \mathrm{d}y\ 1$	$2\pi r\ \mathrm{d}r\ \mathrm{d}y$	$\mathrm{d}x\ \mathrm{d}y\ \mathrm{d}z$
Active displacement	$\mathbf{u}(x,y) = [u,v]^{\mathrm{T}}$	$\mathbf{u}(r,y) = [u,v]^{\mathrm{T}}$	$\mathbf{u}(x,y) = [u,v,w]^{\mathrm{T}}$
DOF / node	2	2	3
Kinematic constraints	$w = 0,\ \dfrac{\partial}{\partial z} = 0$	$w_\theta = 0,\ \dfrac{\partial}{\partial \theta} = 0$	—
Strain vector $\varepsilon = \mathbf{B}\mathbf{d}$	$\left[\varepsilon_{xx}, \varepsilon_{yy}, \gamma_{xy}\right]^{\mathrm{T}}$	$\left[\varepsilon_{xx}, \varepsilon_{yy}, \gamma_{xy}, \varepsilon_{\theta\theta}\right]^{\mathrm{T}}$	$\left[\varepsilon_{xx}, \varepsilon_{yy}, \gamma_{xy}, \varepsilon_{zz}, \gamma_{xz}, \gamma_{yz}\right]^{\mathrm{T}}$
Strain–displacement operator $\mathbf{B}_a$ --- $\mathbf{B} = [\mathbf{B}_a]$ $a = 1, NEN$	$\begin{bmatrix} \dfrac{\partial N_a}{\partial x} & 0 \\ 0 & \dfrac{\partial N_a}{\partial y} \\ \dfrac{\partial N_a}{\partial y} & \dfrac{\partial N_a}{\partial x} \end{bmatrix}$	$\begin{bmatrix} \dfrac{\partial N_a}{\partial r} & 0 \\ 0 & \dfrac{\partial N_a}{\partial y} \\ \dfrac{\partial N_a}{\partial y} & \dfrac{\partial N_a}{\partial r} \\ \dfrac{N_a}{r} & 0 \end{bmatrix}$	$\begin{bmatrix} \dfrac{\partial N_a}{\partial x} & 0 & 0 \\ 0 & \dfrac{\partial N_a}{\partial y} & 0 \\ \dfrac{\partial N_a}{\partial y} & \dfrac{\partial N_a}{\partial x} & 0 \\ 0 & 0 & \dfrac{\partial N_a}{\partial z} \\ \dfrac{\partial N_a}{\partial z} & 0 & \dfrac{\partial N_a}{\partial x} \\ 0 & \dfrac{\partial N_a}{\partial z} & \dfrac{\partial N_a}{\partial x} \end{bmatrix}$

4.2.2   NUMERICAL INTEGRATION

Numerical integration is required for the evaluation all integrals resulting from the problem definition. Gaussian quadrature is used and for a one–dimensional integral can be represented as follows:

$$\int_\Omega f(x)\,\mathrm{d}x = \sum f(\xi_i)\, J_{x,\xi}(\xi_i)\, w_i$$

where:

$$f(\xi_i) - \text{function being integrated, value at } \xi_i$$
$$J_{x,\xi} - \text{jacobian determinant}$$
$$w_i - \text{Gaussian weighting factor}$$

The extension of the above for multidimensional case is straightforward : the double (triple) integration is replaced by a double (triple) summation.

In the case of axisymmetry, all integrands include a factor equal to $2\pi r$ where $r =$ radius of the integration point under consideration, and 2π can be devided out.

Standard quadrature types used for stiffness/forces evaluation for different elements are given in the table below:

Standard quadrature for typical elements

| Element:	T3	Q4	TH4	W6	B8
$Ngauss$	1	2×2	1	2×1	$2 \times 2 \times 2$

Details on integration point positions, weighting factors, for different quadrature types are given in Appendix 4.7.2

4.2.3   STRAINS

Strains at any integration point of a continuum element are evaluated by an unified procedure given in Window 4-8. Beside the standard approach presented here, in the case of incompressible or dilatant media another approach is recommended, see Section 4.3.

Window 4-8: Evaluation of strains
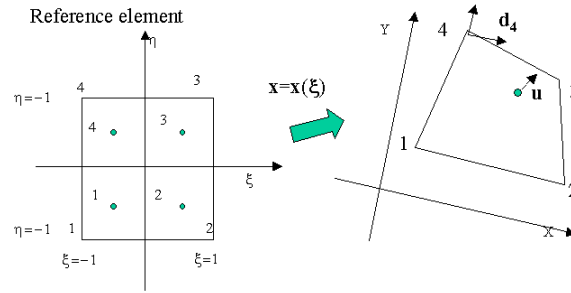
Quadrilateral element (Q4) outlook

An unified procedure for all 2/3D standard continuum elements include:

- isoparametric mapping:

$$\mathbf{x}\left(\boldsymbol{\xi}\right) = \sum_{a=1}^{\text{Nen}} N_a\left(\boldsymbol{\xi}\right)\ \mathbf{x}_a$$

- displacement interpolation:

$$\mathbf{u}\left(\boldsymbol{\xi}\right) = \sum_{a=1}^{\text{Nen}} N_a\left(\boldsymbol{\xi}\right)\ \mathbf{u}_a$$

- strain:

$$\boldsymbol{\varepsilon}\left(\boldsymbol{\xi}\right) = \mathbf{B}\left(\boldsymbol{\xi}\right)\ \mathbf{u} = \sum_{a=1}^{\text{Nen}} \mathbf{B}_a\left(\boldsymbol{\xi}\right)\ \mathbf{u}_a$$

where the standard form of matrix $\mathbf{B}$ is given in section 4.2.1. In the case of strain projection technique (necessary to simulate incompressible media) resulting form of the B–matrix, called B–Bar, will be described in Window 4-9.

- shape function derivatives, present in all concerned $\mathbf{B}_a$ are evaluated as:

$$\frac{\partial N_a}{\partial \mathbf{x}} = \left(\mathbf{J}^{-1}\right)^{\mathrm{T}} \frac{\partial N_a}{\partial \boldsymbol{\xi}}$$

where Jacobian $\mathbf{J} = \partial \mathbf{x}/\partial \boldsymbol{\xi}$ for 2D and 3D is calculated as follows

$$\text{2D:}\quad \mathbf{J} = \begin{bmatrix} \dfrac{\partial x}{\partial \xi} & \dfrac{\partial x}{\partial \eta} \\ \dfrac{\partial y}{\partial \xi} & \dfrac{\partial y}{\partial \eta} \end{bmatrix} ; \qquad \text{3D:}\quad \mathbf{J} = \begin{bmatrix} \dfrac{\partial x}{\partial \xi} & \dfrac{\partial x}{\partial \eta} & \dfrac{\partial x}{\partial \zeta} \\ \dfrac{\partial y}{\partial \xi} & \dfrac{\partial y}{\partial \eta} & \dfrac{\partial y}{\partial \zeta} \\ \dfrac{\partial z}{\partial \xi} & \dfrac{\partial z}{\partial \eta} & \dfrac{\partial z}{\partial \zeta} \end{bmatrix}$$

Window 4-8

4.2.4　STIFFNESS MATRIX

The element stiffness matrix can now be evaluated numerically; recalling that:

$$\mathbf{K}^{\mathrm{e}} = \int_{\Omega} \mathbf{B}^{\mathrm{T}} \mathbf{D} \, \mathbf{B} \ \mathrm{d}\Omega$$

$$\mathbf{F}^{\mathrm{e}} = \int_{\Omega} \mathbf{B}^{\mathrm{T}} \boldsymbol{\sigma} \ \mathrm{d}\Omega$$

Numerical integration yields:

$$\mathbf{K}^{\mathrm{e}} = \sum_{i}^{\mathrm{Ngauss}} \mathbf{B}^{\mathrm{T}}\left(\boldsymbol{\xi}_i\right) \mathbf{D}_i \mathbf{B}\left(\boldsymbol{\xi}_i\right) \det \mathbf{J}\left(\boldsymbol{\xi}_i\right) W_i$$

$$\mathbf{F}^{\mathrm{e}} = \sum_{i}^{\mathrm{Ngauss}} \mathbf{B}^{\mathrm{T}}\left(\boldsymbol{\xi}_i\right) \boldsymbol{\sigma}\left(\boldsymbol{\xi}_i\right) \det \mathbf{J}\left(\boldsymbol{\xi}_i\right) W_i$$

where the integrand is evaluated at the integration point i.

The standard integration rules are used for each element, see Section 4.2.2.

4.2.5   BODY FORCES AND DISTRIBUTED LOADS

The introduction of the interpolation functions into the weak form yields an elemental body force term as follows:

$$\mathbf{F}_{\mathrm{b}}^{\mathrm{e}} = \int_{\Omega^{\mathrm{e}}} \mathbf{N}^{\mathrm{T}} \mathbf{b} \, \mathrm{d}\Omega^{\mathrm{e}}$$

For distributed forces, the equivalent nodal force is seen to be:

$$\mathbf{F}_{\mathrm{t}}^{\mathrm{e}} = \int_{\partial\Gamma^{\mathrm{e}}} \mathbf{N}^{\mathrm{T}} \overline{\mathbf{t}} \, \mathrm{d}\Gamma^{\mathrm{e}}.$$

4.2.6   INITIAL STRESSES, STRAINS

If the initial stress field is in equilibrium the initial stresses can simply be added to the stresses resulting from deformations. If not, equivalent nodal forces must be calculated. Nodal forces equivalent to initial stresses and/or strains can be introduced as follows; this calls for a generalized stress-strain relation.

Let

$$\boldsymbol{\sigma} = \mathbf{D}\left(\boldsymbol{\varepsilon} - \boldsymbol{\varepsilon}_0\right) + \boldsymbol{\sigma}_0$$

where $\boldsymbol{\sigma}_0$ are the initial stresses and $\boldsymbol{\varepsilon}_0$ are the initial strains. By the definition of the internal force term:

$$\mathop{\mathcal{A}}_{e=1,N} \int_\Omega \mathbf{B}^{\mathrm{T}}\boldsymbol{\sigma}\ \mathrm{d}\Omega = \mathop{\mathcal{A}}_{e=1,N} \int_\Omega \mathbf{B}^{\mathrm{T}}\mathbf{D}\left(\boldsymbol{\varepsilon} - \boldsymbol{\varepsilon}_0\right)\ \mathrm{d}\Omega + \mathop{\mathcal{A}}_{e=1,N} \int_\Omega \mathbf{B}^{\mathrm{T}}\boldsymbol{\sigma}_0\ \mathrm{d}\Omega$$

from which the following expression of the nonlinear equilibrium equation results

$$\mathbf{F}^{\mathrm{int}}\left(\mathbf{u}\right) = \mathbf{F} - \mathbf{F}_\varepsilon + \mathbf{F}_{\sigma_0}$$

with

$$\mathbf{F}_{\sigma_0} = \mathop{\mathcal{A}}_{e=1,N} \int_\Omega \mathbf{B}^{\mathrm{T}}\boldsymbol{\sigma}_0\ \mathrm{d}\Omega$$

$$\mathbf{F}_\varepsilon = \mathop{\mathcal{A}}_{e=1,N} \int_\Omega \mathbf{B}^{\mathrm{T}}\boldsymbol{\varepsilon}_0\ \mathrm{d}\Omega.$$

Note that if initial stresses are in equilibrium $\mathbf{F}_{\sigma_0} = \mathbf{0}$ no deformations will result from the initial stresses. If not, deformations will result. Similarly if initial strains are compatible with boundary conditions, no stresses result.

4.3   INCOMPRESSIBLE AND DILATANT MEDIA

A strain projection technique is necessary in order to simulate incompressible media. The resulting form of the B–matrix, called B–Bar, will be described later on.

Another finite element technique to simulate incompressible and highly dilatant plastic media is the Enhanced Assumed Strain method (EAS). The general idea and detailed algorithmic scheme is described in Section 4.3.2. This option is activated in ZSOIL when dilatant plastic flow is active.

INCOMPRESSIBLE MEDIA: B-BAR STRAIN PROJECTION METHOD

DILATANT MEDIA: ENHANCED ASSUMED STRAIN METHOD

4.3.1 INCOMPRESSIBLE MEDIA : B-BAR STRAIN PROJECTION METHOD

Material data include the elastic constants i.e.Young's modulus and Poisson ratio. In fully incompressible cases, Poisson's ratio is 0.5 which within the program is taken as 0.499999. This leads to mesh locking when a full (2×2) integration scheme is used. Underintegration (i.e. the use of a single integration point) is therefore required in the volumetric part of the stiffness, while full integration is used for the shear term.

It can be seen from the iterative scheme that the use of seective underintegration would result in different integration schemes for the left– and right–hand side of the equilibrium equations. This can, and will, disturb convergence, so strain projection is used to circumvent this problem.

First, the B–BAR matrix is established for the case of torsionless axisymmetry and then the plane strain case is derived.

Beginning with the standard B–matrix for node 'a' defined previously in this section, we can split the matrix into dilatational and deviatoric parts as shown in Window 4-9.

In place of using $\mathbf{B}_a$ the $\bar{\mathbf{B}}_a$ is used where the dilatational term has been 'underintegrated'. The dilatational $\bar{\mathbf{B}}$ entries are calculated using a reduced 1×1 integration rule whereas the deviatoric $\bar{\mathbf{B}}$ entries are calculated using the 'normal' (2×2) integration rule.

Window 4-9: Strain projection B-BAR method

$$\mathbf{B}_a = \mathbf{B}_a^{\text{dev}} + \mathbf{B}_a^{\text{dil}}$$

where

$$\mathbf{B}_a^{\text{dil}} = \frac{1}{3} \begin{bmatrix} (B_0 + B_1) & B_2 \\ (B_0 + B_1) & B_2 \\ 0 & 0 \\ \bar{B}_0 + \bar{B}_1 & \bar{B}_2 \end{bmatrix} \quad \text{and} \quad \mathbf{B}_a^{\text{dev}} = \begin{bmatrix} \left(\dfrac{2}{3}B_1 - \dfrac{1}{3}B_0\right) & -\dfrac{1}{3}B_2 \\ \left(-\dfrac{1}{3}B_0 - \dfrac{1}{3}B_1\right) & \dfrac{2}{3}B_2 \\ B_2 & B_1 \\ \dfrac{2}{3}B_0 - \dfrac{1}{3}B_1 & -\dfrac{1}{3}B_2 \end{bmatrix}$$

In place of use $\mathbf{B}_a$ use $\bar{\mathbf{B}}_a$:

$$\bar{\mathbf{B}}_a = \mathbf{B}_a^{\text{dev}} + \bar{\mathbf{B}}_a^{\text{dil}}$$

i.e.:

$$\bar{\mathbf{B}}_a = \begin{bmatrix} B_{12} & B_6 \\ B_{10} & B_7 \\ B_2 & B_1 \\ \bar{B}_{11} & \bar{B}_6 \end{bmatrix}$$

where

$$\begin{array}{lll} B_0 = N_a/x_1 & B_1 = N_{a,x_1} & B_2 = N_{a,x_2} \\ B_4 = \left(\bar{B}_1 - B_1\right)/3 & B_6 = \left(\bar{B}_2 - B_2\right)/3 & B_7 = B_2 + B_6 \\ B_{10} = B_4 + \left(\bar{B}_0 - B_0\right)/3 & B_{11} = B_0 + B_{10} & B_{12} = B_1 + B_{10} \end{array}$$

Window 4-9

Remarks:

1. The plane strain case many be obtained from the above formulation by simply setting $\bar{B}_0 = B_0 = 0$ and using Cartesian rather than cylindrical coordinates. The $2\pi r$ (or r) factor included in the integrands in the case of axisymmetry must also be ignored.

2. Notice that the $\mathbf{D}$ matrix remains 4×4 for plane strain, when $\bar{\mathbf{B}}$ the formulation is used.

4.3.2   DILATANT MEDIA: ENHANCED ASSUMED STRAIN METHOD

INTRODUCTION TO ENHANCED ASSSUMED STRAIN (EAS) APPROACH

EXTENSION OF EAS TO NONLINEAR ELASTO–PLASTIC ANALYSIS

REMARKS AND ASSESSMENT OF EAS ELEMENTS

4.3.2.1   INTRODUCTION TO ENHANCED ASSSUMED STRAIN (EAS) APPROACH

In EAS methods[1] the strain is approximated by two fields, i.e. the compatible and the enhanced one via equation :

$$\varepsilon = \mathbf{Bu} + \mathbf{M\alpha}$$

where $\mathbf{B}$ is the standard strain operator, $\mathbf{M}$ is the interpolation operator for the additional strain field which may be discontinuous across element edges.

The variational basis of the method is the Hu–Washizu functional in the form:

$$U = \int_\Omega \left(\frac{1}{2}\varepsilon^{\mathrm{T}}\mathbf{D}\varepsilon - \sigma^{\mathrm{T}}\varepsilon + \sigma^{\mathrm{T}}\mathbf{Bu} - \mathbf{d}^{\mathrm{T}}\mathbf{N}^{\mathrm{T}}\mathbf{F} \right) \, \mathrm{d}\Omega.$$

Substitution of the modified strain field into functional yields:

$$U = \int_\Omega \left[\frac{1}{2}\left(\mathbf{Bu} + \mathbf{M\alpha}\right)^{\mathrm{T}}\mathbf{D}\left(\mathbf{Bu} + \mathbf{M\alpha}\right) - \sigma^{\mathrm{T}}\left(\mathbf{Bu} + \mathbf{M\alpha}\right) + \sigma^{\mathrm{T}}\mathbf{Bu} - \mathbf{u}^{\mathrm{T}}\mathbf{N}^{\mathrm{T}}\mathbf{F} \right] \, \mathrm{d}\Omega.$$

In order to eliminate the statically admissible stress field from functional the following condition has to be satisfied:

$$\int_\Omega \sigma^{\mathrm{T}}\mathbf{M\alpha} \, \mathrm{d}\Omega = 0.$$

The system of equations obtained by taking the variation of functional with respect to $\mathbf{u}$ and α takes the form:

$$\left[\begin{array}{cc} \mathbf{K}_{uu} & \mathbf{K}_{u\alpha} \\ \mathbf{K}_{\alpha u} & \mathbf{K}_{\alpha\alpha} \end{array} \right] \left[\begin{array}{c} \mathbf{u} \\ \alpha \end{array} \right] = \left[\begin{array}{c} \mathbf{F}^{\mathrm{ext}} \\ \mathbf{0} \end{array} \right]$$

where:

$$\mathbf{K}_{uu} = \int_\Omega \mathbf{B}^{\mathrm{T}}\mathbf{DB} \, \mathrm{d}\Omega \; ; \quad \mathbf{K}_{u\alpha} = \int_\Omega \mathbf{B}^{\mathrm{T}}\mathbf{DM} \, \mathrm{d}\Omega$$

$$\mathbf{K}_{\alpha u} = \int_\Omega \mathbf{M}^{\mathrm{T}}\mathbf{DB} \, \mathrm{d}\Omega \; ; \quad \mathbf{K}_{\alpha\alpha} = \int_\Omega \mathbf{M}^{\mathrm{T}}\mathbf{DM} \, \mathrm{d}\Omega$$

Assuming discontinuous approximation for α these extra degrees of freedom can be eliminated at the element level through standard condensation procedure. The interpolation functions assumed for $\mathbf{M}_\xi$ matrix, defined in isoparametric space, for plane strain case and axisymmetry are given in Windows (4-10) and (4-11).

The forms of $\mathbf{M}_\xi$ matrix for 3D is given in Win. (4-12).

These interpolation functions assumed for $\mathbf{M}_\xi$ (here index ξ is used to distinguish between isoparametric and physical spaces) have to satisfy the orthogonality condition introduced already in 4-th equation in this section. The transformation of $\mathbf{M}_\xi$ matrix from isoparametric space to physical one, summarized in Window (4-13), is performed with aid of Jacobian of the isoparametric mapping.

[1]Simo J.C., Rifai M.S., A class of mixed assumed strain methods and method of incompatible modes. International Journal for Numerical Methods in Engineering. Vol.**29**, pp.1595-1638, 1990

Groen A.E., Improvement of low order elements using assumed strain concepts. TU-Delft report Nr **25.2.94.203**, 1994.

Window 4-10: M matrices for Q4 element in plane strain

EAS–element	Number of extra modes	$\mathbf{M}_\xi$ matrix for plane strain $\left(\boldsymbol{\sigma} = \begin{bmatrix} \sigma_x, & \sigma_y, & \tau_{xy}, & \sigma_z \end{bmatrix}^\mathrm{T} \right)$
EAS2	2	$\mathbf{M}_\xi = \begin{bmatrix} \xi & 0 \\ 0 & \eta \\ 0 & 0 \\ 0 & 0 \end{bmatrix}$
EAS4	4	$\mathbf{M}_\xi = \begin{bmatrix} \xi & 0 & 0 & 0 \\ 0 & \eta & 0 & 0 \\ 0 & 0 & \xi & \eta \\ 0 & 0 & 0 & 0 \end{bmatrix}$
EAS7	7	$\mathbf{M}_\xi = \begin{bmatrix} \xi & 0 & 0 & 0 & \xi\eta & 0 & 0 \\ 0 & \eta & 0 & 0 & 0 & \xi\eta & 0 \\ 0 & 0 & \xi & \eta & 0 & 0 & \xi\eta \\ 0 & 0 & 0 & 0 & 0 & 0 & 0 \end{bmatrix}$

Window 4-10

Window 4-11: M matrices for Q4 element in axisymmetric case

EAS–element	Number of extra modes	$\mathbf{M}_\xi$ matrix for axisymmetry $\left(\boldsymbol{\sigma} = \begin{bmatrix} \sigma_r, & \sigma_y, & \tau_{ry}, & \sigma_\theta \end{bmatrix}^\mathrm{T} \right)$
EAS3	3	$\mathbf{M}_\xi = \begin{bmatrix} \xi - \overline{\xi} & 0 & 0 \\ 0 & \eta - \overline{\eta} & 0 \\ 0 & 0 & 0 \\ 0 & 0 & \xi\eta \dfrac{J(\xi,\eta)}{r(\xi,\eta)\, J_0} \end{bmatrix}$
EAS5	5	$\mathbf{M}_\xi = \begin{bmatrix} \xi - \overline{\xi} & 0 & 0 & 0 & 0 \\ 0 & \eta - \overline{\eta} & 0 & 0 & 0 \\ 0 & 0 & \xi - \overline{\xi} & \eta - \overline{\eta} & 0 \\ 0 & 0 & 0 & 0 & \xi\eta \dfrac{J(\xi,\eta)}{r(\xi,\eta)\, J_0} \end{bmatrix}$

where:

$$\overline{\xi} = \frac{1}{3}\frac{\mathbf{r}^\mathrm{T}\mathbf{a}_1}{\mathbf{r}^\mathrm{T}\mathbf{a}_0} \qquad \overline{\eta} = \frac{1}{3}\frac{\mathbf{r}^\mathrm{T}\mathbf{a}_2}{\mathbf{r}^\mathrm{T}\mathbf{a}_0}$$

$$\mathbf{r}^\mathrm{T}\mathbf{a}_0 = \frac{1}{4}(r_1 + r_2 + r_3 + r_4) \qquad \mathbf{r}^\mathrm{T}\mathbf{a}_1 = \frac{1}{4}(-r_1 + r_2 + r_3 - r_4)$$

$$\mathbf{r}^\mathrm{T}\mathbf{a}_2 = \frac{1}{4}(-r_1 - r_2 + r_3 + r_4)$$

r_1, r_2, r_3, r_4 — radial coordinates of element nodes.

Window 4-11

Window 4-12: M matrices for B8 element in 3D case

EAS-element	Nr of extra modes	$\mathbf{M}_\xi$ matrix for 3D case $(\boldsymbol{\sigma} = \{\ \sigma_x \quad \sigma_y \quad \tau_{xy} \quad \sigma_z \quad \tau_{xz} \quad \tau_{yz}\ \}^{\mathrm{T}})$
EAS6	6	$\mathbf{M}_\xi = \begin{bmatrix} \xi & 0 & 0 & \xi\eta & \xi\zeta & 0 \\ 0 & \eta & 0 & \xi\eta & \eta\zeta & 0 \\ 0 & 0 & 0 & 0 & 0 & 0 \\ 0 & 0 & \zeta & 0 & \xi\zeta & \eta\zeta \\ 0 & 0 & 0 & 0 & 0 & 0 \\ 0 & 0 & 0 & 0 & 0 & 0 \end{bmatrix}$
EAS9	9	$\mathbf{M}_\xi = \begin{bmatrix} \xi & 0 & 0 & 0 & 0 & 0 & 0 & 0 & 0 \\ 0 & \eta & 0 & 0 & 0 & 0 & 0 & 0 & 0 \\ 0 & 0 & 0 & \xi & \eta & 0 & 0 & 0 & 0 \\ 0 & 0 & \zeta & 0 & 0 & 0 & 0 & 0 & 0 \\ 0 & 0 & 0 & 0 & 0 & \xi & \zeta & 0 & 0 \\ 0 & 0 & 0 & 0 & 0 & 0 & 0 & \eta & \zeta \end{bmatrix}$

Window 4-12

Window 4-13: Mapping from isoparametric to physical space

The operator $\mathbf{M}_\xi$ is mapped onto physical space through the Jacobian of the isoparametric transformation at the element centroid (which is the origin of the isoparametric space). For second order tensors the following transformation from the isoparametric to physical space holds (J is evaluated in current integration point while J_0 is evaluated at the center):

$$\varepsilon_{ij}^{\text{isoparametric}} = \frac{\det \mathbf{J}}{\det \mathbf{J}_0} J_{ki_0} \varepsilon_{kl}^{\text{physical}} J_{jl_0}.$$

With matrix notation this mapping can be rewritten in form : $\varepsilon^{\text{physical}} = \dfrac{\det \mathbf{J}_0}{\det \mathbf{J}} \mathbf{T}_0^{-1} \varepsilon^{\text{isoparametric}}.$

From the above equation one gets the definition of $\mathbf{M}$ matrix: $\mathbf{M} = \dfrac{\det \mathbf{J}_0}{\det \mathbf{J}} \mathbf{T}_0^{-1} \mathbf{M}_\xi$

For plane strain and axisymmetry the transformation matrix $\mathbf{T}_0$ takes the form:

$$\mathbf{T}_0 = \begin{bmatrix} J_{11}^2 & J_{21}^2 & J_{11}J_{21} & 0 \\ J_{12}^2 & J_{22}^2 & J_{12}J_{22} & 0 \\ 2J_{11}J_{12} & 2J_{21}J_{22} & J_{11}J_{22} + J_{12}J_{21} & 0 \\ 0 & 0 & 0 & 1 \end{bmatrix} \quad \text{at } (\xi = 0, \eta = 0)$$

For 3D case the transformation matrix $\mathbf{T}_0$ takes the form:

$$\mathbf{T}_0 = \begin{bmatrix} J_{11}^2 & J_{21}^2 & J_{11}J_{21} & J_{31}^2 & J_{11}J_{31} & J_{21}J_{31} \\ J_{12}^2 & J_{22}^2 & J_{12}J_{22} & J_{32}^2 & J_{12}J_{32} & J_{22}J_{32} \\ 2J_{11}J_{12} & 2J_{21}J_{22} & J_{11}J_{22} + J_{21}J_{12} & 2J_{31}J_{32} & J_{11}J_{32} + J_{31}J_{12} & J_{21}J_{32} + J_{31}J_{22} \\ J_{13}^2 & J_{23}^2 & J_{13}J_{23} & J_{33}^2 & J_{13}J_{33} & J_{23}J_{33} \\ 2J_{11}J_{13} & 2J_{21}J_{23} & J_{11}J_{23} + J_{21}J_{13} & 2J_{31}J_{33} & J_{11}J_{33} + J_{31}J_{13} & J_{21}J_{33} + J_{31}J_{23} \\ 2J_{12}J_{23} & 2J_{22}J_{23} & J_{12}J_{23} + J_{22}J_{13} & 2J_{32}J_{33} & J_{12}J_{33} + J_{32}J_{13} & J_{22}J_{33} + J_{32}J_{23} \end{bmatrix}$$

Window 4-13

4.3.2.2   EXTENSION OF THE EAS METHOD TO NONLINEAR ELASTO–PLASTIC ANALYSIS

With the EAS method the resulting nonlinear system of equations to be solved is as follows:

$$\mathcal{A}_{e=1,N} \left[\mathbf{F}^{\text{ext}} - \mathbf{F}^{\text{int}} \left(\mathbf{u}_e, \boldsymbol{\alpha}_e \right) \right] = \mathbf{0}$$

$$\mathbf{h}_e \left(\mathbf{u}_e, \boldsymbol{\alpha}_e \right) = - \int_\Omega \mathbf{M}^{\text{T}} \boldsymbol{\sigma} \ d\Omega = \mathbf{0} \quad (e = 1, 2, \ldots, \text{Nele})$$

Linearization of the above yields:

$$\begin{bmatrix} \mathbf{K}_{uu} & \mathbf{K}_{u\alpha} \\ \mathbf{K}_{\alpha u} & \mathbf{K}_{\alpha\alpha} \end{bmatrix} \begin{bmatrix} \Delta\mathbf{u} \\ \Delta\boldsymbol{\alpha} \end{bmatrix} = \begin{bmatrix} \mathbf{F}^{\text{ext}} - \int_\Omega \mathbf{B}^{\text{T}} \boldsymbol{\sigma} \ d\Omega \\ \mathbf{0} - \int_\Omega \mathbf{M}^{\text{T}} \boldsymbol{\sigma} \ d\Omega \end{bmatrix}$$

where:

$$\mathbf{K}_{uu} = \int_\Omega \mathbf{B}^{\text{T}} \mathbf{D}^{\text{ep}} \mathbf{B} \ d\Omega \qquad \mathbf{K}_{u\alpha} = \int_\Omega \mathbf{B}^{\text{T}} \mathbf{D}^{\text{ep}} \mathbf{M} \ d\Omega$$

$$\mathbf{K}_{\alpha u} = \int_\Omega \mathbf{M}^{\text{T}} \mathbf{D}^{\text{ep}} \mathbf{B} \ d\Omega \qquad \mathbf{K}_{\alpha\alpha} = \int_\Omega \mathbf{M}^{\text{T}} \mathbf{D}^{\text{ep}} \mathbf{M} \ d\Omega$$

4.3.2.3   REMARKS AND ASSESSMENT OF EAS ELEMENTS

1. the EAS2 element in plane strain, EAS3 in axisymmetry and EAS6 in 3D are strongly recommended for stability and ultimate state analysis when using isotropic plastic models with dilatant plastic (for ex. Drucker-Prager if $\psi > 0$)

2. the EAS4 element in plane strain, EAS5 in axisymmetry and EAS9 in 3D are strongly recommended for stability and ultimate state analysis when using anisotropic plastic models with any type of plastic flow (only multilaminate model)

3. if one wants to get highly accurate results for beams/shells modeled with aid of continuum elements (retaining walls, etc...) the Q4-EAS7 (for plane strain case exclusively) and B8-EAS15 (3D) elements give superior results even for coarse distorted meshes, but their application is limited to elastic type of materials only (these elements are activated once `Continuum for structures` instead of `Continuum` is used for `Material formulation` to be defined at the material level).

4.4   FAR FIELD

Standard finite elements can be used only to discretize a bounded domain. In the case of a problem given in an unbounded domain, infinite elements, attached to the boundary of a bounded domain, can be used to describe interaction between bounded domain and its infinite surroundings. The formulation is based on the concept of infinite mapped elements (see [2]). The infinite mapped elements concept is summarized in the following windows.

Formulation of the mapped infinite element

Mapping for 2D infinite element

Mapping for 3D brick type of infinite element

Mapping for 3D wedge type of infinite element

Evaluation of element matrices for infinite mapped elements

---

[2]O.C. Zienkiewicz, C. Emson, P. Bettes, A Novel Boundary Infinite Element, International Journal for Numerical Methods in Engineering, vol. 19, p.393-404, 1983

Window 4-14: Formulation of the mapped infinite element
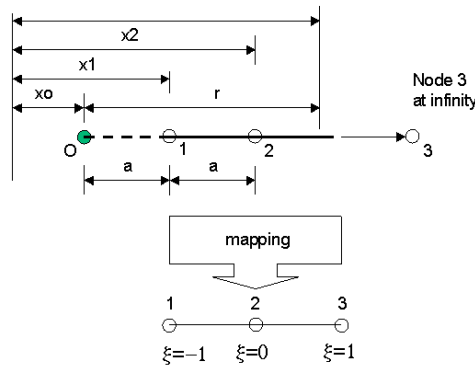
To summarize the concept of infinite mapped elements let us cosider the following one-dimensional situation given in the Fig. The element which extends from node 1 through node 2 up to node 3, placed at infinity, is mapped onto parent element in the local coordinate system. Once the arbitrary position of the pole of expansion x_0 is choosen one can define the position of node 2 using the expression

$$x_2 = 2\,x_1 - x_0$$

The mapping from local coordinate system to the global one can be done in standard way using the following rule

$$x(\xi) = \sum_{i=1}^{2} N_i^\infty(\xi)\,x_i$$

where node 3 is disregarded from the summation.

The infinite mapping functions are defined as follows

$$N_1^\infty(\xi) = -2\xi/(1-\xi)$$
$$N_2^\infty(\xi) = 1 - N_1^\infty(\xi)$$

It can be easily seen that $\xi = -1, 0, +1$ corresponds respectively to positions of node 1, node 2 and node 3 in global coordinate system.

The basic field variable is interpolated using standard shape functions and written in the polynomial form takes the form

$$u(\xi) = a_0 + a_1\xi + a_2\xi^2 + \ldots\ldots\ldots$$

in which coefficients a_i depend on element shape functions. Solving the mapping expression for ξ we get

$$\xi = 1 - \frac{2a}{r}$$

where the distance from the pole O to any point within the element is denoted by r and $a = x_2 - x_1$. Substituting the expression for ξ into expression for basic field variable we can get it in the form expressed in terms of global coordinate r

$$u(\xi) = b_0 + \frac{b_1}{r} + \frac{b_2}{r^2} + \ldots\ldots\ldots$$

where $b_0 = 0$ is implied since the variable u vanishes at infinity. From the above one can show that suitable decay functions $1/r^n$ for basic variable one can get by choosing proper shape functions for it.

Window 4-14

Window 4-15: Mapping for 2D infinite element
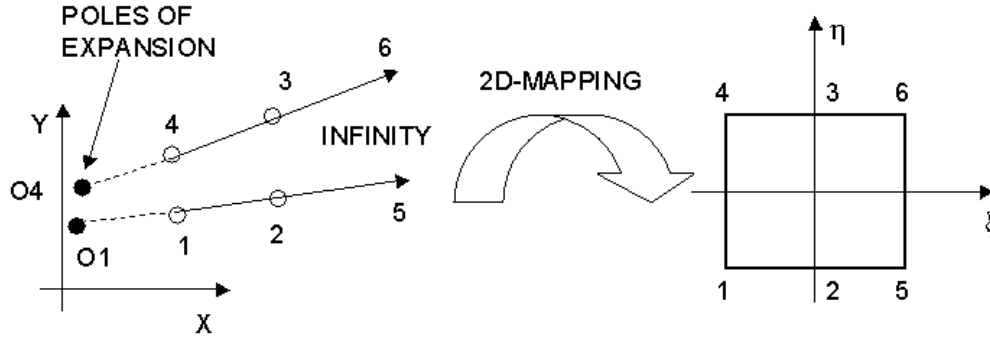
The mapping functions for the 2D element can be easily obtained as a product of one-dimensional Lagrangian shape functions along local direction η and infinite shape functions along direction ξ. If we assume that the poles positions are defined then we can define positions of nodes 2 and 3 as

$$\mathbf{x}_2 = 2\,\mathbf{x}_1 - \mathbf{x}_{O1}$$
$$\mathbf{x}_3 = 2\,\mathbf{x}_4 - \mathbf{x}_{O4}$$

altough the definition of the infinite element geometry is usually done by introduction of nodes 1, 2, 3 and 4 rather then by poles positions O1 and O2.

The set of the infinite shape functions for quadrilateral infinite 4-node element INFQ4 is as follows

$$M_1(\xi,\eta) = N_1^\infty(\xi)\,N_1(\eta)$$
$$M_2(\xi,\eta) = N_2^\infty(\xi)\,N_1(\eta)$$
$$M_3(\xi,\eta) = N_2^\infty(\xi)\,N_2(\eta)$$
$$M_4(\xi,\eta) = N_1^\infty(\xi)\,N_2(\eta)$$

in which the Lagrangian shape functions $N_i(\eta)$

$$N_1(\eta) = \frac{1}{2}\,(1-\eta)$$
$$N_2(\eta) = \frac{1}{2}\,(1+\eta)$$
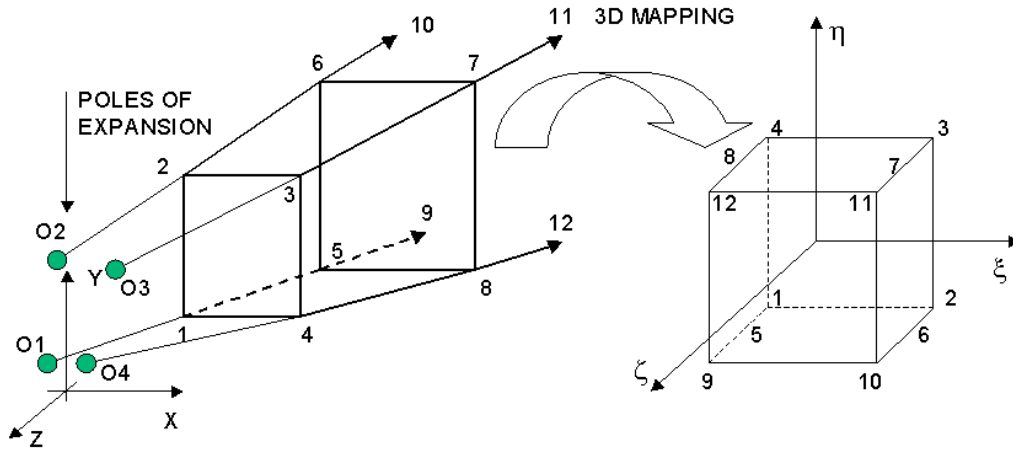
The coordinate element mapping is defined as

$$\mathbf{x}(\xi,\eta) = \sum_{i=1}^{4} M_i(\xi,\eta)\,\mathbf{x}_i$$

The interpolation of the displacement field within the element is assumed in the form

$$\mathbf{u}(\xi,\eta) = N_1(\xi,\eta)\,\mathbf{u}_1 + N_4(\xi,\eta)\,\mathbf{u}_4$$

Window 4-15

Window 4-16: Mapping for 3D brick type of infinite element

The scheme of mapping for 3D brick type of infinite element is shown in the following figure

The appropriate set of the shape functions is as follows

$$M_1(\xi,\eta) = N_1^\infty(\zeta)\, N_1(\xi,\eta)$$
$$M_2(\xi,\eta) = N_1^\infty(\zeta)\, N_2(\xi,\eta)$$
$$M_3(\xi,\eta) = N_1^\infty(\zeta)\, N_3(\xi,\eta)$$
$$M_4(\xi,\eta) = N_1^\infty(\zeta)\, N_4(\xi,\eta)$$

$$M_6(\xi,\eta) = N_2^\infty(\zeta)\, N_1(\xi,\eta)$$
$$M_7(\xi,\eta) = N_2^\infty(\zeta)\, N_2(\xi,\eta)$$
$$M_8(\xi,\eta) = N_2^\infty(\zeta)\, N_3(\xi,\eta)$$
$$M_8(\xi,\eta) = N_2^\infty(\zeta)\, N_4(\xi,\eta)$$

in which the shape functions $N_i(\xi,\eta)$ are the standard shape functions as for standard 4-node quadrilateral element.

The coordinate element mapping is defined as

$$\mathbf{x}(\xi,\eta,\zeta) = \sum_{i=1}^{8} M_i(\xi,\eta,\zeta)\ \mathbf{x}_i$$

The interpolation of the displacement field within the element is assumed in the form

$$\mathbf{u}(\xi,\eta) = \sum_{i=1}^{4} N_i(\xi,\eta)\, \mathbf{u}_i$$

Window 4-16

Window 4-17: Mapping for 3D wedge type of infinite element

The scheme of mapping for 3D wedge type of infinite element is shown in the following figure

The appropriate set of the shape functions is as follows

$$M_1(\xi,\eta) = N_1^\infty(\zeta)\, N_1(\xi,\eta)$$
$$M_2(\xi,\eta) = N_1^\infty(\zeta)\, N_2(\xi,\eta)$$
$$M_3(\xi,\eta) = N_1^\infty(\zeta)\, N_3(\xi,\eta)$$

$$M_4(\xi,\eta) = N_2^\infty(\zeta)\, N_1(\xi,\eta)$$
$$M_5(\xi,\eta) = N_2^\infty(\zeta)\, N_2(\xi,\eta)$$
$$M_6(\xi,\eta) = N_2^\infty(\zeta)\, N_3(\xi,\eta)$$

in which the shape functions $N_i(\xi,\eta)$ are the standard shape functions as for standard 3-node triangular element.

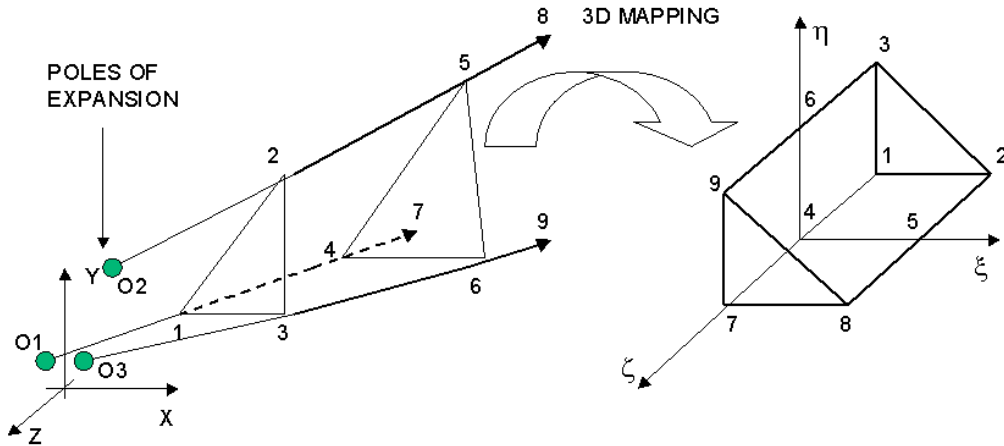The coordinate element mapping is defined as

$$\mathbf{x}(\xi,\eta,\zeta) = \sum_{i=1}^{6} M_i(\xi,\eta,\zeta)\, \mathbf{x}_i$$

The interpolation of the displacement field within the element is assumed in the form

$$\mathbf{u}(\xi,\eta) = \sum_{i=1}^{3} N_i(\xi,\eta)\, \mathbf{u}_i$$

Window 4-17

Window 4-18: Evaluation of element matrices for infinite mapped elements

The numerical integration of required infinite element matrices is performed with aid of standard Gauss integration scheme. The Jacobian, Cartesian derivatives of standard shape functions N_i and domain differential $d\Omega$, for general 3D case, are computed as follows

$$\mathbf{J} = \sum_{i=1}^{NEN^*} \begin{bmatrix} \dfrac{\partial M_i}{\partial \xi} x_i & \dfrac{\partial M_i}{\partial \xi} y_i & \dfrac{\partial M_i}{\partial \xi} z_i \\ \dfrac{\partial M_i}{\partial \eta} x_i & \dfrac{\partial M_i}{\partial \eta} y_i & \dfrac{\partial M_i}{\partial \eta} z_i \\ \dfrac{\partial M_i}{\partial \zeta} x_i & \dfrac{\partial M_i}{\partial \zeta} y_i & \dfrac{\partial M_i}{\partial \zeta} z_i \end{bmatrix}$$

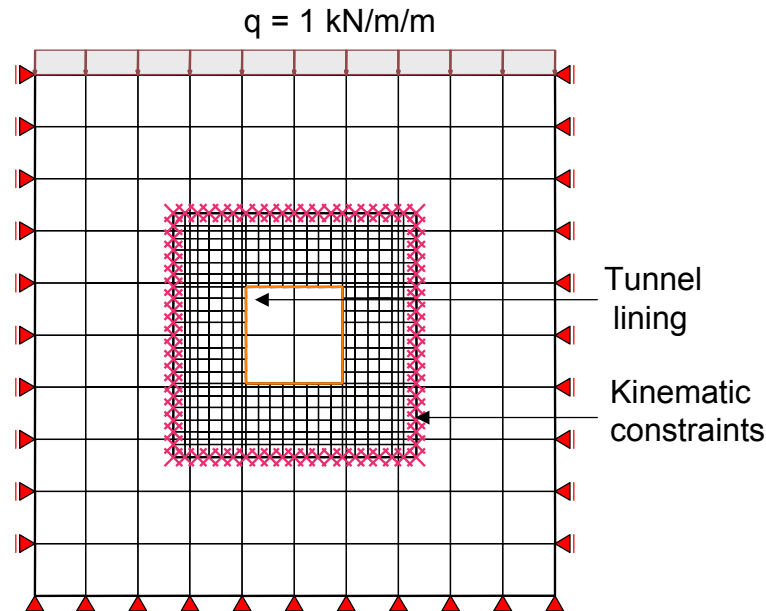$$\left\{ \begin{array}{c} \dfrac{\partial N_i}{\partial x} \\ \dfrac{\partial N_i}{\partial y} \\ \dfrac{\partial N_i}{\partial z} \end{array} \right\} = \mathbf{J}^{-1} \left\{ \begin{array}{c} \dfrac{\partial N_i}{\partial \xi} \\ \dfrac{\partial N_i}{\partial \eta} \\ \dfrac{\partial N_i}{\partial \zeta} \end{array} \right\}$$

$$d\Omega = dx\,dy\,dz = \det(\mathbf{J})\,d\xi\,d\eta\,d\zeta$$

Window 4-18

4.5　OVERLAID MESHES

To explain the idea of overlaid meshes let us consider a 2D domain 30m wide and 30m high, with a square excavation zone of size 6m by 6m placed at the center of the domain. During the excavation a tunnel lining is installed (see Fig. below).


In the context of the overlaid meshes approach we can create a relatively coarse mesh, labeled as layer number 0, which will represent soil behavior far from the excavation zone. In the neighborhood of the excavation zone, to enhance the quality of the results, we need a denser mesh and thus we superpose a second mesh labeled as layer number 1. In the 2D case we could easily generate a mesh in layer 1 in such a way that its external boundary nodes positions coincide with the nodes of the coarse mesh. However, in 3D applications this is usually not that easy and it is simpler, from the user's point of view, to superpose layer 1 with layer 0 without additional restrictions. This corresponds to overlaid meshes for which we have to handle the problem of overlapping of few meshes plus the continuity of primary variables (displacements, pressures etc..) handled via Lagrange multipliers.

In the considered example a mesh consisting of 10 x 10 elements is generated in layer 0 and 20 x 20 elements in layer 1 (layer 1 is 14m wide and 14m high) (see Fig. above). As it is shown in Fig. below some of the elements in layer 0 are fully overlapped (identified with circles) while some others are overlapped only partially (identified with triangles). All these elements which are fully overlapped, and nodes which exclusively belong to these elements, are neglected during computations. Problems arise in the case of partially overlapped elements as part of their domain must be deleted from the resulting stiffness and right-hand-side vector. To handle this case an exact geometrical intersection of a given element in layer 0 and elements in layer 1 must be computed to estimate the overlapped volume. For further application, this intersection is computed for each integration point subdomain of a given element in layer 0 and set of elements in layer 1.

⬤ Element fully overlapped   🔺 Element partially overlapped
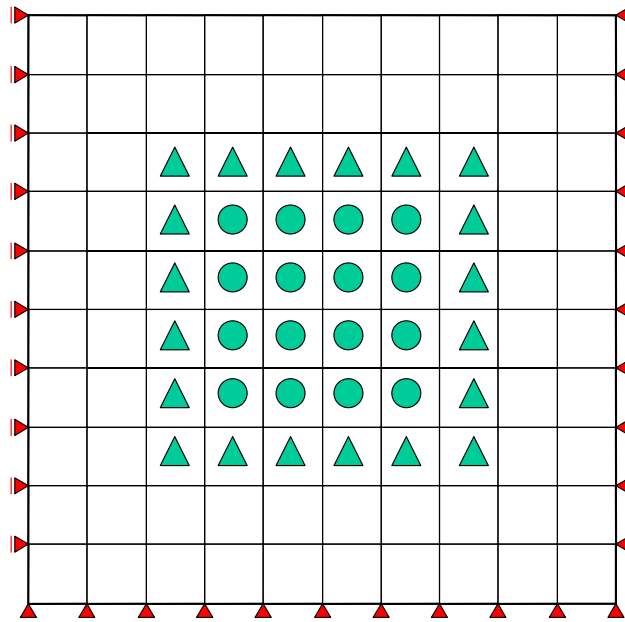
If we analyse the situation shown in Fig. below we can notice that for the integration point number 2 the ratio between nonoverlapped and total volume becomes zero (as the integration area associated with point 2 is entirely overlapped) while for other integration points it is smaller than 1 but greater than zero. Hence a simple computation scheme, in which each integration point volume is weighted by the aforementioned ratio, can be used.
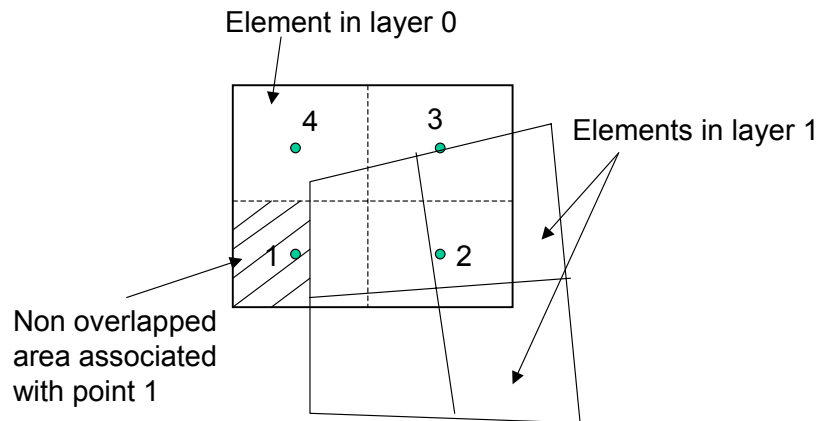
4.6   ALGORITHMS

Several solution algorithms can be activated either individually or in a sequence: initial state, stability, time dependent (driven load/consolidation/creep).

All refer in some way to a Newton–Raphson iterative scheme which is therefore described in Window 4-19. The specific algorithms are described next.

The simulation of excavation/construction stages is managed through existence functions associated with elements at the level of the data preparation.

MODIFIED NEWTON-RAPHSON ALGORITHM

CONVERGENCE NORMS

INITIAL STATE ANALYSIS

STABILITY ANALYSIS

ULTIMATE LOAD ANALYSIS

CONSOLIDATION

CREEP

LOAD TIME FUNCTIONS AND TIME STEPPING

EXCAVATION AND CONSTRUCTION STAGES

4.6.1   FULL/MODIFIED NEWTON-RAPHSON ALGORITHM

Window 4-19: Full/Modified Newton-Raphson algorithm

1. Step initialization : $n = n + 1$

   - set iteration counter $i = 0$
   - set $\Delta\mathbf{u}_{n+1}^{(i=0)} = \mathbf{0}$
   - Accumulate total external force vector $\mathbf{F}_{n+1}^{\text{ext}}$

2. At the element level, at each integration point

   - if creep is active then compute the creep strain increment $\Delta\boldsymbol{\varepsilon}_{n+1}^{\text{cr}}$ according to the Section 3.4 (*MATERIAL MODELS/CREEP*)
   - set the initial stress/strain increments $\Delta\boldsymbol{\sigma}_{0n+1}, \Delta\boldsymbol{\varepsilon}_{0n+1}$

3. $i = i + 1$

4. Assemble internal force vector and stiffness matrix using computed at the element level and at each integration point current total stress $\boldsymbol{\sigma}_{n+1}^{(i+1)\text{tot}}$ and current tangent stiffness matrix $\mathbf{D}_{n+1}^{\text{ep}}$ (an elastic stress state is computed via formula $\boldsymbol{\sigma}_{n+1}^{(i+1)\text{e}} = \boldsymbol{\sigma}_n + \Delta\boldsymbol{\sigma}_{0n+1} + \mathbf{D}^{\text{e}}(\Delta\boldsymbol{\varepsilon}_{n+1}^{(i+1)} - \Delta\boldsymbol{\varepsilon}_{n+1}^{\text{cr}} - \Delta\boldsymbol{\varepsilon}_{0n+1})$)

$$\mathbf{F}_{n+1}^{\text{int}\,(i+1)} = \mathop{\mathcal{A}}_{\text{e}=1,N} \int_{\Omega^{\text{e}}} \mathbf{B}^{\text{T}} \boldsymbol{\sigma}_{n+1}^{(i+1)\text{tot}} \ \mathrm{d}\Omega$$

$$\mathbf{K}_{n+1}^{(i+1)} = \mathop{\mathcal{A}}_{\text{e}=1,N} \int_{\Omega^{\text{e}}} \mathbf{B}^{\text{T}} \mathbf{D}_{n+1}^{\text{ep}(i+1)} \mathbf{B} \ \mathrm{d}\Omega$$

5. Solve system of equations

$$\mathbf{K}_{n+1}^{(i+1)} \, \Delta\mathbf{u}^{(i+1)} = \mathbf{F}_{n+1}^{\text{ext}} - \mathbf{F}_{n+1}^{\text{int}\,(i+1)}$$

   (for modified N–R technique assume $\mathbf{K}_{n+1}^{(i+1)} = \mathbf{K}_n$

   (for full N–R use curent $\mathbf{K}_{n+1}^{(i+1)}$ matrix)

6. Update accumulated increment of displacements: $\Delta\mathbf{u}_{n+1}^{(i+1)} = \Delta\mathbf{u}_{n+1}^{(i)} + \Delta\mathbf{u}^{(i+1)}$

7. If convergence of the iteration process has not been achieved go to step 1

Window 4-19

4.6.2 CONVERGENCE NORMS

RHS OUT OF BALANCE EUCLIDEAN NORM

ENERGY INCREMENT NORM

TOTAL ENERGY NORM

CONVERGENCE/DIVERGENCE/CONTINUATION STRATEGY

The right-hand side (RHS) out of balance Euclidean norm, total energy and incremental energy norms are used in the code to detect convergence or divergence of the Newton-Raphson iterations. These norms are evaluated separtely for solid and for fluid phases in case of two–phase computations. The RHS out of balance norm, incremental energy norm, and total energy norm are defined in Windows 4-20, 4-21, 4-22 respectively. Detection of convergence/divergence state and possible continuation strategy is setup inWindow 4-23.

> **Window 4-20: RHS-out of balance Euclidean norm**

The RHS-out of balance Euclidean norm is defined as follows:

$$\frac{\|\mathbf{F}_{n+1}^{\text{ext}} - \mathbf{F}_{n+1}^{\text{int}\,(i+1)}\|}{\|\mathbf{F}_{n+1}^{\text{ext}} - \mathbf{F}_{n}^{\text{int}}\|} \leq \text{TOL}$$

This norm is evaluated selectively for different degree of freedom (translations $\mathbf{u}$, rotations ϕ, pore pressures p^{F}, temperatures T and humidities W). The following table shows active RHS norms for different analysis types and different degrees of freedom ($+$ means active and - nonactive).

Analysis Type/DOF type	$\mathbf{u}$	p^{F}	ϕ	T	W
Deformation	+	+	$+^{(*)}$	-	-
Deformation+Flow	+	+	$+^{(*)}$	-	-
Flow	-	+	-	-	-
Heat transfer	-	-	-	+	-
Humidity transfer	-	-	-	-	+

The two following tollerances for RHS norm are used i.e. FTOL (set to 0.01 by default) and QTOL (set to 0.001 by default) related to solid phase DOF's and fluid phase DOF's respectively. The following table shows corresponding tollerances for selected DOF's.

DOF	Active tollerance TOL
$\mathbf{u}$	FTOL
p^{F}	QTOL
ϕ	FTOL
T	FTOL
W	FTOL

$^{(*)}$ The reference value, $\|\mathbf{F}_{n+1}^{\text{ext}} - \mathbf{F}_{n}^{\text{int}}\|$, related to rotational DOF's is set to $0.1\,\|\mathbf{F}_{n+1}^{\text{ext}} - \mathbf{F}_{n}^{\text{int}}\|^{u}\,L$ where L is some averaged finite element size, factor 0.1 has been assumed by rule of thumb and $\|\mathbf{F}_{n+1}^{\text{ext}} - \mathbf{F}_{n}^{\text{int}}\|^{u}$ is an Euclidean norm of the RHS corresponding to translational DOF's.

Window 4-20

Window 4-21: Energy increment norm

Th increment of energy and then the energy increment norm (valid for iteration $i \geq 2$) are evaluated as follows (for solid and fluid phase separately):

$$\Delta E_{n+1}^{\mathsf{S}(i+1)} = -\frac{1}{2}\mathbf{F}_{n+1}^{\mathsf{int}\,u(i+1)}\Delta\mathbf{u}^{(i+1)}$$

$$\Delta E_{n+1}^{\mathsf{F}(i+1)} = -\frac{1}{2}\mathbf{F}_{n+1}^{\mathsf{int}\,(i+1)}\Delta p^{\mathsf{F}\,(i+1)}$$

$$\frac{\Delta E_{n+1}^{\mathsf{S}(i+1)} - \Delta E_{n+1}^{\mathsf{S}(i)}}{\Delta E_{n+1}^{\mathsf{S}(i=2)}} \leq \mathsf{ESTOL} \quad \left(\text{ by default } \mathsf{ESTOL} = 10^{-3}\right)$$

$$\frac{\Delta E_{n+1}^{\mathsf{F}(i+1)} - \Delta E_{n+1}^{\mathsf{F}(i)}}{\Delta E_{n+1}^{\mathsf{F}(i=2)}} \leq \mathsf{EFTOL} \quad \left(\text{by default } \mathsf{EFTOL} = 10^{-3}\right)$$

Window 4-21

Window 4-22: Total energy norm

The total energy and then the total energy norm (valid for step $n > 1$) are evaluated as follows (separately for solid and fluid phase):

$$E_{n+1}^{\mathsf{S}(i+1)} = E_n^{\mathsf{S}} + \Delta E_{n+1}^{\mathsf{S}(i+1)}$$

$$E_{n+1}^{\mathsf{F}(i+1)} = E_n^{\mathsf{F}} + \Delta E_{n+1}^{\mathsf{F}(i+1)}$$

$$\frac{\Delta E_{n+1}^{\mathsf{S}(i+1)} - \Delta E_{n+1}^{\mathsf{S}(i)}}{E_n^{\mathsf{S}}} \leq \mathsf{ESTOL} \quad \left(\text{ by default } \mathsf{ESTOL} = 10^{-3}\right)$$

$$\frac{\Delta E_{n+1}^{\mathsf{F}(i+1)} - \Delta E_{n+1}^{\mathsf{F}(i)}}{E_n^{\mathsf{F}}} \leq \mathsf{EFTOL} \quad \left(\text{ by default } \mathsf{EFTOL} = 10^{-3}\right)$$

Window 4-22

Window 4-23: Convergence / divergence / continuation

Convergence strategy

The step is converged if all active RHS out of unbalance norms are satsfied simutaneously (see Window 4-20)

$$\frac{\|\mathbf{F}^{\text{ext}}_{n+1} - \mathbf{F}^{\text{int}\,(i+1)}_{n+1}\|}{\|\mathbf{F}^{\text{ext}}_{n+1} - \mathbf{F}^{\text{int}}_{n}\|} \leq \text{TOL} \quad (\text{FTOL/QTOL})$$

or if the following set of conditions is satisfied:

$$\frac{\|\mathbf{F}^{\text{ext}}_{n+1} - \mathbf{F}^{\text{int}\,(i+1)}_{n+1}\|}{\|\mathbf{F}^{\text{ext}}_{n+1} - \mathbf{F}^{\text{int}}_{n}\|} \leq 10 \ \text{TOL} \ (\text{for all active RHS norms})$$

$$\frac{\Delta E^{\text{S}(i+1)}_{n+1} - \Delta E^{\text{S}(i)}_{n+1}}{E^{\text{S}}_{n}} \leq \text{ESTOL}/10$$

$$\frac{\Delta E^{\text{F}(i+1)}_{n+1} - \Delta E^{\text{F}(i)}_{n+1}}{E^{\text{F}}_{n}} \leq \text{EFTOL}/10 \ (\text{if active})$$

Detection of divergence

The divergence of the iteration process is detected if the following set of conditions is satisfied:

$$\frac{\|\mathbf{F}^{\text{ext}}_{n+1} - \mathbf{F}^{\text{int}\,(i+1)}_{n+1}\|}{\|\mathbf{F}^{\text{ext}}_{n+1} - \mathbf{F}^{\text{int}}_{n}\|} \geq \xi \ (\text{for all active RHS norms})$$

$$\frac{\Delta E^{\text{S}(i+1)}_{n+1} - \Delta E^{\text{S}(i)}_{n+1}}{E^{\text{S}}_{n}} \geq \xi \quad \text{and} \quad \frac{\Delta E^{\text{F}(i+1)}_{n+1} - \Delta E^{\text{F}(i)}_{n+1}}{E^{\text{F}}_{n}} \geq \xi \ (\text{if active})$$

$$\frac{\Delta E^{\text{S}(i+1)}_{n+1} - \Delta E^{\text{S}(i)}_{n+1}}{\Delta E^{(i=2)\text{S}}_{n}} \geq \xi \quad \text{and} \quad \frac{\Delta E^{\text{F}(i+1)}_{n+1} - \Delta E^{\text{F}(i)}_{n+1}}{\Delta E^{(i=2)\text{F}}_{n}} \geq \xi \ (\text{if active})$$

For stability driver $\xi = 5.0$ and for all others $\xi = 10.0$.

Continuation strategy

In case when the maximum number of iterations is reached the following action is performed depending on the status of the check box 'Auto' in calculation window called 'Increase max. nr of iterations'. If it is ON (default setting) and all RHS out of balance norms are below value $1.0\,(100\%)$ then the maximum number of iterations is updated automaticaly (increased by 5) and the process continues unless the new updated maximum number of iterations overreaches the absolute maximum number of iterations (set in the menu under item Control). If this check box is OFF, when reaching current maximum number of iterations a dialog box will be displayed on a screen waiting for new maximum number of iterations to be defined by the user.

Window 4-23

4.6.3   INITIAL STATE ANALYSIS

The initial state in soil mechanics results essentially (but not exclusively) from gravity. The correct implementation of gravity requires simultaneous application (or superposition) of the gravity itself and the corresponding initial stresses, which may undergo additional constraints set by the user (initial state K_0 effect). The corresponding multistep algorithm is described in Window 4-24:

Window 4-24: Initial state multistep algorithm

Initialize:

- set time $t = 0$

- assume first gravity increment and increment size $\Delta\lambda$ for further steps

- set $\lambda = \lambda_0$

- set step counter $n = 0$

- for each element and for each integration point set $\Delta\boldsymbol{\sigma}_0 = \mathbf{0}$

1. Continue

2. Set counter of initial stress reevaluations (for superposition) $l = 0$

3. Set iteration counter $i = 0$

4. Continue

5. Evaluate equivalent partial gravity nodal load: $\mathbf{F}_g = \underset{e=1,N}{\mathcal{A}} \int_{\Omega^e} \mathbf{N}^{\mathrm{T}} \lambda \mathbf{b} \, \mathrm{d}\Omega$, where $\mathbf{b}$ is the gravity load

6. Accumulate total external force vector $\mathbf{F}^{\mathrm{ext}}_{n+1}$ adding to $\mathbf{F}_g$ additional external forces if needed (also weighted by the factor λ)

7. Evaluate corresponding stress state $\boldsymbol{\sigma}^{(i)}_{n+1}$ and constitutive tangent matrix $\mathbf{D}^{\mathrm{ep}(i)}_{n+1}$ for given $\Delta\mathbf{u}^{(i)}_{n+1}$, $\Delta\boldsymbol{\varepsilon}^{(i)}_{n+1} = \mathbf{B}\,\Delta\mathbf{u}^{(i)}_{n+1}$ and given $\Delta\boldsymbol{\sigma}_0$, using the following expression:

$$\boldsymbol{\sigma}^{(i)}_{n+1} = \boldsymbol{\sigma}_n + \Delta\boldsymbol{\sigma}_0 + \mathbf{D}^{\mathrm{e}}(\Delta\boldsymbol{\varepsilon}^{(i)}_{n+1} - \Delta\boldsymbol{\varepsilon}^{\mathrm{p}(i)}_{n+1})$$

where the increment of plastic strain $\Delta\boldsymbol{\varepsilon}^{\mathrm{p}(i)}_{n+1}$ and $\mathbf{D}^{\mathrm{ep}(i)}_{n+1}$ are obtained from return mapping algorithm

8. Assemble internal forces (adding the effect of initial pore pressures if needed, here pore pressures are also weighted by the current gravity multiplier λ)

$$\mathbf{F}^{\mathrm{int}\,(i)}_{n+1} = \underset{e=1,N}{\mathcal{A}} \int_{\Omega^e} \mathbf{B}^{\mathrm{T}} \left(\boldsymbol{\sigma}^{(i)}_{n+1} + \boldsymbol{\delta}^{\mathrm{T}} \lambda p^{\mathsf{F}\,(i)}_{n+1} \right) \, \mathrm{d}\Omega$$

9. Assemble stiffness matrix: $\mathbf{K} = \underset{e=1,N}{\mathcal{A}} \int_{\Omega^e} \mathbf{B}^{\mathrm{T}} \mathbf{D}^{\mathrm{ep}(i)}_{n+1} \mathbf{B} \, \mathrm{d}\Omega$

November 6, 2023   QuickHelp   DataPrep   Benchmarks   Tutorials

ZSoil®-3D-2PHASE v.2023   TM−129

10. Solve system of equations: $\mathbf{K}\,\boldsymbol{\Delta}\mathbf{u}^{(i+1)} = \mathbf{F}^{\text{ext}}_{n+1} - \mathbf{F}^{\text{int}\,(i)}_{n+1}$

11. Update accumulated increment of displacements and strains: $\boldsymbol{\Delta}\mathbf{u}^{(i+1)}_{n+1} = \boldsymbol{\Delta}\mathbf{u}^{(i)}_{n+1} + \boldsymbol{\Delta}\mathbf{u}^{(i+1)}$, $\Delta\boldsymbol{\varepsilon}^{(i+1)}_{n+1} = \mathbf{B}\,\boldsymbol{\Delta}\mathbf{u}^{(i+1)}_{n+1}$

12. If convergence of the iteration process has not been achieved set $i = i + 1$ and go to step 3

13. Increase $l = l + 1$

14. IF $l <$MAX_REPEAT (by default MAX_REPEAT=2) then

    – Update the initial stress increment $\Delta\sigma_0$ (via procedure given in Window 4-25 Initial stress increment correction

    – Repeat last step introducing corrected initial stresses, GO TO step 2

15. Set : $\boldsymbol{\Delta}\mathbf{u}_{n+1} = \boldsymbol{\Delta}\mathbf{u}^{(i+1)}_{n+1} = \mathbf{0}$, $\Delta\boldsymbol{\varepsilon}_{n+1} = \Delta\boldsymbol{\varepsilon}^{(i+1)}_{n+1} = \mathbf{0}$

16. If $n < n_{\max}$ set $n = n + 1$, $\lambda = \lambda + \Delta\lambda$ and GO TO step 1

Window 4-24

Window 4-25: Initial stress increment correction

Correction of the assumed initial stresses is done based on the previous stress state $\boldsymbol{\sigma}_n$, current stress state $\boldsymbol{\sigma}_{n+1}$ and additional set of constraints which include the effect of K_0 (the ratio between selected normal stress components can be defined in a local coordinate system defined by the user). We assume that the y component of the stress state is computed accurately and we want to fulfil the conditions : $\sigma_x^{(*)}/\sigma_y^{(*)} = K_{ox}$ and $\sigma_z^{(*)}/\sigma_y^{(*)} = K_{oz}$. The following steps lead to the evaluation of corrected initial stress increment $\Delta\boldsymbol{\sigma}_0$.

1. Transform $\boldsymbol{\sigma}_{n+1} \to \boldsymbol{\sigma}^{(*)}_{n+1}, \boldsymbol{\sigma}_n \to \boldsymbol{\sigma}^{(*)}_n$ (upper index $(*)$ means local system, one in which K_0 has been set up)

2. Compute stress increment between n and $n + 1$ steps: $\Delta\boldsymbol{\sigma}^{(*)}_{n+1} = \boldsymbol{\sigma}^{(*)}_{n+1} - \boldsymbol{\sigma}^{(*)}_n$

3. Assume : $\Delta\boldsymbol{\sigma}^{(*)}_0 = \Delta\boldsymbol{\sigma}^{(*)}_{n+1}$

4. IF K_{0x} is specified by the user then correct $\Delta\sigma^{(*)\,3}_{0x}$: $\Delta\sigma^{(*)}_{0x} = K_{0x}\,\Delta\sigma^{(*)}_{0y}$

5. IF K_{0z} is specified by the user then correct $\Delta\sigma^{(*)}_{0z}$: $\Delta\sigma^{(*)}_{0z} = K_{0z}\,\Delta\sigma^{(*)}_{0y}$

6. Transform $\Delta\boldsymbol{\sigma}^{(*)}_0$ from local K_0 system to global one: $\Delta\boldsymbol{\sigma}^{(*)}_0 \to \Delta\boldsymbol{\sigma}_0$

Window 4-25

---

[3]Specification of K_0 can be done exclusively in confined directions

4.6.4   STABILITY ANALYSIS

The available definitions of safety factors were introduced in Appendix 3.8.1, i.e.

1. χ, such that global instability corresponds to

$$\boldsymbol{\sigma}_{\text{global failure}} = \sigma_m \boldsymbol{\delta} + \chi \mathbf{s}$$

where χ is a uniform deviatoric stress multiplier in the domain. From the implementation point of view the approach amounts to a progressive modification of the yield criteria parameters until failure occurs.

2. Alternatively for two-parameter $(C - \phi)$ criteria, can be used

$$\mathsf{SF}_2 = \left| \frac{\int_{\Gamma_s} \tau_y \, d\Gamma_s}{\int_{\Gamma_s} \tau \, d\Gamma_s} \right|$$

where $\tau_y = C + \underline{\sigma}'_n \tan \phi'$ is the yield stress according to the Mohr–Coulomb criterion, C the cohesion, $\underline{\sigma}'_n$ the effective normal stress, ϕ the friction angle, SF_2 the safety factor and Γ_s defines the sliding surface. An algorithm which fits the plasticity based approach can be deduced from the above equation; rewriting the equation as

$$\int_{\Gamma_s} \tau \, d\Gamma_s = \frac{\int_{\Gamma_s} \tau_y \, d\Gamma_s}{\mathsf{SF}_2} = \frac{\int_{\Gamma_s} \left(C + \underline{\sigma}'_n \tan \phi' \right) d\Gamma_s}{\mathsf{SF}_2}$$

it is observed that SF_2 can be viewed as the dividing factor of C and $\tan\phi'$ for which instability is reached.

The stability algorithm is summarized in Window 4-26

Window 4-26: Stability algorithm for SF=SF2

1. Initialization

   Set $\mathsf{SF}_n = \mathsf{SF}_0$ (start with the prescribed lower bound of the safety factor SF_0)

2. For each step

$$\mathsf{SF}_{n+1} = \mathsf{SF}_n + \Delta\mathsf{SF} \text{ (increment the safety factor)}$$
$$C_{n+1} = \frac{C}{\mathsf{SF}_{n+1}} \text{(scale the cohesion)}$$
$$\tan \phi'_{n+1} = \frac{\tan \phi'}{\mathsf{SF}_{n+1}} \text{(scale the tangens of friction angle)}$$

3. Solve the boundary-value problem, iterate as needed

4. Go to 2 until divergence occurs

5. At divergence $\mathsf{SF}_n \leq \mathsf{SF} \leq \mathsf{SF}_{n+1}$; estimate of the safety factor

---

Window 4-26

Remarks:

1. Notice that the material characteristics are modified by the algorithm, which is, strictly speaking, only valid 'close' to SF$= 1$.

2. Divergence is normally accompanied by a localized strain field on a slip surface, in which SF corresponds to the given definition.

3. Let SF$_2$ be the default definition of the safety factor for two-parameter $(C - \phi)$ criteria.

4.6.5 ULTIMATE LOAD ANALYSIS

An ultimate load analysis follows the classical Newton–Raphson scheme. Computation are pursued until divergence is reached. Refer to Section 4.6.1. The simulation of drained behaviour should be done using drivers as for 1–phase or 2–phase medium but using large time step. The undrained behavior can be done only with 2–phase algorithm (Section 4.6.6).

4.6.6 CONSOLIDATION ANALYSIS

The consolidation algorithm simulates the transient behavior of the two–phase medium. The time step can vary starting from small values at the beginning up to large steps at the end of the process. The only limitation is that minimum time step should be greater than the critical one estimated via following relation:

$$\Delta t \geq \Delta t_{\text{crit}} = \frac{\gamma^{\text{F}} h^2}{E_{\text{oed}} \theta \ k} \left[\frac{1}{4} + \frac{1}{6} E_{\text{oed}} \ c \right] \tag{4.2}$$

where:

c — compressibility of fluid $= n/\beta_{\text{F}}$; $\quad n$ − porosity, $\quad \beta_{\text{F}}$ − fluid bulk modulus

k — Darcy coefficient

γ^{F} — fluid specific weight

θ — integration coefficient (in Z_SOIL $\theta = 1$)

$E_{\text{oed}} = \dfrac{E \left(1 - \nu \right)}{\left(1 + \nu \right) \left(1 - 2\nu \right)}$ — oedometric stiffness modulus

h — element size.

The one-dimensional test is taken as the basis for the estimation. The condition for nonoscillatory pore pressure distribution can be formulated as $p^{\text{F}} \geq \dfrac{\sigma^{\text{tot}}}{1 + E_{\text{oed}} c}$ (with a positive sign for tensile stresses). In the incompressibility limit $(c = 0)$ this condition means that the stress transferred by the fluid cannot be higher then the total stress value. The estimate will be derived for linear two-node element with an equal interpolation for displacements and pressures. Let us take a mesh which consists of a single finite element, as shown in following figure, and assume that the initial pressure is zero. Solving the resulting system of equations
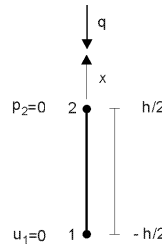
One-dimensional test

with the set of the boundary conditions $\left(u_1 = 0 \text{ and } p_2 = 0 \right)$ we obtain the following value for the pressure increment in the first time step:

$$\Delta p_1 = -\frac{\dfrac{qh}{2E_{\text{oed}}}}{\dfrac{h}{4E_{\text{oed}}} + c\dfrac{h}{3} + \dfrac{\theta \ k \Delta t}{\gamma^{\text{F}}} \dfrac{1}{h}} \tag{4.3}$$

From the consistency condition, which in a general case can be expressed in the form,(see [4]):

$$\Delta p_1 \geq -\frac{q}{1 + E_{\text{oed}} \ c} \tag{4.4}$$

---

[4]Vermeer P., Verruijt A." An accuracy condition for consolidation by finite elements". Int.J.Numer.Anal.Meth.Geomech.**5**, p.1-14, 1981

the condition given in eq. 4.2 for the time step Δt is derived.

Remark:To avoid this restrictive condition the two-phase stabilization method is available in Z_Soil program.

4.6.7   CREEP ANALYSIS

Creep introduces a time dependent deformation at constant or variable stress. The implementation scheme is summarized in Sect. 4.6.1. An important aspect is that the current formulation does not produce creeping effect due to initial stresses. The phenomenon starts due to stress variation starting at time at which the creep is activated. This means that for example the effect of secondary consolidation understood as a result of creeping should be modelled running the consolidation and creep simultaneously. Since creep is a time dependent process it requires therefore a time stepping procedure, which is shown in Window 4-27.

4.6.8   LOAD FUNCTION AND TIME STEPPING PROCEDURE

For time dependent processes like creep, consolidation, transient flow, each item consisting load or prescribed boundary condition may have attached a function describing its variability in time (physical or pseudo) during the process. This is called a `Load Time Function` and is defined as a list of pairs (t_k, v_k), as shown in Window 4-27 assuming linear interpolation for intermediate points. Different loads acting on the model may have attached different load time functions, but its argument must be common for all time function in a job. It must have the meaning of a physical time (consistently with constitutive data) for such a `Time Dependent` problems as: `Transient Fluid, Heat, Humidity Flow, Creep, Consolidation`, while for the remaining (i.e. `Driven Load, Deformation, all Steady State`) ones, may be treated as the non-physical one.
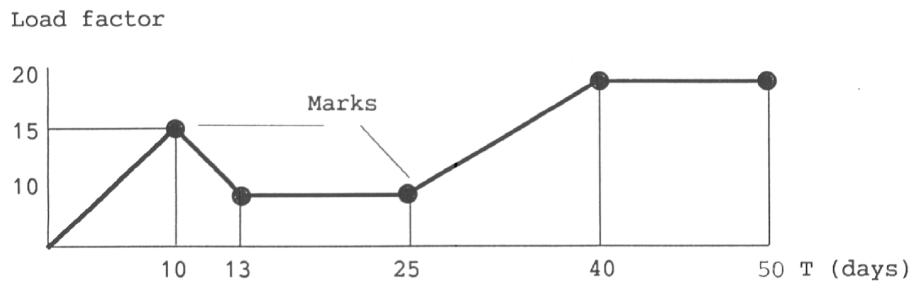
| **Window 4-27: Time stepping procedure** |

•**Load time history**

Applied loads are characterized by a prescribed load amplitude and a load multiplier (load factor). At time t_{n+1} the applied load is then

$$\mathbf{F}_{n+1} = \mathbf{F}_0 LF_{n+1}.$$

The load factor LF is defined as a function of time. Each load can be associated with a different load factor.

Load time–history

•**Time step**

The time dependent processes start always with the initial time step increment defined by the user $\Delta t_1 = \Delta t_{\text{BEG}}$. Each next time step is predicted through relation $\Delta t_{n+1} = \Delta t_n \times \Delta t_{\text{MULT}}$ with time multiplier Δt_{MULT} defined by the user. This next time step increment can be corrected automatically by the system if in between $t_n \Leftrightarrow t_n + \Delta t_{n+1}^{\text{predicted}}$ at least one of the existence functions changes its value (from OFF to ON or vice versa) or some characteristic point on one of the load time functions is detected. Once such situation is detected the time step increment is reset to the initial value Δt_{BEG}.

| Window 4-27 |

4.6.9   SIMULATION OF EXCAVATION AND CONSTRUCTION STAGES

The simulation of excavation/construction stages is normally embedded in every time dependent driver (driven load / consolidation etc..). This type of simulation requires a stiffness update at each excavation stage. The corresponding appropriate algorithmic choice is done automatically by the system.

On the other hand, the input mesh must correspond to the maximal mesh. This may correspond to the final stage in a construction simulation or to the initial state for an excavation simulation.

Management of stiffness

The simulation of construction stages leads to a variable size of the stiffness matrix and therefore to a variable number of nodes and elements. This requires additional data management. The input mesh must correspond to the maximal mesh. The corresponding node and element numbering will be kept throughout the analysis.

At each excavation stage an optimization of the nodal numbering will be performed, and a correspondence table with the input-output node numbering will be established. The optimized mesh node numbering is used for analysis purposes.

Progressive unloading after excavation

If no LTF (unloading function) is specified for excavated elements, interaction forces from excavated media will vanish immediately at the moment of excavation. In the case of elasto-plastic media this may cause difficulties in obtaining converged solution. To prevent this, **progressive unloading after excavation** can be used which helps the system to redistribute stresses in the surroundings of the excavated domain, and in consequence to obtain convergent solution concerning new equilibrium state.

Unloading after excavation can be controlled. The interaction force between the excavated and the remaining medium will be computed by performing

$$\mathbf{F}^{\text{intEXC}} = \int\limits_{\Omega^{\text{exc}}} \mathbf{B}^{\text{T}} \boldsymbol{\sigma}^{\text{tot}} \ \mathrm{d} \cdot \left\{ \begin{array}{l} LTF(t) \\ \quad 0 \text{ if no unloading function is given} \end{array} \right\}$$

over the excavated medium. The association of a load time–history with this set of forces provides the means for the control of unloading. For more details see section 7.6.2.

Related Topics

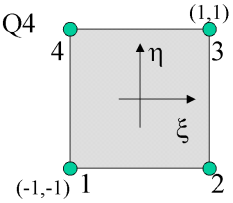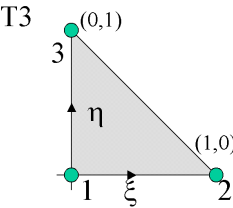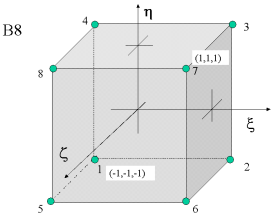- GEOTECHNICAL ASPECT. EXCAVATION, CONSTRUCTION ALGORITHM
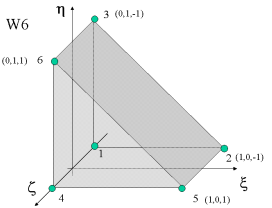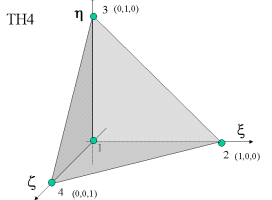
4.7   APPENDICES

SHAPE FUNCTIONS AND REFERENCE ELEMENTS FOR 2D/3D

NUMERICAL INTEGRATION DATA
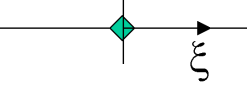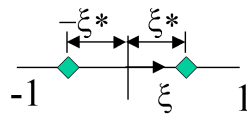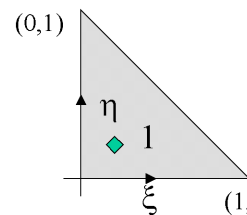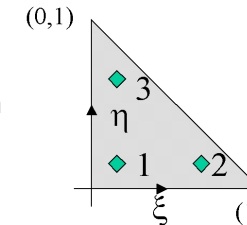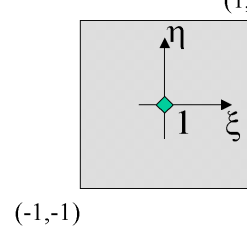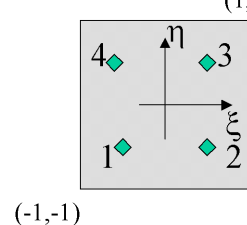
MULTISURFACE PLASTICITY CLOSEST POINT PROJECT ALGORITHM

SINGLE SURFACE PLASTICITY CLOSEST POINT PROJECTION ALGORITHM
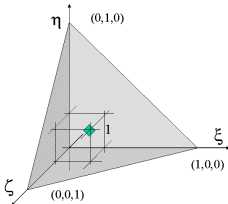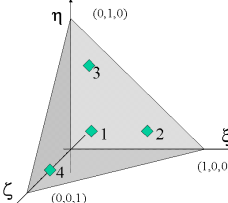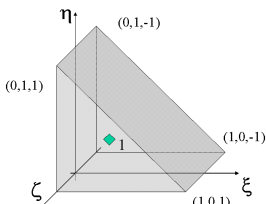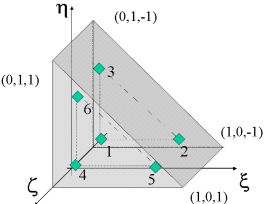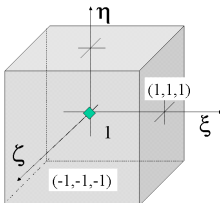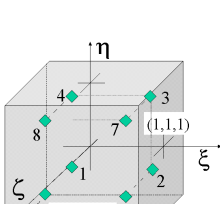
4.7.1   SHAPE FUNCTION DEFINITION AND REFERENCE ELEMENTS FOR 2/3 D

Reference element	Shape functions
	$N_i = \dfrac{1}{4}\left(1 + \xi\xi_i\right)\left(1 + \eta\eta_i\right) \Rightarrow \begin{cases} N_1 = \dfrac{1}{4}\left(1 - \xi\right)\left(1 - \eta\right) \\ N_2 = \dfrac{1}{4}\left(1 + \xi\right)\left(1 - \eta\right) \\ N_3 = \dfrac{1}{4}\left(1 + \xi\right)\left(1 + \eta\right) \\ N_4 = \dfrac{1}{4}\left(1 - \xi\right)\left(1 + \eta\right) \end{cases}$
	$N_1 = 1 - \xi - \eta$ $N_2 = \xi$ $N_3 = \eta.$

	$N_i = \dfrac{1}{8}\left(1 + \xi_i\xi\right)\left(1 + \eta_i\eta\right)\left(1 + \zeta_i\zeta\right) \Rightarrow$ $\begin{cases} N_1 = \dfrac{1}{8}\left(1 - \xi\right)\left(1 - \eta\right)\left(1 - \zeta\right), & N_5 = \dfrac{1}{8}\left(1 - \xi\right)\left(1 - \eta\right)\left(1 + \zeta\right) \\ N_2 = \dfrac{1}{8}\left(1 + \xi\right)\left(1 - \eta\right)\left(1 - \zeta\right), & N_6 = \dfrac{1}{8}\left(1 - \xi\right)\left(1 - \eta\right)\left(1 + \zeta\right) \\ N_3 = \dfrac{1}{8}\left(1 + \xi\right)\left(1 + \eta\right)\left(1 - \zeta\right), & N_7 = \dfrac{1}{8}\left(1 - \xi\right)\left(1 - \eta\right)\left(1 + \zeta\right) \\ N_4 = \dfrac{1}{8}\left(1 - \xi\right)\left(1 + \eta\right)\left(1 - \zeta\right), & N_8 = \dfrac{1}{8}\left(1 - \xi\right)\left(1 - \eta\right)\left(1 + \zeta\right) \end{cases}$
	$N_i = \dfrac{1}{2}\left(1 + \zeta_i\zeta\right) N_{k(i)}^{\mathsf{T3}}\left(\xi, \eta\right)$ where: $k\left(i\right) = \left(i - 1\right)\bmod 3 + 1$
	$N_1 = 1 - \xi - \eta - \zeta$ $N_2 = \xi$ $N_3 = \eta$ $N_4 = \zeta$

4.7.2   NUMERICAL INTEGRATION DATA FOR DIFFERENT ELEMENTS IN 1/2/3D

$$\xi^* = \frac{\sqrt{3}}{3} = 0.5773502691896$$

Element shape	Integration points				
	number	Positions			Weigthing
	N_gauss	$i:$	ξ_i	η_i	factors W_i
	1	1	0.0		2.0
	2	1 : 2 :	$-\xi^*$ ξ^*		1.0 1.0
	1	1:	0.33333	0.33333	0.5
	2	1 : 2 : 3 :	0.16666 0.16666 0.66666	0.16666 0.66666 0.16666	0.16666 0.16666 0.16666
	1	1:	0.0	0.0	4.0
	2×2=4	1 : 2 : 3 : 4 :	$-\xi^*$ ξ^* ξ^* $-\xi^*$	$-\xi^*$ $-\xi^*$ ξ^* ξ^*	1.0 1.0 1.0 1.0

Element shape	number N_{gauss}	Integration points				
			Positions			Weigthing factors W_i
		$i:$	ξ_i	η_i	ζ_i	
	1	1:	0.25	0.25	0.25	0.16666
	4	1 :	0.13819	0.13819	0.13819	0.04166
		2 :	0.58541	0.13819	0.13819	0.04166
		3 :	0.13819	0.58541	0.13819	0.04166
		4 :	0.13819	0.13819	0.58541	0.04166
	1	1:	0.33333	0.33333	0.0	1.0
	$2 \times 3 = 6$	1 :	0.166666	0.166666	$-\xi^*$	0.166666
		2 :	0.666666	0.166666	$-\xi^*$	0.166666
		3 :	0.166666	0.666666	$-\xi^*$	0.166666
		4 :	0.166666	0.166666	ξ^*	0.166666
		5 :	0.666666	0.166666	ξ^*	0.166666
		6 :	0.166666	0.666666	ξ^*	0.166666
	1	1:	0.0	0.0	0.0	1.0
	$2 \times 2 \times 2$ $=$ 8	1 :	$-\xi^*$	$-\xi^*$	$-\xi^*$	1.0
		2 :	ξ^*	$-\xi^*$	$-\xi^*$	1.0
		3 :	ξ^*	ξ^*	$-\xi^*$	1.0
		4 :	$-\xi^*$	ξ^*	$-\xi^*$	1.0
		5 :	$-\xi^*$	$-\xi^*$	ξ^*	1.0
		6 :	ξ^*	$-\xi^*$	ξ^*	1.0
		7 :	ξ^*	ξ^*	ξ^*	1.0
		8 :	$-\xi^*$	ξ^*	ξ^*	1.0

4.7.3 MULTISURFACE PLASTICITY CLOSEST POINT PROJECTION ALGORITHM

A generalized, unconditionally stable, algorithm designed for the integration of constitutive equations for class of multisurface elasto–plastic models is presented here. This subject has been worked out first by Simo & Hughes but procedures described therein were not as general as needed. Three crucial problems e.a.: selection of the reduced set of active mechanisms solving the plastic corrector problem in case when the number of active mechanisms is greater than the stress space dimension , activation of initially nonactive plastic mechanisms due to effects of hardening/softening and finally definition of the general form of a consistent tangent matrix for multimechanism models with generally nonassociated flow rule, and including hardening/softening, were introduced later by Szarliński and Truty. Slightly modified algorithm including an additional substeping scheme is described here. The complete set of information on Multisurface Closest Point Projection Stress Return Algorithm (MCPPSS) can be found in the following Windows:

Notation

Basic set of equations

Consistent tangent operator $\mathbf{D^{ep}}$

Window 4-28: Notation

M	—	number of all plastic mechanisms,
Jact	—	actual set of active plastic mechanisms,
α	—	mechanism index,
$^a\gamma = \dot{\gamma}\Delta t$	—	plastic multiplier value,
$^\alpha\mathbf{r}\,(\boldsymbol{\sigma},\mathbf{q})$	—	flow vector,
$^\alpha\mathbf{h}\,(\boldsymbol{\sigma},\mathbf{q})$	—	column matrix of hardening/softening functions,
$^\alpha\mathbf{q}$	—	column matrix of plastic (hardening/softening) parameters
ε^p	—	column matrix of total plastic strains,
$^\alpha F$	—	the value of plasticity condition for given stress state and plastic parameters
$\mathbf{D}$	—	elastic stiffness matrix
$\mathbf{C}$	—	elastic compliance matrix
k	—	index of previous closest point projection algorithm iteration
$k+1$	—	index of actual iteration
n	—	index of last configuration of equilibrium
$n+1$	—	index of actual configuration of equilibrium

Window 4-28

Window 4-29: Set of basic equations

The integration of constitutive equations for any elasto–plastic model consists of two stages e.g. elastic predictor and plastic corrector one. Assuming the fully implicit integration scheme

for plastic strains and hardening/softening parameters this second stage is expressed by the following set of equations which is the basis of the closest point projection algorithm (**in the following windows this will be called the basic set of equations**):

$$
\left.
\begin{aligned}
\boldsymbol{\varepsilon}_{n+1}^{\mathsf{p}(k+1)} &= \boldsymbol{\varepsilon}_n^{\mathsf{p}} + \sum_{\alpha=1,M} {}^{\alpha}\gamma_{n+1}^{(k+1)}\; {}^{\alpha}\mathbf{r}_{n+1}^{(k+1)} \\
\mathbf{q}_{n+1}^{(k+1)} &= \mathbf{q}_n + \sum_{\alpha=1,M} {}^{\alpha}\gamma_{n+1}^{(k+1)}\; {}^{\alpha}\mathbf{h}_{n+1}^{(k+1)} \\
{}^{\alpha}F_{n+1}^{(k+1)} &= {}^{\alpha}F_{n+1}^{(k)} + \Delta\; {}^{\alpha}F_{n+1}^{(k)} = 0 \quad \underset{\alpha\in\mathsf{Jact}}{\forall} \\
\Delta\boldsymbol{\sigma}_{n+1}^{(k+1)} &= -\mathbf{D}\Delta\boldsymbol{\varepsilon}_{n+1}^{\mathsf{p}(k)}
\end{aligned}
\right\}
$$

In most cases this system is nonlinear and Newton–Raphson procedure is needed for its solution. To apply this procedure the consistent linerization of the above set of equations has to be done. Denoting by $\mathbf{R}_\varepsilon$ and $\mathbf{R}_q$ the residuals of the first two equations which are defined by the following expressions:

$$
\mathbf{R}_\varepsilon = \boldsymbol{\varepsilon}_n^{\mathsf{p}} - \boldsymbol{\varepsilon}_{n+1}^{\mathsf{p}(k)} + \sum_{\alpha=1,M} {}^{\alpha}\gamma_{n+1}^{(k)}\; {}^{\alpha}\mathbf{r}_{n+1}^{(k)}
$$

$$
\mathbf{R}_q = \mathbf{q}_n - \mathbf{q}_{n+1}^{(k)} + \sum_{\alpha=1,M} {}^{\alpha}\gamma_{n+1}^{(k)}\; {}^{\alpha}\mathbf{h}_{n+1}^{(k)}
$$

the linearized system of first two equations of the basic set using expressions for $\mathbf{R}_\varepsilon$ and $\mathbf{R}_q$ and 4th equation from basic set is as follows (summation for $\underset{\alpha\in\mathsf{Jact}}{\forall}$):

$$
\left(\mathbf{A}_{n+1}^{(k)}\right)^{-1} = \begin{bmatrix} \mathbf{D} & \mathbf{0} \\ \mathbf{0} & -\mathbf{I} \end{bmatrix} \left\{ \begin{array}{c} \Delta\boldsymbol{\varepsilon}_{n+1}^{\mathsf{p}(k)} \\ \Delta\mathbf{q}_{n+1}^{(k)} \end{array} \right\} = \left\{ \begin{array}{c} \mathbf{R}_\varepsilon + \sum_{\alpha=1,M} {}^{\alpha}\gamma_{n+1}^{(k)}\; {}^{\alpha}\mathbf{r}_{n+1}^{(k)} \\ \mathbf{R}_q + \sum_{\alpha=1,M} {}^{\alpha}\gamma_{n+1}^{(k)}\; {}^{\alpha}\mathbf{h}_{n+1}^{(k)} \end{array} \right\}
$$

where:

$$
\mathbf{A}_{n+1}^{(k)} = \begin{bmatrix} \mathbf{D}^{-1} + \sum_{\alpha=1,M} {}^{\alpha}\gamma\dfrac{\partial\; {}^{\alpha}\mathbf{r}^{(k)}}{\partial\underline{\boldsymbol{\sigma}}} & \sum_{\alpha=1,M} {}^{\alpha}\gamma\dfrac{\partial\; {}^{\alpha}\mathbf{r}^{(k)}}{\partial\underline{\mathbf{q}}} \\ \sum_{\alpha=1,M} {}^{\alpha}\gamma\dfrac{\partial\; {}^{\alpha}\mathbf{h}^{(k)}}{\partial\boldsymbol{\sigma}} & \sum_{\alpha=1,M} {}^{\alpha}\gamma\dfrac{\partial\; {}^{\alpha}\mathbf{h}^{(k)}}{\partial\mathbf{q}} - \mathbf{I} \end{bmatrix}^{-1}.
$$

In order to find increments of plastic multipliers the third equation from basic set written for each mechanism ${}^{\alpha}F : \alpha\in\mathsf{Jact}$ has to be solved. After linearization it takes the form:

$$
{}^{\alpha}F_{n+1}^{(k+1)} = {}^{\alpha}F_{n+1}^{(k+1)} + \Delta\; {}^{\alpha}F_{n+1}^{(k)} = {}^{\alpha}F_{n+1}^{(k+1)} + \frac{\partial\; {}^{\alpha}F_{n+1}^{(k)}}{\partial\boldsymbol{\sigma}}\Delta\boldsymbol{\sigma}_{n+1}^{(k)} + \frac{\partial\; {}^{\alpha}F_{n+1}^{(k)}}{\partial\mathbf{q}}\Delta\mathbf{q}_{n+1}^{(k)} \qquad (1)
$$

It can be written in matrix form using 4-th equation from basic set which leads finally to the following:

$$
{}^{\alpha}F_{n+1}^{(k)} = \left[\frac{\partial\; {}^{\alpha}F_{n+1}^{(k)}}{\partial\boldsymbol{\sigma}}\mathbf{D} \quad -\frac{\partial\; {}^{\alpha}F_{n+1}^{(k)}}{\partial\underline{\mathbf{q}}} \right] \qquad (2)
$$

In the above equation vector of unknowns which consists of plastic strain and plastic variables increments can be eliminated via expression derived for $\left(\mathbf{A}_{n+1}^{(k)}\right)^{-1}$ and finally after some matrix manipulations this expression can be rewritten in the form:

$$
\mathbf{U}_{n+1}^{(k)}\mathbf{A}_{n+1}^{(k)}\mathbf{P}_{n+1}^{(k)}\Delta\boldsymbol{\gamma}^{(k)} = \mathbf{f}_{n+1}^{(k)} - \mathbf{U}_{n+1}^{(k)}\mathbf{A}_{n+1}^{(k)}\mathbf{R}_{n+1}^{(k)}
$$

where:

$$\mathbf{R}_{n+1}^{(k)} = \left\{ \begin{array}{c} \mathbf{R}_{\varepsilon} \\ \mathbf{R}_q \end{array} \right\}$$

$$\mathbf{P}_{n+1}^{(k)} = \left[\begin{array}{ccc} \mathbf{r}^{\alpha_1} & \ldots & \mathbf{r}^{\alpha_N} \\ \mathbf{h}^{\alpha_1} & \ldots & \mathbf{h}^{\alpha_n} \end{array} \right]$$

$$\mathbf{U}_{n+1}^{(k)} = \left[\begin{array}{cc} \left(\dfrac{\partial f^{\alpha_1}}{\partial \boldsymbol{\sigma}} \right)^{\mathrm{T}} & \left(\dfrac{\partial f^{\alpha_1}}{\partial \mathbf{q}} \right)^{\mathrm{T}} \\ \vdots & \vdots \\ \left(\dfrac{\partial f^{\alpha N}}{\partial \boldsymbol{\sigma}} \right)^{\mathrm{T}} & \left(\dfrac{\partial f^{\alpha N}}{\partial \mathbf{q}} \right)^{\mathrm{T}} \end{array} \right]$$

Window 4-29

Window 4-30: Consistent tangent operator $\mathbf{D}^{\mathsf{ep}}$

The general definition of the tangent matrix is as follows:

$$\mathbf{D}^{\mathsf{ep}} = \frac{\mathrm{d}\boldsymbol{\sigma}}{\mathrm{d}\boldsymbol{\varepsilon}}.$$

This definition after introducing of the applied integration scheme leads to the so called consistent tangent matrix. The starting point for its derivation is the basic set of equations given in Window 4-29 which expresses the fully implicit scheme applied for the integration of plastic strains and plastic variables. All next steps will lead to derivation of the relation between $\mathrm{d}\boldsymbol{\sigma} - \mathrm{d}\boldsymbol{\varepsilon}$ and encapsulating from it the algorithmic constitutive operator. To do that let's differentiate this basic set of equations which yields:

$$\begin{aligned}
\mathrm{d}\boldsymbol{\varepsilon}^{\mathsf{p}} &= \sum_{\alpha=1,M} {}^{\alpha}\gamma \frac{\partial \, {}^{\alpha}\mathbf{r}}{\partial \boldsymbol{\sigma}} \mathrm{d}\boldsymbol{\sigma} + \sum_{\alpha=1,M} {}^{\alpha}\gamma \frac{\partial \, {}^{\alpha}\mathbf{r}}{\partial \mathbf{q}} \mathrm{d}\mathbf{q} + \sum_{\alpha=1,M} {}^{\alpha}\mathrm{d}\gamma^{\alpha}\mathbf{r} \\
\mathrm{d}\mathbf{q} &= \sum_{\alpha=1,M} {}^{\alpha}\gamma \frac{\partial \, {}^{\alpha}\mathbf{h}}{\partial \boldsymbol{\sigma}} \mathrm{d}\boldsymbol{\sigma} + \sum_{\alpha=1,M} {}^{\alpha}\gamma \frac{\partial \, {}^{\alpha}\mathbf{h}}{\partial \mathbf{q}} \mathrm{d}\mathbf{q} + \sum_{\alpha=1,M} {}^{\alpha}\mathrm{d}\gamma^{\alpha}\mathbf{h} \\
\mathrm{d}\,{}^{\alpha}F &= \frac{\partial \, {}^{\alpha}F}{\partial \boldsymbol{\sigma}} \mathrm{d}\boldsymbol{\sigma} + \frac{\partial \, {}^{\alpha}F}{\partial \mathbf{q}} \mathrm{d}\mathbf{q} = 0; \qquad \mathop{\forall}_{\alpha \in \mathsf{Jact}} \\
\mathrm{d}\boldsymbol{\sigma} &= \mathbf{D}\left(\mathrm{d}\boldsymbol{\varepsilon} - \mathrm{d}\boldsymbol{\varepsilon}^{\mathsf{p}} \right)
\end{aligned}$$

Considering only first two equations from the above set and eliminating the increment of plastic strains using fourth equation we can write the following matrix equation:

$$\underbrace{\left[\begin{array}{cc} \mathbf{C} + \sum_{\alpha=1,M} {}^{\alpha}\gamma \dfrac{\partial \, {}^{\alpha}\mathbf{r}}{\partial \boldsymbol{\sigma}} & \sum_{\alpha=1,M} {}^{\alpha}\gamma \dfrac{\partial \, {}^{\alpha}\mathbf{r}}{\partial \mathbf{q}} \\ \sum_{\alpha=1,M} {}^{\alpha}\gamma \dfrac{\partial \, {}^{\alpha}\mathbf{h}}{\partial \boldsymbol{\sigma}} & \sum_{\alpha=1,M} {}^{\alpha}\gamma \dfrac{\partial \, {}^{\alpha}\mathbf{h}}{\partial \mathbf{q}} - \underline{\mathbf{I}} \end{array} \right]}_{\mathbf{A}^{-1}} \left(\begin{array}{c} \mathrm{d}\boldsymbol{\sigma} \\ \mathrm{d}\mathbf{q} \end{array} \right) = \left(\begin{array}{c} \mathrm{d}\boldsymbol{\varepsilon} \\ \mathbf{0} \end{array} \right) - \left(\begin{array}{c} \sum_{\alpha=1,M}^{\alpha} \mathrm{d}\gamma^{\alpha}\mathbf{r} \\ \sum_{\alpha=1,M}^{\alpha} \mathrm{d}\gamma^{\alpha}\mathbf{h} \end{array} \right)$$

Let us evaluate the stress increment considering once again the fourth equation from linearized

basic set

$$d\boldsymbol{\sigma} = \mathbf{D}\,(\,d\boldsymbol{\varepsilon} - d\boldsymbol{\varepsilon}^{\mathbf{p}}) = \mathbf{D}\left(\sum_{\alpha=1,M}{}^{\alpha}\gamma\frac{\partial\,{}^{\alpha}\mathbf{r}}{\partial\boldsymbol{\sigma}}\,d\boldsymbol{\sigma} - \sum_{\alpha=1,M}{}^{\alpha}\gamma\frac{\partial\,{}^{\alpha}\mathbf{r}}{\partial\mathbf{q}}\,d\mathbf{q} - \sum_{\alpha=1,M}d\,{}^{\alpha}\gamma\,{}^{\alpha}\mathbf{r}\right)$$

$$= \mathbf{D}\left(d\boldsymbol{\varepsilon} - \underbrace{\left[\sum_{\alpha=1,M}{}^{\alpha}\gamma\frac{\partial\,{}^{\alpha}\mathbf{r}}{\partial\boldsymbol{\sigma}}\quad\sum_{\alpha=1,M}{}^{\alpha}\gamma\frac{\partial\,{}^{\alpha}\mathbf{r}}{\partial\mathbf{q}}\right]}_{\mathbf{a}}\left[\begin{array}{c}d\boldsymbol{\sigma}\\d\mathbf{q}\end{array}\right] - \sum_{\alpha=1,M}d\,{}^{\alpha}\gamma\,{}^{\alpha}\mathbf{r}\right).$$

By elimination of the plastic strain differential from the above equation we can rewrite as:

$$d\boldsymbol{\sigma} = \mathbf{D}\left(d\boldsymbol{\varepsilon} - \mathbf{aA}\left[\begin{array}{c}d\boldsymbol{\varepsilon}\\\mathbf{0}\end{array}\right] + \mathbf{aA}\left[\begin{array}{c}\sum\limits_{\alpha=1,M}d\,{}^{\alpha}\gamma\,{}^{\alpha}\mathbf{r}\\\sum\limits_{\alpha=1,M}d\,{}^{\alpha}\gamma\,{}^{\alpha}\mathbf{h}\end{array}\right]\right).$$

Let us introduce some auxiliary matrices to simplify further derivations:

– matrix $\widetilde{\mathbf{r}}$ which consists of column stored flow vectors for each active mechanism　　$\widetilde{\mathbf{r}} = [\mathbf{r}_1,\ldots,\mathbf{r}_N]$

– vector of plastic multiplier increments:　　$d\boldsymbol{\gamma} = \left[\begin{array}{c}d\gamma_1\\\vdots\\d\gamma_N\end{array}\right]$

– matrix $\mathbf{K}_{\;[(\text{NSTRE}+\text{NHARD})\times\text{NSTRE}]} : \mathbf{K} = \left[\begin{array}{c}\mathbf{I}\\\mathbf{0}\end{array}\right].$

With these defnitions one can reform the equation for $d\boldsymbol{\sigma}$:

$$d\boldsymbol{\sigma} = \mathbf{D}\left\{d\boldsymbol{\varepsilon} - \mathbf{aA}\left[\begin{array}{c}d\boldsymbol{\varepsilon}\\\mathbf{0}\end{array}\right] + (\mathbf{aAP} - \widetilde{\mathbf{r}})\,d\boldsymbol{\gamma}\right\}$$

but still it is necessary to define vector $d\boldsymbol{\gamma}$. It can be done writing appropriate consistency condition for each active mechanism. Thus for all (NJACT) active mechanisms one gets the following system

$$\left[\begin{array}{cc}\dfrac{\partial\,{}^{\alpha}F}{\partial\boldsymbol{\sigma}} & \dfrac{\partial\,{}^{\alpha}F}{\partial\mathbf{q}}\\\vdots & \vdots\\\dfrac{\partial\,{}^{N}F}{\partial\boldsymbol{\sigma}} & \dfrac{\partial\,{}^{N}F}{\partial\mathbf{q}}\end{array}\right]\left[\begin{array}{c}d\boldsymbol{\sigma}\\d\mathbf{q}\end{array}\right] = \left[\begin{array}{c}0\\\vdots\\0\end{array}\right].$$

Eliminating vector of unknowns the expression for increments of plastic multipliers will take finally the form:

$$d\boldsymbol{\gamma} = (\mathbf{UAP})^{-1}\,\mathbf{UA}\left[\begin{array}{c}d\boldsymbol{\varepsilon}\\\mathbf{0}\end{array}\right].$$

Introducing the above formula into the equation for $d\boldsymbol{\sigma}$, after some matrix manipulations, we get the most general form of the multimechanism consistent elasto-plastic matrix:

$$d\boldsymbol{\sigma} = \mathbf{D}\underbrace{\left[\mathbf{I} - \mathbf{aAK} + (\mathbf{aAP} - \widetilde{\mathbf{r}})\,(\mathbf{UAP})^{-1}\,\mathbf{UAK}\right]}_{\mathbf{D}^{\text{ep-consistent}}}d\boldsymbol{\varepsilon}.$$

4.7.4 SINGLE SURFACE PLASTICITY CLOSEST POINT PROJECTION ALGORITHM

The case of a single surface plasticity with/without hardening is handled via multisurface plasticity theory and algorithms assuming M=1 (nr of plastic surfaces), see Appendix 4.7.3

Chapter 5

STRUCTURES

TRUSSES

BEAMS

SHELLS

MEMBRANES

APPENDICES

5.1   TRUSSES

TRUSS ELEMENT

RING ELEMENT

ANCHORING OF TRUSS AND RING ELEMENTS

PRE-STRESSING OF TRUSS AND RING ELEMENTS

UNI-AXIAL ELASTO-PLASTIC MODEL

5.1.1 TRUSS ELEMENT

GENERAL IDEA OF TRUSS ELEMENT

GEOMETRY AND DOF OF TRUSS ELEMENTS

**INTERPOLATION OF THE DISPLACEMENTS AND STRAINS**

WEAK FORMULATION OF THE EQUILIBRIUM

STIFFNESS MATRIX AND ELEMENT FORCE VECTOR

5.1.1.1   GENERAL IDEA OF TRUSS ELEMENT

Elements are designed to model the presence of different kind of anchors, reinforcements , or separate bar (**3D case**). Note the difference between truss/anchor and **2D** membrane elements , see Section 5.4 .
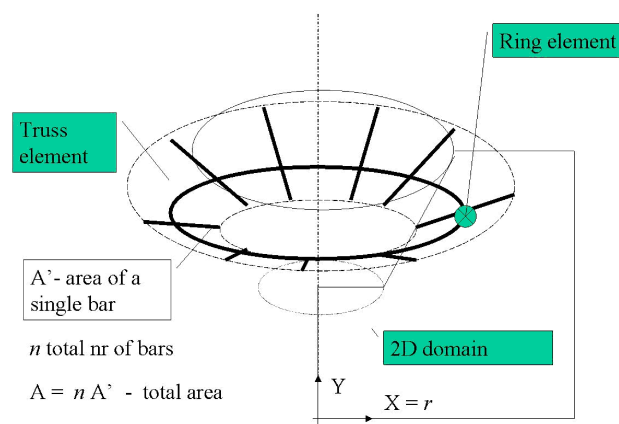

Window 5-1: Truss elements in Plane Strain

A' - area of single bar

A = A'/a - area per unit slice
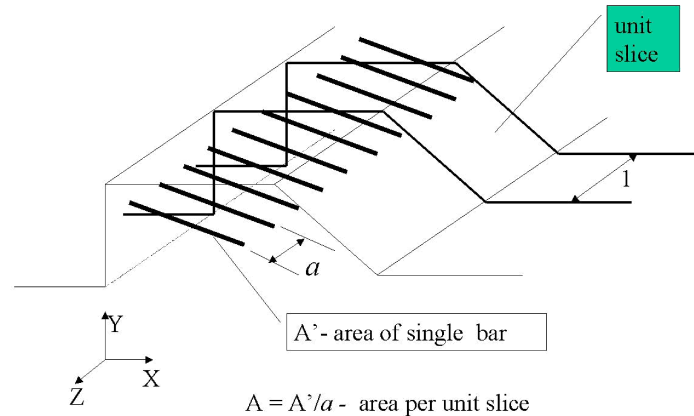
Plane Strain case

Window 5-1

Window 5-2: Truss elements in axisymmetry

A' - area of a single bar

n total nr of bars

A = n A' - total area
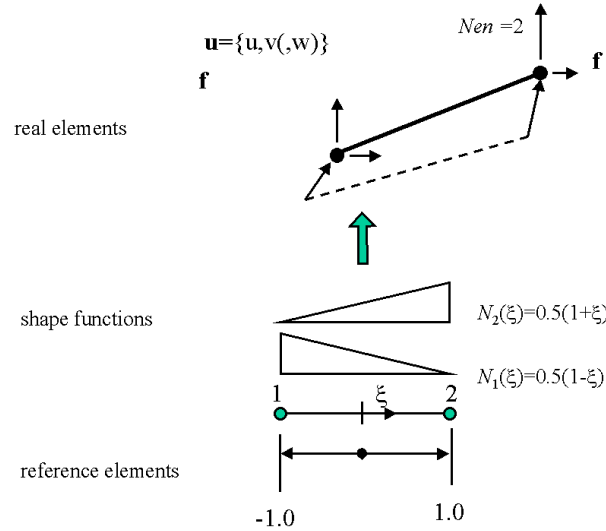
Axisymmetric case

Window 5-2

Window 5-3: Truss elements in 3D analysis type
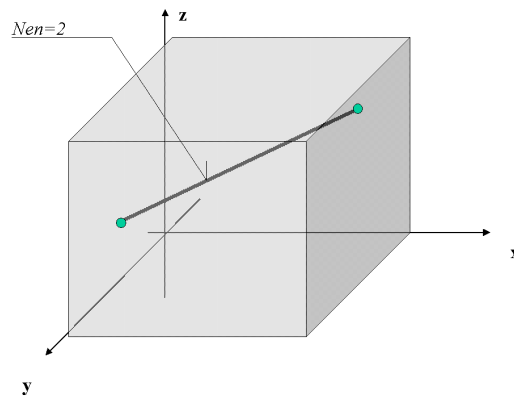
3D case: single bar

Window 5-3

5.1.1.2   GEOMETRY AND DOF OF TRUSS ELEMENTS

Window 5-4: Truss element geometry

The reference element, shape functions, construction of isoparametric mapping, DOF setting for 2/3 node truss element

Window 5-4

Geometry of the truss element is identified by the geometry of the centroid line:

$$°\mathbf{x}(\xi) = \sum_{i=1,2} N_i(\xi)\mathbf{x}_i$$

Local cross-sectional coordinate system $\{x_\mathsf{L}, y_\mathsf{L}, z_\mathsf{L}\}$ directions are set as:

$$\mathbf{e}_{x_\mathsf{L}} = \frac{°\mathbf{x}_{,\xi}}{\|°\mathbf{x}_{,\xi}\|}; \quad \mathbf{e}_{z_\mathsf{L}} = \left\{\begin{array}{ccc} 0, & 0, & 1 \end{array}\right\}^\mathrm{T}; \quad \mathbf{e}_{y_\mathsf{L}} = \mathbf{e}_{z_\mathsf{L}} \times \mathbf{e}_{x_\mathsf{L}},$$

which for 2D cases correspond to the following rules:

1. x_L – axis is tangent to element with the direction pointing from 1–st to 2–nd node of the element,

2. z_L – is perpendicular to global XY plane (meridian plane for *Axisymmetric*) and equal to global Z axis,

3. y_L – is set from $x_\mathsf{L}, z_\mathsf{L}$ by right–hand screwdriver rule .

For an arbitrary point of an element identified by its reference co–ordinate ξ and local cross sectional positions $\mathbf{r}\{y_\mathsf{L}, (z_\mathsf{L})\}$, the mapping to the global co–ordinate may be put as:

$$\mathbf{x}(\xi, y_\mathsf{L}, z_\mathsf{L}) =° \mathbf{x}(\xi) + y_\mathsf{L}\mathbf{e}_{y_\mathsf{L}} + z_\mathsf{L}\mathbf{e}_{z_\mathsf{L}}$$

The Jacobi matrix of the above mapping may be put as:

$$\mathbf{J} = \left[\; ^\circ\mathbf{x}_{,\xi}\,;\quad \mathbf{e}_{y_{\mathsf{L}}}\,;\quad \mathbf{e}_{z_{\mathsf{L}}}\;\right].$$

The local–global $\{x_{\mathsf{L}}\} \leftrightarrow \{x_{\mathsf{G}}\}$ transformation matrix may be put as:

$$\mathbf{T} = \left[\; \mathbf{e}_{x_{\mathsf{L}}}\,;\quad \mathbf{e}_{y_{\mathsf{L}}}\,;\quad \mathbf{e}_{z_{\mathsf{L}}}\;\right],\quad \mathbf{T}^{\mathrm{T}} = \left[\begin{array}{c} \langle\mathbf{e}_{x_{\mathsf{L}}}\rangle \\ \langle\mathbf{e}_{y_{\mathsf{L}}}\rangle \\ \langle\mathbf{e}_{z_{\mathsf{L}}}\rangle \end{array}\right]$$

For for any vector:

$$\mathbf{v}_{\mathsf{G}} = \mathbf{T}\mathbf{v}_{\mathsf{L}},\; \mathbf{v}_{\mathsf{L}} = \mathbf{T}^{\mathrm{T}} v_{\mathsf{G}}$$

Evaluation of strains requires the derivatives of displacement components versus local x_{L} axis :

$$\mathbf{v}_{,x_{\mathsf{L}}} = \mathbf{v}_{,\xi}\, \frac{\partial\xi}{\partial x_{\mathsf{L}}} = \mathbf{v}_{,\xi}\, D \quad \text{with} \quad D = \langle\mathbf{J}^{-1}\rangle_1 \mathbf{e}_{x_{\mathsf{L}}}$$

For *2D cases* a relation between local and global DOF as well as forces may be established in a form :

$$\mathbf{v}_{\mathsf{G}} = \mathbf{T}\mathbf{v}_{\mathsf{L}},\; \mathbf{v}_{\mathsf{L}} = \mathbf{T}^{\mathrm{T}}\mathbf{v}_{\mathsf{G}},\quad \text{with} \quad \mathbf{T} = \left[\begin{array}{cc} c & -s \\ s & c \end{array}\right],$$

where:

$$\mathbf{e}_{x_{\mathsf{L}}} = \left\{\; c,\quad s\;\right\}^{\mathrm{T}},\quad \mathbf{e}_{y_{\mathsf{L}}} = \left\{\; -s,\quad c\;\right\}^{\mathrm{T}}$$

5.1.1.3   INTERPOLATION OF THE DISPLACEMENTS AND STRAINS

For the point with given reference coordinate ξ translation displacement components $\mathbf{u}_\mathsf{G}$ (referred to global coordinate system $\{\mathbf{x}_\mathsf{G}\}$) are interpolated from its values at nodal points

$$\mathbf{u}_\mathsf{G}(\xi) = \sum_{i=1,2} N_i(\xi)\mathbf{u}_{\mathsf{G}_i}$$

The only strain component taken into account while evaluating element stress is strain along the element, and, as no bending is taken into account, this strain is assumed to remain constant in the whole cross-section of the element:

$$\varepsilon_{xx_\mathsf{L}}(x_\mathsf{L}, y_\mathsf{L}) = \frac{\partial u_\mathsf{L}}{\partial x_\mathsf{L}} = \mathbf{e}_{x_\mathsf{L}}{}^\mathrm{T}\frac{\partial \mathbf{u}_\mathsf{G}}{\partial x_\mathsf{L}},$$

The formulae relating the only strains component $\varepsilon_{xx_\mathsf{L}}$ any point within the element, with its DOF vector $\mathbf{u}$ may put in general for:

$$\varepsilon_{xx_\mathsf{L}}(\xi) = \mathbf{B}_{\varepsilon_{x_\mathsf{L}}}(\xi)\mathbf{u} = \sum_{i=1}^{Nen}\mathbf{B}_{i\varepsilon_{x_\mathsf{L}}}(\xi)\mathbf{u}_i,$$

For each analysis type in takes form:

- Plane Strain, Axisymmetry:

$$\mathbf{u}_i = \begin{bmatrix} u_i & v_i \end{bmatrix}^\mathrm{T}$$
$$\mathbf{B}_{i\varepsilon_{x_\mathsf{L}}} = \begin{bmatrix} e_{x_\mathsf{L}x}DN_{i,\xi} & e_{x_\mathsf{L}y}DN_{i,\xi} \end{bmatrix}$$

- *3D:*

$$\mathbf{u}_i = \begin{bmatrix} u_i, & v_i, & w_i \end{bmatrix}^\mathrm{T},$$
$$\mathbf{B}_{i\varepsilon_{x_\mathsf{L}}} = \begin{bmatrix} e_{x_\mathsf{L}x}DN_{i,\xi} & e_{x_\mathsf{L}y}DN_{i,\xi} & e_{x_\mathsf{L}z}DN_{i,\xi} \end{bmatrix}.$$

5.1.1.4 WEAK FORMULATION OF THE EQUILIBRIUM

The virtual work principle expressing equilibrium of a system may be put in the general form:

find σ such that:

for any $\delta\varepsilon$, $\delta\mathbf{u}$

$$\int_V \delta\varepsilon^{\mathrm{T}}\sigma dV - \int_{\partial V} \delta\mathbf{u}^{\mathrm{T}}\mathbf{p}d\partial V = 0$$

The contribution of the truss elements in the above may be easily derived, with integrals taken along the element length. A is an area attributed to the assumed computational domain i.e. to the unit slice for the *Plane strain, Generalized Plane Strain* , to the whole circumference (independently from current radius) for the *Axisymmetric* case or to one distinct bar for the *3D* case.

for any $\delta\varepsilon$, $\delta\mathbf{u}$

$$\int_L \delta\varepsilon_{xx_\mathsf{L}}\sigma_{xx_\mathsf{L}}A\mathrm{d}L - \int_L \delta\mathbf{u}^{\mathrm{T}}\mathbf{p}\mathrm{d}L = 0$$

For the description of $1D$ uni–axial elasto–plastic material model used for truss elements see the Window 5-29.

5.1.1.5   STIFFNESS MATRIX AND ELEMENT FORCE VECTOR

Stiffness matrix $\mathbf{K}^{\mathsf{e}}$ and force vector $\mathbf{f}^{\mathsf{e}}$ of the truss element are derived in a standard way from the weak formulation of a problem. It would require constitutive module D_{xxxx} as well as $\sigma_{xx_{\mathsf{L}}}$ stress evaluation for given strain increment. This will be performed by $1D$ uni–axial elasto–plastic model.

Numerical integration technique is used to evaluate integrals over the length of the element. In the case of a 2–node linear element, 1 integration point is used ($Ngaus = 1$, $W_1 = 2.0$, $\xi_1 = 0.0$). Integration over the cross section of the element is hidden in given values of integral characteristics of the cross section area A.

$$\mathbf{K}^{\mathsf{e}} = \int_{-1}^{1} \mathbf{B}_{\varepsilon_{x_{\mathsf{L}}}}{}^{\mathrm{T}}(\xi) D_{xxxx} \mathbf{B}_{\varepsilon_{x_{\mathsf{L}}}}(\xi) \|^{\mathsf{o}}\mathbf{x}(\xi)\| \mathrm{d}\xi =$$

$$\sum_{igaus=1}^{Ngaus} \mathbf{B}_{\varepsilon_{x_{\mathsf{L}}}}{}^{\mathrm{T}}(\xi_{igaus}) D_{xxxx} \mathbf{B}_{\varepsilon_{x_{\mathsf{L}}}}(\xi_{igaus}) \|^{\mathsf{o}}\mathbf{x}(\xi)\| W_{igaus}$$

$$\mathbf{f}^{\mathsf{e}} = \int_{-1}^{1} \mathbf{B}_{\varepsilon_{x_{\mathsf{L}}}}{}^{\mathrm{T}}(\xi) \sigma_{xx}(\xi) \|^{\mathsf{o}}\mathbf{x}(\xi)\| \mathrm{d}\xi =$$

$$\sum_{igaus=1}^{Ngaus} \mathbf{B}_{\varepsilon_{x_{\mathsf{L}}}}{}^{\mathrm{T}}(\xi_{igaus}) \sigma_{xx}(\xi_{igaus}) \|^{\mathsf{o}}\mathbf{x}(\xi_{igaus})\| W_{igaus}$$

The element $\mathbf{p}$ load is assumed to act along the centroid line leading to load induced forces evaluated as:

$$\mathbf{f}_p = \int_{-1}^{1} \mathbf{N}^{\mathrm{T}}(\xi) \mathbf{p} \|^{\mathsf{o}}\mathbf{x}(\xi)\| \mathrm{d}\xi =$$

$$\sum_{igaus=1}^{Ngaus} \mathbf{N}^{\mathrm{T}}(\xi_{igaus}) \mathbf{p} \|^{\mathsf{o}}\mathbf{x}(\xi_{igaus})\| W_{igaus}$$

where:

$$\mathbf{N}(\xi) = \left[N_i(\xi) \mathbf{I}_{(\mathrm{dim})} \right], \quad i = 1, Nen$$

5.1.2 RING ELEMENT

**GEOMETRY AND KINEMATICS OF A RING ELEMENT**

WEAK FORMULATION OF THE EQUILIBRIUM

STIFFNESS MATRIX AND ELEMENT FORCES

5.1.2.1   GEOMETRY AND KINEMATICS OF A RING ELEMENT

The geometry of the ring element (available exclusively for *Axisymmetric* analysis type) is represented by the coordinates of its 1st node and attached area.

Window 5-5: Geometry and DOF of a ring elements
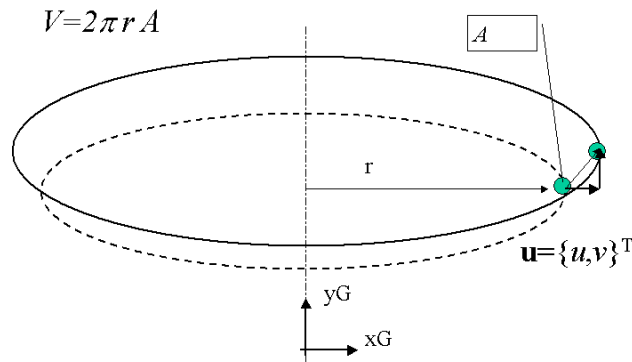
Ring element. Geometry and DOF

Window 5-5

Although only u contribute to element strain both $\{u, v\}$ displacement components are kept as element DOF, to allow force resulting from vertical load to be transmitted to the system via ring element.

The only strain component taken into account while evaluating element stress is strain in circumferential direction, constant in the whole cross–section of the element, related only to the radial component of the displacement and current radius:

$$\varepsilon_{zz} = \frac{u}{r}$$

The formulae relating ε_{zz} , with elements DOF vector **u**:

$$\varepsilon_{zz} = \mathbf{B}_{\varepsilon_{zz}} \mathbf{u}, \qquad \mathbf{u} = \begin{bmatrix} u, & v \end{bmatrix}^{\mathrm{T}}$$

$$\mathbf{B}_{\varepsilon_{zz}} = \begin{bmatrix} \dfrac{1}{r}, & 0 \end{bmatrix}$$

5.1.2.2   WEAK FORMULATION OF THE EQUILIBRIUM

From the general form of the V.W.P it may be stated as:

for any $\delta\varepsilon, \delta\mathbf{u}$:

$$\delta\varepsilon_{zz}\sigma_{zz}(2\pi rA) - \delta\mathbf{u}^{\mathrm{T}}\mathbf{p}(2\pi r) = 0$$

For the description of $1D$ uni–axial elasto–plastic material model used for ring element see the Window 5-29

5.1.2.3   STIFFNESS MATRIX AND ELEMENT FORCES

Stiffness matrix $\mathbf{K^e}$ and force vector $\mathbf{f^e}$ of the truss element is derived in a standard way from the weak formulation of a problem. It would require constitutive module D_{zzzz} as well as σ_{zz} stress evaluation for given strain increment. This will be performed by $1D$ uni–axial elasto–plastic model, see the Window 5-29

$$\mathbf{K^e} = \mathbf{B}_{\varepsilon_{zz}}^{\mathrm{T}} D_{zzzz} \mathbf{B}_{\varepsilon_{zz}} 2\pi r A$$

$$\mathbf{f^e} = \mathbf{B}_{\varepsilon_{zz}}^{\mathrm{T}} \sigma_{zz} 2\pi r A$$

5.1.3   ANCHORING OF TRUSS AND RING ELEMENTS

For the sake of generality the nodal points of truss elements may be placed in arbitrary position within the domain occupied by continuum or structural element. Despite modeling convenience, the option also possesses some physical meaning as then the truss element force are distributed over surrounding nodes of continuum element and the effect of force concentration is diminished.

Window 5-6: Anchoring of truss and ring elements

Conditions to be fulfilled:

- displacement compatibility:

$$\mathbf{u}_{Truss} = \mathbf{u}_{Cont}$$

- force equivalence (weak form):

  for any $\delta \mathbf{u}$:

$$\delta \mathbf{u}_{Truss}^{\mathrm{T}} \mathbf{f}_{Truss} = \sum_{i=1}^{Nen} \delta \mathbf{u}_{Cont}^{(i)\mathrm{T}} \mathbf{f}_{Cont}^{(i)}$$
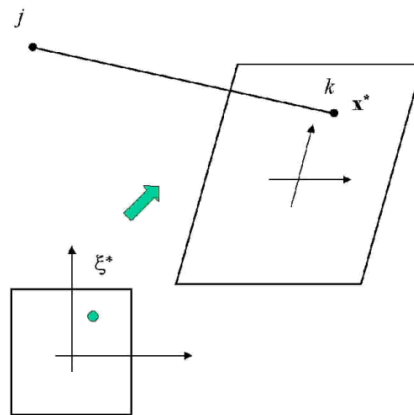
Anchoring of a truss/ring node within continuum element

Window 5-6

5.1.3.1   NUMERICAL REALIZATION OF ANCHORING

Let N_i are shape functions of the element in which k–th node of a truss is anchored, and ξ^* are local coordinates of the anchorage point within its reference element. Displacement of a truss node $\mathbf{u}_{Truss}$ are to be evaluated from displacement of surrounding element $\mathbf{u}_{Cont}$ via compatibility condition :

$$\mathbf{u}_{Truss} = \mathbf{u}_{Cont}(\xi^*) = \sum_{i=1}^{NenCont} N_i(\xi^*)\mathbf{u}_{iCont} = \mathbf{N}^{\mathrm{T}}\mathbf{u}_{Cont}$$

where:

$$\mathbf{N} = \left[N_i(\xi^*)\mathbf{I}_{Ndm} \right], \qquad i = 1, NenCont$$

In the case of anchoring within structural (i.e. beam or shell element), shape function matrix $\mathbf{N}$ must be understood in more general sense i.e. as a matrix relating translation displacement at arbitrary point within the element with all its DOF and takes the form given in point 1.2, 1.3.

In turn, forces evaluated at the node of a truss $\mathbf{f}_{Truss}$ are transferred to the nodes of the surrounding element as $\mathbf{f}_{Cont}$ basing on (weakly formulated) equivalency

for any $\delta\mathbf{u}$:

$$\delta\mathbf{u}_{Truss}^{\mathrm{T}}\mathbf{f}_{Truss} = \sum_{i=1}^{Nen} \delta\mathbf{u}_{Cont}^{(i)\mathrm{T}}\mathbf{f}_{Cont}^{(i)} = \delta\mathbf{u}_{Cont}\mathbf{f}_{Cont} \Rightarrow$$

$$\delta\mathbf{u}_{Truss}^{\mathrm{T}}\mathbf{f}_{Truss} = \delta\mathbf{u}_{Cont}^{\mathrm{T}}\mathbf{N}\mathbf{f}_{Cont} = \delta\mathbf{u}_{Cont}\mathbf{f}_{Cont} \Rightarrow \quad \mathbf{f}_{Cont} = \mathbf{N}\mathbf{f}_{Truss}$$

Finally, the stiffness of the truss element is assembled on the DOF of surrounding element, and takes a form as bellow, where K_{jk} are j–th and k–th nodal sub–matrix of the truss stiffness:

$$\widehat{\mathbf{K}} = \left[\begin{array}{ccc} \mathbf{K}_{jj} & \vdots & \mathbf{K}_{jk}\mathbf{N}^{\mathrm{T}} \\ s & s & s \\ \mathbf{N}\mathbf{K}_{kj} & \vdots & \mathbf{N}\mathbf{K}_{kk}\mathbf{N}^{\mathrm{T}} \end{array} \right]$$

In the case of the ring element, its stiffness assembled on the DOF of surrounding elements takes form:

$$\widehat{\mathbf{K}} = \mathbf{N}\mathbf{K}_{kk}\mathbf{N}^{\mathrm{T}}.$$

5.1.4   PRE–STRESSING OF TRUSS AND RING ELEMENTS

Pre-stress can be applied only to anchor/truss or ring elements. Pre–stress differs from a standard initial stress situation by the fact, that the internal force is assumed to be known *a priori*. According to the definition of current tangent stiffness matrix it follows that:

$$\mathbf{K} = \frac{\partial \mathbf{f}(\mathbf{u})}{\partial \mathbf{u}} = \mathbf{0}$$

since internal force $\mathbf{f}(\mathbf{u})$ is constant. As a consequence, if pre-stress is being applied then the stiffness of the anchor is always set to zero while it is evaluated via standard procedures if pre- stress is non–active.

Strains in the anchor / ring element are monitored during the pre-stress as:

$$
\begin{aligned}
\varepsilon^i &= \varepsilon^{i-1} + \Delta\varepsilon^i \\
\Delta\varepsilon^i &= \frac{\sigma^{prestres}(t^i) - \sigma^{i-1}}{E}
\end{aligned}
$$

5.2   BEAMS

GEOMETRY OF BEAM ELEMENT

KINEMATICS OF BEAM THEORY

WEAK FORMULATION OF THE EQUILIBRIUM

INTERPOLATION OF THE DISPLACEMENT FIELD

STRAIN REPRESENTATION

STIFFNESS MATRIX AND ELEMENT FORCES

MASTER-CENTROID (OFFSET) TRANSFORMATION

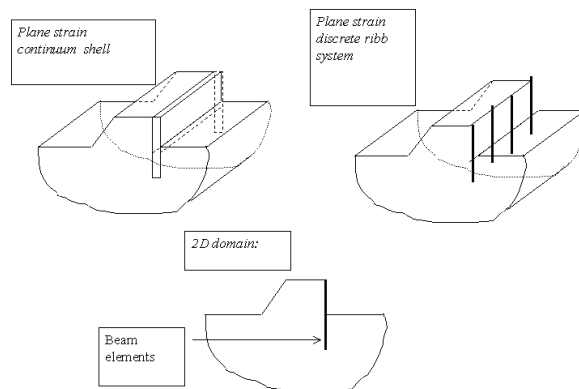**RELAXATION OF INTERNAL DOF**

BEAM ELEMENT RESULTS

5.2.1   GEOMETRY OF BEAM ELEMENT

- **Beams in 2D analysis types (Plane Strain , Generalized Plane Strain, Axisymmetry, Plane Stress)**

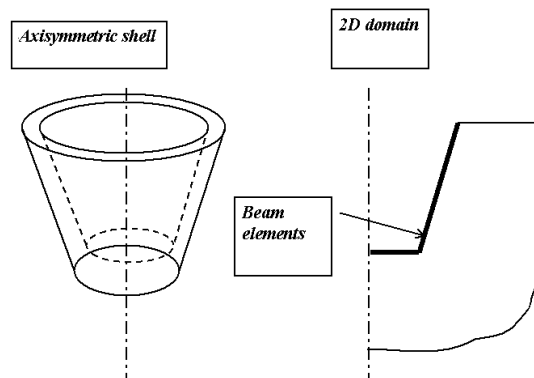**Window 5-7: Beams in 2D analysis type modeling situations**

In the case of *Plane Strain*

analysis, beam elements can be used for two - modeling situations:

Modeling situations for beam elements in `Plane Strain` and `2.5D` analysis

In the case of *Axisymmetric* analysis, only *continuum shell* option can be used:


Beam elements in axisymmetric analysis

Window 5-7

System $\{x_G, y_G, z_G\}$ is the global one. Local element system $\{x_L, y_L, z_L\}$ is created in the element in a following way:

1. x_L - axis is tangent to the element's centroid axis at a given point, with the direction pointing from 1-st to 2-nd centroid node of the element

2. z_L - is perpendicular to global XY plane (meridian plane for Axisymmetric case) and corresponds to global Z axis

3. y_L -is set from x_L, z_L by right-hand screw driver rule
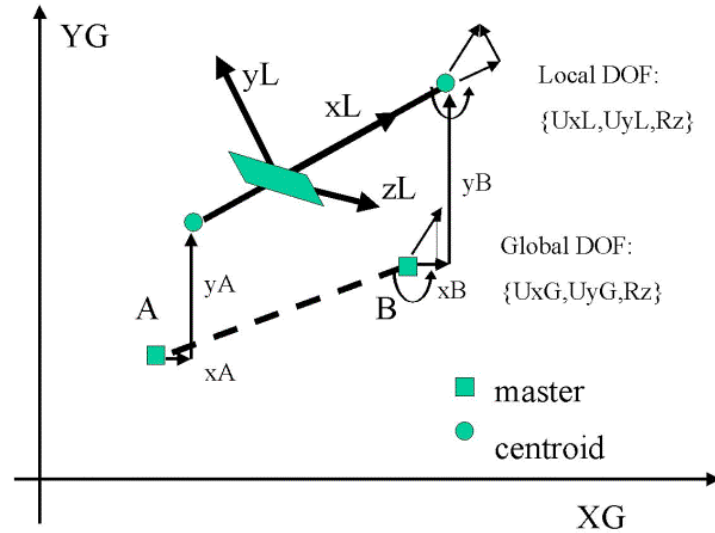
2D beam element: nodal DOF and coordinates systems

$$\mathbf{e}_{x_L} = \frac{{}^{\circ}\mathbf{x}_{,\xi}}{\|{}^{\circ}\mathbf{x}_{,\xi}\|}, \quad \mathbf{e}_{z_L} = \left\{ \begin{array}{ccc} 0, & 0, & 1 \end{array} \right\}^{\mathrm{T}}, \quad \mathbf{e}_{y_L} = \mathbf{e}_{z_L} \times \mathbf{e}_{x_L}$$

Relation between local and global DOF (degrees of freedom) as well as forces may be established in a form :
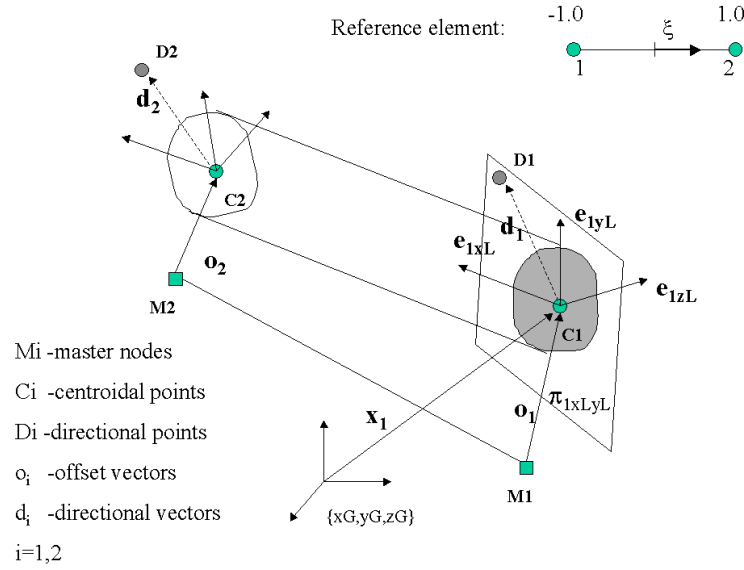
$$\mathbf{v}_G = \mathbf{T}\mathbf{v}_L, \quad \mathbf{v}_L = \mathbf{T}^{\mathrm{T}}\mathbf{v}_G, \qquad \mathbf{T} = \begin{bmatrix} c & -s & 0 \\ s & c & 0 \\ 0 & 0 & 1 \end{bmatrix}$$

are local coordinate unit vectors.

- **Beams in 3D analysis type**

The geometry of a 2 node beam element allowing for moderate (when 3 nodes are used) and data, shown on the plot for the most general situation.

Window 5-8: Beams in 3D analysis type

Beam element in 3D analysis

Window 5-8

The versors of local cross sectional axis are evaluated from the above data at any point of the element with reference coordinates ξ as:

$$\mathbf{e}_{x_L} = \frac{{}^{\circ}\mathbf{x}_{,\xi}}{\|{}^{\circ}\mathbf{x}_{,\xi}\|}, \quad \mathbf{e}_{z_L} = \frac{\mathbf{e}_{x_L} \times \mathbf{d}(\xi)}{\|\mathbf{e}_{x_L} \times \mathbf{d}(\xi)\|}, \quad \mathbf{e}_{y_L} = \mathbf{e}_{z_L} \times \mathbf{e}_{x_L}$$

Note, that iso-parametric mapping is used to interpolate both centroid position vector ${}^{\circ}\mathbf{x}(\boldsymbol{\xi})$ and directional vector $\mathbf{d}(\xi)$ from their nodal representatives.

$$ {}^{\circ}\mathbf{x}(\xi) = \sum_{i=1,2} N_i(\xi)\mathbf{x}_i, \quad \mathbf{d}(\xi) = \sum_{i=1,2} N_i(\xi)\mathbf{d}_i$$

Centroids may coincide with corresponding masters. Directional nodes may be different for each node enabling for moderate twist of cross-sectional axis or only 1 common point for all nodes in the element may be given. The directional planes may be different then the element curvature plane. The only obligation for the positions of the directional nodes is to omit the situation when cross product is indeterminable, i.e. when tangent vector $\mathbf{e}_{x_L}$ is parallel to the directional vector $\mathbf{d}$.

Local cross sectional axis are these to which the geometry of the cross–section is referred. In the case of *elastic beam* model they must strictly correspond to centroidal and principal cross–sectional inertia axis . In the case of *layered, non–linear beam* model this demand may be satisfied only approximately, as most meaningful effects, related to axial strain and stresses resulting from axial force and bi–directional bending action are taken into account by cross–sectional numerical integration. Then cross sectional axis setting will be used to input layer centers positions. Moreover, cross sectional axis setting will be used to refer bi–directional shear and torsion elastic characteristics.

For local cross sectional positions $\mathbf{r}\{y_\mathsf{L}, (z_\mathsf{L})\}$, the mapping to the global co–ordinate may be put as:

$$\mathbf{x}(\xi, y_\mathsf{L}, z_\mathsf{L}) = {}^\mathrm{o}\mathbf{x}(\xi) + y_\mathsf{L}\mathbf{e}_{y_\mathsf{L}} + z_\mathsf{L}\mathbf{e}_{z_\mathsf{L}}$$

The Jacobi matrix of the above mapping may be put as:

$$\mathbf{J}(\xi, y_\mathsf{L}, z_\mathsf{L}) = \left[\ {}^\mathrm{o}\mathbf{x}_{,\xi} + y_\mathsf{L}\mathbf{e}_{y_\mathsf{L},\xi} + z_\mathsf{L}\mathbf{e}_{z_\mathsf{L},\xi}\ ; \quad \mathbf{e}_{y_\mathsf{L}}; \quad \mathbf{e}_{z_\mathsf{L}}\ \right]$$

The local-global $\{x_\mathsf{L}\} \leftrightarrow \{x_\mathsf{G}\}$ transformation matrix may be put as:

$$\mathbf{T} = \left[\ \mathbf{e}_{x_\mathsf{L}}; \quad \mathbf{e}_{y_\mathsf{L}}; \quad \mathbf{e}_{z_\mathsf{L}}\ \right], \quad \mathbf{T}^\mathrm{T} = \begin{bmatrix} \langle \mathbf{e}_{x_\mathsf{L}} \rangle \\ \langle \mathbf{e}_{y_\mathsf{L}} \rangle \\ \langle \mathbf{e}_{z_\mathsf{L}} \rangle \end{bmatrix} \quad \text{thus for any vector :} \begin{cases} \mathbf{v}^\mathsf{G} = \mathbf{T}\mathbf{v}^\mathsf{L}, \\ \mathbf{v}^\mathsf{L} = \mathbf{T}^\mathrm{T}\mathbf{v}^\mathsf{G}. \end{cases}$$

Evaluation of strains requires the derivatives of any displacement components versus local xL axis :

$$\mathbf{v}_{,x_\mathsf{L}} = \mathbf{v}_{,\xi}\frac{\partial \xi}{\partial xL} = \mathbf{v}_{,\xi}D \quad \text{with} \quad D = \langle \mathbf{J}^{-1} \rangle_1 \mathbf{e}_{x_\mathsf{L}}$$

In *3D analysis case* ξ–derivatives of base vectors $\mathbf{e}_{\square\mathsf{L}}$ appear, evaluated as:

$$\mathbf{e}_{x_\mathsf{L},\xi} = \frac{1}{\|{}^\mathrm{o}\mathbf{x}_{,\xi}\|}\left(\mathbf{I} - \frac{{}^\mathrm{o}\mathbf{x}_{,\xi} \otimes {}^\mathrm{o}\mathbf{x}_{,\xi}}{{}^\mathrm{o}\mathbf{x}_{,\xi} \cdot {}^\mathrm{o}\mathbf{x}_{,\xi}}\right){}^\mathrm{o}\mathbf{x}_{,\xi\xi}$$

$$\mathbf{e}_{z_\mathsf{L}} = \frac{1}{\|\mathbf{e}_{x_\mathsf{L}} \times \mathbf{d}\|}\left(\mathbf{I} - \frac{(\mathbf{e}_{x_\mathsf{L}} \times \mathbf{d}) \otimes (\mathbf{e}_{x_\mathsf{L}} \times \mathbf{d})}{(\mathbf{e}_{x_\mathsf{L}} \times \mathbf{d}) \cdot (\mathbf{e}_{x_\mathsf{L}} \times \mathbf{d})}\right)(\mathbf{e}_{x_\mathsf{L},\xi} \times \mathbf{d} + \mathbf{e}_{x_\mathsf{L}} \times \mathbf{d}_{,\xi})$$

$$\mathbf{e}_{y_\mathsf{L}} = \mathbf{e}_{z_\mathsf{L},\xi} \times \mathbf{e}_{x_\mathsf{L}} + \mathbf{e}_{z_\mathsf{L}} \times \mathbf{e}_{x_\mathsf{L},\xi}$$

5.2.2   KINEMATICS OF BEAM THEORY

The adopted kinematics of a beam is based on Timoshenko's hypothesis, i.e. that originally plane cross- section perpendicular to beam centroid line remains plane but not necessarily perpendicular to deformed beam axis . Moreover small displacements & strains are assumed

---

Window 5-9: Kinematic assumption of beam theory
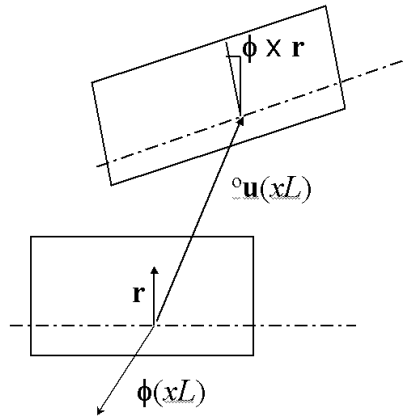
Kinematic assumption of beam theory

Window 5-9

Displacements at any point $\mathbf{r}$ with given local coordinate $\{x_\mathsf{L}, y_\mathsf{L}, z_\mathsf{L}\}$ are then given by displacement $°\mathbf{u}$ of centroid line and independent rotation ϕ of a cross section plane (fiber) as :

$$\mathbf{u}(\mathbf{x}) = °\mathbf{u}(x_\mathsf{L}) + \phi(x_\mathsf{L}) \times \mathbf{r}$$

For *2D* case this leads to:

$$u_\mathsf{L} = °u_\mathsf{L}(x_\mathsf{L}) - \phi(x_\mathsf{L})y_\mathsf{L}$$

$$v_\mathsf{L} = °v_\mathsf{L}(x_\mathsf{L})$$

Two formulations of beam element are used:

- **layered approach** (*Nonlinear Beam* option, analysis type *Plane Strain, Axisymmetry,*

  3D analysis)

  composite sections allowed, nonlinear or elastic material models, setting of the centroid of the cross–section may be done in approximate manner as $M - N$ coupling is taken into account in the model);

- **integral approach** (*Elastic Beam* option, *Plane strain, Axisymmetry,*   3D analysis), uniform section described by its integral characteristics, elastic material model only, setting of the centroid of the cross–section must be done in rigorously exact way, as $M - N$ coupling is disregarded by the model)

For the layered approach strains are evaluated at each layer. These (related to local coordinate system) are:

(*2D* case)

normal strain

$$\varepsilon_{xx_{\mathsf{L}}}(x_{\mathsf{L}}, y_{\mathsf{L}}) = \frac{\partial u_{\mathsf{L}}}{\partial x_{\mathsf{L}}} = \mathbf{e}_{x_{\mathsf{L}}}^{\mathsf{T}} \frac{\partial\,{}^{\circ}\mathbf{u}_{\mathsf{G}}(x_{\mathsf{L}})}{\partial x_{\mathsf{L}}} - y_{\mathsf{L}} \frac{\partial \phi_{z_{\mathsf{L}}}(x_{\mathsf{L}})}{\partial x_{\mathsf{L}}},$$

shear strain

$$\gamma_{xy_{\mathsf{L}}} = \frac{\partial v_{\mathsf{L}}}{\partial x_{\mathsf{L}}} + \frac{\partial u_{\mathsf{L}}}{\partial y_{\mathsf{L}}} = \mathbf{e}_{y_{\mathsf{L}}}^{\mathsf{T}} \frac{\partial\,{}^{\circ}\mathbf{u}_{\mathsf{G}}(x_{\mathsf{L}})}{\partial x_{\mathsf{L}}} - \phi_{z_{\mathsf{L}}}(x_{\mathsf{L}})$$

additionally, for *Axisymmetry* , circumferential strain is set as:

$$\varepsilon_{zz_{\mathsf{L}}}(x_{\mathsf{L}}, y_{\mathsf{L}}) = \frac{u_{\mathsf{G}}}{r} = \frac{1}{r}\left({}^{\circ}u_{\mathsf{G}}(x_{\mathsf{L}}) - cy_{\mathsf{L}}\phi_{z_{\mathsf{L}}}(x_{\mathsf{L}})\right)$$

In *3D analysis* case and *layered beam* model strains related to the cross sectional axis are:

normal strain:

$$\varepsilon_{xx_{\mathsf{L}}}(x_{\mathsf{L}}, y_{\mathsf{L}}) = \frac{\partial u_{\mathsf{L}}}{\partial x_{\mathsf{L}}} = \mathbf{e}_{x_{\mathsf{L}}}^{\mathsf{T}}\left(\frac{\partial\,{}^{\circ}\mathbf{u}_{\mathsf{G}}(x_{\mathsf{L}})}{\partial x_{\mathsf{L}}} + \frac{\partial(\boldsymbol{\phi}(x_{\mathsf{L}}) \times \mathbf{r})}{\partial x_{\mathsf{L}}}\right)$$

average strains due to shear:

$$\gamma_{xy_{\mathsf{L}}}(x_{\mathsf{L}}) = \frac{\partial v_{\mathsf{L}}}{\partial x_{\mathsf{L}}} + \frac{\partial u_{\mathsf{L}}}{\partial y_{\mathsf{L}}} = \frac{\partial v_{\mathsf{L}}}{\partial x_{\mathsf{L}}} - \phi_{z_{\mathsf{L}}} = \mathbf{e}_{y_{\mathsf{L}}}^{\mathsf{T}} \frac{\partial\,{}^{\circ}\mathbf{u}_{\mathsf{G}}(x_{\mathsf{L}})}{\partial x_{\mathsf{L}}} - \mathbf{e}_{z_{\mathsf{L}}}^{\mathsf{T}} \boldsymbol{\phi}(x_{\mathsf{L}})$$

$$\gamma_{xz_{\mathsf{L}}}(x_{\mathsf{L}}) = \frac{\partial w_{\mathsf{L}}}{\partial x_{\mathsf{L}}} + \frac{\partial u_{\mathsf{L}}}{\partial z_{\mathsf{L}}} = \frac{\partial w_{\mathsf{L}}}{\partial x_{\mathsf{L}}} + \phi_{y_{\mathsf{L}}} = \mathbf{e}_{z_{\mathsf{L}}}^{\mathsf{T}} \frac{\partial\,{}^{\circ}\mathbf{u}_{\mathsf{G}}(x_{\mathsf{L}})}{\partial x_{\mathsf{L}}} - \mathbf{e}_{y_{\mathsf{L}}}^{\mathsf{T}} \boldsymbol{\phi}(x_{\mathsf{L}})$$

torsion angle:

$$\psi(x_{\mathsf{L}}) = \frac{\partial \phi_{x_{\mathsf{L}}}}{\partial x_{\mathsf{L}}} = \mathbf{e}_{x_{\mathsf{L}}}^{\mathsf{T}} \frac{\partial \boldsymbol{\phi}(x_{\mathsf{L}})}{\partial x_{\mathsf{L}}}$$

For the integral approach strains (in generalized sense) are (for *Plane Strain*):

extension of $\{x_{\mathsf{L}}, 0, 0\}$ *line:*

$${}^{\circ}\varepsilon_{xx_{\mathsf{L}}}(x_{\mathsf{L}}) = \frac{\partial\,{}^{\circ}u_{\mathsf{L}}}{\partial x_{\mathsf{L}}} = \mathbf{e}_{x_{\mathsf{L}}}^{\mathsf{T}} \frac{\partial\,{}^{\circ}\mathbf{u}_{\mathsf{G}}(x_{\mathsf{L}})}{\partial x_{\mathsf{L}}},$$

curvature:

$$\kappa_z(x_{\mathsf{L}}) = -\frac{\partial \phi_{z_{\mathsf{L}}}(x_{\mathsf{L}})}{\partial x_{\mathsf{L}}},$$

average shear strain:

$$\gamma_{xy_{\mathsf{L}}}(x_{\mathsf{L}}) = \frac{\partial v_{\mathsf{L}}}{\partial x_{\mathsf{L}}} + \frac{\partial u_{\mathsf{L}}}{\partial y_{\mathsf{L}}} = \mathbf{e}_{y_{\mathsf{L}}}^{\mathrm{T}} \frac{\partial^{\circ}\mathbf{u}_{\mathsf{G}}(x_{\mathsf{L}})}{\partial x_{\mathsf{L}}} - \phi_{z_{\mathsf{L}}}(x_{\mathsf{L}}).$$

In *3D* case (integral approach) generalized strains are:

extension of $\{x_{\mathsf{L}}, 0, 0\}$ *line:*

$$^{\circ}\varepsilon_{xx_{\mathsf{L}}}(x_{\mathsf{L}}) = \frac{\partial^{\circ}u_{\mathsf{L}}}{\partial x_{\mathsf{L}}} = \mathbf{e}_{x_{\mathsf{L}}}^{\mathrm{T}} \frac{\partial^{\circ}\mathbf{u}_{\mathsf{G}}(x_{\mathsf{L}})}{\partial x_{\mathsf{L}}},$$

curvatures:

$$\kappa_y(x_{\mathsf{L}}) = \frac{\partial \phi_{y_{\mathsf{L}}}(x_{\mathsf{L}})}{\partial x_{\mathsf{L}}} = \mathbf{e}_{y_{\mathsf{L}}}^{\mathrm{T}} \frac{\partial \boldsymbol{\phi}(x_{\mathsf{L}})}{\partial x_{\mathsf{L}}},$$

$$\kappa_z(x_{\mathsf{L}}) = -\frac{\partial \phi_{z_{\mathsf{L}}}(x_{\mathsf{L}})}{\partial x_{\mathsf{L}}} = -\mathbf{e}_{z_{\mathsf{L}}}^{\mathrm{T}} \frac{\partial \boldsymbol{\phi}(x_{\mathsf{L}})}{\partial x_{\mathsf{L}}},$$

Also *average strains due to shear* and *torsion angle* taking the form identical as for *layered beam* are taken into account.

5.2.3 WEAK FORMULATION OF THE EQUILIBRIUM

In both **layered** and **integral** approach, the treatment of a transversal shear (and torsion for the 3D case) is de–coupled from bending and extension state analysis and limited to linear stress- strain relation. This kind of procedure is exact in linear cases, while for the nonlinear one, consists a commonly accepted simplification. Coupled treatment of both, shear & bending / extension state would require additional significant numerical effort and much more complex formulation. In both formulations, the shear behavior is treated in "integral" way, with usage of averaged shear angle, stress-resultant tangent force and a shear correction factor.

The virtual work principle expressing the equilibrium of a beam may be put in the general form:

find σ such that:

for any $\delta\varepsilon, \delta\mathbf{u}$

$$\int_V \delta\varepsilon^{\mathrm{T}}\sigma \, \mathrm{d}V - \int_{\partial V} \delta\mathbf{u}^{\mathrm{T}}\mathbf{p} \, \mathrm{d}\partial V = 0$$

From the above, taking into account kinematic assumptions both **layered** and **integral** approach, detailed formulation for each *analysis type* may be derived, i.e.:

layered formulation:

(*2D, Plane Strain* case)

for any $\delta\varepsilon, \delta\gamma, \delta\mathbf{u}$:

$$\sum_i \int_{V^{(i)}} \delta\varepsilon_{xx_{\mathsf{L}}}^{(i)}\sigma_{xx_{\mathsf{L}}} \, \mathrm{d}V^{(i)} + \int_L \delta\gamma_{xy_{\mathsf{L}}}(k_y GA)\gamma_{xy_{\mathsf{L}}} \, \mathrm{d}L - \int_{\partial V} \delta\mathbf{u}^{\mathrm{T}}\mathbf{p} \, \mathrm{d}\partial V = 0$$

(*2D, Axisymmetric case*, $\mathrm{d}V$ is conical volume element)

for any $\delta\varepsilon, \delta\gamma, \delta\mathbf{u}$:

$$\sum_i \int_{V^{(i)}} \left(\delta\varepsilon_{xx_{\mathsf{L}}}^{(i)}\sigma_{xx_{\mathsf{L}}} + \delta\varepsilon_{zz_{\mathsf{L}}}^{(i)}\sigma_{zz_{\mathsf{L}}}^{(i)}\right) \mathrm{d}V^{(i)} + 2\pi \int_L \delta\gamma_{xy_{\mathsf{L}}}(k_y GA)\gamma_{xy_{\mathsf{L}}} r \, \mathrm{d}L - \int_{\partial V} \delta\mathbf{u}^{\mathrm{T}}\mathbf{p} \, \mathrm{d}\partial V = 0$$

(*2D analysis case* – anti–plane shear included optionally ($\langle\rangle$),in each layer separately

for any $\delta\varepsilon, \delta\gamma, \delta\mathbf{u}$:

$$\sum_i \int_{V^{(i)}} \left(\delta\varepsilon_{xx_{\mathsf{L}}}^{(i)}\sigma_{xx_{\mathsf{L}}} + \langle\delta\gamma_{xz_{\mathsf{L}}}^{(i)}\sigma_{xz_{\mathsf{L}}}^{(i)}\rangle\right) \mathrm{d}V^{(i)} + \int_L \delta\gamma_{xy_{\mathsf{L}}}(k_y GA)\gamma_{xy_{\mathsf{L}}} \, \mathrm{d}L - \int_{\partial V} \delta\mathbf{u}^{\mathrm{T}}\mathbf{p} \, \mathrm{d}\partial V = 0$$

(*3D* case)

for any $\delta\varepsilon, \delta\gamma, \delta\psi, \delta\mathbf{u}$:

$$\sum_i \int\limits_{V^{(i)}} \delta\varepsilon_{xx_\mathsf{L}}^{(i)} \sigma_{xx_\mathsf{L}}\, \mathrm{d}V^{(i)} + \sum_{\langle\rangle=y,z} \int\limits_L \delta\gamma_{x\langle\rangle_\mathsf{L}} (k_{\langle\rangle}GA)\gamma_{x\langle\rangle_\mathsf{L}}\, \mathrm{d}L + \int\limits_L \delta\psi GI_x\psi\, \mathrm{d}L - \int\limits_{\partial V} \delta\mathbf{u}^\mathrm{T}\mathbf{p}\, \mathrm{d}\partial V = 0$$

integral formulation for *elastic beam* model

(*2D, Plane Strain* case)

for any $\delta\varepsilon, \delta\gamma, \delta\kappa_z, \delta\mathbf{u}$:

$$\int\limits_L [\delta°\varepsilon_{xx_\mathsf{L}}N + \delta\kappa_z M + \delta\gamma(k_yGA)\gamma]\, \mathrm{d}L - \int\limits_{\partial V} \delta\mathbf{u}^\mathrm{T}\mathbf{p}\, \mathrm{d}\partial V = 0$$

(*3D* case)

for any $\delta\varepsilon, \delta\gamma_{\langle\rangle}, \delta\kappa_{\langle\rangle}, \delta\mathbf{u}$:

$$\int\limits_L (\delta°\varepsilon_{xx_\mathsf{L}}N + \sum_{\langle\rangle=y,z} [\delta\kappa_{\langle\rangle}M_{\langle\rangle} + \delta\gamma_{x\langle\rangle}(k_{\langle\rangle}GA)\gamma_{x\langle\rangle}) + \delta\psi GI_x\psi]\, \mathrm{d}L - \int\limits_{\partial V} \delta\mathbf{u}^\mathrm{T}\mathbf{p}\, \mathrm{d}\partial V = 0$$

In the above–shear correction factor k is introduced to account for non–uniform shear stress – strain distribution over the cross section. On the basis of energetic equivalency this may be put as:

$$\frac{1}{k} = \frac{A}{I^2} \int\limits_A \frac{S^2}{b^2}\, \mathrm{d}A.$$

Moreover, shear module G must be specified by the user.   For material model description see the Appendix, Window 5-29.

5.2.4   INTERPOLATION OF THE DISPLACEMENT FIELD

For the point lying on the element centroid line with given reference coordinate ξ, both translations $\mathbf{u}$ and rotational ϕ, displacement components (referred to global coordinate system) are interpolated from its values at the centroid nodes Ci. Note, that these may be obtained from element DOF by "master" to "centroid" offset transformation ,see the Appendix, Window 5-26.

$$^{\circ}\mathbf{u}^{\mathsf{G}}(\xi) = \sum_{i=1,2} N_i(\xi)\mathbf{u}^{\mathsf{G}}_{\mathrm{Ci}}$$

$$^{\circ}\boldsymbol{\phi}^{\mathsf{G}}(\xi) = \sum_{i=1,2} N_i(\xi)\boldsymbol{\phi}^{\mathsf{G}}_{\mathrm{Ci}}$$

5.2.5   STRAIN REPRESENTATION

The formulae relating strains any point within the element with its DOF vector $\mathbf{q}$, based on kinematic assumptions is given in general form:

$$\varepsilon(\xi, y_{\mathsf{L}}, z_{\mathsf{L}}) = \mathbf{B}(\xi, y_{\mathsf{L}}, z_{\mathsf{L}})\mathbf{q} = \sum_{i=1}^{Nen} \mathbf{B}_i(\xi, y_{\mathsf{L}}, z_{\mathsf{L}})\mathbf{q}_i, \quad \mathbf{q}_i = \left[\begin{array}{c} \mathbf{u}_i^{\mathsf{C}} \\ \boldsymbol{\phi}_i^{\mathsf{C}} \end{array} \right]$$

The displacement vector $\mathbf{q}$ consist of:

2D–Plane Strain, Axisymmetry:

$$\mathbf{q}_i = \left[\begin{array}{ccc} u, & v, & \phi_z \end{array} \right]^{\mathrm{T}}$$

3D analysis:

$$\mathbf{q}_i = \left[\begin{array}{cccccc} u, & v, & w, & \phi_x, & \phi_y, & \phi_z \end{array} \right]^{\mathrm{T}}$$

i-th node submatrix of B-matrix relating shear strain with nodal DOF has a form in the case of:

2D–Plane Strain, Axisymmetry:

$$\mathbf{B}_{\gamma_i} = \left[\begin{array}{ccc} e_{y_{\mathsf{L}}x}DN_{i,\xi}\,; & e_{y_{\mathsf{L}}y}DN_{i,\xi}\,; & -N_i \end{array} \right]$$

3D analysis:

$$\mathbf{B}_{\gamma_{xy_i}} = \left[\begin{array}{cc} DN_{i,\xi}\,\mathbf{e}_{y_{\mathsf{L}}}^{\mathrm{T}}\,; & -N_i\mathbf{e}_{y_{\mathsf{L}}}^{\mathrm{T}} \end{array} \right]$$
$$\mathbf{B}_{\gamma_{xz_i}} = \left[\begin{array}{cc} DN_{i,\xi}\,\mathbf{e}_{z_{\mathsf{L}}}^{\mathrm{T}}\,; & -N_i\mathbf{e}_{z_{\mathsf{L}}}^{\mathrm{T}} \end{array} \right]$$

In that case also torsion angle matrix $\mathbf{B}_\psi$ should be set as :

$$\mathbf{B}_{\psi_i} = \left[\begin{array}{cc} \mathbf{0}_{1\times3}\,; & DN_{i,\xi}\,\mathbf{e}_{x_{\mathsf{L}}}^{\mathrm{T}} \end{array} \right]$$

Remaining strain component one–node sub–matrix $\mathbf{B}_i$ takes form (for straight geometry element):

- **layered** approach:

   2D–Plane Strain:

   axial strain

$$\mathbf{B}_{\varepsilon x_{\mathsf{L}_i}} = \left[\begin{array}{ccc} e_{x_{\mathsf{L}}x}DN_{i,\xi}\,; & e_{x_{\mathsf{L}}y}DN_{i,\xi}\,; & -DN_{i,\xi}\,y_{\mathsf{L}} \end{array} \right]$$

   2D–Axisymmetry:

   axial strain:

$$\mathbf{B}_{\varepsilon x_{\mathsf{L}i}} = \left[\ e_{x_{\mathsf{L}}x} DN_{i,\xi}\,;\ \ e_{x_{\mathsf{L}}y} DN_{i,\xi}\,;\ \ -DN_{i,\xi}\, y_{\mathsf{L}}\ \right]$$

circumferential strain:

$$\mathbf{B}_{\varepsilon x_{\mathsf{L}i}} = \left[\frac{N_i}{r};\quad 0;\quad -\frac{N_i}{r} y_{\mathsf{L}} e_{y_{\mathsf{L}}y}\right]$$

3D analysis:

$$\mathbf{B}_{\varepsilon x_{\mathsf{L}i}} = \left[\ DN_{i,\xi}\,\mathbf{e}_{x_{\mathsf{L}}}^{\mathsf{T}};\ \ D(N_i \mathbf{r} \times \mathbf{e}_{x_{\mathsf{L}}} + N_{i,\xi}\,\mathbf{r}_{,\xi} \times \mathbf{e}_{x_{\mathsf{L}}})^{\mathsf{T}}\ \right]$$

where:

$$\mathbf{r} = y_{\mathsf{L}} \mathbf{e}_{y_{\mathsf{L}}} + z_{\mathsf{L}} \mathbf{e}_{z_{\mathsf{L}}}$$

- **integral** approach*:*

2D-Plane Strain:

   axial strain at centroid line:

$$\mathbf{B}_{\varepsilon_i} = \left[\ e_{x_{\mathsf{L}}x} DN_{i,\xi}\,;\ \ e_{x_{\mathsf{L}}y} DN_{i,\xi}\,;\ \ 0\ \right]$$

curvature:

$$\mathbf{B}_{\kappa_i} = \left[\ 0;\ \ 0;\ \ -DN_{i,\xi}\ \right]$$

3D analysis:

   axial strain at centroid line:

$$\mathbf{B}_{\varepsilon_i} = \left[\ DN_{i,\xi}\,\mathbf{e}_{x_{\mathsf{L}}}^{\mathsf{T}};\ \ \mathbf{0}_{1\times 3}\ \right],$$

curvature in $x_{\mathsf{L}} z_{\mathsf{L}}$ plane:

$$\mathbf{B}_{\kappa y_i} = \left[\ \mathbf{0}_{1\times 3};\ \ D(N_{i,\xi}\,\mathbf{e}_{y_{\mathsf{L}}}^{\mathsf{T}} + N_i \mathbf{e}_{y_{\mathsf{L}},\xi}^{\mathsf{T}})\ \right],$$

curvature in $x_{\mathsf{L}} y_{\mathsf{L}}$ plane:

$$\mathbf{B}_{\kappa z_i} = \left[\ \mathbf{0}_{1\times 3};\ \ -D(N_{i,\xi}\,\mathbf{e}_{z_{\mathsf{L}}}^{\mathsf{T}} + N_i \mathbf{e}_{z_{\mathsf{L}},\xi}^{\mathsf{T}})\ \right].$$

5.2.6   STIFFNESS MATRIX AND ELEMENT FORCES

Stiffness matrix $\mathbf{K}^e$ and force vector $\mathbf{f}^e$ of a beam element are derived in a standard way from the weak formulation of a problem. It would require constitutive module matrix $\mathbf{D}$ for each stress–strain component. Numerical integration technique is used to evaluate integrals over the length of the element. In the case of a 2–node linear element selected reduced integration technique (SRI) with 1 integration point is used ($Ngaus = 1$, $W_1 = 2.0$, $\xi_1 = 0.0$).

Integration over the cross section of the element is performed numerically in the case of layered approach, or it is hidden in given values of integral characteristics of the cross section (shear area for uncoupled treatment of shear, area and rotational inertia for elastic beam).

Integrals in **layered** approach case use longitudinal jacobians $^l J = \det(\mathbf{J}(\xi, y_{\mathsf{L}^l}, z_{\mathsf{L}^l}))$ evaluated at each layer l separately, in order to enhance accuracy in case of curved elements., while other integrals over the element length use jacobians referred to centroid line $^\circ J = \det(\mathbf{J}(\xi, 0, 0))$. For all *2D* cases, contribution of shear part is evaluated in a common way as:

$$\mathbf{K}_{\gamma\gamma} = \int_{-1}^{1} \mathbf{B}_\gamma^{\mathrm{T}}(\xi)(kGA)\mathbf{B}_\gamma(\xi)\,{}^\circ J \, \mathrm{d}\xi$$

$$= \sum_{igaus=1}^{Ngaus} \mathbf{B}_\gamma^{\mathrm{T}}(\xi_{igaus})(kGA)\mathbf{B}_\gamma(\xi_{igaus})\,{}^\circ J_{igaus} W_{igaus}$$

$$\mathbf{f}_\gamma = \int_{-1}^{1} \mathbf{B}_\gamma^{\mathrm{T}}(\xi)(kGA\gamma(\xi))\,{}^\circ J \, \mathrm{d}\xi$$

$$= \sum_{igaus=1}^{Ngaus} \mathbf{B}_\gamma^{\mathrm{T}}(\xi_{igaus})(kGA\gamma(\xi_{igaus}))\,{}^\circ J_{igaus} W_{igaus}$$

2D–Plane Strain, **layered** approach (*Nonlinear beam*):

$$\mathbf{K}^e = \int_{-1}^{1} \sum_l \mathbf{B}_{\varepsilon x_{\mathsf{L}}}^{\mathrm{T}}(\xi, y_{\mathsf{L}^l}) D_{xxxx}^l \mathbf{B}_{\varepsilon x_{\mathsf{L}}}(\xi, y_{\mathsf{L}^l})\,{}^l J \, \mathrm{d}\xi + \mathbf{K}_{\gamma\gamma}$$

$$= \sum_{igaus=1}^{Ngaus} \sum_l \mathbf{B}_{\varepsilon x_{\mathsf{L}}}^{\mathrm{T}}(\xi_{igaus}, y_{\mathsf{L}^l}) D_{xxxx}^l \mathbf{B}_{\varepsilon x_{\mathsf{L}}}(\xi_{igaus}, y_{\mathsf{L}^l})\,{}^l J_{igaus} W_{igaus} + \mathbf{K}_{\gamma\gamma}$$

$$\mathbf{f}^e = \int_{-1}^{1} \sum_l \mathbf{B}_{\varepsilon x_{\mathsf{L}}}^{\mathrm{T}}(\xi, y_{\mathsf{L}^l}) \sigma_{xx}(\xi, y_{\mathsf{L}^l})\,{}^l J \, \mathrm{d}\xi + \mathbf{f}_{\gamma\gamma}$$

$$= \sum_{igaus=1}^{Ngaus} \sum_l \mathbf{B}_{\varepsilon x_{\mathsf{L}}}^{\mathrm{T}}(\xi_{igaus}, y_{\mathsf{L}^l}) \sigma_{xx_{\mathsf{L}}}(\xi_{igaus}, y_{\mathsf{L}^l})\,{}^l J_{igaus} W_{igaus} + \mathbf{f}_\gamma$$

Plane Strain , **integral** approach (*Elastic beam model*):

$$\mathbf{K}^{\mathrm{e}} = \int\limits_{-1}^{1} \left[\ \mathbf{B}_{\varepsilon}^{\mathrm{T}}(\xi);\ \ \mathbf{B}_{\kappa}^{\mathrm{T}}(\xi)\ \right] \left[\begin{array}{cc} EA & 0 \\ 0 & EL_z \end{array}\right] \left[\begin{array}{c} \mathbf{B}_{\varepsilon}(\xi) \\ \mathbf{B}_{\kappa}(\xi) \end{array}\right]\ {}^{\circ}J\,\mathrm{d}\xi + \mathbf{K}_{\gamma\gamma}$$

$$= \sum_{igaus=1}^{Ngaus} \left[\ \mathbf{B}_{\varepsilon}^{\mathrm{T}}(\xi_{igaus});\ \ \mathbf{B}_{\kappa}^{\mathrm{T}}(\xi_{igaus})\ \right] \left[\begin{array}{cc} EA & 0 \\ 0 & EL_z \end{array}\right] \left[\begin{array}{c} \mathbf{B}_{\varepsilon}(\xi_{igaus}) \\ \mathbf{B}_{\kappa}(\xi_{igaus}) \end{array}\right]$$

$${}^{\circ}J_{igaus}W_{igaus} + \mathbf{K}_{\gamma\gamma}$$

$$\mathbf{f}^{\mathrm{e}} = \int\limits_{-1}^{1} \left[\ \mathbf{B}_{\varepsilon}^{\mathrm{T}}(\xi);\ \ \mathbf{B}_{\kappa}^{\mathrm{T}}(\xi)\ \right] \left[\begin{array}{c} EA\varepsilon(\xi) \\ EI_z\kappa(\xi) \end{array}\right]\ {}^{\circ}J\,\mathrm{d}\xi + \mathbf{f}_{\gamma} =$$

$$\sum_{igaus=1}^{Ngaus} \left[\ \mathbf{B}_{\varepsilon}^{\mathrm{T}}(\xi_{igaus});\ \ \mathbf{B}_{\kappa}^{\mathrm{T}}(\xi_{igaus})\ \right] \left[\begin{array}{c} EA\varepsilon(\xi_{igaus}) \\ EI_z\kappa(\xi_{igaus}) \end{array}\right]\ {}^{\circ}J_{igaus}W_{igaus} + \mathbf{f}_{\gamma}$$

2D–Axisymmetry, **layered** approach (*Nonlinear beam*):

$$\mathbf{K}^{\mathrm{e}} = 2\pi \left(\int\limits_{-1}^{1} \sum_l \left[\ \mathbf{B}_{\varepsilon x_{\mathsf{L}}}^{\mathrm{T}}(\xi, y_{\mathsf{L}^l});\ \ \mathbf{B}_{\varepsilon z_{\mathsf{L}}}^{\mathrm{T}}(\xi, y_{\mathsf{L}^l})\ \right] \left[\mathbf{D}^l\right] \left[\begin{array}{c} \mathbf{B}_{\varepsilon x_{\mathsf{L}}}(\xi, y_{\mathsf{L}^l}) \\ \mathbf{B}_{\varepsilon z_{\mathsf{L}}}(\xi, y_{\mathsf{L}^l}) \end{array}\right] r(\xi)\ {}^lJ\mathrm{d}\xi + r\mathbf{K}_{\gamma\gamma} \right)$$

$$= 2\pi \left(\sum_{igaus=1}^{Ngaus} \sum_l \left[\ \mathbf{B}_{\varepsilon x_{\mathsf{L}}}^{\mathrm{T}}(\xi_{igaus}, y_{\mathsf{L}^l});\ \ \mathbf{B}_{\varepsilon z_{\mathsf{L}}}^{\mathrm{T}}(\xi_{igaus}, y_{\mathsf{L}^l})\ \right] \left[\mathbf{D}^l\right] \left[\begin{array}{c} \mathbf{B}_{\varepsilon x_{\mathsf{L}}}(\xi_{igaus}, y_{\mathsf{L}^l}) \\ \mathbf{B}_{\varepsilon z_{\mathsf{L}}}(\xi_{igaus}, y_{\mathsf{L}^l}) \end{array}\right] \right)$$

$$r(\xi_{igaus})\ {}^lJ_{igaus}W_{igaus} + 2\pi r\mathbf{K}_{\gamma\gamma}$$

$$\mathbf{f}^{\mathrm{e}} = 2\pi \left(\int\limits_{-1}^{1} \sum_l \left[\ \mathbf{B}_{\varepsilon x_{\mathsf{L}}}^{\mathrm{T}}(\xi, y_{\mathsf{L}^l});\ \ \mathbf{B}_{\varepsilon z_{\mathsf{L}}}^{\mathrm{T}}(\xi, y_{\mathsf{L}^l})\ \right] \left[\begin{array}{c} \sigma_{xx}(\xi, y_{\mathsf{L}^l}) \\ \sigma_{xz}(\xi, y_{\mathsf{L}^l}) \end{array}\right] r(\xi)\ {}^lJ\,\mathrm{d}\xi + r\mathbf{f}_{\gamma} \right) =$$

$$2\pi \left(\sum_{igaus=1}^{Ngaus} \sum_l \left[\ \mathbf{B}_{\varepsilon x_{\mathsf{L}}}^{\mathrm{T}}(\xi_{igaus}, y_{\mathsf{L}^l});\ \ \mathbf{B}_{\varepsilon z_{\mathsf{L}}}^{\mathrm{T}}(\xi_{igaus}, y_{\mathsf{L}^l})\ \right] \left[\begin{array}{c} \sigma_{xx}(\xi_{igaus}, y_{\mathsf{L}^l}) \\ \sigma_{xz}(\xi_{igaus}, y_{\mathsf{L}^l}) \end{array}\right] \right)$$

$$r(\xi_{igaus})\ {}^lJ_{igaus}W_{igaus} + 2\pi r\mathbf{f}_{\gamma}$$

where constitutive module matrix: $\quad \mathbf{D}^l_{(2\times2)} = \left[\begin{array}{cc} D_{xxxx} & D_{xxzz} \\ D_{zzxx} & D_{zzzz} \end{array}\right].$

3D analysis:

For both **layered** and **integral** approaches, treatment of transversal shear and torsion is de–coupled from treatment of bending and extension states. Thus element stiffness and forces are split according to:

$$\mathbf{K}^{\mathrm{e}} = \mathbf{K}^{\mathrm{e}}_{N-M} + \sum_{i=x,y} \mathbf{K}^{\mathrm{e}}_{\gamma i} + \mathbf{K}^{\mathrm{e}}_{\Psi}$$

$$\mathbf{f}^{\mathrm{e}} = \mathbf{f}^{\mathrm{e}}_{N-M} + \sum_{i=x,y}\mathbf{f}^{\mathrm{e}}_{\gamma i} + \mathbf{f}^{\mathrm{e}}_{\Psi}$$

The contributions common for **layered** and **integral** approaches are:

shear :

$$\mathbf{K}^{\mathrm{e}}_{\gamma i} = \int_{-1}^{1}\mathbf{B}^{\mathrm{T}}_{\gamma x_i}(\xi)k_i GA\mathbf{B}_{\gamma x_i}(\xi)\,^{\circ}\!J\,\mathrm{d}\xi$$

$$= \sum_{igaus=1}^{Ngaus}\mathbf{B}^{\mathrm{T}}_{\gamma x_i}(\xi_{igaus})k_i GA\mathbf{B}_{\gamma x_i}(\xi_{igaus})\,^{\circ}\!J_{igaus}W_{igaus}$$

$$\mathbf{f}^{\mathrm{e}}_{\gamma i} = \int_{-1}^{1}\mathbf{B}^{\mathrm{T}}_{\gamma x_i}(\xi)k_i GA\gamma_{x_i}(\xi)\,^{\circ}\!J\,\mathrm{d}\xi$$

$$= \sum_{igaus=1}^{Ngaus}\mathbf{B}^{\mathrm{T}}_{\gamma x_i}(\xi_{igaus})k_i GA\gamma_{x_i}(\xi_{igaus})\,^{\circ}\!J_{igaus}W_{igaus}$$

torsion:

$$\mathbf{K}^{\mathrm{e}}_{\Psi} = \int_{-1}^{1}\mathbf{B}^{\mathrm{T}}_{\Psi}(\xi)GI_x\mathbf{B}_{\Psi}(\xi)\,^{\circ}\!J\,\mathrm{d}\xi$$

$$= \sum_{igaus=1}^{Ngaus}\mathbf{B}^{\mathrm{T}}_{\Psi}(\xi_{igaus})GI_x\mathbf{B}_{\Psi}(\xi_{igaus})\,^{\circ}\!J_{igaus}W_{igaus}$$

$$\mathbf{f}^{\mathrm{e}}_{\Psi} = \int_{-1}^{1}\mathbf{B}^{\mathrm{T}}_{\Psi}(\xi)GI_x\mathbf{\Psi}(\xi)\,^{\circ}\!J\,\mathrm{d}\xi$$

$$= \sum_{igaus=1}^{Ngaus}\mathbf{B}^{\mathrm{T}}_{\Psi}(\xi_{igaus})GI_x\mathbf{\Psi}(\xi_{igaus})\,^{\circ}\!J_{igaus}W_{igaus}$$

Bending and extension states are treated in different ways:

layered approach (*Nonlinear beam model*):

$$\mathbf{K}^{\mathrm{e}}_{N-M} = \int_{-1}^{1}\sum_{l}\mathbf{B}^{\mathrm{T}}_{\varepsilon x_{\mathsf{L}}}(\xi,y_{\mathsf{L}^l},z_{\mathsf{L}^l})D^l_{xxxx}\mathbf{B}_{\varepsilon x_{\mathsf{L}}}(\xi,y_{\mathsf{L}^l},z_{\mathsf{L}^l})\,^l\!J\,\mathrm{d}\xi$$

$$= \sum_{igaus=1}^{Ngaus}\sum_{l}\mathbf{B}^{\mathrm{T}}_{\varepsilon x_{\mathsf{L}}}(\xi_{igaus},y_{\mathsf{L}^l},z_{\mathsf{L}^l})D^l_{xxxx}\mathbf{B}_{\varepsilon x_{\mathsf{L}}}(\xi_{igaus},y_{\mathsf{L}^l},z_{\mathsf{L}^l})\,^l\!J_{igaus}W_{igaus}$$

$$\mathbf{f}^{\mathsf{e}}_{N-M} = \int\limits_{-1}^{1} \sum_{l} \mathbf{B}^{\mathsf{T}}_{\varepsilon x_{\mathsf{L}}}(\xi, y_{\mathsf{L}^l}, z_{\mathsf{L}^l}) \sigma_{xx}(\xi, y_{\mathsf{L}^l}, z_{\mathsf{L}^l})\,^l J \, \mathrm{d}\xi$$

$$= \sum_{igaus=1}^{Ngaus} \sum_{l} \mathbf{B}^{\mathsf{T}}_{\varepsilon x_{\mathsf{L}}}(\xi_{igaus}, y_{\mathsf{L}^l}, z_{\mathsf{L}^l}) \sigma_{xx}(\xi_{igaus}, y_{\mathsf{L}^l}, z_{\mathsf{L}^l})\,^l J_{igaus} W_{igaus}$$

integral approach (*Elastic beam model*):

$$\mathbf{K}^{\mathsf{e}}_{N-M} = \int\limits_{-1}^{1} \begin{bmatrix} \mathbf{B}^{\mathsf{T}}_{\varepsilon}(\xi); & \mathbf{B}^{\mathsf{T}}_{\kappa y}(\xi); & \mathbf{B}^{\mathsf{T}}_{\kappa z}(\xi) \end{bmatrix} \begin{bmatrix} EA & 0 & 0 \\ 0 & EI_y & 0 \\ 0 & 0 & EI_z \end{bmatrix} \begin{bmatrix} \mathbf{B}_{\varepsilon}(\xi) \\ \mathbf{B}_{\kappa y}(\xi) \\ \mathbf{B}_{\kappa z}(\xi) \end{bmatrix} {}^{\circ}J \, \mathrm{d}\xi$$

$$= \sum_{igaus=1}^{Ngaus} \begin{bmatrix} \mathbf{B}^{\mathsf{T}}_{\varepsilon}(\xi_{igaus}); & \mathbf{B}^{\mathsf{T}}_{\kappa y}(\xi_{igaus}); & \mathbf{B}^{\mathsf{T}}_{\kappa z}(\xi_{igaus}) \end{bmatrix} \begin{bmatrix} EA & 0 & 0 \\ 0 & EI_y & 0 \\ 0 & 0 & EI_z \end{bmatrix}$$

$$\begin{bmatrix} \mathbf{B}_{\varepsilon}(\xi_{igaus}) \\ \mathbf{B}_{\kappa y}(\xi_{igaus}) \\ \mathbf{B}_{\kappa z}(\xi_{igaus}) \end{bmatrix} {}^{\circ}J_{igaus} W_{igaus}$$

$$\mathbf{f}^{\mathsf{e}}_{N-M} = \int\limits_{-1}^{1} \begin{bmatrix} \mathbf{B}^{\mathsf{T}}_{\varepsilon}(\xi) & \mathbf{B}^{\mathsf{T}}_{\kappa y}(\xi) & \mathbf{B}^{\mathsf{T}}_{\kappa z}(\xi) \end{bmatrix} \begin{bmatrix} EA\varepsilon(\xi) \\ EI_y \kappa_y(\xi) \\ EI_z \kappa_z(\xi) \end{bmatrix} {}^{\circ}J \, \mathrm{d}\xi$$

$$= \sum_{igaus=1}^{Ngaus} \begin{bmatrix} \mathbf{B}^{\mathsf{T}}_{\varepsilon}(\xi_{igaus}); & \mathbf{B}^{\mathsf{T}}_{\kappa y}(\xi_{igaus}); & \mathbf{B}^{\mathsf{T}}_{\kappa z}(\xi_{igaus}) \end{bmatrix}$$

$$\begin{bmatrix} EA\varepsilon(\xi_{igaus}) \\ EI_y \kappa_y(\xi_{igaus}) \\ EI_z \kappa_z(\xi_{igaus}) \end{bmatrix} {}^{\circ}J_{igaus} W_{igaus}$$

The element load $\mathbf{p}$ is assumed to act along the centroid line leading to load induced forces evaluated as:

$$\mathbf{f}_p = \int\limits_{-1}^{1} \mathbf{N}^{\mathsf{T}}(\xi)\mathbf{p}\,{}^{\circ}J \, \mathrm{d}\xi = \sum_{igaus=1}^{Ngaus} \mathbf{N}^{\mathsf{T}}(\xi_{igaus})\mathbf{p}\,{}^{\circ}J_{igaus} W_{igaus}$$

$$\mathbf{N}(\xi) = \begin{bmatrix} N_i(\xi)\mathbf{I}_{(\dim)} \end{bmatrix}, \qquad i = 1, Nen$$

All element forces and stiffness, as given above, are referred to centroidal nodes of the element. Prior to the agregation to global ones, they are submitted to *Master–centroid (offset) transformation*, see Appendix 5.6.1 .

5.2.7 MASTER-CENTROID (OFFSET) TRANSFORMATION

In order to deal with the frequently encountered situation where beam elements are connected to other elements of the model by nodes, which are not the centroids of a beam cross section, offset transformation of element displacement, forces and stiffness is introduced. The DOF of the element are placed on its "master" nodes defining connectivity. Based on rigid body movement of the "master", translation and rotation displacements of the "centroid" are evaluated.

For the details of "master-slave" offset transformation see the Appendix 5.6.1 .

5.2.8   RELAXATION OF INTERNAL DOF

Stiffness matrix and force vector derived above concerns element with all DOF active. Situation when user demanded group of DOF is relaxed (what means that no forces are transmitted by the element in selected directions).The directions of relaxed DOF might be related to local element directions at both ends of the element.

If given directions at beam node are relaxed, the node is implicitly duplicated and DSC (Node-to-node interface) elements are introduced to the model. The stiffness of that interface remains 0 at relaxed direction, while it is assumed to take penalty values, estimated automaticaly from beam stiffness on fixed DOF.

5.2.9   BEAM ELEMENT RESULTS

Element stress resultants are referred to cross section local coordinate system at the integration point. The sign convention is as follows:

N normal force	–	positive in tension
M_i bending moment	–	positive, are such which leads to positive (tensile) stresses in the points with positive local coordinate on the complementary axis
Q_i shear forces	–	positive is such that produce positive shear stresses acting in the i–th local direction
M_x torsion moment	–	positive moment is represented by the vector directed towards outer normal

Note, that in case of all analysis types, signs of some stress resultants are related to node order $C1 - C2$

Window 5-10: 2D beam element result setting

2D Beam element results sign convention, case of:

-Plane strain,

-Generalized PS
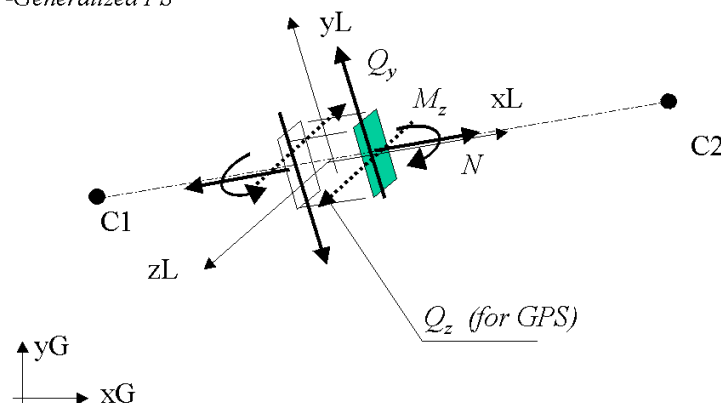
2D beam element results sign convention

Window 5-10

Note, that for *Plane Strain* and case of discrete beam system in Z direction stress resultants are referred to single beam but not a unit slice of a model.

Window 5-11: Axisymetric shell element result setting

2D Beam element results sign convention, case of:
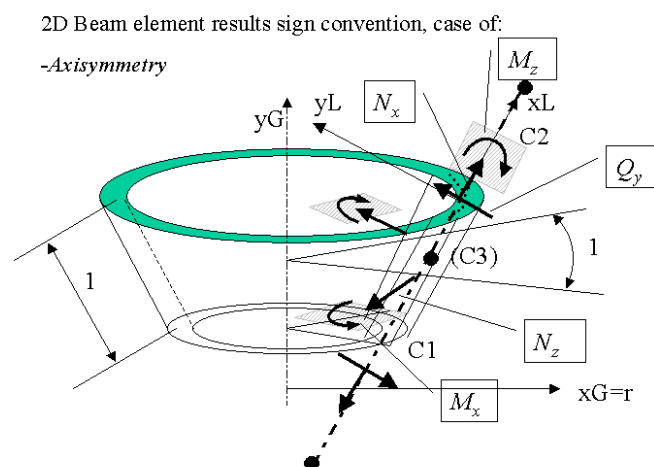
-Axisymmetry

Axisymmetric shell element results sign convention

Window 5-11

Note, that in the case of *Axisymmetry*, evaluated stress resultants are referred to the unit length of the axi–symmetric shell both in circumference and meridian direction.

Window 5-12: 3D beam element result setting

3D Beam element results sign convention
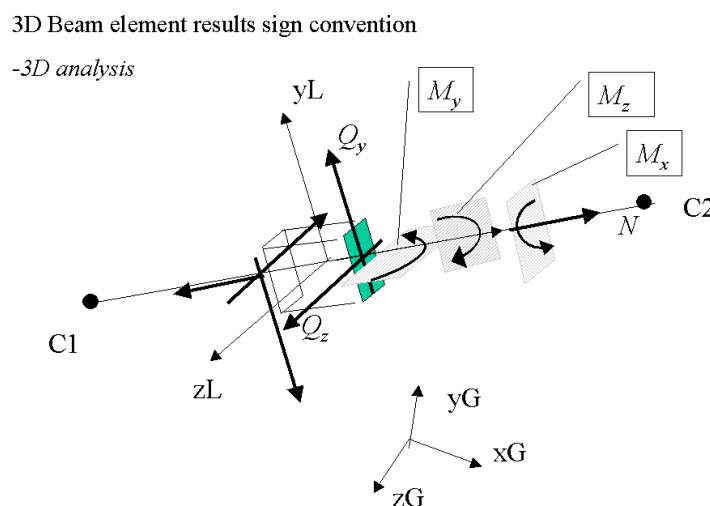
-3D analysis

3D beam element results sign convention

Window 5-12

5.3   SHELLS

Following paragraphs present most important aspects of applied shell elements

BASIC ASSUMPTIONS OF SHELL ANALYSIS

SETTING OF THE ELEMENT GEOMETRY

ELEMENT MAPPING AND COORDINATE SYSTEMS

CROSS–SECTION MODELS

DISPLACEMENT AND STRAIN FIELD WITHIN THE ELEMENT

TREATMENT OF TRANSVERSAL SHEAR

WEAK FORMULATION OF EQUILIBRIUM

STIFFNESS MATRIX AND ELEMENT FORCES

LOADS

SHELL ELEMENT RESULTS

5.3.1   BASIC ASSUMPTIONS OF SHELL ANALYSIS

Shell elements are 2D elements in 3D space, which are of course compatible with the continuum, beam, truss and, contact elements. The degenerated continuum approach is used, in which deformation field within the element is described by translations and independent fiber rotations field (Mindlin-Reissner hypothesis) of the "reference surface". The fiber is assumed to be in-extensive. The principles of the shell kinematics are shown in the following Figure.
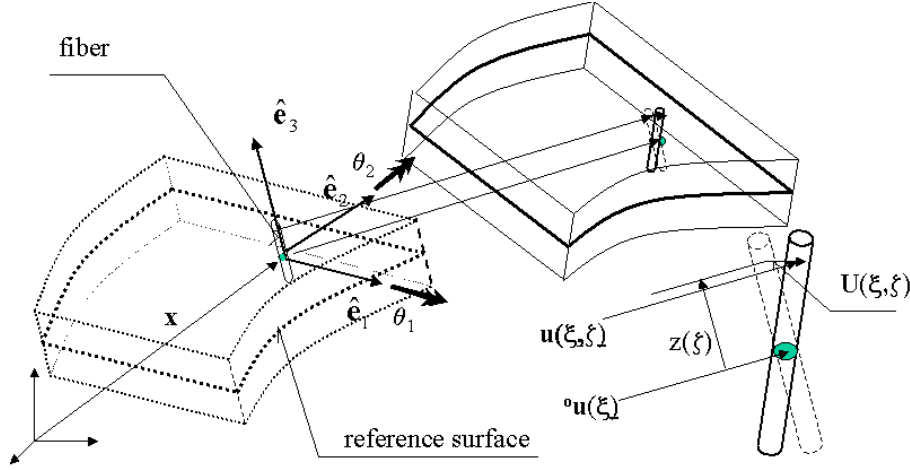
Shell kinematics principle

The displacement field $\mathbf{u}$ within the element is split into two parts. First is related to reference surface translation $\mathbf{^0u}$, and second $\mathbf{U}$ is related to fiber rotation:

$$\mathbf{u}(\boldsymbol{\xi}, \zeta) = \mathbf{^0u}(\boldsymbol{\xi}) + \mathbf{U}(\boldsymbol{\xi}, \zeta)$$

$$\mathbf{U}(\boldsymbol{\xi}, \zeta) = z(\zeta)(\theta_2(\boldsymbol{\xi}) \, \hat{\mathbf{e}}_1 - \theta_1(\boldsymbol{\xi}) \, \hat{\mathbf{e}}_2)$$

where:

$\boldsymbol{\xi} = [\xi, \eta]^{\mathrm{T}}$ – point coordinates at the reference element,

$\left\{ \hat{\mathbf{e}}_i(\boldsymbol{\xi}), i = 1, 2, 3 \right\}$ – fiber coordinate system,

$\theta_i(\boldsymbol{\xi}), i = 1, 2$ – fiber rotation vector components referred to fiber coordinate system,

$z(\zeta)$ – lamina coordiante.

In each lamina plane stress hypothesis is adopted. Moreover transversal shear strains and stresses are accounted for. Each node of the reference surface posses 6 DOF, i.e.:

$$\mathbf{q} = \left\{ u_1, u_2, \phi_1, \phi_2, \phi_3 \right\}^{\mathrm{T}}$$

Nodal rotations ϕ are transformed to nodal fiber coordinate systems

$$\left\{ \hat{\mathbf{e}}_{ai}(\boldsymbol{\xi}), i = 1, 2, 3; \ a = 1, Nen \right\}.$$

Bending rotation components $\theta_i(\boldsymbol{\xi}), i = 1, 2$ are used to evaluate element strains and then stresses, while only stabilization ε–stiffness is attached to so called "drilling rotation" θ_3.

5.3.2   SETTING OF THE ELEMENT GEOMETRY

Four (8) and eight (16) nodes shell elements are available. Two modeling options and related classes of shell elements are:

A. Shell elements with 2 layers of nodes (Window 5-13)

B. Shell elements with 1 layer of nodes (Window 5-14)

Window 5-13: Shell elements − 2 layers

SHQ4

Master nodes

Slave nodes

Reference surface
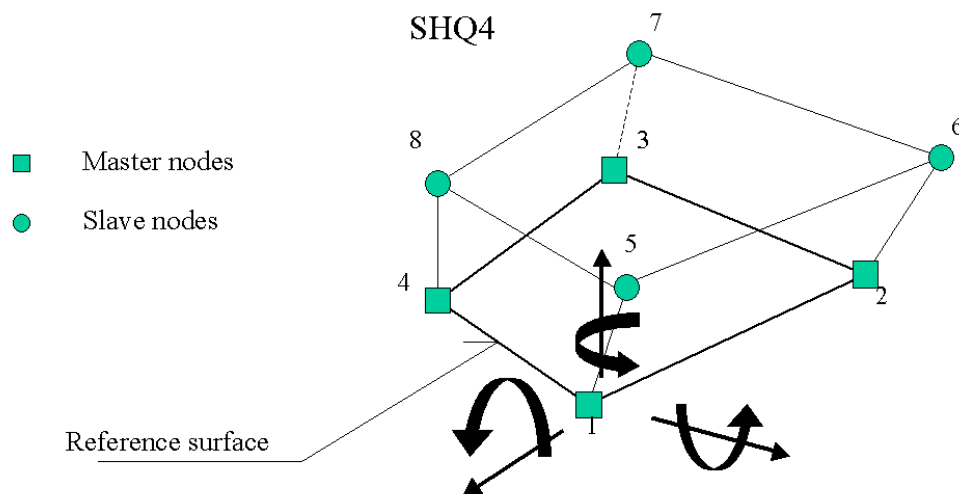
Shell elements with 2 layers of nodes

Window 5-13

Elements are designed to be fully compatible in all kind of connections with surrounding volume elements, without overlapping. They have DOF attached only to one (master) layer of nodes creating "reference surface", slave nodes are used to define the geometry. Master nodes 1 to 4 characterize the SHQ4 element with bilinear interpolation are slave nodes which help constructing meshes and manage variable thickness. Shell elements are connected (or not) to the other elements through either master or slave elements. As the only degrees-of-freedom retained for analysis correspond to master nodes all loads applied to slave nodes will be transferred to master nodes assuming a rigid link, with possibly resulting moments. Similarly results (displacements) obtained at master nodes are transferred to slave nodes assuming a rigid link, so that a master node rotation may result in an additional slave node translation. Moreover, **offset transformation**, see Appendix 5.6.1 , is performed on force vectors and stiffness matrices of all other elements adjacent to the slave node layer. Described modeling option posses however following <u>limitations</u>:

1. mechanical boundary conditions can not be applied to slave nodes,

2. while connecting beam to shell elements Master-to-Master and slave-to-slave condition must be respected.

Window 5-14: Shell elements – 1 layer

SXQ4

■ Master nodes

Reference surface
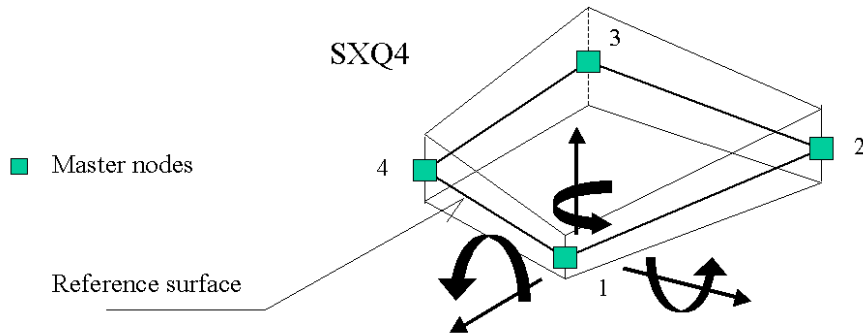
Shell elements with 1 layer of nodes

Window 5-14

Elements are designed to be used in thin shell-structural systems. Element thickness (variable allowed) must be set as an additional data. It is of course taken into account during element stiffness/forces evaluation, but in the sense of geometrical modeling 0 thickness is in fact assumed. This means that the volume occupied by a shell may be over-lapped in the case when a volume element is adjacent to the shell element (i.e. when shell nodes consist a face of a volume element). Fiber is assumed to be strictly orthogonal to the reference surface.

Window 5-15: Setting of the variable thickness data

Variable thickness of the shell elements is set using the following algorithm:

- A family of fictitious (and temporary) thickness interpolation macro-elements is introduced. It consist of linear L1, surface triangular T3,T6 and surface quadrilateral Q4, elements. User has to define the thickness values $\{h_i, i = 1, Nen\}$ at the nodes of these macro-elements.

- Current point $\mathbf{x}$ at the shell element is projected ortogonally onto the surface of fictitious element $\mathbf{x} \rightarrow \mathbf{x}'$, and then local coordinates ξ' of a point $\mathbf{x}'$ at the macro-element are set.

- The thickness at the current point $h(\mathbf{x})$ is equal to the value at the projection point $h(\mathbf{x}')$ and, as such, is interpolated from the nodal values of the thickness using macro-element shape functions N_i'.

$$h(\mathbf{x}) = h(\mathbf{x}') = \sum_{i=1,Nen} h_i N_i'(\xi'(\mathbf{x}'))$$

Window 5-15

Despite above difference in element geometry description all others mechanical features of the element (kinematics, constitutive modeling) are common for both classes A. and B.
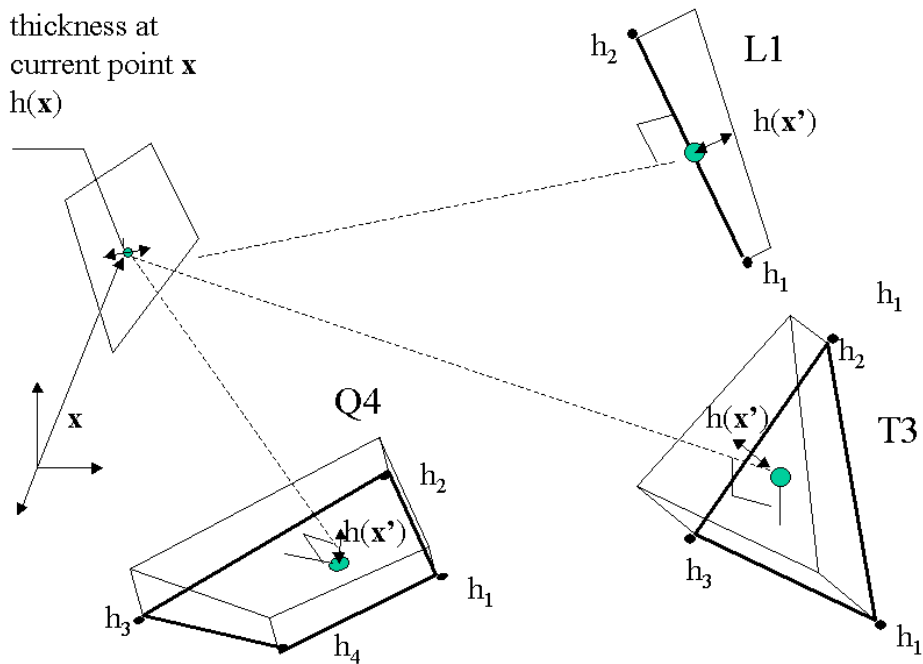
Different possibilities of variable thickness setting
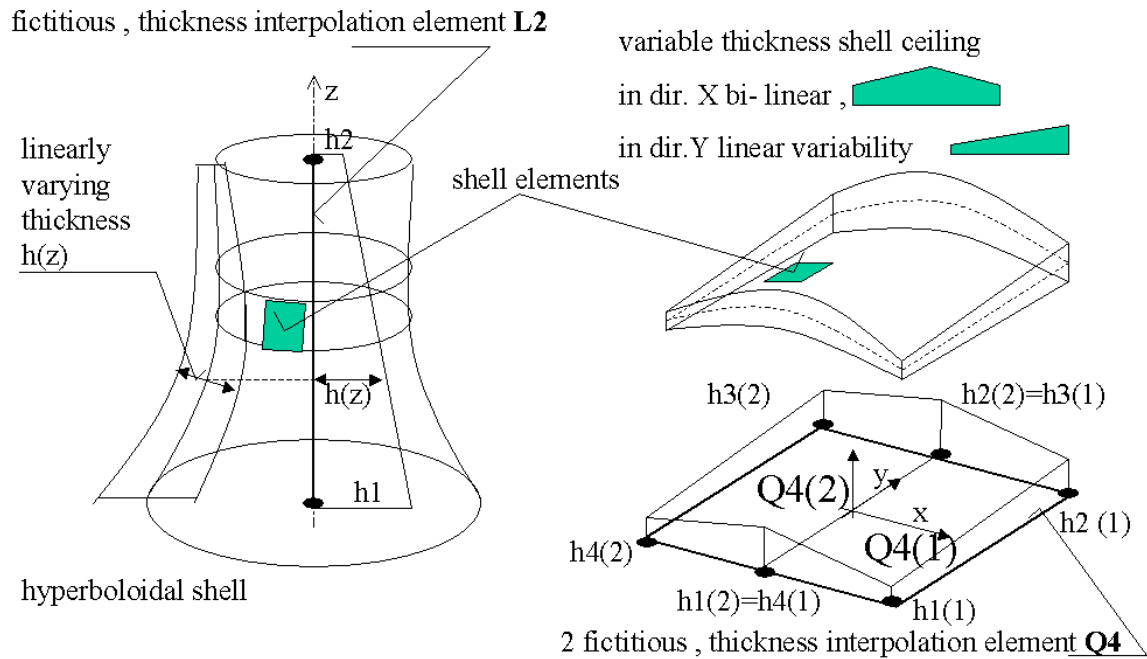
Practical examples of the variable thickness setting

5.3.3   ELEMENT MAPPING AND COORDINATE SYSTEMS

Given construction of the shell element is common for each type of shell element SXQ4, SHQ4.

Window 5-16: Shell elements coordinate systems and mapping

- Nodal basis, after [1]

for each node $a = 1, Nen$

$$\{\widehat{\mathbf{e}}_{ai}, \quad i = 1,2,3\} =$$

$$[\widehat{\mathbf{e}}_{a1}, \widehat{\mathbf{e}}_{a2}, \widehat{\mathbf{e}}_{a3}] = \begin{cases} \begin{bmatrix} n_z + \dfrac{1}{1+n_z}n_y^2 & -\dfrac{1}{1+n_z}n_x n_y & n_x \\ -\dfrac{1}{1+n_z}n_x n_y & n_z + \dfrac{1}{1+n_z}n_x^2 & n_y \\ -n_x & -n_y & n_z \end{bmatrix} &, if\, n_z \neq -1 \\[6pt] \begin{bmatrix} 1 & 0 & 0 \\ 0 & -1 & 0 \\ 0 & 0 & -1 \end{bmatrix} &, if\, n_z = -1 \end{cases}$$

where: $\mathbf{n}_a = [n_x, n_y, n_z]^{\mathrm{T}}$ is element reference surface normal at node a.

- Mapping from the reference element is constructed as follows, after[2]: $\mathbf{x}(\xi,\eta,\zeta) = {}^{\mathbf{o}}\mathbf{x}(\xi,\eta) + \mathbf{X}(\xi,\eta,\zeta)$
  with:

  reference surface:

  $$^{\mathbf{o}}\mathbf{x}(\xi,\eta) = \sum_{a=1,Nen} N_a(\xi,\eta) \,{}^{\mathbf{o}}\mathbf{x}_a;$$

  position on the director:

  $$\mathbf{X}(\xi,\eta,\zeta) = \sum_{a=1,Nen} N_a(\xi,\eta) \, z_a(\zeta)\widehat{\mathbf{e}}_{a3;}$$

  where:

  $$z_a(\zeta) = \frac{1}{2}(1+\zeta)z_a^+ + \frac{1}{2}(1-\zeta)z_a^-$$

---

[1]J.L. Batoz, G. Dhatt, Modelisation des structures par element finis, Ed.Hermes, Paris 1992.
[2]T.J.R. Hughes, The Finite Element method, Ed.Prentice–Hall Inc.1988.

$$
\left.
\begin{array}{ll}
z_a^+ = h_a; & z_a^- = 0; \qquad \text{for SHQ4} \\[2mm]
z_a^+ = h_a/2; & z_a^- = -h_a/2; \quad \text{for SXQ4}
\end{array}
\right\} \Rightarrow z_{a,\zeta} = h_a/2.
$$

Jacobi matrix of the mapping:

$$
\begin{aligned}
\mathbf{J} &= \left[\mathbf{x}_{,\xi}; \mathbf{x}_{,\eta}; \mathbf{x}_{,\zeta}\right] = \left[{}^{\mathbf{o}}\mathbf{x}_{,\xi}; {}^{\mathbf{o}}\mathbf{x}_{,\eta}; 0\right] + \\
&+ \sum_{a=1,Nen} z_a(\zeta) \left[\widehat{\mathbf{e}}_{a3} N_{a,\xi}; \widehat{\mathbf{e}}_{a3} N_{a,\eta}; 0\right] + \sum_{a=1,Nen} \left[0; 0; \widehat{\mathbf{e}}_{a3} N_{a,\zeta}\right]
\end{aligned}
$$

Shape function global derivatives:

$$
\frac{\partial N_a}{\partial \mathbf{x}} = \mathbf{J}^{-\mathrm{T}}
\begin{bmatrix} N_{a,\xi} \\ N_{a,\eta} \\ 0 \end{bmatrix};
\qquad
\frac{\partial z N_a}{\partial \mathbf{x}} = \mathbf{J}^{-\mathrm{T}}
\left(z \begin{bmatrix} N_{a,\xi} \\ N_{a,\eta} \\ 0 \end{bmatrix} + N_a \begin{bmatrix} 0 \\ 0 \\ z_{,\zeta} \end{bmatrix} \right)
$$

Derivatives versus local directions $\{x_{iL}\}, i = 1, 2, 3$ are evaluated as:

$$
\frac{\partial}{\partial x_{iL}} = \mathbf{e}_i^{\mathrm{T}} \frac{\partial}{\partial \mathbf{x}}.
$$

- Gauss point base, at layer ζ after[3], see Appendix: 5.6.3
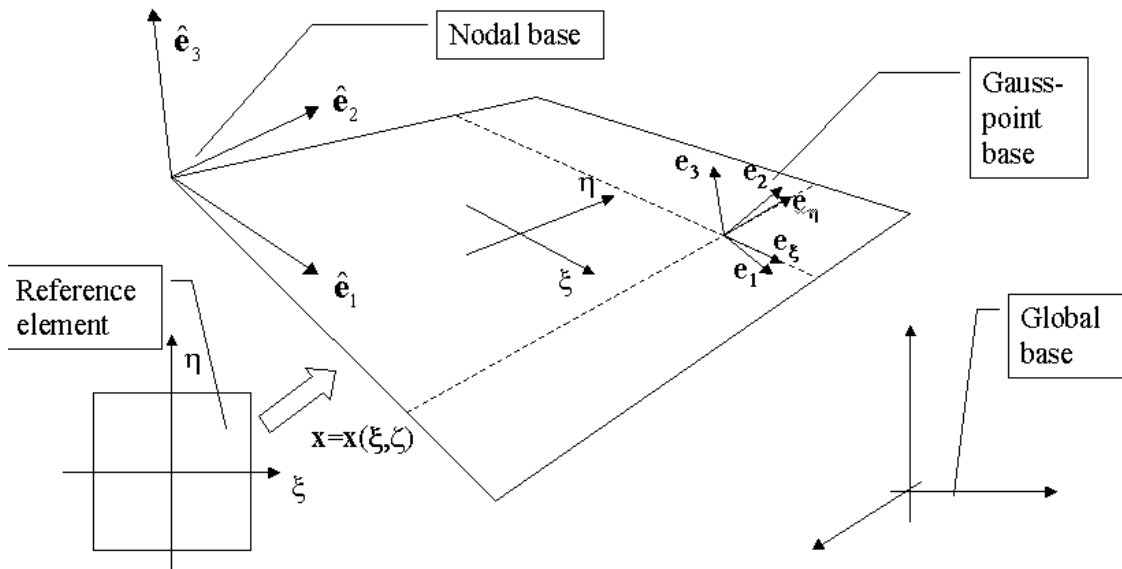
Shell element coordinate systems and mapping

Window 5-16

---

[3]T.J.R. Hughes, The Finite Element method, Ed.Prentice–Hall Inc.1988.

5.3.4   CROSS–SECTION MODELS

Independently from the element geometry description, two approaches to modeling of the cross sectional behavior of a shell are available. They are:

(i) *homogeneous section, elastic model.*

The cross section is fully described by elastic material data, i.e. Young module E and Poisson ratio ν. Note, that element thickness is set as geometric data, independent from cross section model. Numerical integration along the depth of an element is performed using 2-point Gauss rule.

(ii) *layered model* (non–homogenous section or/and material non–linearity).

The cross section is understood as a set of layers with possible different material models in each. In the case of homogenous section but non-linear material model introduction of layers may be understood as the specification of integration rule, different than 2-point Gauss rule used in the case of homogenous elastic section.

The following data must be specified for the whole section:

– number of layers $Nlayer \leq NLAYER\_MAX = 20$

– elastic properties E, ν

– averaged volume unit weight (for evaluation of gravity load)

while for each layer required are:

– z_i, the position of the layer center (relative or the distance from top/bottom)

– $w_i = \frac{h_i}{h}$, the relative depth of the layer or, for the fiber model, the area of fiber

per unit length.

– indication of a material model attached to the layer.

The models to be used in that context are : elastic , elasto-plastic Menetrey–

Willam, $1D$ elasto-plastic fiber model, In the latter case, for each elasto–

plastic fiber model

– E, the elastic modulus,

– f_{ty}, the tensile yield stress,

– f_{cy}, the compressive yield stress,

– n_x, n_y, n_z direction cosines of a unit vector; the projection of **n** on the element

surface will define the fiber orientation, see Appendix 5.6.2   and example in the following figure.
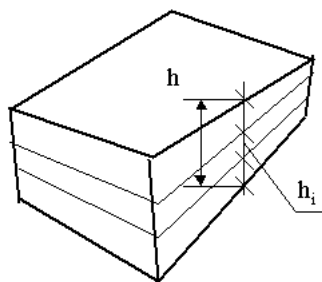
variable thickness, constant h_i/h ratio preserved
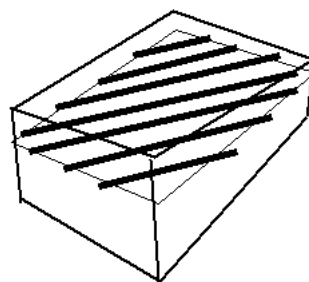
2 options of fiber layer position setting, i.e. preserved is:

or: $\dfrac{\text{relative distance } \zeta \in (-1.0, 1.0)}{\text{distance from top/bottom}}$

Example:

$\mathbf{n_1} = \{0,0,1\}^T$

fiber 1

$\mathbf{n_2} = \{0,1,0\}^T$

fiber 2

Setting of fiber direction as a projection of direction versor $\mathbf{n}$
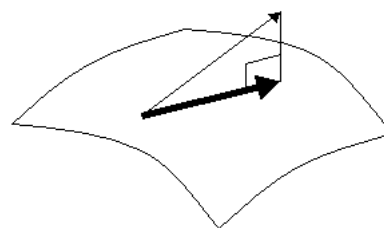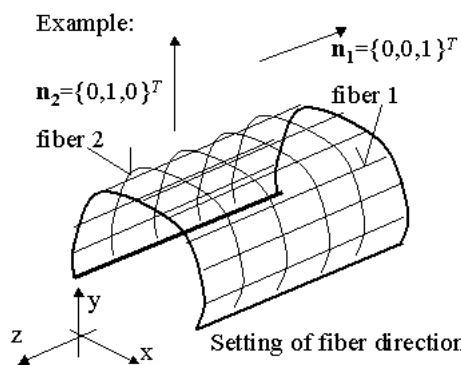
Shell cross–section and fiber orientation models

5.3.5 DISPLACEMENT AND STRAIN FIELD WITHIN THE ELE-MENT

Assumed kinematic hypothesis together with interpolating (shape) functions built upon reference element with node number $Nen = 4$ (SHQ4, SXQ4) lead to the following expressions for the displacement field within the element. The displacement field may be expressed :

- in terms of nodal translations $\mathbf{u}_a$ and rotations θ_{a1}, θ_{a2} in the directions of nodal base vectors $\widehat{\mathbf{e}}_1, \widehat{\mathbf{e}}_2$ tangent to the element reference surface, as:

$$\mathbf{u}(\boldsymbol{\xi}, \zeta) = \sum_{a=1,Nen} N_a(\boldsymbol{\xi})\mathbf{u}_a + \sum_{a=1,Nen} N_a(\boldsymbol{\xi})z(\zeta)(\widehat{\mathbf{e}}_{a1}\theta_{a2} - \widehat{\mathbf{e}}_{a2}\theta_{a1})$$

Above will be used to evaluate element strains.

- in terms of element DOF vector $\mathbf{q}$, including global components of rotations ϕ using generalized shape function matrix $\mathbf{N}$, as:

$$\mathbf{u}(\boldsymbol{\xi}, \zeta) = \mathbf{N}(\boldsymbol{\xi}, \zeta)\mathbf{q}$$

$$\mathbf{q} = [u_{a1}, u_{a2}, u_{a3}, \phi_{a1}, \phi_{a2}, \phi_{a3}]^{\mathrm{T}}, \quad a = 1, Nen$$

$$\mathbf{N}(\boldsymbol{\xi}, \zeta) = \left[N_a(\boldsymbol{\xi})\mathbf{I}_{3\times3}; \quad z(\zeta)N_a(\boldsymbol{\xi})(\widehat{\mathbf{e}}_{a1}\widehat{\mathbf{e}}_{a2}^{\mathrm{T}} - \widehat{\mathbf{e}}_{a2}\widehat{\mathbf{e}}_{a1}^{\mathrm{T}}) \right], \quad a = 1, Nen$$

Above, will be used for evaluation of element equivalent forces, and for numerical realization of anchoring, see p. Strain approximation is built upon nodal translations $\mathbf{u}_a$ and rotations θ_{a1}, θ_{a2} in the directions of nodal base vectors $\widehat{\mathbf{e}}_1, \widehat{\mathbf{e}}_2$ tangent to the element reference surface, consisting 5 components of DOF vector $\mathbf{q}_{(5)}$

$$\mathbf{q}_{(5)} = [u_{a1}, u_{a2}, u_{a3}, \theta_{a1}, \theta_{a2}]^{\mathrm{T}}, \quad a = 1, Nen$$

$$\boldsymbol{\varepsilon}_m = \left[\frac{\partial u_{1L}}{\partial x_{1L}}, \quad \frac{\partial u_{2L}}{\partial x_{2L}}, \quad \frac{\partial u_{1L}}{\partial x_{2L}} + \frac{\partial u_{2L}}{\partial x_{1L}} \right] = \mathbf{B}_m \mathbf{q}_{(5)}$$

$$\boldsymbol{\varepsilon}_s = \left[\frac{\partial u_{1L}}{\partial x_{3L}} + \frac{\partial u_{3L}}{\partial x_{1L}}, \quad \frac{\partial u_{2L}}{\partial x_{3L}} + \frac{\partial u_{3L}}{\partial x_{2L}} \right] = \mathbf{B}_s \mathbf{q}_{(5)}$$

Membrane strains are evaluated in unified way for all options considered, with $\mathbf{B}_m$ matrix taking form:

$$\mathbf{B}_m = \begin{array}{c} \vdots \qquad\quad \mathbf{u} \quad \vdots \qquad \theta_\alpha, \alpha = 1, 2 \quad \vdots \\ \left[\begin{array}{ccc} \mathbf{e}_1^{\mathrm{T}} \dfrac{\partial N_a}{\partial x_{1L}} & & \omega_{a1\alpha} \dfrac{\partial z N_a}{\partial x_{1L}} \\[2ex] \mathbf{e}_1^{\mathrm{T}} \dfrac{\partial N_a}{\partial x_{1L}} & \vdots & \omega_{a2\alpha} \dfrac{\partial z N_a}{\partial x_{2L}} \\[2ex] \mathbf{e}_1^{\mathrm{T}} \dfrac{\partial N_a}{\partial x_{2L}} + \mathbf{e}_2^{\mathrm{T}} \dfrac{\partial N_a}{\partial x_{1L}} & & \omega_{a1\alpha} \dfrac{\partial z N_a}{\partial x_{2L}} + \omega_{a2\alpha} \dfrac{\partial z N_a}{\partial x_{1L}} \end{array} \right] \end{array}, \quad a = 1, Nen$$

where:

$$\omega_{ak1} = -\mathbf{e}_k^{\mathrm{T}}\widehat{\mathbf{e}}_{a2}; \quad \omega_{ak2} = -\mathbf{e}_k^{\mathrm{T}}\widehat{\mathbf{e}}_{a1}.$$

For transversal shear strains (i.e. mean shear angles), evaluated at the mid-surface *standard* and *enhanced* options are provided. While *standard* option is used, shear strains are evaluated with use of:

$$\vdots \qquad \mathbf{u} \quad \vdots \qquad \theta_\alpha, \alpha = 1, 2 \quad \vdots$$

$$
{}^o\mathbf{B}_s = \begin{bmatrix}
\mathbf{e}_1^{\mathrm{T}}\dfrac{\partial N_a}{\partial x_{3L}} + \mathbf{e}_3^{\mathrm{T}}\dfrac{\partial N_a}{\partial x_{1L}} & \omega_{a1\alpha}\dfrac{\partial z N_a}{\partial x_{3L}} + \omega_{a3\alpha}\dfrac{\partial z N_a}{\partial x_{1L}} \\
& \vdots & \\
\mathbf{e}_2^{\mathrm{T}}\dfrac{\partial N_a}{\partial x_{3L}} + \mathbf{e}_3^{\mathrm{T}}\dfrac{\partial N_a}{\partial x_{2L}} & \omega_{a2\alpha}\dfrac{\partial z N_a}{\partial x_{3L}} + \omega_{a3\alpha}\dfrac{\partial z N_a}{\partial x_{2L}}
\end{bmatrix}, \quad a = 1, Nen.
$$

For *enhanced* option, in order to omit shear-locking problem in low order Q4 elements *Mixed Interpolation of Tensorial Components* (MITC) approach is optionally introduced, after Batoz[4]. In that case appropriate form of the ${}^o\mathbf{B}_s$ matrix may be derived from following consideration. Covariant components of mean shear angle $\boldsymbol{\gamma}_\alpha = [\gamma_\xi, \gamma_\eta]^{\mathrm{T}}$ are interpolated from its mid–side representatives as:
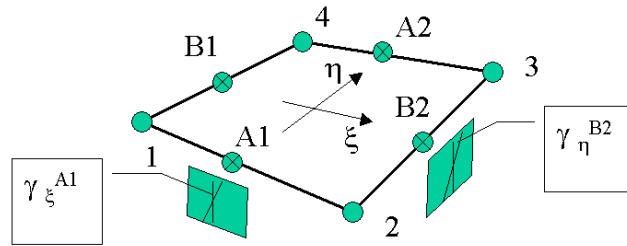
Mean shear angle components

$$\gamma_\xi = \frac{1-\eta}{2}\gamma_\xi^{A1} + \frac{1+\eta}{2}\gamma_\xi^{A2}; \quad \gamma_\eta = \frac{1-\xi}{2}\gamma_\eta^{B1} + \frac{1+\xi}{2}\gamma_\eta^{B2};$$

where

$$\gamma_\xi^{A1} = (\mathbf{a}_1^{\mathrm{T}}\boldsymbol{\beta} + \mathbf{n}^{\mathrm{T}}\, {}^o\mathbf{u}_{,\xi})|_{\xi=0,\eta=-1}; \qquad \gamma_\xi^{A2} = (\mathbf{a}_1^{\mathrm{T}}\boldsymbol{\beta} + \mathbf{n}^{\mathrm{T}}\, {}^o\mathbf{u}_{,\xi})|_{\xi=0,\eta=1}$$

$$\gamma_\eta^{B1} = (\mathbf{a}_2^{\mathrm{T}}\boldsymbol{\beta} + \mathbf{n}^{\mathrm{T}}\, {}^o\mathbf{u}_{,\eta})|_{\xi=-1,\eta=0}; \qquad \gamma_\eta^{B2} = (\mathbf{a}_2^{\mathrm{T}}\boldsymbol{\beta} + \mathbf{n}^{\mathrm{T}}\, {}^o\mathbf{u}_{,\eta})|_{\xi=1,\eta=0}$$

$$\mathbf{a}_1 = {}^o\mathbf{x}_{,\xi}; \quad \mathbf{a}_1 = {}^o\mathbf{x}_{,\eta}; \qquad \boldsymbol{\beta} = \sum_{a=1,Nen} N_a(\boldsymbol{\xi})(\widehat{\mathbf{e}}_{a1}\theta_{a2} - \widehat{\mathbf{e}}_{a2}\theta_{a1}).$$

---

[4]J.L.Batoz, G.Dhatt, Modelisation des structures par element finis, Ed.Hermes, Paris 1992.

After transformation components of mean shear angle $\varepsilon_S = [\gamma_{1L}, \gamma_{2L}]^{\mathrm{T}}$ in local Gauss point base $\{Q\}$ are obtained as:

$$\varepsilon_S = \mathbf{C}^{\mathrm{T}}\boldsymbol{\gamma}_\alpha; \qquad \text{with: } \mathbf{C} = \begin{bmatrix} \mathbf{a}_1^{\mathrm{T}}\mathbf{a}_1 & \mathbf{a}_1^{\mathrm{T}}\mathbf{a}_2 \\ symm & \mathbf{a}_2^{\mathrm{T}}\mathbf{a}_2 \end{bmatrix}^{-1} \begin{bmatrix} \mathbf{a}_1^{\mathrm{T}}\mathbf{e}_1 & \mathbf{a}_1^{\mathrm{T}}\mathbf{e}_2 \\ \mathbf{a}_1^{\mathrm{T}}\mathbf{e}_2 & \mathbf{a}_2^{\mathrm{T}}\mathbf{e}_2 \end{bmatrix}.$$

5.3.6   TREATMENT OF TRANSVERSAL SHEAR

Standard and *enhanced* options of treatment of the transversal shear are available. This concern interpolation of the shear strain, constitutive modeling and shear strain decomposition along the cross-section depth as summarized in widow below.

Window 5-17: Options of transversal shear treatment

Treatment:	Context:			
	Shear interpolation and numerical integration rule for elements of type:		Constitutive treatment of shear in case of *layered model*	Assumed shear strain decomposition along the cross–section depth in case of *layered model*
	Q4 (SHQ4, SXQ4)			
Standard	SRI	Linear, shear behavior decoupled from in–plane nonlinear modeling	Uniform shear correction factor $\kappa = 5/6$ is used	
Enhanced	MITC/URI	Shear included to nonlinear model,	Non–uniform, resulting from elastic stiffness (*)	

URI – Uniform Reduced Integration (2x2).

SRI – Selective Reduced Integration 1x1 (for shear), 2x2 (for membrane & bending part).

MITC – Mixed Interpolation of Tensorial Components approach.

$$(*) \qquad \gamma(z) = \frac{\frac{S(z)}{G(z)}}{\frac{1}{h}\int_{-h/2}^{h/2} \frac{S(z)}{G(z)}\, \mathrm{d}z}\; {}^{o}\gamma = \psi(z){}^{o}\gamma, \quad S(z) = \int_{-h/2}^{z} E(z)z\, \mathrm{d}z.$$

Window 5-17

5.3.7   WEAK FORMULATION OF EQUILIBRIUM

Formulation of the equilibrium equations are derived from virtual work principle (VWP), which in takes general form:

find σ such that:

for any $\delta\varepsilon$, $\delta\mathbf{u}$

$$\int_V \delta\boldsymbol{\varepsilon}^{\mathrm{T}}\boldsymbol{\sigma}\,\mathrm{d}V - \int_V \delta\mathbf{u}^{\mathrm{T}}\mathbf{b}\,\mathrm{d}V = 0$$

In each detailed case, the particular form of VWP is as follows, using the notation:

$\boldsymbol{\varepsilon}_m = \begin{bmatrix} \varepsilon_{xxL} & \varepsilon_{yyL} & \gamma_{xyL} \end{bmatrix}^{\mathrm{T}}$ – membrane strains

$\boldsymbol{\sigma}_m = \begin{bmatrix} \sigma_{xxL} & \sigma_{yyL} & \sigma_{xyL} \end{bmatrix}^{\mathrm{T}}$ – membrane stresses

$\boldsymbol{\varepsilon}_s = \begin{bmatrix} \gamma_{xzL} & \gamma_{yzL} \end{bmatrix}^{\mathrm{T}}$ – shear strains

$\boldsymbol{\sigma}_s = \begin{bmatrix} \sigma_{xzL} & \sigma_{yzL} \end{bmatrix}^{\mathrm{T}}$ – shear stresses

$\boldsymbol{\varepsilon} = [\boldsymbol{\varepsilon}_m, \boldsymbol{\varepsilon}_s]^{\mathrm{T}}$ – full strains and stresses

V – volume of the element

Ω – reference surface area

$\mathbf{b}$ – body forces

$\mathbf{D}_{ss}^{el} = \begin{bmatrix} G & 0 \\ 0 & G \end{bmatrix}$ – shear part of linear constituive matrix

with

     κ – shear correction factor (=5/6 for homogeneous section)

     G – Kirchhoff moduli

     h – element thickness.

- *homogenous section, elastic model*
    find σ such that:
    for any $\delta\varepsilon, \delta\gamma, \delta\mathbf{u}$

$$\int_V \delta\boldsymbol{\varepsilon}_m^{\mathrm{T}}\boldsymbol{\sigma}_m\,\mathrm{d}V + \int_\Omega \delta\boldsymbol{\gamma}_s^{\mathrm{T}}\kappa h\mathbf{D}_{ss}^{el}\boldsymbol{\gamma}_s\,\mathrm{d}\Omega - \int_V \delta\mathbf{u}^{\mathrm{T}}\mathbf{b}\,\mathrm{d}V = 0$$

- *layered section, possible nonlinear model, standard treatment of shear (shear de-coupled from membrane part in constitutive model)*
    find σ such that:
    for any $\delta\varepsilon, \delta\gamma, \delta\mathbf{u}$

$$\int_\Omega \sum_i (\delta\boldsymbol{\varepsilon}_m^l)^{\mathrm{T}}\boldsymbol{\sigma}_m^l \Delta h_l\,\mathrm{d}\Omega + \int_\Omega \delta\boldsymbol{\gamma}_s^{\mathrm{T}}\kappa h\mathbf{D}_{ss}^{el}\boldsymbol{\gamma}_s\,\mathrm{d}\Omega - \int_V \delta\mathbf{u}^{\mathrm{T}}\mathbf{b}\,\mathrm{d}V = 0$$

- *layered section, possible nonlinear model, enhanced treatment of shear (shear included in constitutive model)*
    find σ such that:
    for any $\delta\varepsilon, \delta\gamma, \delta\mathbf{u}$

$$\int_\Omega \sum_i (\delta\boldsymbol{\varepsilon}_m^l)^{\mathrm{T}}\boldsymbol{\sigma}_m^l \Delta h_l\,\mathrm{d}\Omega - \int_V \delta\mathbf{u}^{\mathrm{T}}\mathbf{b}\,\mathrm{d}V = 0$$

Moreover, in the case of enhanced shear treatment for SHQ4,SXQ4 elements MITC (Mixed Interpolation of Tensorial Components) approach is applied.

5.3.8 STIFFNESS MATRIX AND ELEMENT FORCES

The formulas for element stiffness matrix $\mathbf{K}_{(5\times5)}$ and force vectors concern $5DOF$ component vectors $\mathbf{q}_{(5)}, \mathbf{f}_{(5)}$ with rotations /moments related to nodal tangent directions.

- *layered model with standard treatment of shear or homogenous section , elastic model:*

$$\mathbf{K}_{(5\times5)} = \int_\Omega \sum_{ilayer=1}^{Nlayer} \mathbf{B}_m^\mathrm{T} \mathbf{D}_{mm} \mathbf{B}_m j h_{ilayer} \,\mathrm{d}\xi\,\mathrm{d}\eta + \int_\Omega {}^o\mathbf{B}_s^\mathrm{T} \kappa h \mathbf{D}_{ss}^{el}\, {}^o\mathbf{B}_s j \,\mathrm{d}\xi\,\mathrm{d}\eta$$

$$\mathbf{f}_{(5)} = \int_\Omega \sum_{ilayer=1}^{Nlayer} \mathbf{B}_m^\mathrm{T} \boldsymbol{\sigma}_m j h_{ilayer} \,\mathrm{d}\xi\,\mathrm{d}\eta + \int_\Omega {}^o\mathbf{B}_s^\mathrm{T} \kappa h \mathbf{D}_{ss}^{el}\, {}^o\boldsymbol{\varepsilon}_s j \,\mathrm{d}\xi\,\mathrm{d}\eta$$

where ${}^o()$ concerns mean shear strains.

- *layered model with enhanced treatment of shear:*

$$\mathbf{K}_{(5\times5)} = \int_\Omega \sum_{ilayer=1}^{Nlayer} [\mathbf{B}_m^\mathrm{T}, \mathbf{B}_s^\mathrm{T}] \begin{bmatrix} \mathbf{D}_{mm} & \mathbf{D}_{ms} \\ \mathbf{D}_{sm} & \mathbf{D}_{ss} \end{bmatrix} \begin{bmatrix} \mathbf{B}_m \\ \mathbf{B}_s \end{bmatrix} j h_{ilayer} \,\mathrm{d}\xi\,\mathrm{d}\eta$$

$$\mathbf{f}_{(5)} = \int_\Omega \sum_{ilayer=1}^{Nlayer} [\mathbf{B}_m^\mathrm{T}, \mathbf{B}_s^\mathrm{T}] \begin{bmatrix} \boldsymbol{\sigma}_m \\ \boldsymbol{\sigma}_s \end{bmatrix} j h_{ilayer} \,\mathrm{d}\xi\,\mathrm{d}\eta$$

$$\mathbf{B}_s = \psi(z_{ilayer})\, {}^o\mathbf{B}_s$$

In all above integrals Gauss type integration is performed over the surface of the element as specified in Window 5-17. Integration in the direction of element depth is based on user defined layer setting (*layered model*) or on 2 point Gauss rule in case of *homogenous section, elastic model*.

$5 - DOF$ vectors and matrix put into full $6 - DOF$ ones and stabilizing terms are added to stiffness matrix on the positions of $6th\ DOF$ (drilling rotations), in order to avoid singularity in case of co-planarity of elements adjacent to a node.

$$\mathbf{K} = \begin{bmatrix} \mathbf{K}_{ab(5\times5)} & 0 \\ 0 & k_{ab}^{\mathsf{drill}} \end{bmatrix}, \qquad a,b = 1, Nen$$

$$\mathbf{f} = [\ \mathbf{f}_{a(5)}, \quad 0\ , \qquad a = 1, Nen]$$

$$k_{ab}^{\mathsf{drill}} = \alpha \int_\Omega N_a N_b G h \,\mathrm{d}\Omega, \qquad \alpha \cong 10^{-6}$$

Subsequently, rotational part is transformed to global coordinate system :

$$\mathbf{f}^G = \mathbf{Tf}$$

$$\mathbf{K}^G = \mathbf{TKT}^\mathrm{T}$$

where

$$\mathbf{T} = \begin{bmatrix} \mathbf{T}_1 & s & \mathbf{0} & s & \mathbf{0} \\ \vdots & \ddots & & & \vdots \\ \mathbf{0} & & \mathbf{T}_a & & \mathbf{0} \\ \vdots & & & \ddots & \vdots \\ \mathbf{0} & s & \mathbf{0} & s & \mathbf{T}_{Nen} \end{bmatrix},$$

$$\mathbf{T}_a = \begin{bmatrix} \mathbf{I}_{3\times3} & \mathbf{0} \\ \mathbf{0} & [\widehat{\mathbf{e}}_{a1}, \widehat{\mathbf{e}}_{a2}, \widehat{\mathbf{e}}_{a3}] \end{bmatrix}, \quad a = 1, Nen.$$

5.3.9   LOADS

Gravity, nodal and surface loads can be applied. Gravity corresponds to body forces. In a case of shell 2 node layer elements (option A) nodal forces can be applied to either master or slave nodes. Also surface loads are specified on fictitious surface elements S_Q4 which may be set on slave or master layer of nodes. Equivalent nodal force vector consist of forces as well as moments, evaluated with use of generalized shape function matrix $\mathbf{N}$ as:

$$\mathbf{f}_p = \int\limits_{V^e} \mathbf{N}^{\mathrm{T}}\mathbf{p}\,dV$$

Thermal loads can also be accounted for; thermal analysis is always performed on a continuum element and then ε thermal is projected into shell material data at each layer.

5.3.10   SHELL ELEMENT RESULTS

Nodal results include 3 translations and 3 rotations. Element results include (at each numerical integration point) membrane forces , moments and shear forces .

Window 5-18: Shell element stress resultants and sign convention
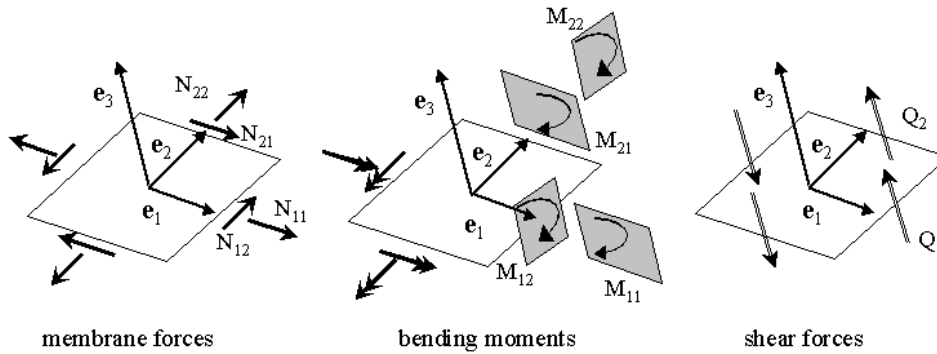
Shell element stress resultants and sign convention

Window 5-18

Window 5-18 indicates the sign convention. These results are evaluated, stored and printed into text file at integration point and are referred to integration point fiber coordinate system and to the mid–surface (not to the reference surface). During the visualization phase users reference system must be defined. This is documented in the reference manual, under post–processing.

5.4   MEMBRANES

ELEMENT GEOMETRY MAPPING AND COORDINATE SYSTEM

DISPLACEMENTS AND STRAINS FIELD

CONSTITUTIVE MODELS

WEAK FORMULATION OF THE EQUILIBRIUM

STIFFNESS MATRIX AND ELEMENT FORCES

Elements are designed to model different kind of soil reinforcement (solid phase) such as geo–textiles, geo-grids. In modern geo-technical practice there is a variety of different types of such a means. Membrane elements are available in all 2D and 3D analysis types. Although membrane and truss elements use the same DOF (at least for statics), note the difference between membrane and truss elements for all 2D analysis. The difference concerns the possibility of using a wider list of constitutive models in the case of membrane elements.

Window 5-19: Membrane elements

Membrane elements in 3D analysis:

M_T3   M_Q4
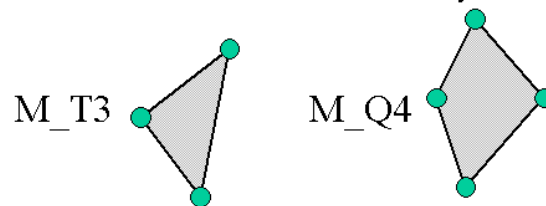
Membrane elements in 2D analysis: M_L2

2D model:
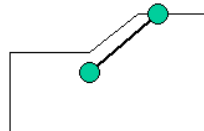
unit slice   1
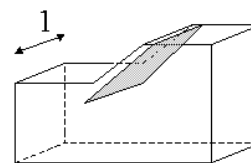
Plane strain, Gen. P.S =>

Axisymmetry =>

Note: elementary volume:

$dV = 2\pi\, r \cdot dL$
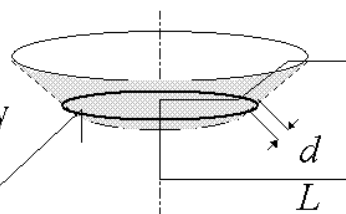
The family of membrane elements

Window 5-19

Note the significant difference between *membrane* and *truss* elements for the *Axisymmetry* analysis. For the *membrane* elementary volume dV changes with the current point radius r, while for the *truss* elements

it remains constant, see the Window 5-1. The geometry of the element is set as iso-parametric surface element (all T3/Q4) in 3D space or as 2 node linear element in 2D space. It posses one layer of nodes - as it is required in statics. As element has only 1 layer of nodes it can not be used to model a flow in the normal direction - (2 node layer necessary) -thus membrane elements can not be used to model impermeable surface. When necessary to simulate the drainage or impermeable surface in the normal direction, one node layer membrane element should be placed together with 2-node layer flow interface:

Window 5-20: Flow trough membrane elements

2-node layer (◯, ●)
INTERFACE element -to control the flow in the normal direction and to simulate drainage -flow in the surface direction

1-node layer (●) **MEMBRANE**
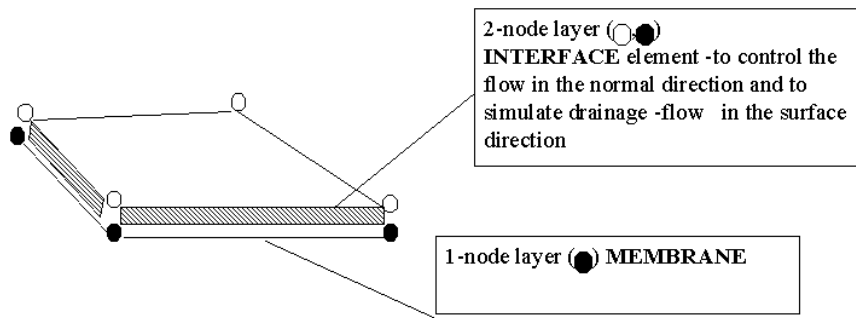
Modelling of flow trough membrane elements

Window 5-20

5.4.1   ELEMENT GEOMETRY MAPPING AND COORDINATE SYSTEM

3D case

Window 5-21: 3D membrane elements co-ordinate systems and mapping

- Mapping from the reference element is constructed as:

$$\mathbf{x}(\xi,\eta) = \sum_{a=1,Nen} N_a(\xi,\eta)\mathbf{x}_a;$$

- Gauss point local base, by unified procedure see Appendix 5.6.3

- Derivatives of any function f versus local directions x_L, y_L are evaluated as:

$$\begin{bmatrix} \dfrac{\partial f}{\partial x_L} \\ \dfrac{\partial f}{\partial y_L} \end{bmatrix} = (\mathbf{J}^{-1})^{\mathsf{T}} \cdot \begin{bmatrix} f_{,\xi} \\ f_{,\eta} \end{bmatrix}, \quad \text{with: } \mathbf{J} = \begin{bmatrix} \mathbf{e}_1^{\mathsf{T}}\cdot\mathbf{x}_{,\xi} & \mathbf{e}_1^{\mathsf{T}}\cdot\mathbf{x}_{,\eta} \\ \mathbf{e}_2^{\mathsf{T}}\cdot\mathbf{x}_{,\xi} & \mathbf{e}_1^{\mathsf{T}}\cdot\mathbf{x}_{,\eta} \end{bmatrix}$$

Window 5-21

In all 2D cases geometry setting for *membrane* element is identical with these for *truss* element, see Window 5-4.

5.4.2   DISPLACEMENTS AND STRAINS FIELD

The displacements within the element are interpolated from nodal values as:

$$\mathbf{u}(\xi) = \sum_{a=1,Nen} N_a(\xi)\mathbf{u}_a$$

The strains within the element (only in-plane are taken into account)

- *3D case:*

$$\boldsymbol{\varepsilon} = \begin{bmatrix} \varepsilon_{xxL} \\ \varepsilon_{yyL} \\ \gamma_{xyL} \end{bmatrix} = \begin{bmatrix} \dfrac{\partial u_{xL}}{\partial x_L} \\ \dfrac{\partial u_{yL}}{\partial y_L} \\ \dfrac{\partial u_{xL}}{\partial y_L} + \dfrac{\partial u_{yL}}{\partial x_L} \end{bmatrix} = \begin{bmatrix} \mathbf{e}_{xL}^{\mathsf{T}} \cdot \dfrac{\partial \mathbf{u}}{\partial x_L} \\ \mathbf{e}_{yL}^{\mathsf{T}} \cdot \dfrac{\partial \mathbf{u}}{\partial y_L} \\ \mathbf{e}_{yL}^{\mathsf{T}} \cdot \dfrac{\partial \mathbf{u}}{\partial x_L} + \mathbf{e}_{xL}^{\mathsf{T}} \cdot \dfrac{\partial \mathbf{u}}{\partial y_L} \end{bmatrix}$$

- 2D analysis types:

  ★ *Plane Strain:*

$$\boldsymbol{\varepsilon} = \begin{bmatrix} \varepsilon_{xxL} \\ \varepsilon_{yyL} \\ \gamma_{xyL} \end{bmatrix} = \begin{bmatrix} \dfrac{\partial u_{xL}}{\partial x_L} \\ 0 \\ 0 \end{bmatrix} = \begin{bmatrix} \mathbf{e}_{xL}^{T} \cdot \dfrac{\partial \mathbf{u}}{\partial x_L} \\ 0 \\ 0 \end{bmatrix}$$

  ★ *Axisymmetry:*

$$\boldsymbol{\varepsilon} = \begin{bmatrix} \varepsilon_{xxL} \\ \varepsilon_{yyL} \\ \gamma_{xyL} \end{bmatrix} = \begin{bmatrix} \dfrac{\partial u_{xL}}{\partial x_L} \\ \dfrac{u_{xG}}{r} \\ 0 \end{bmatrix} = \begin{bmatrix} \mathbf{e}_{xL}^{\mathsf{T}} \cdot \dfrac{\partial \mathbf{u}}{\partial x_L} \\ \dfrac{u_{xG}}{r} \\ 0 \end{bmatrix}$$

The formulae relating strains ε any point within the element, with its DOF vector $\mathbf{u}$ may be put in the general form:

$$\boldsymbol{\varepsilon} = \mathbf{B}\mathbf{u} = \sum_{a=1}^{Nen} \mathbf{B}_a \mathbf{u}_a,$$

- *Plane Strain:*

$$\mathbf{u}_a = [u_a, v_a]$$
$$\mathbf{B}_a(\xi) = [e_{\mathsf{xLx}} \cdot DN_{a'\xi}, \quad e_{\mathsf{xLy}} \cdot DN_{a'\xi}]$$

- *Axisymmetry:*

$$\mathbf{B}_a(\xi) = \begin{bmatrix} e_{\mathsf{xLx}} \cdot DN_{a'\xi} & e_{\mathsf{xLx}} \cdot DN_{a'\xi} \\ \dfrac{N_a}{r} & 0 \\ 0 & 0 \end{bmatrix},$$

- *3D:*

$$\mathbf{u}_a = [u_a, v_a, w_a]^\mathsf{T}$$

$$\mathbf{B}_a(\xi, \eta) = \begin{bmatrix} e_{1x} N_{a'xL} & e_{1y} N_{a'xL} & e_{1z} N_{a'xL} \\ e_{2x} N_{a'yL} & e_{2y} N_{a'yL} & e_{2z} N_{a'yL} \\ e_{1x} N_{a'yL} + e_{2x} N_{a'xL} & e_{1y} N_{a'yL} + e_{2y} N_{a'xL} & e_{1z} N_{a'yL} + e_{2z} N_{a'xL} \end{bmatrix}.$$

- *3D:*

5.4.3 CONSTITUTIVE MODELS

Constitutive models used in membrane elements (solid phase) for all *analysis types* relate in- Plane Strains $\boldsymbol{\varepsilon} = [\varepsilon_{xxL}, \varepsilon_{yyL}, \gamma_{xyL},]^\mathsf{T}$ with membrane stress components $\boldsymbol{\sigma} = [\sigma_{xxL}, \sigma_{yyL}, \sigma_{xyL},]^\mathsf{T}$ in local directions of membrane element. For some models, constitutive data concerning stiffness and strength must be given in reference to the whole thickness of the element, in units [force/length]. The models are:

- Elasto-plastic membrane (isotropic)

Data:	stiffness K [force/length], Poisson ratio ν, tensile and compressive strength f_t, f_c [force/length]
Applications:	geo–textile
Stress criterion:	$\sigma_1 \leq f_t, \quad \sigma_2 > -f_c$ where: σ_1, σ_2 principal stresses
Elasticity matrix:	$\mathbf{D_e} = \begin{bmatrix} K & \nu K & 0 \\ \nu K & K & 0 \\ 0 & 0 & \dfrac{K}{2(1+\nu)} \end{bmatrix}$

- Elasto-plastic membrane (an–isotropic)

Data:	stifness K_{11}, K_{22}, K_{12} [force/length] tensile strength f_{t1}, f_{t2} [force/length] compressive strength f_{c1}, f_{c2} [force/length] α – angle between local element axis x_L and an-isotropy *1-st* axis $\mathbf{x}_1$, evaluated from projection of a direction vector onto element surface (see Appendix 5.6.2) .
Applications:	geo-grids
Stress criterion:	$\begin{bmatrix} \sigma_{11} \\ \sigma_{22} \end{bmatrix} = \mathbf{T}\boldsymbol{\sigma}$
Elasticity matrix:	$\mathbf{D}_e = \mathbf{T}^T \cdot \begin{bmatrix} K_{11} & K_{12} \\ K_{12} & K_{22} \end{bmatrix} \cdot \mathbf{T}$ where: $\mathbf{T} = \begin{bmatrix} c^2 & s^2 & sc \\ s^2 & c^2 & -sc \end{bmatrix}$; $s = \sin\alpha, \quad c = \cos\alpha$

- Elasto-plastic fibre

Data:	elasticity module–E, area per unit length–A, tensile and compressive strength–f_t, f_c, α– angle between local element axis x_L and fibre direction $\mathbf{x_1}$, evaluated from projection of a direction vector onto element surface , see Appendix 5.6.2 .
Applications:	reinforcement layer

Note: In case of *Axisymmetry*, the model is suitable for modelling circumferential reinforcement ($\alpha = 90°$), while for longitudinal one, usage of *truss* elements is recommended.

Stress criterion	$\sigma \leq f_t, \quad \sigma > -f_c$ σ– uni–axial stress in the fibre direction
Elasticity matrix:	$\mathbf{D}_e = E\mathbf{t} \cdot \mathbf{t}^\mathsf{T}$ where: $\mathbf{t} = \begin{bmatrix} c^2 & s^2 & sc \end{bmatrix}^\mathsf{T}$

- Elasto plastic-plane stress member

Data:	elasticity module–E, Poisson ratio ν, area per unit length–A, Menetrey–Willam criterion data
Applications:	thin lining (steel, concrete, etc.)
Stress criterion	Menetrey–Willam (plane stress)
Elasticity matrix:	standard plane stress

5.4.4   WEAK FORMULATION OF EQUILIBRIUM

The contribution of the membrane elements to the virtual work principle expressing equilibrium of a system may be put as:

find $\boldsymbol{\sigma}$ such that:

for any $\delta\boldsymbol{\varepsilon}$, $\delta\mathbf{u}$

$$\int_S \delta\boldsymbol{\varepsilon}^\mathsf{T}\sigma \; A\mathrm{d}S - \int_S \delta\mathbf{u}^\mathsf{T}\mathbf{p} \; dS = 0$$

with

$$\boldsymbol{\varepsilon} = \left[\varepsilon_{xxL}, \varepsilon_{yyL}, \gamma_{xyL},\right]^\mathsf{T};$$

$$\boldsymbol{\sigma} = \left[\sigma_{xxL}, \sigma_{yyL}, \sigma_{xyL},\right]^\mathsf{T};$$

$$\mathbf{u} = \begin{cases} \begin{bmatrix} u & v \end{bmatrix}^\mathsf{T} & \textit{for Plane Strain, Axisymmetry} \\ \begin{bmatrix} u & v & w \end{bmatrix}^\mathsf{T} & \textit{for Gen. plane strain, 3D} \end{cases}$$

$A-$ thickness of the element ($= 1$ for models using membrane forces instead of stresses).

Integrals are taken over the surface of the element. S is an area attributed to the assumed computational domain i.e. to the unit slice for the *Plane Strain* or to the whole circumference for the Axisymmetric case.

5.4.5   STIFFNESS MATRIX AND ELEMENT FORCES

Stiffness matrix $\mathbf{K^e}$ and force vector $\mathbf{f^e}$ of the membrane element are derived in a standard way from weak formulation of a problem. It would require constitutive module matrix $\mathbf{D}$ as well as stress evaluation for given strain increment. Numerical integration technique is used to evaluate integrals over the element with inegration point number as shown in the table.

Element	M_L2	M_T3	M_Q4
Ngaus	1	1	2×2

- *3D* case:

$$\mathbf{K^e} = \int\limits_{-1}^{1}\int\limits_{-1}^{1} \mathbf{B^T D B}|\mathbf{J}|\; A\mathrm{d}\eta\mathrm{d}\xi = \sum_{igaus=1}^{Ngaus} \mathbf{B^T D B}|\mathbf{J}|{\cdot}A\cdot W_{igaus}$$

$$\mathbf{f^e} = \int\limits_{-1}^{1}\int\limits_{-1}^{1} \mathbf{B^T}\cdot\boldsymbol{\sigma}|\mathbf{J}|\; A\mathrm{d}\eta\mathrm{d}\xi = \sum_{igaus=1}^{Ngaus} \mathbf{B^T}\cdot\boldsymbol{\sigma}|\mathbf{J}|{\cdot}A\cdot W_{igaus}$$

- *2D* cases:

  ★ *Plane Strain:*

$$\mathbf{K^e} = \int\limits_{-1}^{1}\int\limits_{-1}^{1} \mathbf{B^T D B} \parallel \mathbf{x},_{\xi}\parallel\; A\mathrm{d}\xi = \sum_{igaus=1}^{Ngaus} \mathbf{B^T D B}{\cdot}\parallel \mathbf{x},_{\xi}\parallel\cdot A\cdot W_{igaus}$$

$$\mathbf{f^e} = \int\limits_{-1}^{1}\int\limits_{-1}^{1} \mathbf{B^T}\cdot\boldsymbol{\sigma}\parallel \mathbf{x},_{\boldsymbol{\xi}}\parallel\; A\mathrm{d}\eta\mathrm{d}\xi = \sum_{igaus=1}^{Ngaus} \mathbf{B^T}\cdot\boldsymbol{\sigma}\parallel \mathbf{x},_{\boldsymbol{\xi}}\parallel\cdot A\cdot W_{igaus}$$

  ★ *Axisymmetry*

$$\mathbf{K^e} = \int\limits_{-1}^{1}\int\limits_{-1}^{1} \mathbf{B^T D B}\parallel \mathbf{x},_{\xi}\parallel\cdot 2\pi r\cdot A d\xi = \sum_{igaus=1}^{Ngaus} \mathbf{B^T D B}{\cdot}\parallel \mathbf{x},_{\xi}\parallel\cdot 2\pi r{\cdot}A\cdot W_{igaus}$$

$$\mathbf{f^e} = \int\limits_{-1}^{1}\int\limits_{-1}^{1} \mathbf{B^T}\cdot\boldsymbol{\sigma}\parallel \mathbf{x},_{\boldsymbol{\xi}}\parallel\cdot 2\pi r{\cdot}A\mathrm{d}\eta\mathrm{d}\xi = \sum_{igaus=1}^{Ngaus} \mathbf{B^T}\cdot\boldsymbol{\sigma}\parallel \mathbf{x},_{\boldsymbol{\xi}}\parallel\cdot 2\pi r{\cdot}A\cdot W_{igaus}.$$

5.5   NONLINEAR HINGES

NONLINEAR BEAM HINGES

NONLINEAR SHELL HINGES

Nonlinear hinge elements can be used to model complex behavior of a beam-beam or shell-shell connections. These hinge elements may be used in the uncoupled form for each specific degree of freedom (defined in local coordinate system) (to model no tension condition for instance)or in the coupled one (using Janssen formula) where the current bending moment may strongly depend on the axial(for beams) or membrane (for shells) force. Uncoupled/coupled hinge models (different for each degree of freedom) can be mixed within one hinge element.

5.5.1   NONLINEAR BEAM HINGES

Window 5-22: Nonlinear beam hinges

Hinge element may be defined at the beam or axisymmetric shell element vertex. This element is of node-node interface type. The local base of the element is inherited from the adjacent beam/axisymmetric shell element as shown in the figure. Nonlinear hinge behavior can be defined as a user given generalized force-relative generalized displacement relation for each distinct degree of freedom without couplings among them, or it may undergo so-called Janssen formula that couples bending moment and axial force. User given generalized force-relative generalized displacement relation can be sensitive to the sign of the relative displacement but exclusively for axial force and two bending moments (unsymmetric relations). Relations for torsion and shear in two directions can only be symmetric.

Beam hinge element

Window 5-22

Window 5-23: Modeling joint using Janssen's formula
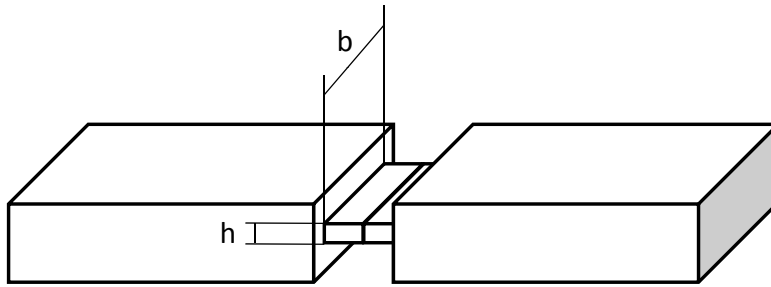
Modeling joint in segmental lining require complex nonlinear hinge model to be used in beam-beam connection (see figure). One of the simplest formula that quite well approximates the aforementioned joint behavior is the one proposed by Janssen. In Janssen's formula for joint that is in full stick mode along whole interface depth (h) (joint must transfer compressive axial force ($N < 0$)) bending moment and elastic joint stiffness are described by the following expressions

$$M = k_{el}\Delta\phi \qquad (1)$$

$$k_{el} = E\,b\,\frac{h^2}{12} \qquad (2)$$

When the joint opens (bending moment $|M| > |N|\dfrac{h}{6}$ and $N < 0$), a nonlinear relation between M and $\Delta\phi$ is observed in the experiments and numerical FE models as well. The corresponding bending moment M and tangent joint stiffness for bending k_t are as follows (for $N \geq 0$ (tension in joint) $M{=}0$)

$$M = 1/6\,\frac{\left(3\,|\Delta\phi|\,Ebh - 2\sqrt{2}\sqrt{|\Delta\phi|\,Ebh\,|N|}\right)|N|\,sign\,(\Delta\phi)}{|\Delta\phi|\,Eb} \qquad (3)$$

$$k_t = 1/6\,\frac{N^2\sqrt{2}h}{|\Delta\phi|\,\sqrt{|\Delta\phi|\,Ebh\,|N|}} \qquad (4)$$

$$\qquad (5)$$

NB. To model no tension condition one may set an uncoupled hinge model for the axial behavior and coupled one (Janssen) for bending.

Window 5-23

5.5.2 NONLINEAR SHELL HINGES

Window 5-24: Nonlinear shell hinges

Hinge element may be defined at the shell element edge. This element is of segment-segment interface type. The local base of the element for each shell edge is shown in the figure. Nonlinear hinge behavior can be defined as a user given generalized force-relative generalized displacement relation for each distinct degree of freedom without couplings among them, or it may undergo so-called Janssen formula that couples bending moment and membrane force. User given generalized force-relative generalized displacement relation can be sensitive to the sign of the relative displacement but exclusively for axial force and two bending moments (unsymmetric relations). Relations for shear in two directions can only be symmetric.
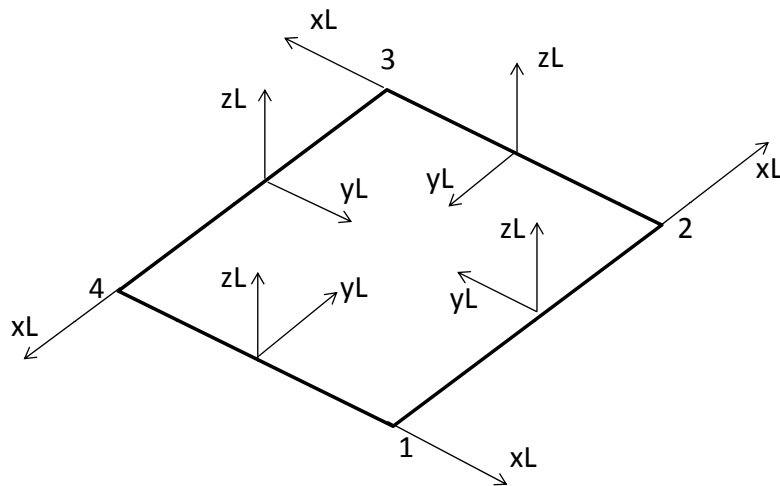
Local bases for shell hinge element

Window 5-24

Window 5-25: Modeling joint using Janssen's formula
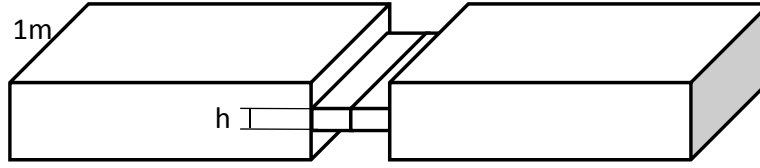
Modeling joints in segmental lining require complex nonlinear hinge model to be used in shell-shell connection (see figure). One of the simplest formula that quite well approximates the aforementioned joint behavior is the one proposed by Janssen. In Janssen's formula for joint that is in full stick mode along whole interface depth (h) (joint must transfer compressive membrane force ($N < 0$)) bending moment and elastic joint stiffness are described by the following expressions (same as for the beam hinge but $b = 1m$)

$$M = k_{el}\Delta\phi \tag{1}$$

$$k_{el} = E\,\frac{h^2}{12} \tag{2}$$

When the joint opens (bending moment $|M| > |N|\,\dfrac{h}{6}$ and $N < 0$), a nonlinear relation between M and $\Delta\phi$ is observed in the experiments and numerical FE models as well. The corresponding bending moment M and tangent joint stiffness for bending k_t are as follows (for $N \geq 0$ (tension in joint) $M=0$)

$$M = 1/6\,\frac{\left(3\,|\Delta\phi|\,Eh - 2\,\sqrt{2}\sqrt{|\Delta\phi|\,Eh\,|N|}\right)|N|\,sign\,(\Delta\phi)}{|\Delta\phi|\,E} \tag{3}$$

$$k_t = 1/6\,\frac{N^2\sqrt{2}h}{|\Delta\phi|\,\sqrt{|\Delta\phi|\,Eh\,|N|}} \tag{4}$$

$$\tag{5}$$

NB. To model no tension condition one may set an uncoupled hinge model for the axial behavior and coupled one (Janssen) for bending.

Window 5-25

5.6   APPENDICES

MASTER-SLAVE (OFFSET) TRANSFORMATION

SETTING THE DIRECTION ON SURFACE ELEMENTS

SETTING OF THE LOCAL BASE ON A SURFACE ELEMENT

UNI-AXIAL ELASTO-PLASTIC MODEL

UNI-AXIAL USER DEFINED MODEL

5.6.1   MASTER-SLAVE (OFFSET) TRANSFORMATION

In order to deal with the frequently encountered situation where elements are connected to other elements of the model by nodes, which are not the centroids of a cross section, offset transformation of element displacement, forces and stiffness is introduced. The DOF of the element are placed on its "master" nodes defining connectivity. Based on rigid body movement of the "master", translation and rotation displacements of the centroid being the "slave" node are evaluated. The above concerns beams as well as shell elements.

Window 5-26: Master-slave (offset) transformation

Displacements at the "slave":

$$\begin{aligned}
\mathbf{u}^{\mathsf{S}} &= \mathbf{u}^{\mathsf{M}} + \phi^{\mathsf{M}} \times \mathbf{o} \\
\phi^{\mathsf{S}} &= \phi^{\mathsf{M}}
\end{aligned}$$

where offset vector is used:

$$\mathbf{o} = \mathbf{x}_{\mathsf{Slave}} - \mathbf{x}_{\mathsf{Master}}$$

$$\mathbf{o} = \{xi, yi, (zi)\}^{\mathrm{T}}.$$

In turn, forces and moments evaluated initially at "slave" are moved to "masters" in a way preserving static equivalency:

$$\begin{aligned}
\mathbf{t}^{\mathsf{M}} &= \mathbf{t}^{\mathsf{S}} \\
\mathbf{m}^{\mathsf{M}} &= \mathbf{m}^{\mathsf{S}} + \mathbf{o} \times \mathbf{t}^{\mathsf{S}}
\end{aligned}$$

Expressing the above in a matrix form one can get:

displacement transformation :

$$\mathbf{q}^{\mathsf{S}} = \mathbf{O}\mathbf{q}^{\mathsf{M}}$$

force transformation:

$$\mathbf{f}^{M} = \mathbf{O}^{\mathrm{T}}\mathbf{f}^{S}$$

stiffness transformation:

$$as \quad : \quad \mathbf{f}^{\mathsf{M}} = \mathbf{O}^{\mathrm{T}}\mathbf{f}^{\mathsf{S}} = \mathbf{O}^{\mathrm{T}}\mathbf{K}^{\mathsf{S}}\mathbf{q}^{\mathsf{S}} = \mathbf{O}^{\mathrm{T}}\mathbf{K}^{\mathsf{S}}\mathbf{O}\mathbf{q}^{\mathsf{M}} = \mathbf{K}^{\mathsf{M}}\mathbf{q}^{\mathsf{M}}$$

$$\mathbf{K}^{M} = \mathbf{O}^{\mathrm{T}}\mathbf{K}^{\mathsf{S}}\mathbf{O}$$

Offset transformation matrix takes the form:

(all 2D cases)

$$\mathbf{O} = \begin{bmatrix} 1 & 0 & -yi \\ 0 & 1 & xi \\ 0 & 0 & 1 \end{bmatrix}$$

(3D case)

$$\mathbf{O} = \begin{bmatrix} 1 & 0 & 0 & 0 & zi & -yi \\ 0 & 1 & 0 & -zi & 0 & xi \\ 0 & 0 & 1 & yi & -xi & 0 \\ 0 & 0 & 0 & 1 & 0 & 0 \\ 0 & 0 & 0 & 0 & 1 & 0 \\ 0 & 0 & 0 & 0 & 0 & 1 \end{bmatrix}$$

Window 5-26

5.6.2　SETTING THE DIRECTION ON SURFACE ELEMENTS

A unified procedure of setting the direction on the surface element (shell, membrane, surface load, interface) is proposed. The direction setting is independent from node order, orientation of the element, what is not the case of local element base $\{\mathbf{e1}, \mathbf{e2}, \mathbf{e3}\}$ Moreover the same method of setting user defined coordinate system to present the stress resultants in shell and membrane element is used in post-processor

---

Window 5-27: Direction on the surface elements
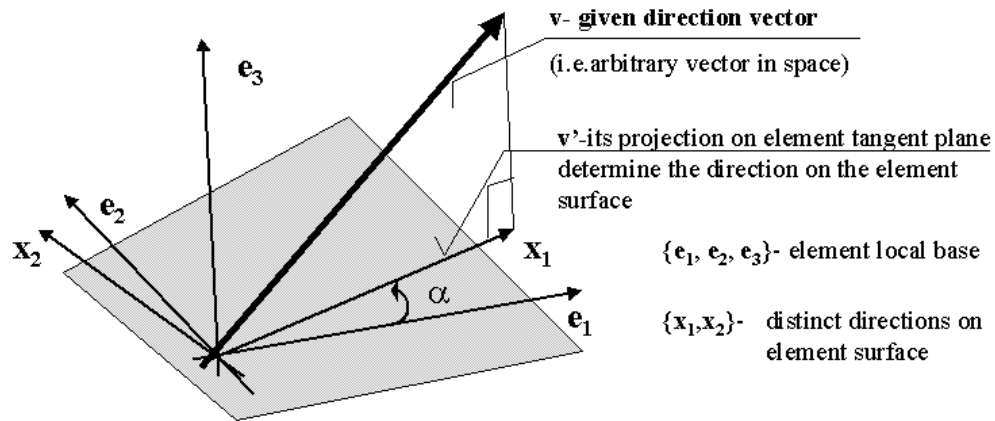
Distinction of the direction on the surface elements

Evaluation of the angle α:

$$\mathbf{v}' = \mathbf{v} - (\mathbf{e}_3^T\mathbf{v})\mathbf{e}_3$$
$$\cos\alpha = \frac{\mathbf{e}_1^T\mathbf{v}'}{\parallel \mathbf{v}' \parallel}; \qquad \sin\alpha = \frac{\mathbf{e}_2^T\mathbf{v}'}{\parallel \mathbf{v}' \parallel}$$

Note:

1. An error will be reported in the case when $\mathbf{v}$ is orthogonal to element surface, leading to $\parallel \mathbf{v}' \parallel =0$.

2. $\mathbf{x}_i$ is the direction closest to given $\mathbf{v}$ among all directions tangent to the element surface.

3. In a case when $\mathbf{v}$ is tangent to element surface, $\mathbf{x}_i$ coincide with $\mathbf{v}$, i.e. $\mathbf{x}_i \Uparrow \mathbf{v}$.

Window 5-27

5.6.3 SETTING OF THE LOCAL BASE ON A SURFACE ELEMENT

The following construction of the local base in the integration point, after T.J.R.Hughes[5], is used in all kind of surface elements (i.e. shell, membrane, contact, fictitious for surface load elements). Moreover for these elements, stress-type results which are stored in *.str ASCII file, are referred to defined bellow coordinate system.

Note, that element local base depends on node numbering order and its orientation.

Window 5-28: Local base on a surface element
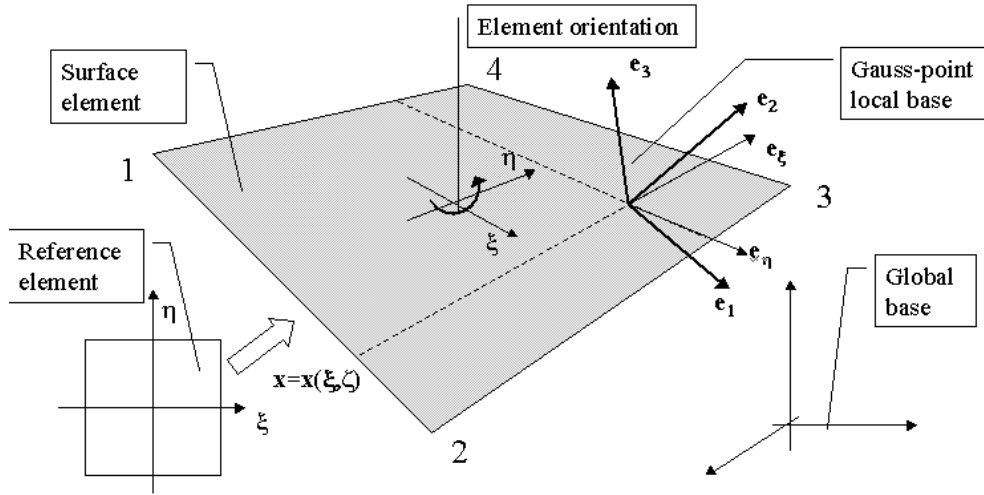
Setting of the local base on a surface element

$$\{Q\}(\xi, \eta) = [\mathbf{e}_1, \mathbf{e}_2, \mathbf{e}_3]$$

$$\mathbf{e}_3 = \frac{\mathbf{e}_\xi \times \mathbf{e}_\eta}{\parallel \mathbf{e}_\xi \times \mathbf{e}_\eta \parallel}; \quad \mathbf{e}_1 = \frac{\sqrt{2}}{2}(\mathbf{a} - \mathbf{b}); \quad \mathbf{e}_2 = \frac{\sqrt{2}}{2}(\mathbf{a} + \mathbf{b});$$

where

$$\mathbf{e}_\xi = \frac{\mathbf{x}_{,\xi}}{\parallel \mathbf{x}_{,\xi} \parallel}; \quad \mathbf{e}_\eta = \frac{\mathbf{x}_{,\eta}}{\parallel \mathbf{x}_{,\eta} \parallel}; \quad \mathbf{a} = \frac{\mathbf{e}_\xi + \mathbf{e}_\eta}{\parallel \mathbf{e}_\xi + \mathbf{e}_\eta \parallel}; \quad \mathbf{b} = \frac{\mathbf{e}_3 \times \mathbf{a}}{\parallel \mathbf{e}_3 \times \mathbf{a} \parallel};$$

Window 5-28

---

[5]T.J.R.Hughes, Finite Element Method, Ed.Prentice–Hall 1988

5.6.4   UNI-AXIAL ELASTO-PLASTIC MATERIAL MODEL

The uni-axial stress-strain relationship to be used commonly for truss, ring, beam, fibers is given as follows:

Window 5-29: Uni–axial elasto–plastic material model
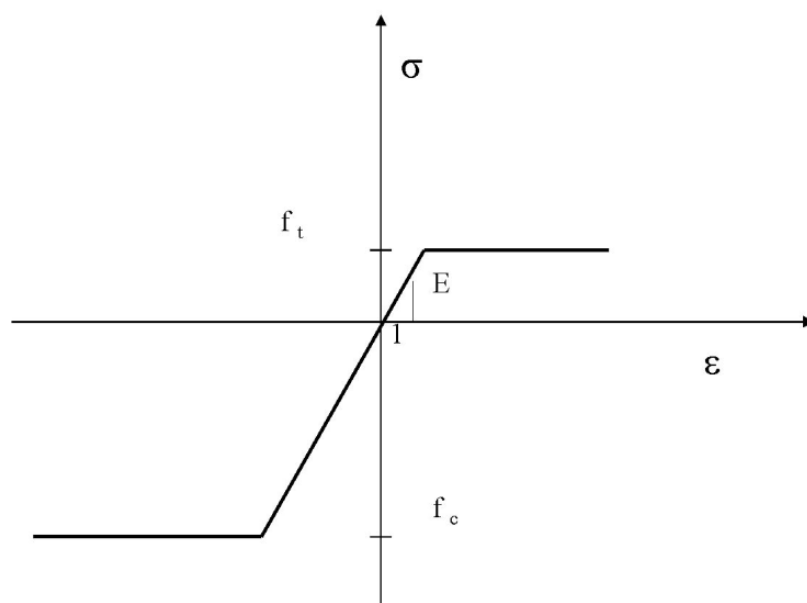
Uni–axial elasto-plastic material model

Window 5-29

5.6.5   UNI-AXIAL USER DEFINED MODEL

The uniaxial user defined $\sigma - \varepsilon$ laws can be used to model beam fibers. To set up such a model both tensile and compresive branches must be defined with a minimum 2 points $\{\varepsilon_i - \sigma_i(\varepsilon_i)\}$ on each curve. The linear interpolation is used to compute stress for a given strain value. These branches describe primary loading paths while the unloading ones tend towards the origin of $\sigma - \varepsilon$ axes (like in damage models). All values in set $\{\varepsilon_i - \sigma_i(\varepsilon_i)\}$ must be positive no matter whether tensile or compressive branch is defined. In this model softening can be assumed but it may require a certain regularization to handle strain localization effects and resulting mesh dependency of results. To handle that one may activate regularization through softening scaling in which a characteristic length L_c must be declared (to reproduce properly fracture energy in pure tension). As the assumed law generates variable elastic stiffness an extra assumption must be made with respect to the value of the equivalent E modulus to be used in dynamics, pushover, creep, but also to compute shear stiffness of the whole beam cross section. Three possibilities can be used

1. $E = \max\left(\mathrm{d}\sigma^+/\mathrm{d}\varepsilon^+\right)$

2. $E = \max\left(\mathrm{d}\sigma^-/\mathrm{d}\varepsilon^-\right)$

3. $E = 1/2\left(\max\left(\mathrm{d}\sigma^+/\mathrm{d}\varepsilon^+\right) + \max\left(\mathrm{d}\sigma^-/\mathrm{d}\varepsilon^-\right)\right)$

As far as softening scaling is concerned user supplied curves are traced to identify whether softening effects occur. If the softening effect is detected then in the descending branch strains are scaled by factor L_c/h^e where h^e is an element length. Usually element size is larger than L_c hence descending branch is usually shortened along strain axis. For reinforced concrete beams when percentage of reinforcement in the cross section is high this regularization may not be needed as the resulting stiffness of composite material will always be positive definite.

Window 5-30: Uniaxial user defined model
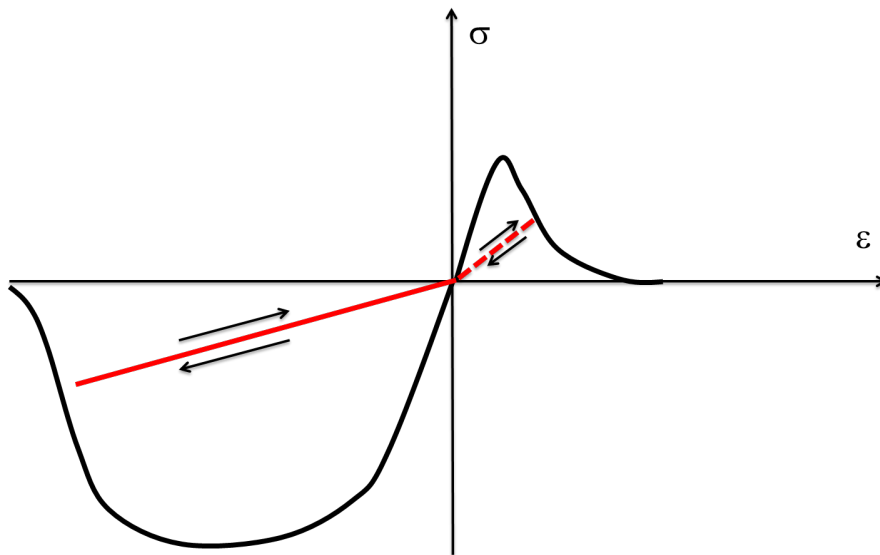
Uniaxial user defined material model

Window 5-30

Chapter 6

INTERFACE

CONTACT
PILE INTERFACE
PILE TIP INTERFACE

6.1   CONTACT OF SOLIDS AND FLUID INTERFACE

GENERAL OUTLOOK

DISPLACEMENT & STRAINS

CONSTITUTIVE MODEL

STIFFNESS MATRIX AND FORCE VECTOR

AUGMENTED LAGRANGIAN APPROACH

CONTRIBUTION TO CONTINUITY EQUATION

6.1.1   GENERAL OUTLOOK

Window 6-1: Interface elements: General remarks

Mechanical contact as well as flux (of fluid, heat, humidity) through the surface between two bodies is modelled by finite element discretization of the interface between them. The interface elements use nodes belonging to the FE–mesh of both adjacent solids with assumed invariable topology (small displacement theory). Moreover the compatibility of the initial positions of nodes is required (this is assured by pre–processing tools, see `Interface` option).
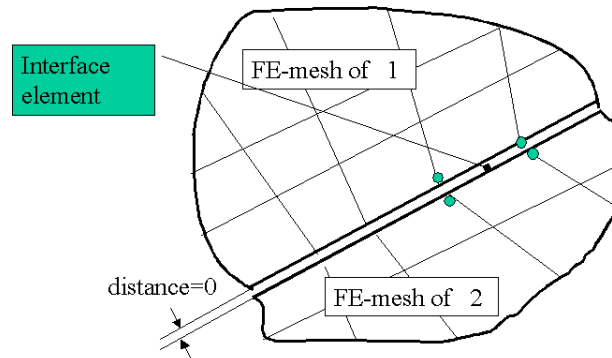
Interface (contact) elements between 2 adjacent bodies

Interface element geometry is based on the iso-parametric mapping from the reference element. As nodes of both layers of element are assumed to occupy the same position :

$$\mathbf{x}(\xi) = \sum_{i=1,..,Nen} N_i(\xi)\mathbf{x}_i.$$

Interface elements in 3D analysis:

C_T3   C_Q4
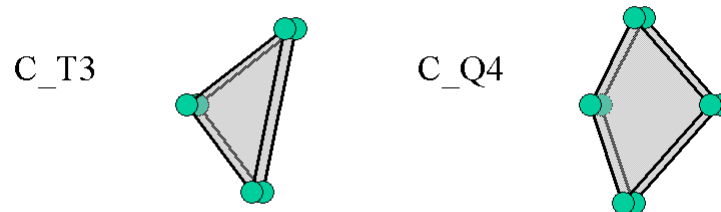
Interface elements in 2D analysis:

C_L2
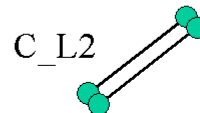
Family of interface elements

Window 6-1

Window 6-2: Interface: Mechanical contact

As an additional feature, for mechanical contact, the displacements continuity option is introduced. This is related to interface element status.

Status CONTACT: The interface elements reproduce the force action between the two bodies based on the relative displacements of the interface nodes. The elasto–plastic friction model is used, allowing for sliding and separation, while the elastic properties of the interface impose penalty constraints multipliers excluding penetration, see **Window** 6-4 for the details.

Status CONTINUITY(u,p,T) or CONTINUITY(u,T): Displacements continuity across the interface is enforced. Nodes on both sides of the interface share the same kinematical DOFs.

| Window 6-2 |

Window 6-3: Fluid Phase

In case of `Flow` or `Deformation+Flow` analysis mode, interface elements may posses pressure DOF at nodes of both layers. Interface elements can be used to model following situations:

Fully permeable interface

Pressures continuity across the interface is enforced. Nodes on both sides of the interface share the same pressure DOFs.

Impermeable interface

No flow takes place in the direction normal to the interface ("no flux" $q_n = 0$ condition on both faces is imposed). Resulting pressures on both interface faces will be (in general) discontinuos. In this case the interface element does not contribute to the equation system.

Permeable interface

Both isotropic and anisotropic flow conditions can be handled.

| Window 6-3 |

6.1.2 DISPLACEMENTS AND STRAINS

Displacements at each layer of the interface *L1* and *L2* are interpolated using standard approach, from given nodal displacements $\mathbf{u}$:

$$\mathbf{u}_{\frac{L1}{L2}}(\xi) = \sum_{\substack{i=1,\ldots,Nen \\ i=Nen+1,\ldots,2Nen}} N_i(\xi)\mathbf{u}_i$$

. The generalized strains at the integration point of the interface element are mutual displacements of both layers transformed to the local basis $\{t, n\}$ of the element. In $3D$ case local base on the element surface is created according to unified procedure given in **Appendix**, Window 5-28.
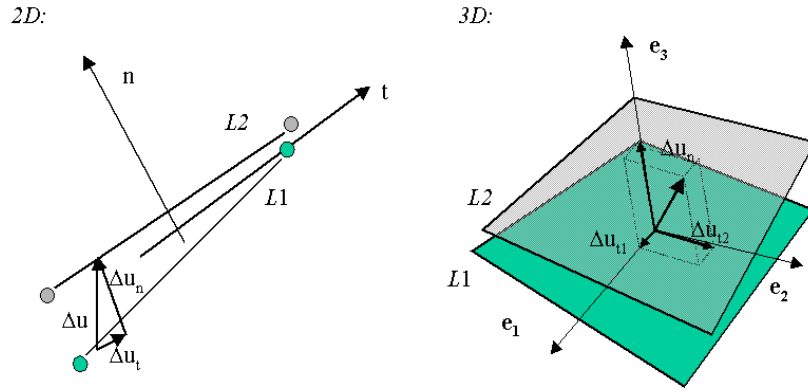
Generalized strains in contact element

The relation between the above generalized strain and nodal displacements may be put in unified form,

$$\boldsymbol{\varepsilon}(\xi) = \mathbf{B}(\xi)\mathbf{u} = \sum_{i=1}^{2Nen} \mathbf{B}_i(\xi)\mathbf{u}_i$$

with $\mathbf{B}$ − matrix given as:

$$\mathbf{B}(\xi) = \mathbf{T}(\xi)\left[-N_i(\xi)\mathbf{I}_{NDOF}, N_i(\xi)\mathbf{I}_{NDOF}\right]^{\mathrm{T}}, \quad i = 1, Nen$$

where:

$$\mathbf{T}(\xi)-\text{transormation matrix such that } \mathbf{U}_{TN} = \mathbf{T}(\xi)\mathbf{u}$$

$$\mathbf{I}_{NDOF}-\text{unit matrix, } NDOF \text{ is displacement component number per node}$$

2D cases

Plane Strain, Axisymmetry:

$$\mathbf{u}_i = [u_i, v_i]^{\mathrm{T}}$$

$$\boldsymbol{\varepsilon}(\xi) = [\Delta u_t, \Delta u_n]^{\mathsf{T}} = [u_{t_{L2}} - u_{t_{L1}}, u_{n_{L2}} - u_{n_{L1}}]^{\mathsf{T}}$$

$$\mathbf{T}(\xi) = \begin{bmatrix} c, & s \\ -s, & c \end{bmatrix}, \quad c = \frac{x_{,\xi}}{\sqrt{x_{,\xi}^2 + y_{,\xi}^2}}, \quad s = \frac{y_{,\xi}}{\sqrt{x_{,\xi}^2 + y_{,\xi}^2}}$$

3D case:

$$\mathbf{u}_i = [u_i, w_i, v_i]^{\mathrm{T}}$$

$$\boldsymbol{\varepsilon}(\xi, \eta) = [\Delta u_{t1}, \Delta u_{t2}, \Delta u_n]^{\mathrm{T}} = [u_{t1_{L1}} - u_{t1_{L1}}, u_{t2_{L2}} - u_{t2_{L1}}, u_{n_{L2}} - u_{n_{L1}}]^{\mathrm{T}}$$

$$\mathbf{T}(\xi, \eta) = \left[\mathbf{e}_1 \vdots \mathbf{e}_2 \vdots \mathbf{e}_3\right]^{\mathrm{T}}$$

Moreover, initial gap may be accounted for while evaluating element strains.

6.1.3   CONSTITUTIVE MODEL

Constitutive behavior of the interface is described in the terms of:

- generalized strains ε, evaluated from nodal displacements of the interface

- effective stresses $\boldsymbol{\sigma}'$, submitted to appropriate stress criterions resulting from

  1. cohesive Mohr - Coulomb condition

  2. no-tension condition.

For *Plane Strain* and *Axisymmetry* number of stress components $Nstre = 2$, while for $3D$ analysis $Nstre = 3$. In the case of *analysis mode Deformation+Flow*, the concept of effective stress is used taking into account pressures p and saturation ratio S or the effective saturation S_e (in the formula given below $\tilde{S}$ can be equal to S or to $S_e^{1/(nm)}$ depending on the user's choice) and enforced Biot coefficient value $\tilde{\alpha}$

$$
\begin{array}{cc}
Nstre = 2 & Nstre = 3 \\
\boldsymbol{\sigma} = \boldsymbol{\sigma}' + \tilde{\alpha}\tilde{S} \begin{bmatrix} 0 \\ p \end{bmatrix} & \boldsymbol{\sigma} = \boldsymbol{\sigma}' + \tilde{\alpha}\tilde{S} \begin{bmatrix} 0 \\ 0 \\ p \end{bmatrix}
\end{array}
$$

- flow rule with a flow potential in the form analogous to Mohr-Coulomb yield function allowing for non-associative flow rule in the case when $\phi \neq \psi$,

- constitutive matrix $\mathbf{D}$.

Both $\boldsymbol{\sigma}'$ and $\mathbf{D}$ are evaluated within the frame of perfect multi–surface elasto–plasticity theory, with components related to the plane of the interface and its normal.

Formulation of both cases of contact constitutive law is given in the **Window** 6-4.
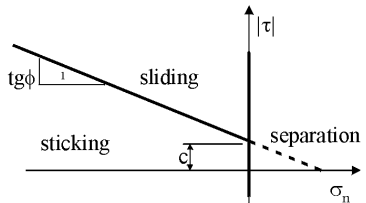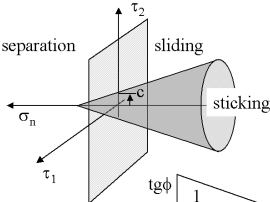
The trial stresses $\boldsymbol{\sigma}^*$ are evaluated as:

$$\boldsymbol{\sigma}^* = \boldsymbol{\sigma}^n + \mathbf{D}_{el}\Delta\varepsilon$$

using the previous stress $\boldsymbol{\sigma}^n$, strain increment $\Delta\varepsilon$, the elastic (penalty) interface stiffness $\mathbf{D}_{el}$.

The elastic stiffness K_n should be large enough to prevent significant penetration in the case of compression, but can not undertake arbitrarily large values as it might spoil conditioning of the resulting FE equation system and lead to difficulties in obtaining convergence of the solution. Estimation of penalty stiffness is done as follows in the **Window** 6-5.

Window 6-4: Constitutive law of frictional contact

Analysis type:	Plane Strain, Axisymmetry	3D
Nstre	2	3
Data:	c – cohesion φ – friction angle ψ – dilatancy angle $(0 \leq \psi \leq \phi)$	
Stresses:	$\sigma = [\tau, \sigma_n]^{\mathrm{T}}$ with: $\quad \tau \quad$ the shear interface stress $\quad \sigma_n \quad$ the stress normal to the interface	$\sigma = [\tau_1, \tau_2, \sigma_n]^{\mathrm{T}}$ with: $\quad \tau_1, \tau_2 \quad$ the shear interface stresses in local directions $\mathbf{e_1}, \mathbf{e_2}$ $\quad \sigma_n \quad$ the stress normal to the interface

Stress conditions	Slip activated when:	
	$F_1(\boldsymbol{\sigma}') = \tau + \tan(\phi)\sigma_n' - c > 0 \quad$ if $\quad \tau \geq 0$ $F_2(\boldsymbol{\sigma}') = \tau + \tan(\phi)\sigma_n' - c > 0 \quad$ if $\quad \tau < 0$	$F_1(\boldsymbol{\sigma}') = \sqrt{\tau_1^2 + \tau_2^2} +$ $\tan(\phi)\sigma_n' - c > 0$
	No tension ("cut–off") activated when:	
	$F_3(\boldsymbol{\sigma}') = \sigma_n' > 0$	$F_2(\boldsymbol{\sigma}') = \sigma_n' > 0$
	Graphic presentation:	

Flow potential	$Q_1(\boldsymbol{\sigma}') = \tau + \tan(\psi)\sigma_n' - c > 0 \quad$ if $\quad \tau \geq 0$ $Q_2(\boldsymbol{\sigma}') = -\tau + \tan(\psi)\sigma_n' - c > 0 \quad$ if $\quad \tau < 0$	$Q_1(\boldsymbol{\sigma}') = \sqrt{\tau_1^2 + \tau_2^2} +$ $\tan(\psi)\sigma_n' - c > 0$
Gradients $\quad \mathbf{a} = \frac{\partial F}{\partial \boldsymbol{\sigma}},$ $\mathbf{b} = \frac{\partial Q}{\partial \boldsymbol{\sigma}}$:	$\mathbf{a}_{1/2} = \begin{bmatrix} \pm 1, & \tan\varphi \end{bmatrix}^{\mathrm{T}},$ $\mathbf{b}_{1/2} = \begin{bmatrix} \pm 1, & \tan\psi \end{bmatrix}^{\mathrm{T}}.$	$\mathbf{a}_1 = \begin{bmatrix} \frac{\tau_1}{\tau}, & \frac{\tau_2}{\tau}, & \tan\varphi \end{bmatrix}^{\mathrm{T}}$ $\mathbf{b}_1 = \begin{bmatrix} \frac{\tau_1}{\tau}, & \frac{\tau_2}{\tau}, & \tan\psi \end{bmatrix}^{\mathrm{T}}$ $\tau = \sqrt{\tau_1^2 + \tau_2^2}$
Elasticity matrix:	$\mathbf{D}_{\mathrm{el}} = \begin{bmatrix} K_t & 0 \\ 0 & K_n \end{bmatrix}$	$\mathbf{D}_{\mathrm{el}} = \begin{bmatrix} K_t & 0 & 0 \\ 0 & K_t & 0 \\ 0 & 0 & K_n \end{bmatrix}$

Window 6-4

Window 6-5: Estimation of the penalty stiffness and permeability

This is done automatically (default) based on the following algorithm:

1. Find neighbouring elements (active at the current time $t_n + 1$)

2. For neighbouring elements find the maximum size in the direction normal to the interface
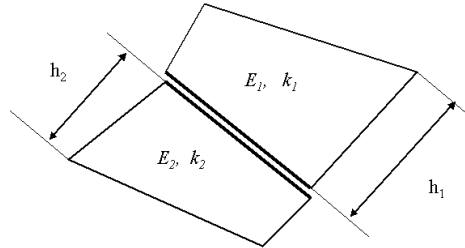
Penalty stiffness estimation

1. Estimate normal stiffness as:
$$K_n = \min \left(\frac{E_1}{h_1}, \frac{E_2}{h_2} \right) \frac{A}{\sqrt{Neq\varepsilon}}$$

2. Set tangent stiffness K_t of the interface as:
$$K_t = 0.01 K_n$$

3. In the case of *Flow* or *Deformation+Flow* analysis mode estimate penalty permeability:
$$k_f = \frac{B}{\gamma_w \sqrt{Neq\varepsilon}} \min \left(\frac{k_1}{h_1}, \frac{k_2}{h_2} \right) \quad \text{where } k_m = \sqrt{\sum_{i=1, N \text{ dim}} k_{ii}^2 k_r(S(p))}$$

taking into account permeability multiplier k_r dependent on current saturation $S = S(p)$

In the above:

A, B — arbitrary factors(default $A = 10^{-4}, B = 10^3$)set by numerical experience
Neq — total equation number in the system
ε — precision (machine dependent small number)

Parameters adopted under points $3, 4, 5$ may be multiplied by user-defined factors.

Window 6-5

Window 6-6: Stress point algorithm

Depending on the trial stress σ^*, 3 different types of the behavior will be modelled:

- sticking,

- sliding,

- separation.

The algorithm of stress and constitutive matrix evaluation is as follows:

Stress-point algorithm

$if \ \sigma_n^* > 0 \ then$

    separation:

        $\sigma^{n+1} = \mathbf{0}$

        $\mathbf{D} = \mathbf{0}$

$else$

$$if \quad F_1(\sigma^*) \leq 0 \overbrace{\wedge F_2(\sigma^*) \leq 0}^{if \quad Nstre=2} then$$

    sticking

    $\sigma^{n+1} = \sigma^*$

    $\mathbf{D} = \mathbf{D}_{el}$

    $else$

    sliding $(F_1(\sigma^*) > 0):$

    $\sigma^{n+1} = \sigma^n + \mathbf{D}_{el}(\Delta\boldsymbol{\varepsilon} - \Delta\gamma\mathbf{b})$

    $\Delta\gamma = \dfrac{F_i(\sigma^*)}{\mathbf{a}^{\mathrm{T}}\mathbf{D}_{el}\mathbf{b}}$

    $\mathbf{D} = \mathbf{D}_{el} - \dfrac{(\mathbf{D}_{el}\mathbf{b}) : (\mathbf{D}_{el}\mathbf{a})^{\mathrm{T}}}{\mathbf{a}^{\mathrm{T}}\mathbf{D}_{el}\mathbf{b}}$

    $where: \quad \mathbf{a} = \dfrac{\partial F_i}{\partial \sigma}, \quad \mathbf{b} = \dfrac{\partial Q_i}{\partial \sigma}$

    $end \ if$

$end \ if$

Note that stress return for the 'sliding' case is performed with a one step 'cutting-plane' procedure. This is due to the linear form of the yield function and flow potential in $2D$ case ($Nstre = 2$) as well as possible radial return for the $3D$ case ($Nstre = 3$).

Window 6-6

6.1.4 STIFFNESS MATRIX AND ELEMENT FORCE VECTOR

These are evaluated as: 3D case:

$$\mathbf{K}^e = \int_{-1}^{1}\int_{-1}^{1} \overline{\mathbf{B}}^{\mathrm{T}}\mathbf{D}\overline{\mathbf{B}} \mid \mathbf{J} \mid \mathrm{d}\eta \mathrm{d}\xi = \sum_{igaus=1}^{Ngaus} \overline{\mathbf{B}}^{\mathrm{T}}\mathbf{D}\overline{\mathbf{B}} \mid \mathbf{J} \mid W_{igaus}$$

$$\mathbf{f}^e = \int_{-1}^{1}\int_{-1}^{1} \overline{\mathbf{B}}^{\mathrm{T}}\boldsymbol{\sigma} \mid \mathbf{J} \mid \mathrm{d}\eta \mathrm{d}\xi = \sum_{igaus=1}^{Ngaus} \overline{\mathbf{B}}^{\mathrm{T}}\boldsymbol{\sigma} \mid \mathbf{J} \mid W_{igaus}$$

2D cases:

Plane Strain

$$\mathbf{K}^e = \int_{-1}^{1} \overline{\mathbf{B}}^{\mathrm{T}}\mathbf{D}\overline{\mathbf{B}} \parallel \mathbf{x}_{,\xi} \parallel \mathrm{d}\xi = \sum_{igaus=1}^{Ngaus} \overline{\mathbf{B}}^{\mathrm{T}}\mathbf{D}\overline{\mathbf{B}} \parallel \mathbf{x}_{,\xi} \parallel W_{igaus}$$

$$\mathbf{f}^e = \int_{-1}^{1} \overline{\mathbf{B}}^{\mathrm{T}}\boldsymbol{\sigma} \parallel \mathbf{x}_{,\xi} \parallel \mathrm{d}\xi = \sum_{igaus=1}^{Ngaus} \overline{\mathbf{B}}^{\mathrm{T}}\boldsymbol{\sigma} \parallel \mathbf{x}_{,\xi} \parallel W_{igaus}$$

Axisymmetry

$$\mathbf{K}^e = \int_{-1}^{1} \overline{\mathbf{B}}^{\mathrm{T}}\mathbf{D}\overline{\mathbf{B}} \parallel \mathbf{x}_{,\xi} \parallel 2\pi r\mathrm{d}\xi = \sum_{igaus=1}^{Ngaus} \overline{\mathbf{B}}^{\mathrm{T}}\mathbf{D}\overline{\mathbf{B}} \parallel \mathbf{x}_{,\xi} \parallel 2\pi r W_{igaus}$$

$$\mathbf{f}^e = \int_{-1}^{1} \overline{\mathbf{B}}^{\mathrm{T}}\boldsymbol{\sigma} \parallel \mathbf{x}_{,\xi} \parallel 2\pi r\mathrm{d}\xi = \sum_{igaus=1}^{Ngaus} \overline{\mathbf{B}}^{\mathrm{T}}\boldsymbol{\sigma} \parallel \mathbf{x}_{,\xi} \parallel 2\pi r W_{igaus}$$

with constitutive matrix $\mathbf{D}$ and stresses $\boldsymbol{\sigma}$ being the result of the point level algorithm, see **Window 6.5.4** . Note that in the case of *Analysis mode Deformation +Flow*, the total stresses $\boldsymbol{\sigma}$ including pressure is used to evaluate element forces. In order to avoid oscillatory patterns of normal stress, integration is performed at nodes and not standard Gauss points. In addition normal vectors at each node are averaged from all adjacent elements. The $\overline{\mathbf{B}}$ matrix is evaluated as follows:

$$\overline{\mathbf{B}}(\boldsymbol{\xi}_{igaus}) = \left[\begin{array}{c} \mathbf{B}_t(\boldsymbol{\xi}_{igaus}) \\ s \\ \mathbf{B}_n(\boldsymbol{\xi}_{igaus}) \end{array} \right]$$

6.1.5   AUGMENTED LAGRANGIAN APPROACH

[1] A common problem of the standard penalty approach used for problems of contacting elasto-plastic media is that the resulting overpenetration is too large and contact stresses may be underestimated. Usage of high values of penalty stifnesses usually results in loss of convergence and oscillatory contact stress distribution. In the case of soil-structure contact interaction the stress resultants may be underestimated as well. To handle this deficiency an Augmented Lagrangian Approach can be used. In the current contact formulation (segment to segment approach) each time the state of the global static equilibrium is achieved the contact resulting normal stresses are memorized, penalty stiffness is increased (by default through factor of 2). The Augmented Lagrangian Approach is summarized in window given below.

> **Window 6-7: Augmented Lagrangian Approach**
>
> 1. initialize: $\alpha = 0$, $^{(\alpha=0)}f = 1$
>
> 2. at each integration point at contact element set: $^{(\alpha=0)}\sigma_{n_{N+1}} = \sigma_{n_N}$
>
> 3. solve: $\mathbf{F}_{\text{ext}_{N+1}} - \mathbf{F}_{\text{int}}(\mathbf{u}_{N+1}) = \mathbf{0}$ assuming that that the trial normal stress at each integration point of contact element is computed as: $\sigma_{n_{N+1}}^{\text{trial}} = ^{(\alpha)}\sigma_{n_{N+1}} + ^{(\alpha)}f\, k_n\, \Delta\varepsilon_{n_{N+1}}$
>
> 4. at each integration point of contact element check overpenetration: $|\Delta\varepsilon_{n_{N+1}}| > $TOL (?)
>
> 5. if overpenetration is too large (at any integration point) perform augmentation procedure:
>
> 6. set: $\alpha = \alpha + 1$
>
> 7. increase penalty parameter: $^{(\alpha)}f = ^{(\alpha-1)}f \times g$ ($g = 2$ by default)
>
> 8. if $^{(\alpha)}f > f_{\max}$ set: $^{(\alpha)}f = f_{\max}$
>
> 9. if $\alpha <$MAX-AUGMENTATIONS go to step (2)
>
> Window 6-7

---

[1]concerns versions: **ACADEMIC, PROFESSIONAL, EXPERT** only

6.1.6   CONTRIBUTION TO CONTINUITY EQUATION

In the case of active fluid phase interface elements contribute to matrix $\mathbf{H}$ and flux vector $\mathbf{Q}$ (see Section 4.1.2) with the following:

$$\mathbf{H}_{\text{Interface}} = -\int_{\Gamma} \begin{bmatrix} \mathbf{N} \\ -\mathbf{N} \end{bmatrix} k_f \begin{bmatrix} \mathbf{N}^{\text{T}}, & -\mathbf{N}^{\text{T}} \end{bmatrix} d\Gamma$$

$$\mathbf{Q}_{\text{Interface}} = -\mathbf{H}_{\text{Interface}} \mathbf{t}_w$$

where:

$$\mathbf{N}^{\text{T}} = \begin{bmatrix} N_1(\xi) & \dots & N_{Nen}(\xi) \end{bmatrix} \quad \text{– shape function vector}$$
$$\mathbf{t}_w^{\text{T}} = \begin{bmatrix} t_{w1}, & \dots & t_{wNen} \end{bmatrix} \quad \text{– nodal pressure vector.}$$

The integration technique analogous to the one used for *Stiffness matrix and element force vector* evaluation is used.

## 6.2   PILE CONTACT INTERFACE

GENERAL OUTLOOK

DISPLACEMENT & STRAINS

CONSTITUTIVE MODEL

6.2.1   GENERAL OUTLOOK

Window 6-8: Pile interface element: General remarks

Pile interface element is used to model frictional contact between pile (beam elements) and continuum in which pile is embedded. This element consists of the two linear segments called master and slave respectively. Nodal points of the master segment are linked to the continuum via `Nodal link` option while slave segment coincides with beam element. This element allows to model relative movement of the pile and continuum while the interface behavior is controlled by the standard Coulomb's friction law. This element assumes full displacement continuity, enforced by the penalty method, in the plane perpendicular to the pile axis. Two formulations can be adopted ie. local or non-local. A comprehensive analysis and explanation of these two formulations is given in dedicated report.
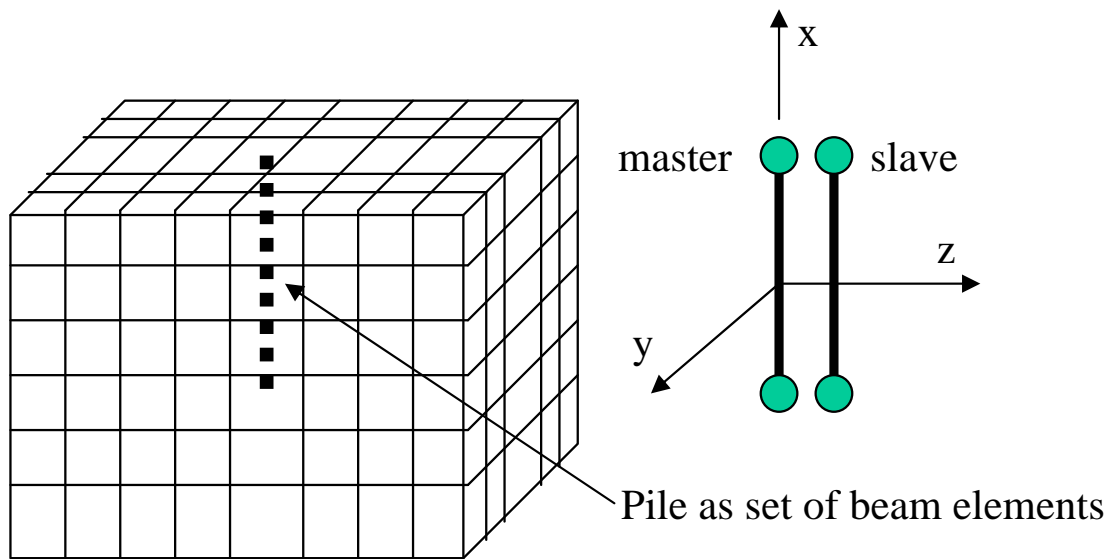
Window 6-8

6.2.2 DISPLACEMENTS AND STRAINS

Window 6-9: Pile interface: Generalized strains

Displacements at slave and master segments are interpolated by using standard approach, from given nodal displacements at master segment $\mathbf{u}_i^{\text{master}}$ and slave segment $\mathbf{u}_i^{\text{slave}}$:

$\mathbf{u}^{\text{master}}(\xi) = \sum_{i=1..Nen} N_i(\xi)\mathbf{u}_i^{\text{master}}$

$\mathbf{u}^{\text{slave}}(\xi) = \sum_{i=Nen+1..2*Nen} N_i(\xi)\mathbf{u}_i^{\text{slave}}$

The generalized strains at any integration point of the interface element are understood as relative displacements of both segments transformed to the local element basis $\{t, n_1, n_2\}$. The local n_1 and n_2 axes are created in a random way due to axial symmetry. If t axis is parallel to the global y axis (standard situation) then local n_1 and n_2 axes are parallel to the global x and z axes.
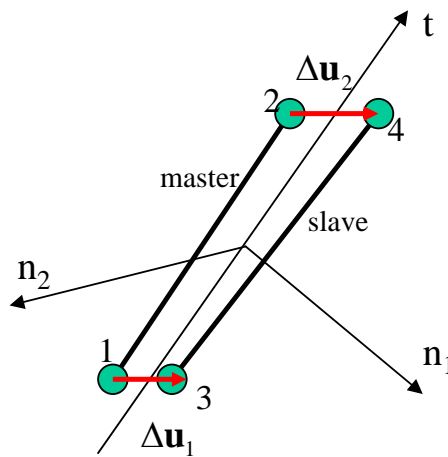
The relation between generalized strains and nodal global displacements:

$$\boldsymbol{\varepsilon}(\xi) = \mathbf{B}(\xi)\mathbf{u} = \sum_{i=1}^{2*Nen} \mathbf{B}_i(\xi)\mathbf{u}_i$$

where $\mathbf{B}$ is defined as:

$$\mathbf{B}(\xi) = [-N_i(\xi)\mathbf{T}(\xi), N_i(\xi)\mathbf{T}(\xi)]^{\text{T}} \quad \text{for } i = 1..Nen$$

$$\mathbf{T}(\xi)\text{–transformation matrix such that } \mathbf{u}^{local} = \mathbf{T}(\xi)\mathbf{u}^{global}$$

$$\mathbf{u}_i = [u_i, w_i, v_i]^{\text{T}}$$

$$\boldsymbol{\varepsilon}(\xi) = [\Delta u_t, \Delta u_{n_1}, \Delta u_{n_2}]^{\text{T}} = \left[u_t^{\text{slave}} - u_t^{\text{master}}, u_{n_1}^{\text{slave}} - u_{n_1}^{\text{master}}, u_{n_2}^{\text{slave}} - u_{n_2}^{\text{master}}\right]^{\text{T}}$$

Transformation matrix is composed of unit vectors $\mathbf{e}_t$, $\mathbf{e}_{n_1}$, $\mathbf{e}_{n_2}$ expressed in global coordinate system

$$\mathbf{T}(\xi) = [\mathbf{e}_t, \mathbf{e}_{n_1}, \mathbf{e}_{n_2}]^{\text{T}}$$

Window 6-9

6.2.3   CONSTITUTIVE MODEL

Window 6-10: Pile interface: Constitutive aspects and stress return algorithm

Constitutive behavior of the pile interface is described in terms of:

- Generalized strain ε_t, evaluated from nodal tangential displacements of the interface

- Effective stress $\boldsymbol{\sigma}'_n$ estimated in an explicit manner from the continuum in which pile is embedded; note that displacement continuity along n_1 and n_2 directions is always preserved

- Frictional Colulomb's law: $F(\sigma'_n, \tau) = |\tau| + \sigma'_n \, \tan(\phi) - c$

- Constitutive elastic matrix

$$\mathbf{D}^e = \begin{bmatrix} K_t & 0 & 0 \\ 0 & K_n & 0 \\ 0 & 0 & K_n \end{bmatrix}$$

Stress evaluation consists of the following steps:

- Compute trial averaged shear stress $\tau_{N+1}^{\text{trial}} = \tau_N + K_t \, \Delta\mathbf{u}_t$

- If $\sigma'_n > 0$ set $\tau_{N+1} = 0$ and

$$\mathbf{D}^{ep} = \begin{bmatrix} 0 & 0 & 0 \\ 0 & K_n & 0 \\ 0 & 0 & K_n \end{bmatrix}$$

- If $\sigma'_n \leq 0$ check plasticity condition: $F(\sigma'_n, \tau)$

   ★ If $F(\sigma'_n, \tau) < 0$ (sticking) then set $\tau_{N+1} = \tau_{N+1}^{\text{trial}}$ and $\mathbf{D}^{ep} = \mathbf{D}^e$

   ★ If $F(\sigma'_n, \tau) > 0$ (sliding) then set $\tau_{N+1} = (-\sigma'_n \, \tan(\phi) + c) \, sign(\tau_{N+1}^{\text{trial}})$ and

$$\mathbf{D}^{ep} = \begin{bmatrix} 0 & 0 & 0 \\ 0 & K_n & 0 \\ 0 & 0 & K_n \end{bmatrix}$$

- Compute the two remaining stress vector components σ_{n_1}, σ_{n_2} which are concerned with the enforced displacement continuity in n_1 and n_2 directions
$\sigma_{n_1 N+1} = \sigma_{n_1 N} + K_n \, \Delta\mathbf{u}_{n_1}$
$\sigma_{n_2 N+1} = \sigma_{n_2 N} + K_n \, \Delta\mathbf{u}_{n_2}$

- Compose stress vector $\boldsymbol{\sigma} = \{\tau_{N+1}, \sigma_{n_1}, \sigma_{n_2}\}^{\text{T}}$

Remarks:

1. The elastic stiffness K_t should be large enough to prevent significant loss of displacement continuity in the tangential direction for case of full sticking

2. The normal elastic stiffness K_n should also be large enough to prevent loss of continuity of the displacement fields in the plane perpendicular to the pile axis; however, too large values for K_n and K_t may lead to the lack of convergence, oscillations.

3. Dilatancy angle ψ is not meaningful for this type of the interface

4. Estimation of K_n and K_t factors follows the procedure described in Win.(6-5)

Window 6-10

6.2.4   STIFFNESS MATRIX AND ELEMENT FORCE VECTOR

$$\mathbf{K}^e = 2\pi \; r^{\text{pile}} \int_{-1}^{1} \mathbf{B}^{\mathrm{T}} \mathbf{D} \mathbf{B} \mid \mathbf{J} \mid \mathrm{d}\xi = 2\pi \; r^{\text{pile}} \sum_{igaus=1}^{Ngaus} \mathbf{B}^{\mathrm{T}} \mathbf{D} \mathbf{B} \mid \mathbf{J} \mid W_{igaus}$$

$$\mathbf{f}^e = 2\pi \; r^{\text{pile}} \int_{-1}^{1} \mathbf{B}^{\mathrm{T}} \boldsymbol{\sigma} \mid \mathbf{J} \mid \mathrm{d}\xi = 2\pi \; r^{\text{pile}} \sum_{igaus=1}^{Ngaus} \mathbf{B}^{\mathrm{T}} \boldsymbol{\sigma} \mid \mathbf{J} \mid W_{igaus}$$

Remarks:

1. r^{pile} is a radius of pile (reinforcement)

6.3   PILE TIP CONTACT INTERFACE

GENERAL OUTLOOK

DISPLACEMENT & STRAINS

CONSTITUTIVE MODEL

6.3.1   GENERAL OUTLOOK

| **Window 6-11: Pile tip interface element: General remarks** |

Pile tip interface element is a simple node to node interface element which is used to put limits on the tensile and compressive stresses in the contact zone of tip of the pile and underlying subsoil. This element consists of the two nodes called master (it is linked to the continuum via `Nodal link` option) and slave ((pile) beam element endpoint). This element allows to model separation of the tip of the pile and soil during pull out and limited compressive strength. The latter effect is important as due to coarseness of the continuum finite element mesh in the zone of the tip of the pile bearing capacity of the pile could be overestimated. This interface controls relative movement of the pile and continuum only in the axial pile direction (x_L); in the two remaining directions (y_L, z_L) full continuity is enforced. Two formulations can be adopted ie. local or non-local. A comprehensive analysis and explanation of these two formulations is given in dedicated report.
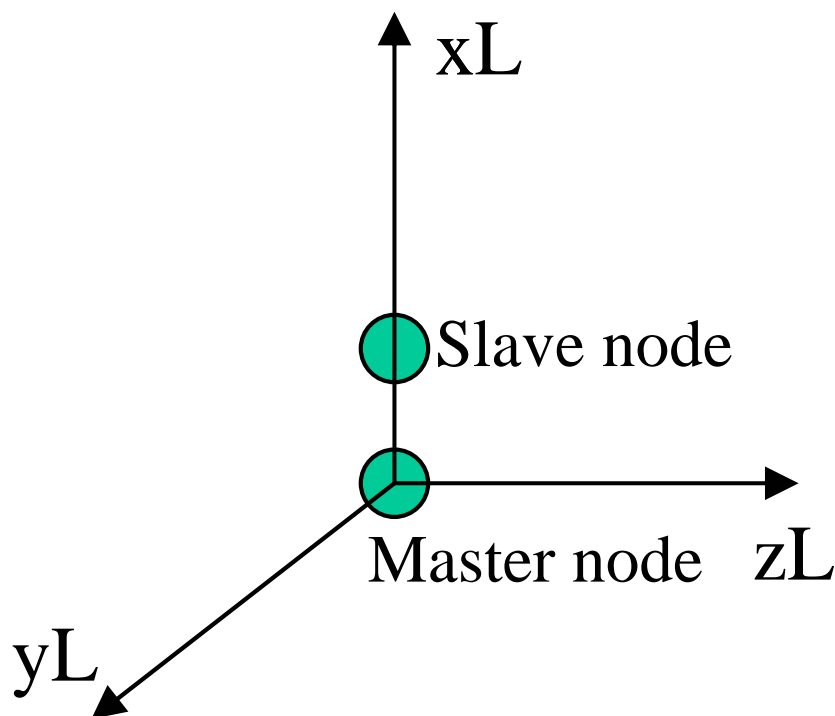
| Window 6-11 |

6.3.2　DISPLACEMENTS AND STRAINS

Window 6-12: Pile tip interface: Generalized strains

The generalized strains in the interface are understood as relative displacements of both nodes transformed to the local element basis $\{x_L, y_L, z_L\}$. The local y_L and z_L axes are created in a random way due to axial symmetry. If x_L axis is parallel to the global y axis (standard situation) then local y_L and z_L axes are parallel to the global x and z axes.
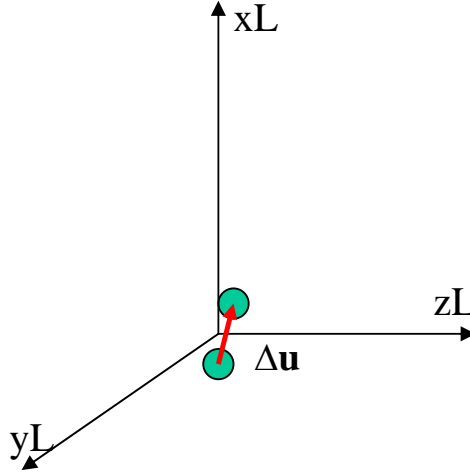
The relation between generalized strains and nodal global displacements:

$$\varepsilon = \mathbf{B}\mathbf{u} = \sum_{i=1}^{2} \mathbf{B}_i \mathbf{u}_i$$

where $\mathbf{B}$ is defined as:

$$\mathbf{B} = [-1\ \mathbf{T}, 1\ \mathbf{T}]^{\mathrm{T}}$$

$\mathbf{T}$–transformation matrix such that $\mathbf{u}^{local} = \mathbf{T}\mathbf{u}^{global}$

$$\mathbf{u}_i = [u_i, w_i, v_i]^{\mathrm{T}}$$

$$\varepsilon = [\Delta u_{x_L}, \Delta u_{y_L}, \Delta u_{z_L}]^{\mathrm{T}} = \left[u_{x_L}^{\text{slave}} - u_{x_L}^{\text{master}}, u_{y_L}^{\text{slave}} - u_{y_L}^{\text{master}}, u_{z_L}^{\text{slave}} - u_{z_L}^{\text{master}} \right]^{\mathrm{T}}$$

Transformation matrix is composed of unit vectors $\mathbf{e}_{x_L}$, $\mathbf{e}_{y_L}$, $\mathbf{e}_{z_L}$ expressed in global coordinate system

$$\mathbf{T} = [\mathbf{e}_t, \mathbf{e}_{n_1}, \mathbf{e}_{n_2}]^{\mathrm{T}}$$

Window 6-12

6.3.3   CONSTITUTIVE MODEL

Window 6-13: Pile tip interface: Constitutive aspects and stress return algorithm

Constitutive behavior of the pile tip interface is described in terms of:

- Generalized strain ε_x, evaluated from nodal displacements of the interface

- Stick-separation law: $-q_c \leq \sigma_x \leq q_t$; q_t is a tensile bearing capacity (default $q_t = 0$ kPa) and q_c is the compressive bearing capacity (can be found in standard codes for pile design) (default $q_c = 10^{38}$ kPa)

- Constitutive elastic matrix

$$\mathbf{D}^e = \begin{bmatrix} K_n & 0 & 0 \\ 0 & K_n & 0 \\ 0 & 0 & K_n \end{bmatrix}$$

Stress evaluation consists of the following steps:

- Compute trial normal stress $\sigma_{x\,N+1}^{\text{trial}} = \sigma_{x\,N} + K_n\,\Delta\mathbf{u}_x$

- If $\sigma_{x\,N+1}^{\text{trial}} > q_t$ set $\sigma_{x\,N+1} = q_t$ and

$$\mathbf{D}^{ep} = \begin{bmatrix} 0 & 0 & 0 \\ 0 & K_n & 0 \\ 0 & 0 & K_n \end{bmatrix}$$

- If $\sigma_{x\,N+1}^{\text{trial}} < -q_c$ set $\sigma_{x\,N+1} = -q_c$ and

$$\mathbf{D}^{ep} = \begin{bmatrix} 0 & 0 & 0 \\ 0 & K_t & 0 \\ 0 & 0 & K_t \end{bmatrix}$$

- If $-q_c < \sigma_{x\,N+1}^{\text{trial}} < q_t$ set $\sigma_{x\,N+1} = \sigma_{x\,N+1}^{\text{trial}}$ and $\mathbf{D}^{ep} = \mathbf{D}^e$

- Compute the two remaining stress vector components τ_{xz}, τ_{xy} which are concerned with the enforced displacement continuity in y_L and z_L directions
  $\tau_{xy\,N+1} = \tau_{xy\,N} + K_n\,\Delta\mathbf{u}_y$
  $\tau_{xz\,N+1} = \tau_{xz\,N} + K_n\,\Delta\mathbf{u}_z$

- Compose stress vector $\boldsymbol{\sigma} = \{\sigma_x, \tau_{xy}, \tau_{xz}\}^{\text{T}}$

Remarks:

1. The elastic stiffness K_n should be large enough to prevent significant over-penetration in case of full sticking

2. Too large values for K_n may lead to the lack of convergence (oscillations)

3. Estimation of K_n follows the procedure described in Win.(6-5)

Window 6-13

6.3.4   STIFFNESS MATRIX AND ELEMENT FORCE VECTOR

$$\mathbf{K}^e = \pi \, r^{\mathsf{pile}^2} \mathbf{B}^{\mathrm{T}} \mathbf{D} \mathbf{B}$$

$$\mathbf{f}^e = \pi \, r^{\mathsf{pile}^2} \mathbf{B}^{\mathrm{T}} \boldsymbol{\sigma}$$

Remarks:

1. r^{pile} is a radius of pile

6.4   NAIL INTERFACE

This interface is fully compatible with the interface designed for 3D piles. However, there exist the three major differences among them. The first is such that the nail interface can be used both for 2D and 3D problems, the radius appearing in the integration of the internal force vector and interface stiffness matrix is equal to the radius of the injection zone, and contact constitutive model is purely adhesive. Hence, firictional terms in the formulation are cancelled.   The detailed explanations are given in sections devoted to piles treated as beam elements embedded in the continuum 6.2.

6.5   FIXED ANCHOR INTERFACE

This interface is fully compatible with the interface designed for 3D piles. However, there exist the three major differences among them. The first is such that the fixed anchor interface can be used both for 2D and 3D problems, the radius appearing in the integration of the internal force vector and interface stiffness matrix is equal to the radius of the injection zone and contact constitutive model is purely adhesive. Hence, firictional terms in the formulation are canceled.   The detailed explanations are given in sections devoted to piles treated as beam elements embedded in the continuum 6.2.

Chapter 7

GEOTECHNICAL ASPECTS

TWOPHASE MEDIUM

EFFECTIVE STRESSES

SOIL PLASTICITY

INITIAL STATE

SOIL RHEOLOGY

ALGORITHMIC STRATEGIES

7.1   TWO-PHASE MEDIUM

In this section, an attempt is made to relate modelling parameters to geotechnical aspects. The soil is modeled as a two-phase medium, this means that equilibrium of the medium requires the solution of a coupled system of differential equations where one set of equations represents the equilibrium of the solid and the second set of equations represents the continuity of the fluid flow. Both sets include coupling terms. Drained and undrained conditions are limiting cases of particular interest. The corresponding boundary conditions are shown in **Window** 7-1

- **Drained conditions**

  Boundary conditions are such that, in the long term, the local stress is carried by the skeleton $(\underline{\sigma} = \underline{\sigma}')$.

- **Undrained conditions**

  When boundary conditions and material properties are such that no fluid motion relative to the solid is possible, the condition is undrained and the medium behaves in an essentially incompressible manner.

Window 7-1: Drained and undrained condition
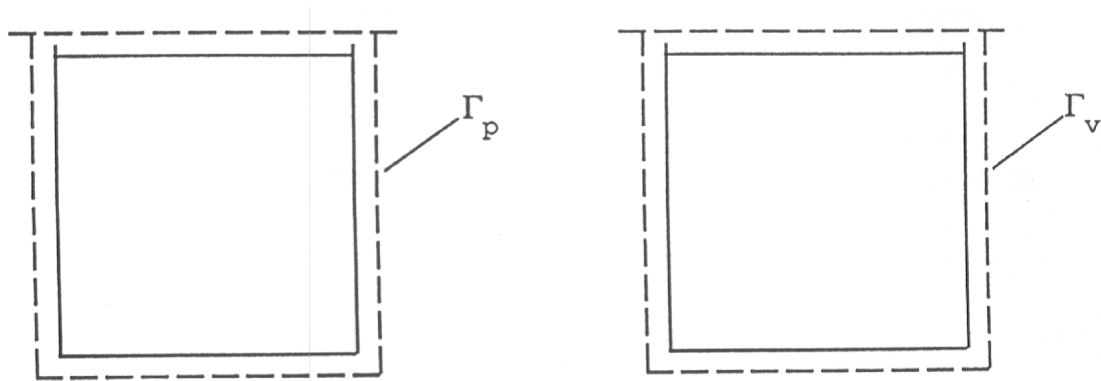
Drained condition: $p^{\mathsf{F}} = \overline{p^{\mathsf{F}}}$ on Γ_p (left); Undrained condition $q = 0$ on Γ_v (right)

Window 7-1

7.2   EFFECTIVE STRESSES

Effective stresses allow a unified approach to the analysis of the drained and undrained conditions, this concept is extended here to account for partially saturated media. Let:

$$\boldsymbol{\sigma} = \boldsymbol{\sigma}' + \tilde{\alpha}\,\tilde{S}\boldsymbol{\delta}p$$

where $\boldsymbol{\sigma}'$ is the effective (grain to grain stress), $\tilde{\alpha}$ is the Biot coefficient, p the interstitial pressure, and $\tilde{S} = S$ (saturation ratio) or $\tilde{S} = S_e^{1/(nm)}$ (corrected effective saturation) depending on the user's choice.

7.3   SOIL PLASTICITY

DRUCKER-PRAGER VERSUS MOHR-COULOMB CRITERION

CAP MODEL

DILATANCY

7.3.1   DRUCKER-PRAGER VERSUS MOHR-COULOMB CRITE-RION

It is common to describe soils as elastic–perfectly plastic Mohr–Coulomb materials. A smooth Mohr–Coulomb criterion described earlier is available in this program. If a Drucker–Prager criterion with cap closure is preferred, the size of the Drucker–Prager criterion can be adjusted to match the Mohr–Coulomb criterion. This is illustrated in **Window** 7-2. The various matching options are derived in the theoretical section; for plane strain, the most meaningful matching for an ultimate load analysis is the matching of collapse loads. The most important size–adjustments are summarized in **Window** 7-2.

Window 7-2: Matching Mohr-Coulomb and Drucker-Prager criteria
---
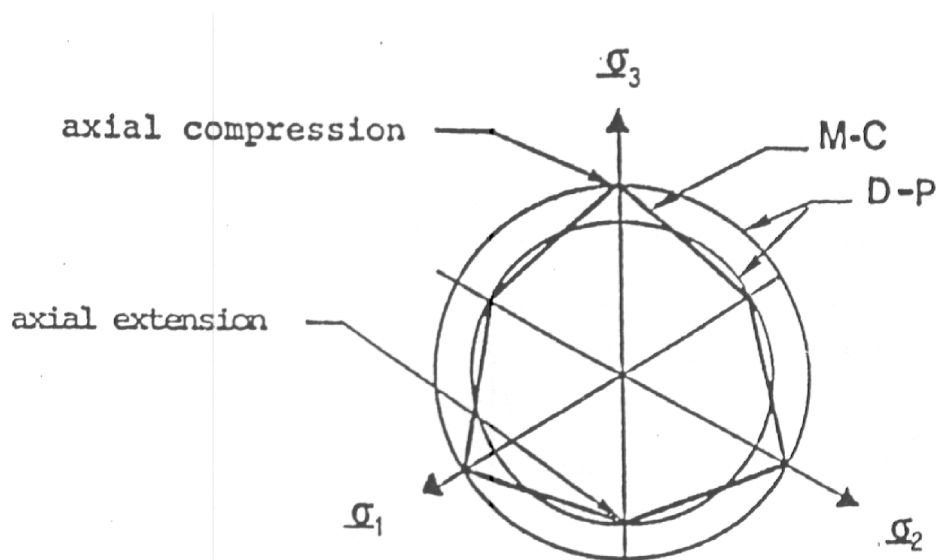
Deviatoric sections of Mohr–Coulomb (M–C) and Drucker–Prager

Matching	a_ϕ	k
External apices	$\dfrac{2\sin\phi}{\sqrt{3}(3-\sin\phi)}$	$\dfrac{6c\cos\phi}{\sqrt{3}(3-\sin\phi)}$
Internal apices	$\dfrac{2\sin\phi}{\sqrt{3}(3+\sin\phi)}$	$\dfrac{6c\sin\phi}{\sqrt{3}(3+\sin\phi)}$
Plane–strain collapse	$\dfrac{\sin\phi}{3D}; \quad D=\left(a_\psi\sin\phi+\sqrt{1-3a_\psi^2}\right)$	$c\cos\phi D^{-1}$
Elastic domain (plane strain $\nu_t=0.5$)[1]	$\dfrac{\sin\phi}{3}$	$c\cos\phi$

a_ϕ, k :   parameters of the Drucker–Prager criterion
ϕ :   friction angle
C :   cohesion
ψ :   angle of non–associativity (in doubt, use default value)

Window 7-2

Related Topics

- THEORY: M-C VERSUS D-P

7.3.2   CAP MODEL

The cap model accounts for nonlinear behavior of soil under dominant volumetric (pressure) stress. The initial size of the cap is derived from the oedometric test, it is determined by the preconsolidation pressure. Once the yield point (i.e. the cap) is reached by the stress, hardening takes place.

Hardening results from the reduction of the void ratio under increasing pressure, it is again controlled by the oedometric test.

Related Topics

- CAP MODEL
- CAP MODEL - STRESS POINT ALGORITHM
- OEDOMETRIC TEST

7.3.3 DILATANCY

Two alternative dilatancy parameters can be accommodated by the material models proposed earlier. The first parameter, d, relies on the availability of experimental results. The second one, ψ, assumes the empirical knowledge of ψ, by analogy with the friction angle ϕ.

- **Dilatancy parameter d**

  Volumes changes in soils, in the plastic regime, are conveniently described as follows; let d be the dilatancy

  $$d = \frac{d\varepsilon_V^p}{d\varepsilon_D^p} = \frac{\partial Q/\partial p}{\partial Q/\partial q} = \frac{r_p}{r_q}$$

  where $d\varepsilon_V^p$ is the volumetric plastic strain increment and $d\varepsilon_D^p$ is the plastic deviatoric strain increment. Q is the plastic potential, r_p is the norm of the volumetric plastic flow component and r_q, the deviatoric one. $d\varepsilon_V^p$, $d\varepsilon_D^p$ will usually be retrieved from a tri-axial test and r_p/r_q will be derived from the plastic model.

- **Dilatancy extraction from triaxial test**

  Experimental results from a triaxial test can be plotted as follows:
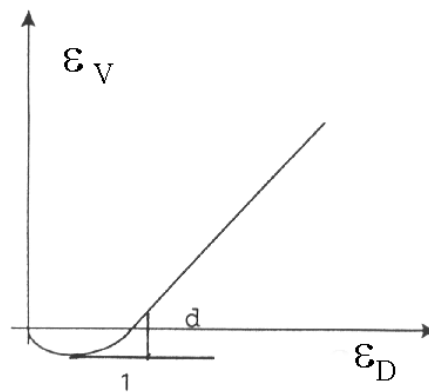
  $$\varepsilon_V = \varepsilon_1 + 2\varepsilon_3$$

  $$\varepsilon_D = (2/3)(\varepsilon_1 - \varepsilon_3)$$

  In the plastic regime $d\varepsilon_V \cong d\varepsilon_V^P$ and $d\varepsilon \cong d\varepsilon^P$ hence: $\dfrac{d\varepsilon_V}{d\varepsilon_D} = d$

- **Dilatancy with Drucker-Prager plasticity**

  The plastic potential is in this case:

  $$Q = a_\psi I_1 + \sqrt{J_2}$$

  then,

  $$r_p = \frac{\partial Q}{\partial p} = \frac{\partial Q}{\partial I_1}\frac{\partial I_1}{\partial p} = 3a_\psi$$

  $$r_q = \frac{\partial Q}{\partial q} = \frac{\partial Q}{\partial \sqrt{J_2}}\frac{\partial \sqrt{J_2}}{\partial p} = 1/\sqrt{3}$$

  and finally,

  $$d = 3\sqrt{3}a_\psi$$

  Given d from the experiment, a_ψ can be found for the material model.

- **Dilatancy with Mohr-Coulomb plasticity**

  Plastic flow is again governed by a Drucker-Prager type surface in the program, even when yield is governed by a Mohr-Coulomb criterion. The rate of non-associativity generated by a given (experimental) d is therefore dependent on the size adjustment.

  In 2D, for size adjustment option "matching plane strain collapse load" , given ϕ, c and d, one gets:

$$a_\psi = d/3\sqrt{3}$$
$$a_\phi = \frac{1}{3}\sin\phi \cdot [a_\psi \sin\phi + \sqrt{1 - 3a_\psi^2}]^{-1}$$
$$k = C\cos\phi[a_\psi \sin\phi + \sqrt{1 - 3a_\psi^2}]^{-1}$$

For a 3D situation in which ξ defines the size adjustment with respect to external and internal matching, we get

$$a_\psi = d/3\sqrt{3}$$
$$a_\phi = (1-\xi)[2\sin\phi/(\sqrt{3}(3-\sin\phi))] + \xi[2\sin\phi/(\sqrt{3}(3+\sin\phi))]$$
$$k = (1-\xi)[6C\cos\phi/(\sqrt{3}(3-\sin\phi))] + \xi[6C\cos\phi/(\sqrt{3}(3+\sin\phi))]$$

NB: a_ψ should be such that $(0 < a_\psi < a_\phi)$.

Alternative experimental results can also be used in order to define d, as illustrated next.

- **Alternative experimental representations**

$$d = \frac{3}{2}\left(\frac{1 + 2d'}{1 - d'}\right) \qquad\qquad d = \frac{d''}{1 - \dfrac{d''}{3}}$$
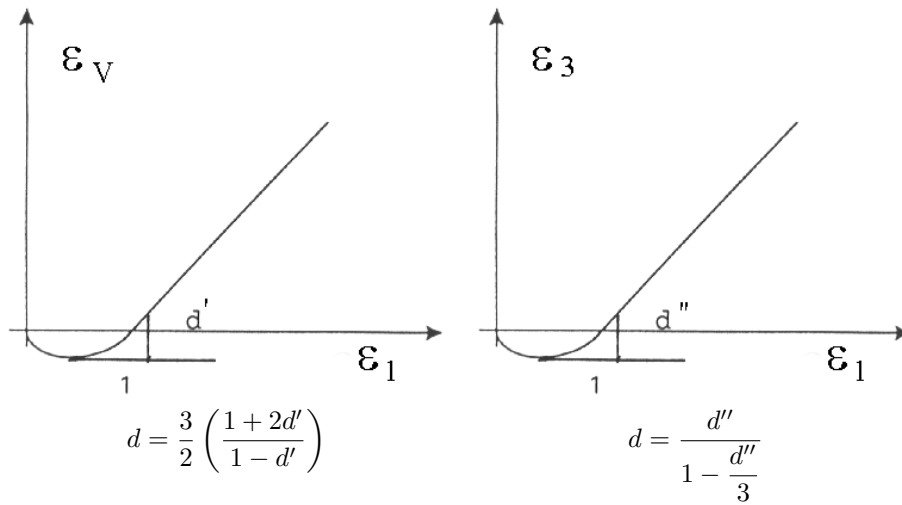
- **Dilatancy angle** ψ

  Assuming a plastic potential given by $Q = |\tau| - \sigma_n \tan\psi$. The value of ψ can result from empirical knowledge or be retrieved from experiments as before, using the following formula,

$$\tan\psi = -\frac{\dot{\varepsilon}_n^p}{\dot{\varepsilon}_t^p}$$

  where $\dot{\varepsilon}_n^p$ and $\dot{\varepsilon}_t^p$ are normal and tangential plastic strain increments or alternatively:

$$\sin\psi = -\frac{\dot{\varepsilon}_V^p}{\dot{\gamma}_{\max}^p} = -\frac{\dot{\varepsilon}_1^p + \dot{\varepsilon}_3^p}{\dot{\varepsilon}_1^p - \dot{\varepsilon}_3^p}$$

- **Application with Drucker-Prager plasticity**

  If ψ is specified, then the same size adjustment as for ϕ will be assumed in order to retrieve a_ψ. For example, assuming a 2D situation for which ϕ, C, ψ and size adjustment "plane strain collapse" are specified, then ψ introduced into the associated flow option yields:

$$a_\psi = \tan\psi/\sqrt{9 + 12\tan^2\psi}$$

  can then in turn be introduced into formulas in order to retrieve k and a_ϕ.

  In a 3D situation with f, k, ψ and ξ specified, a_ψ can be retrieved from formula, ψ replacing ϕ; a_ϕ and k are, in this case independent of α_ψ. These operations are, of course, done automatically and hidden to the user.

- **Dilatancy with smooth Hoek-Brown criterion**

  Flow options available on Hoek-Brown criterion include:

* Deviatoric, corresponding to incompressible flow.

* Tensile meridian. The flow will be radial in the deviatoric plane and follow the normal to the tensile meridian in the meridian plane.

* ψ_c prescribed (Hoek-Brown flow).

  ψ_c is defined as the angle of dilatancy at failure under uniaxial compression $\psi_c = \arctan(d\xi/d\rho)$ and

$$\left[\arctan(\frac{f_t}{\sqrt{2}f_c}) < \psi_c < \arctan(\frac{1}{\sqrt{2}}) \right].$$

Alternatively $\psi_c = \arctan[\dfrac{1}{\sqrt{6}}\dfrac{dI_1}{d\sqrt{J_2}}]$; the resulting dilatancy will vary with loading paths: from coincidence with the loading path under uniaxial tension to ψ_c under uniaxial compression.

Following table contains indicative values of **dilatancy characteristics**

	ψ/ϕ	d	$\psi_c, []^o$
Clay	0	0	-
Sand	-	-	-
Gravel	-	-	-
Rock	$0.67 - 1$	-	-
Concrete	-	-	$4^o - 35^o$

7.4   INITIAL STATE

COEFFICIENT OF EARTH PRESSURE AT REST, K0

STATES OF PLASTIC EQUILIBRIUM

INFLUENCE OF POISSON'S RATIO

COMPUTATION OF THE INITIAL STATE

INFLUENCE OF WATER

7.4.1   COEFFICIENT OF EARTH PRESSURE AT REST, K0

K_0 is by definition the ratio of horizontal effective stresses to vertical effective stresses

$$K_0 = \frac{\sigma_1'}{\sigma_2'}.$$

The coefficient can be determined from triaxial experiments, measured with a pressuremeter or evaluated using approximate formula. Commonly used formula are given in **Window** 7-3.

Window 7-3: Coefficient of earth pressure at rest, K_0

Normally consolidated soil (NC)	$(K_0)_{NC} = 1 - \sin\phi$	[JAK48]
Overconsolidated soil (OC)	$(K_0)_{OC} = (K_0)_{NC} OCR^\alpha$ $\alpha = \sin\phi$	
Confined elastic medium	$K_0 = \frac{\nu}{1-\nu}$	

Window 7-3

- **Overconsolidation ratio (OCR)**

  The overconsolidation ratio OCR is obtained from an oedometric test. It is maximum close to soil surface and tends to 1 a depth. The identification of OCR is illustrated in

Window 7-4.

Given the void ratio, the water content, a preconsolidation pressure can be associated with each vertical stress and the corresponding overconsolidation ratio can be computed as illustrated in Figs 7-4, 7-4.

Window 7-4: Overconsolidation ratio OCR

- Effective stress at depth z :

$$\underline{\sigma}'_z = \gamma' z,$$

- initial void ratio:

$$e_0 = \left(\gamma_s \frac{1+w}{\gamma}\right) - 1$$

where:

γ_s : unit weight of solid particles
w : water content ratio
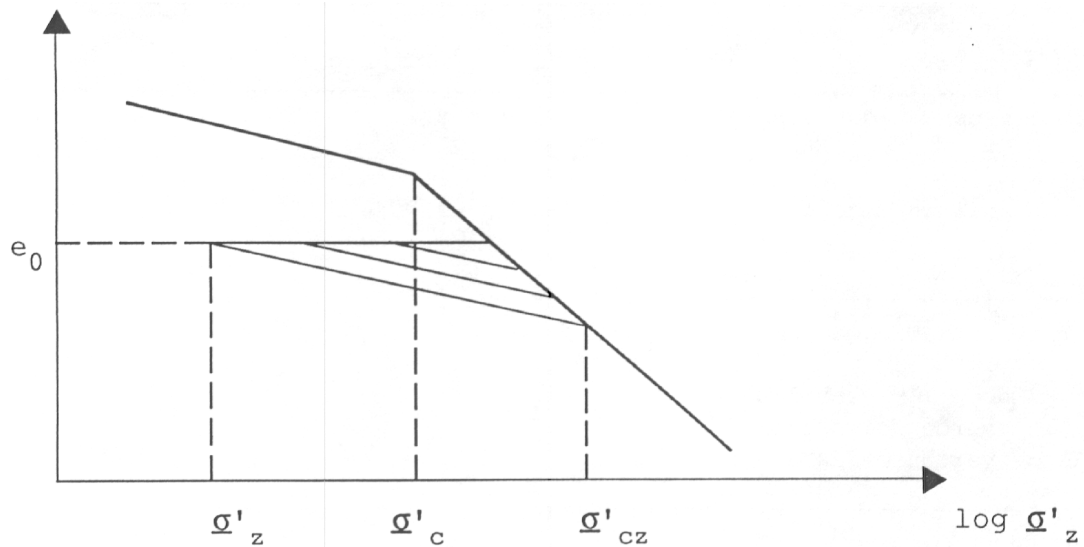
Oedometric test
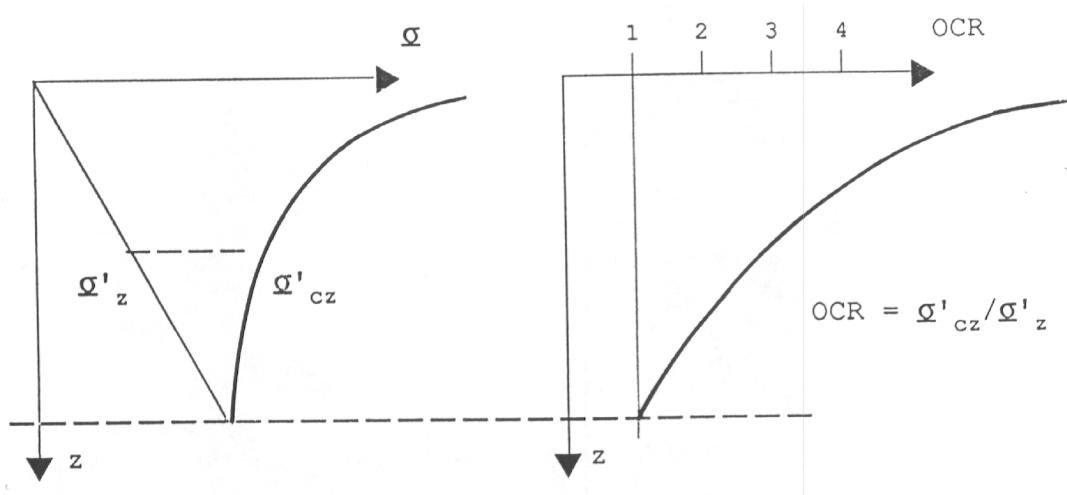
Vertical stresse and preconsolidation pressure as a function of depth
(right).Overconsolidation ratio as a function of stress (left)

Window 7-4

7.4.2   STATES OF PLASTIC EQUILIBRIUM

The section deals with the case of semi-infinite soil mass with horizontal or inclined surface subjected to gravity load. Coefficients of horizontal pressure K fulfilling different stress criterion are investigated.

MOHR-COULOMB CRITERION

DRUCKER-PRAGER CRITERION

7.4.2.1 MOHR-COULOMB MATERIAL

The plastic equilibrium at depth h of a semi–infinite soil mass with horizontal surface, considered as a Mohr–Coulomb material, subjected to gravity loading is characterized by two circles in a Mohr diagram (**Window** 7-5).

The two Mohr circles correspond to Rankine states. The small circle corresponds to the active Rankine state, the large circle to the passive state.

A cohesionless material is considered first. Note that the principal stress orientation coincides with axes 1 (horizontal) and 2 (vertical). The plastic stress state at depth h is

$$\underline{\sigma}_2 = \gamma h \qquad \text{(vertical)}$$
$$\underline{\sigma}_1 = \underline{\sigma}_3 \qquad \text{(assumption)}$$
$$\underline{\sigma}_1 = \underline{\sigma}_A = K_A \gamma h \qquad \text{(horizontal, active state)}$$
$$\underline{\sigma}_1 = \underline{\sigma}_p = K_A \gamma h \qquad \text{(horizontal, passive state)}$$

Stress states such that,

$$\underline{\sigma}_1 = K_0 \gamma h \qquad \text{with } K_A < K_0 < K_P$$

are elastic. K_0 is the earth pressure coefficient at rest.

From geometrical considerations equations 1 and 2 (**Window** 7-5) can be derived for K_A and K_P are plotted and provide a useful way to define possible horizontal stress states, given the friction angle. For an elastic perfectly plastic material, no stress state outside of these limits is tolerable.

Window 7-5: Rankine state
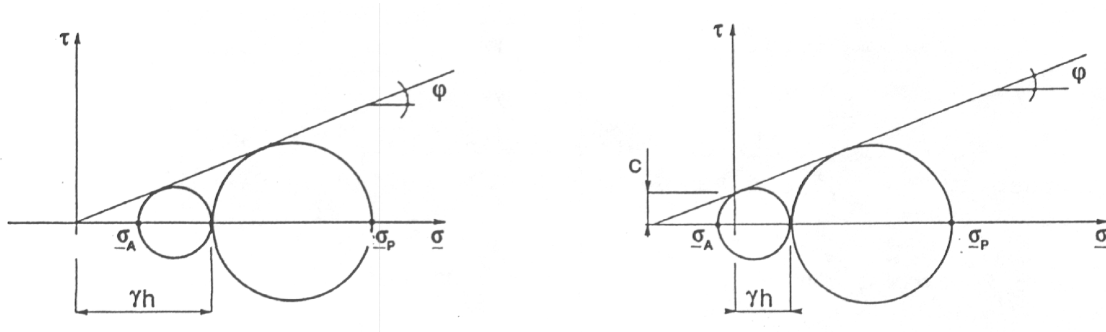
Mohr diagram of the plastic state of a semi-infinite medium: Cohesionless material (left), Cohesive material (right)
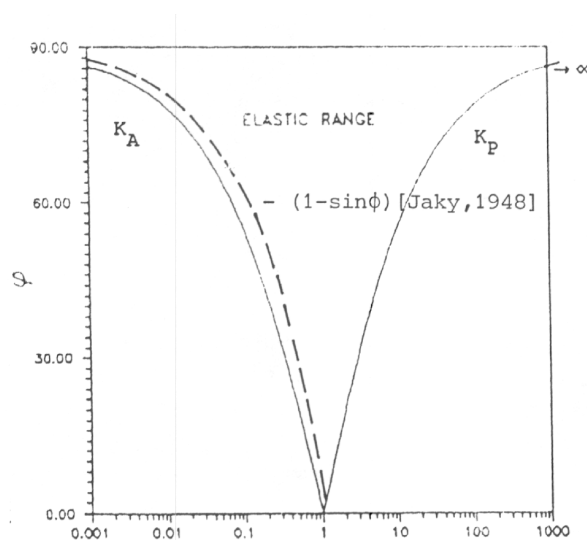
Earth pressure coefficient at rest K_0, for a cohesionless semi-infinite soil mass with horizontal surface

- Active state:

$$K_A = \frac{1 - \sin\phi}{1 + \sin\phi} = \tan^2\left(45° - \frac{\phi}{2}\right) = \frac{1}{N_\phi} \tag{1}$$

- Passive state:

$$K_P = \frac{1 + \sin\phi}{1 - \sin\phi} = \tan^2\left(45° + \frac{\phi}{2}\right) = N_\phi \tag{2}$$

Window 7-5

Similar expressions for the horizontal stress are derived in **Window 7-5** for a **cohesive material**, from **Window 7-6** and geometrical considerations.

Window 7-6: Rankine states for a Cohesive Mohr–Coulomb material

- Active state

$$\underline{\sigma}_1 = K_A \left(\underline{\sigma}_2 + \frac{C}{\tan \phi} \right) - \frac{C}{\tan \phi}$$

  or

$$\underline{\sigma}_1 = K_A \underline{\sigma}_2 - (1 - K_A) \frac{C}{\tan \phi}.$$

- Passive state

$$\underline{\sigma}_1 = K_P \left(\underline{\sigma}_2 + \frac{C}{\tan \phi} \right) - \frac{C}{\tan \phi}$$

  or

$$\underline{\sigma}_1 = K_P \underline{\sigma}_2 - (1 - K_P) \frac{C}{\tan \phi}.$$

Window 7-6

Given the friction angle, K_A and K_P can be read from **Window** 7-5. Introducing the cohesion C, f and K_A or K_P into the expressions for $\underline{\sigma}_1$ yields limiting values of the horizontal stress $\underline{\sigma}_1$. These values define the elastic range. The same discussion holds when the semi–finite soil mass is loaded on its surface by a uniform load q. In this case $\underline{\sigma}_2 = \gamma h$ is replaced by $\underline{\sigma}_2 = (\gamma h + q)$.

The presence of a **water table** can be accounted for similarly. Plastic states are defined in terms of effective stresses. The limiting values K_A and K_P of K_0 are therefore the same for a saturated medium as for a dry medium.

If the water table is located at a depth d, the upper layer can be viewed as a surface load on a saturated medium, and K_A and K_P are again the same.

Particular situations

If the semi–infinite soil mass is limited by an upper surface inclined at an angle $\beta \leq \phi$ the Mohr diagram is given in Window 7-7.

The stress state at depth h on a plane inclined at angle β can be calculated as:

$$\underline{\sigma} = \gamma h \cos^2 \beta$$
$$\underline{\tau} = \gamma h \sin \beta \cos \beta.$$

The corresponding point in the Mohr diagram is Z and the Mohr circles corresponding to active and passive states can be constructed. The values obtained for K_A^* and K_P^* ($K^* = \underline{\sigma}_{11}/\gamma h$) are reported in Window 7-7 as functions of the friction angle ϕ and the angle of the slope β.

The case of a semi–infinite soil mass limited by an upper surface inclined at an angle $\beta \leq \phi$, submerged by water can be solved similarly and the same values of , K_A^*, K_P^* apply, associated with γ'.

The case of an infinite slope under conditions of seepage flow leads to the following stress state on a plane inclined at angle β:

$$\underline{\sigma} = \gamma h \cos^2 \beta$$
$$\underline{\tau} = \gamma_{\text{sat}} h \sin \beta \cos \beta.$$

A Mohr circle can be drawn as in the previous case and the corresponding limiting states can be calculated. The values of K_A^* and K_P^* can again be read from Window 7-5 , with $\tan \beta$ replaced by

$$\tan \beta^* = \frac{\gamma_{\text{sat}}}{\gamma_b} \tan \beta.$$

Similar derivations can be performed for the case of a cohesive material leading to the same expressions for K_A^* and K_P^* if β is replaced by β^0 such that:

$$\tan \beta^0 = \tan \beta \left(\frac{\sigma}{\underline{\sigma} + C/\tan \phi} \right).$$

For seepage flow β^* replaces β.

Window 7-7: Rankine states, inclined surface
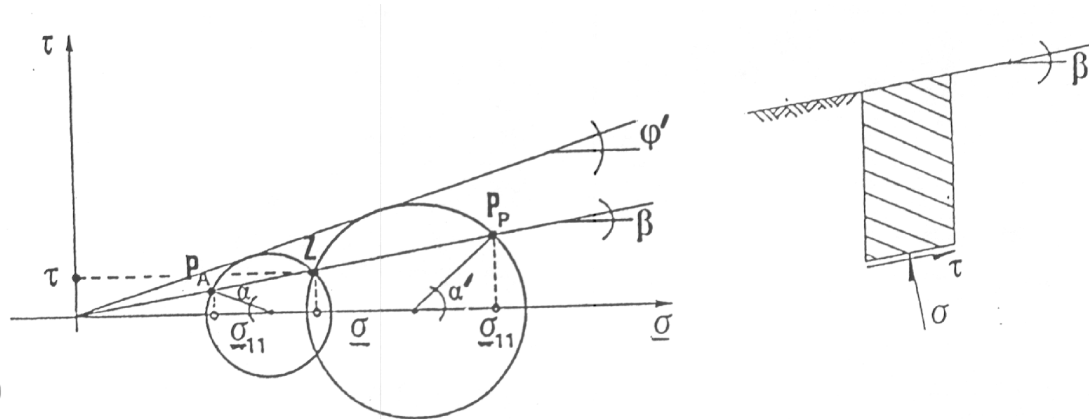
Mohr diagram for a semi–infinite soil mass with inclined surface. Cohesionless soil
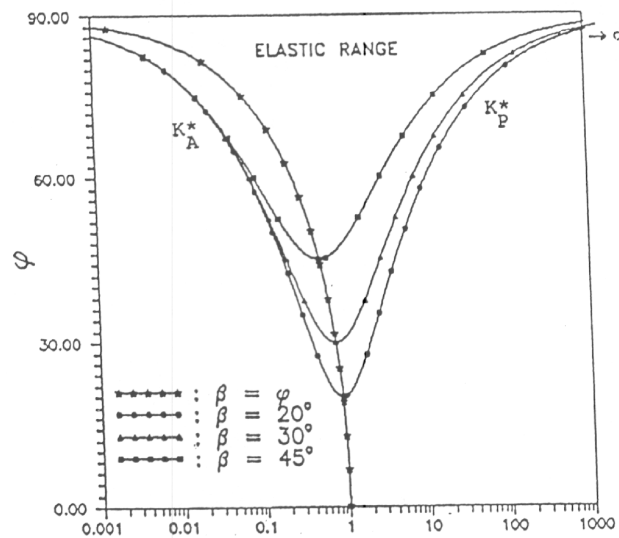
Earth pressure coefficient at rest K_0^*, for a cohesionless semi–infinite soil mass with surface inclined at angle β

$$K_A^* = \left(\cos^2\beta - \cos\beta\sqrt{\cos^2\beta - \cos^2\phi}\right)\left(\cos^2\phi\right)^{-1}\left(1 - \sin\phi\cos\alpha\right) \tag{1}$$

$$K_P^* = \left(\cos^2\beta - \cos\beta\sqrt{\cos^2\beta - \cos^2\phi}\right)\left(\cos^2\phi\right)^{-1}\left(1 - \sin\phi\cos\alpha\right) \tag{2}$$

with

$$\alpha = \arcsin\left(\frac{\sin\beta}{\sin\phi}\right) - \beta; \quad \beta \le \phi$$

$$\alpha = \arcsin\left(\frac{\sin\beta}{\sin\phi}\right) + \beta$$

The horizontal stresses corresponding to active and passive states are expressed as:

- active state:

$$(\sigma_{11})_A = K_A^*\gamma h - \frac{C}{\tan\phi}$$

- passive state:

$$(\sigma_{11})_P = K_P^* \gamma h - \frac{C}{\tan\phi}$$

where K_A^* and K_P^* are read from Window 7-7.

Window 7-7

7.4.2.2 DRUCKER-PRAGER MATERIAL

Rankine states can be derived similarly for a Drucker–Prager cohesionless material, with the stress state defined previously. With the assumption $\underline{\sigma}_3 = \underline{\sigma}_1$, equations (DP1) Window 7-8 are derived. With the assumption $\underline{\sigma}_3 = 0.5\,(\underline{\sigma}_1 + \underline{\sigma}_2)$, relations (DP2) result.

The results obtained for K_A and K_P as function of ϕ are reported in Window 7-8. It is observed that the elastic ranges of Mohr–Coulomb and Drucker–Prager materials coincide, for the assumption that $\underline{\sigma}_3 = 0.5\,(\underline{\sigma}_1 + \underline{\sigma}_2)$.

As before, the presence of a surface load or of a water table can be accounted for, as for the Mohr–Coulomb case.

Window 7-8: Rankine states for Drucker-Prager material
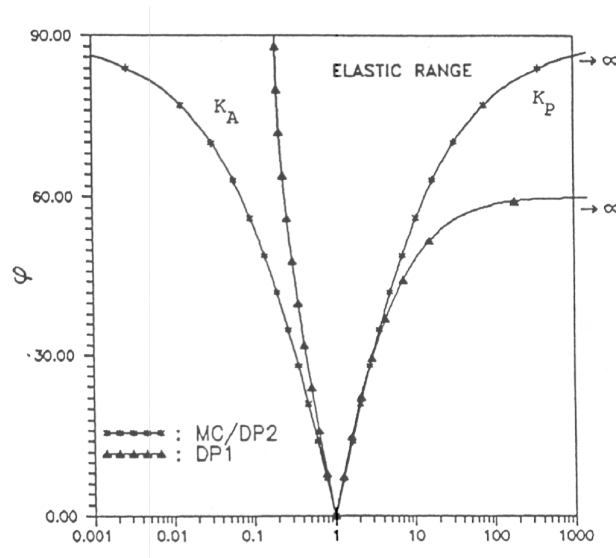
Earth pressure coefficient at rest K_0 for cohesionless material, Mohr–Coulomb (M–C),
Drucker–Prager $\underline{\sigma}_3 = \underline{\sigma}_1$ (DP1) and Drucker-Prager with $\underline{\sigma}_3 = 0.5\,(\underline{\sigma}_1 + \underline{\sigma}_2)$ (DP2)

$$K_A = \frac{\sqrt{3} - \sin\phi}{2\sin\phi + \sqrt{3}}, \quad K_P = \frac{-\left(\sqrt{3} - \sin\phi\right)}{2\sin\phi - \sqrt{3}} \tag{1}$$

$$K_A = \frac{1 - \sin\phi}{1 + \sin\phi}, \quad K_P = \frac{1 + \sin\phi}{1 - \sin\phi} \tag{2}$$

Window 7-8

If the semi–infinite soil mass, always considered as a cohesionless material, is limited by an upper surface inclined at an angle $\beta \leq \phi$, values of K_A^* and K_P^* can again be derived for both case, i.e.:

$$K_A^* = \cos^2 \beta \frac{1 - D \tan \beta}{1 + D \tan \beta}, \quad K_P^* = \cos^2 \beta \frac{1 + D \tan \beta}{1 - D \tan \beta}$$

with

$$D = \tan \left[\arccos \left(\sin \beta \frac{6 - \sqrt{3} \sin \phi}{3\sqrt{3} \sin \phi} \right) \right] \quad \text{if} \quad \underline{\sigma}_3 = \underline{\sigma}_1$$

$$D = \tan \left[\arccos \left(\frac{\sin \beta}{\sin \phi} \right) \right] \quad \text{if} \quad \underline{\sigma}_3 = 0.5 \left(\underline{\sigma}_1 + \underline{\sigma}_2 \right).$$

The obtained values of K_A^* and K_P^* ($K^* = \underline{\sigma}_{11}/\gamma h$) are plotted in Window 7-9 as functions of the friction angle ϕ and the angle of slope β, the same assumptions for $\underline{\sigma}_3$ as before are made.

It is noted again that the elastic ranges of Mohr–Coulomb and Drucker–Prager materials, with the assumption of $\underline{\sigma}_3 = 0.5 \left(\underline{\sigma}_1 + \underline{\sigma}_2 \right)$, coincide (see Window 7-8 and Window 7-9).

Similar derivation can be performed for the case of a cohesive material. The case of a horizontal surface can be treated using K_A and K_P from Window 7-7. The horizontal stresses corresponding to active and passive states are obtained from:

- Active state:

$$(\underline{\sigma}_{11})_A = K_A \gamma h - \frac{3C \cos \phi}{\sqrt{3} + 2 \sin \phi} \quad \text{if} \quad \underline{\sigma}_3 = \underline{\sigma}_1$$

$$(\underline{\sigma}_{11})_A = K_A \gamma h - \frac{2C \cos \phi}{1 + \sin \phi} \quad \text{if} \quad \underline{\sigma}_3 = 0.5 \left(\underline{\sigma}_1 + \underline{\sigma}_2 \right)$$

- Passive state:

$$(\underline{\sigma}_{11})_P = K_P \gamma h - \frac{3C \cos \phi}{\sqrt{3} + 2 \sin \phi} \quad \text{if} \quad \underline{\sigma}_3 = \underline{\sigma}_1$$

$$(\underline{\sigma}_{11})_P = K_P \gamma h - \frac{2C \cos \phi}{1 - \sin \phi} \quad \text{if} \quad \underline{\sigma}_3 = 0.5 \left(\underline{\sigma}_1 + \underline{\sigma}_2 \right).$$

Under condition of seepage flow the value of K_A^* and K_P^* cannot be read directly from Window 7-9, they need to be derived explicitly. The same remark holds for the case of a cohesive material with surface inclined at angle β.

Window 7-9: Rankine states. Inclined surface
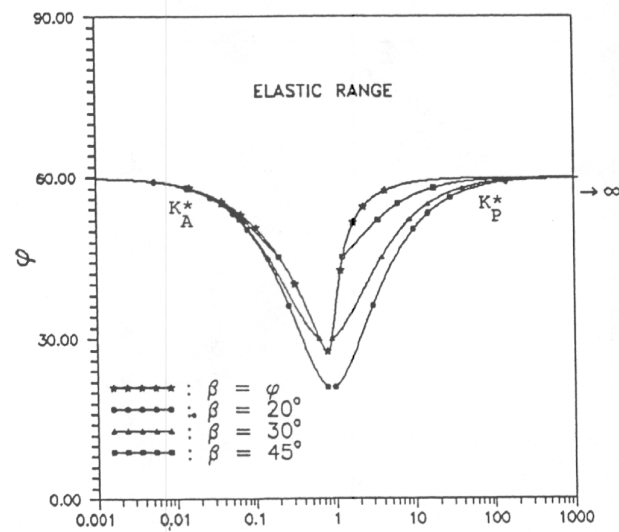
Earth pressure coefficient at rest K^* for a cohesionless semi–infinite soil mass with surface inclined at angle β. Drucker–Prager with $\sigma_1 = \sigma_3$.
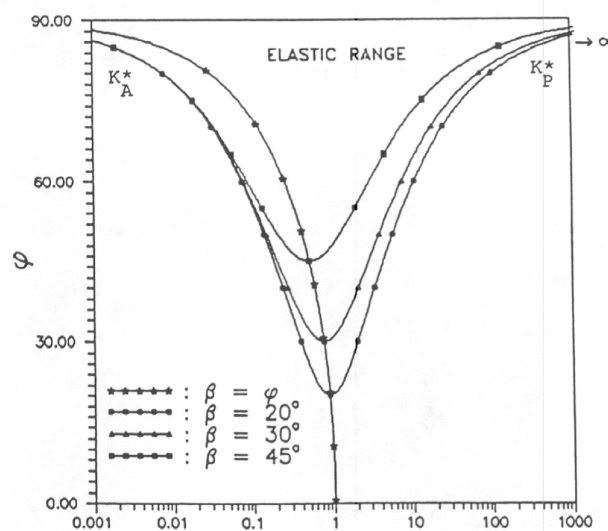
Earth pressure coefficient at rest K^* for a cohesionless semi–infinite soil mass with surface inclined at angle β. Drucker–Prager with $\beta_3 = 0.5(\sigma_1 + \sigma_2)$.

Window 7-9

7.4.3   INFLUENCE OF POISSON'S RATIO

Let Π_{12} be the plane containing axes 1 and 2 in which the plane strain problem is defined. If failure is to occur in the Π_{12} plane, $\underline{\sigma}_3$ must be the intermediate stress; hence the following condition must apply:

$$\underline{\sigma}_1 \leq \underline{\sigma}_3 \leq \underline{\sigma}_2.$$

Simultaneously, plane strain holds, i.e. for the elastic case:

$$\underline{\sigma}_3 = \nu \left(\underline{\sigma}_1 + \underline{\sigma}_2 \right) \quad \text{and} \quad \nu \leq 0.5.$$

The following limiting conditions results:

1.

$$\underline{\sigma}_3 = \underline{\sigma}_1 = \left(\frac{\nu}{1 - \nu} \right) \underline{\sigma}_2$$

2.

$$\underline{\sigma}_3 = 0.5 \left(\underline{\sigma}_1 + \underline{\sigma}_2 \right).$$

The second one result from the limits of Poisson's ratio. If no tectonic stresses are present, all elastic states lies within these limits.

These conditions are sometimes met a priori by the boundary–value problem (e.g. for the box shaped medium) or by the adopted matching of Drucker–Prager/Mohr–Coulomb criteria, as e.g. for the elastic matching proposed earlier. Violating these conditions can have a significant effect on the solution.

In addition, some choices of material data lead to plastic behavior already under gravity loading. Since this is the most common loading in soil mechanics, it is interesting to investigate the corresponding limits of elastic behavior. Some situations of special interest are analyzed next for a cohesionless material.

Case 1: Box-shaped medium under gravity load, dry, matching collapse load.

The box-shaped medium is the default configuration adopted in the program. Combining plane strain and the boundary conditions associated with the box–shaped medium leads for the isotropic medium to:

$$\underline{\sigma}_1 = \underline{\sigma}_3 = \left(\frac{\nu}{1 - \nu} \right) \underline{\sigma}_2; \quad \underline{\sigma}_2 = \gamma h$$

Notice that this coincides with a limiting condition established previously for failure to occur in the plane Π_{12} and to the active Rankine state. This condition is therefore satisfied a priori. The invariants corresponding to this stress state are:

$$I_1 = \left(\frac{1 + \nu}{1 - \nu} \right) \underline{\sigma}_2 = 3\overline{\sigma} \qquad J_2 = \frac{1}{3} \left(\frac{1 - 2\nu}{1 - \nu} \right)^2 \underline{\sigma}_2.$$

In stress space, the corresponding stress point is located on a cone with its vertex at the origin, characterized by:

$$a_\sigma I_1 - \sqrt{J_2} = 0$$

from which,

$$3a_\sigma = \frac{\sqrt{J_2}}{\overline{\sigma}} = \sqrt{3} \left(\frac{1 - 2\nu}{1 + \nu} \right).$$

For a cohesionless soil, a_σ characterizes the position of the stress point with respect to the yield surface. Elastic and plastic stress states can be identified as follows:

$a_\sigma < a_\phi$: elastic state
$a_\sigma = a_\phi$: plastic limit
$a_\sigma > a_\phi$: out–of–balance state

Using the matching rules discussed earlier with a_σ replacing a_ϕ, relations are established which define the elastic limit as a function of ϕ and ν.

Matching the collapse loads corresponding to Mohr–Coulomb and Drucker–Prager criteria, under plane strain conditions and deviatoric flow, yields the following result:

$$a_\sigma = \frac{\sin\phi}{3} \qquad \text{or} \qquad \sin\phi_y = \sqrt{3}\frac{1-2\nu}{1+\nu}.$$

The lower index y denotes yielding. This curve is shown in **Window** 7-10.

Note that a similar curve can be derived using directly the Mohr–Coulomb criterion without any consideration of matching with the Drucker–Prager criterion, leading to:

$$\sin\phi_y = 1 - 2\nu.$$

Material data corresponding to a point located below the curve will automatically generate a plastic state, and a point located above will generate elastic behavior. Different situations can be analyzed in a similar way.

Window 7-10: Influence of Poisson's ratio
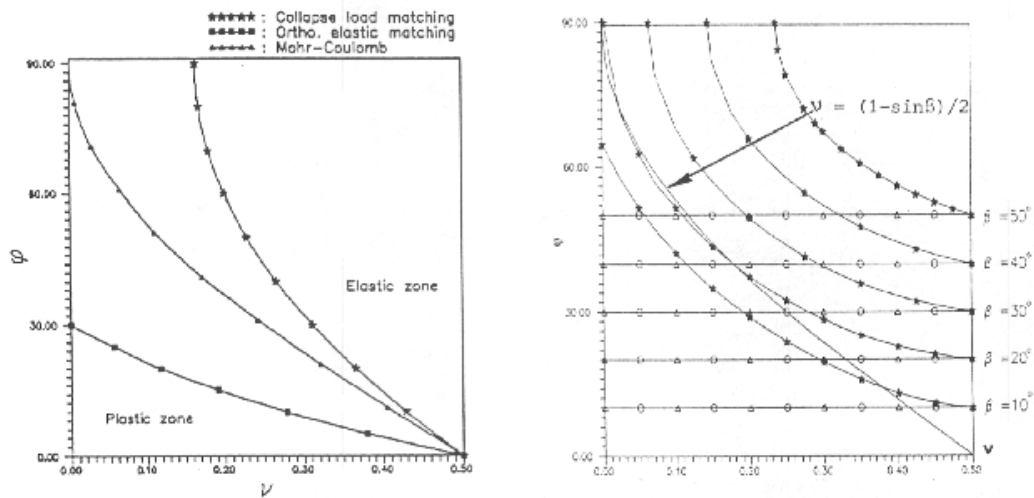
Influence of Poisson's ratio (box-shaped medium, cohesionless soil) (left); Influence of Poisson's ratio (infinite slope, cohesionless soil, dry medium) (right)

Window 7-10

Case 2: Box-shaped medium under gravity load, dry, matching elastic domains.

Matching of orthotropic elastic domains of Drucker–Prager and Mohr–Coulomb criteria yields:

$$\underline{\sigma}_1 = \left(\frac{4\nu+1}{3}\right)\underline{\sigma}_2; \qquad \underline{\sigma}_2 = \gamma h$$

$$\underline{\sigma}_3 = 0.5\left(\underline{\sigma}_1 + \underline{\sigma}_2\right).$$

The corresponding invariants were computed earlier and (see matching of elastic domains) ratio a_σ is such that yielding occurs if:

$$3a_\sigma = \frac{\sqrt{J_2}}{\overline{\sigma}} = \frac{1-2\nu}{2(1+\nu)} \geq \sin\phi$$

This curve is plotted in **Window** 7-10. Material data corresponding to a point located below the curve will generate a plastic state.

Case 3: Saturated medium.

The same results as before apply to effective stresses.

Case 4: Infinite slope at angle β, dry, matching collapse loads.

Principal stresses are:

$$\underline{\sigma}_1 = \gamma h(1 - \sin\beta)$$

$$\underline{\sigma}_2 = \gamma h(1 + \sin\beta)$$

$$\underline{\sigma}_3 = \gamma(\underline{\sigma}_1 + \underline{\sigma}_2) = 2\nu\gamma h$$

Corresponding invariants are:

$$I_1 = 2(1+\nu)\gamma h$$

$$J_2 = \frac{1}{3}(\gamma h)^2 \left(3\sin^2\beta + 1 - 4\nu + 4\nu^2\right)$$

then

$$3a_\sigma = \frac{\sqrt{J_2}}{\underline{\sigma}} = \frac{\sqrt{3\left(3\sin^2\beta + (1-2\nu^2)\right)}}{2(1+\nu)}.$$

Note that, for failure to occur in plane Π_{12}, $\underline{\sigma}_3$ must be the intermediate stress. This yields:

$$\nu \geq \frac{1 - \sin\beta}{2} \qquad \text{(see } \mathbf{Window}\ 7\text{-}10 \text{)}.$$

Similarly, the adjustment of yield criteria for place strain collapse load yields:

$$3a_\sigma = \frac{\sqrt{3\left(3\sin^2\beta + (1-2\nu^2)\right)}}{2(1+\nu)} > \sin\phi.$$

For each given slope β in a cohesionless soil, a curve $\phi = f(\nu)$ can be drawn, which characterizes the limit of elastic behavior and, for the given boundary-value-problem, the limit of stability (**Window** 7-5).

Case 5: Infinite slope at angle β, dry medium, matching elastic domains (Window 7-10).

Adjustment of yield criteria for coincidence of elastic domains, with $\nu_t = 0.5$. The state of principal stresses is:

$$\underline{\sigma}_1 = \gamma h(1 - \sin\beta)$$

$$\underline{\sigma}_2 = \gamma h(1 + \sin\beta)$$

$$\underline{\sigma}_3 = 0.5(\underline{\sigma}_1 + \underline{\sigma}_2) = \gamma h$$

The corresponding invariants are:

$$I_1 = 3\gamma h$$

$$J_2 = \gamma^2 h^2 \sin^2\beta$$

with elastic matching of failure criteria, this corresponds to yield if:

$$\sin\beta > \sin\phi.$$

The stress state in a cohesionless soil, for the adopted adjustment with the Mohr–Coulomb criterion, will be elastic if $\beta < \phi$ and plastic if $\beta > \phi$. Poisson's ratio has no influence in this particular case.

Case 6: Infinite slope at angle β, saturated.

The same results as before apply, corresponding to effective stresses.

7.4.4   COMPUTATION OF THE INITIAL STATE

Box-shaped medium in plane strain

For most static plane strain problems the soil half–plane can be conveniently approximated by a box–shaped medium with smooth lateral boundaries (**Window 5.4.9**). The particular stress-strain state which results can easily be derived.

From plane strain and lateral boundary conditions :

$$\varepsilon_3 = 0 \rightarrow \underline{\sigma}_3 = \nu \left(\underline{\sigma}_1 + \underline{\sigma}_2 \right)$$

$$\varepsilon_1 = 0 \rightarrow \underline{\sigma}_1 = \nu \left(\underline{\sigma}_2 + \underline{\sigma}_3 \right)$$

therefore:

$$\underline{\sigma}_1 = \frac{\nu}{1 - \nu} \underline{\sigma}_2$$

The stress-strain fields which result for some typical loading cases are summarized in **Window 7-11**.

Gravity field

As can be seen in **Window 7-11** the correct implementation of gravity requires simultaneous application of γ and corresponding initial stresses. This combination is characterized by the capital Γ in this text.

An initial state corresponding to an urban environment can be established using the same procedure.

Axisymmetric medium

The default boundary conditions for the axisymmetric case are the same as for plane–strain.

Window 7-11: Box-shaped medium with smooth lateral boundaries
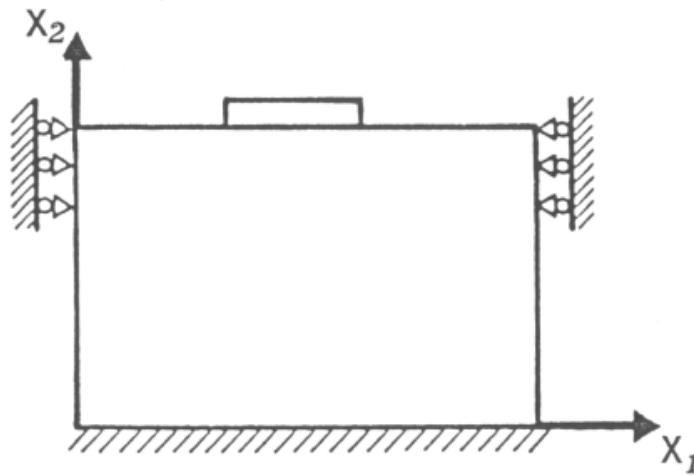
Box-shaped medium ($\varepsilon_1 = \varepsilon_3 = 0$)

No	APPLICATION OF:	YIELDS:	WHERE:
1	Deadweight γ downwards	$\sigma_2 = -\gamma h$ $\sigma_1 = \sigma_3 = -\frac{\nu}{1-\nu}\gamma h$ $\varepsilon_2 = -\frac{\gamma h}{E}\left(1 - \frac{2\nu^2}{1-\nu}\right)$	$h-$depth $\gamma-$unit weight (BOXD1)
2	Initial stress σ_{02}	$\sigma_2 = 0$ $\sigma_1 = \sigma_3 = \frac{\nu}{1-\nu}\sigma_{02}$ $\varepsilon_2 = \frac{\sigma_{02}}{E}\left(1 - \frac{2\nu^2}{1-\nu}\right)$	(BOXD2)
3	Initial stress σ_{01}	$\sigma_2 = 0, \; \sigma_1 = \sigma_{01}$ $\sigma_3 = 0, \; \varepsilon_2 = 0$	(BOXD3)
4	$\Gamma-$gravity field γ $\sigma_{02} = -\gamma h$ $\sigma_{01} = K_0\sigma_{02}$ $\sigma_{03} = K_0\sigma_{02}$ NB: $K_0 = \frac{\nu}{1-\nu}$ by default	$\sigma_2 = -\gamma h$ $\sigma_1 = K_0\sigma_{02}$ $\sigma_3 = K_0\sigma_{02}$ $\varepsilon_2 = 0$	(BOXD4)

Window 7-11

7.4.5   INFLUENCE OF WATER

A steady state Darcy flow model only is included, although the pressure b.c. can vary in time and for each step steady state solution can be obtained.

7.5 SOIL RHEOLOGY

Soil is subjected to long term deformations which cannot be avoided. This phenomenon is called consolidation.

Modern consolidation theories split the deformations into several mechanisms and two time periods associated with **primary** and **secondary** consolidation.

Primary consolidation is dominated by a mechanism of stress–induced seepage flow which transfers progressively the part of load carried by the interstitial water to the soil skeleton. During secondary consolidation, after stabilization of primary consolidation, the deformation is dominated by creep mechanisms.

Creep can be split into volumetric and deviatoric components.

A carreful choice of boundary to avoid meaningless results.

7.6   ALGORITHMIC STRATEGIES

SEQUENCES OF ANALYSES

EXCAVATION, CONSTRUCTION ALGORITHM

7.6.1   SEQUENCES OF ANALYSES

Most combinations of drivers are possible provided they are meaningful: initial state, stability, ultimate load, prestress, consolidation, creep, flow. Obviously, an initial state analysis should come first; a stability analysis should not be followed by any other type of analysis unless provisions are taken to restart before the stability analysis; recall that the stability analysis goes through the change of the material properties.

7.6.2 EXCAVATION, CONSTRUCTION ALGORITHM

The excavation–construction process shows an analogy with loads and associated load–time histories. Each element is associated with an existence time–history which takes values (0 or 1) depending if the element exists at a given time.

It is possible to simulate excavation and construction processes; corresponding restrictions are specified in the following remarks.

Remarks

1. The initial mesh numbering will be referred to throughout the analysis, for display of results. It must therefore include all elements appearing during analysis; some may however, be inactive at the beginning of the analysis.

2. When performing an excavation–construction analysis, stiffness update must obviously be required at the beginning of each step. The corresponding algorithmic choice must be done in the input definition.

3. Excavation stages can not be associated with some types of stability e.g. algorithms; this options would not be meaningful.

4. If an excavation is followed by a time dependent analysis, progressive unloading will occur.

5. Unloading can be controlled using **load time functions** attached to the elements, named as **unloading functions**. The interaction forces of the excavated medium on the surrounding medium can be computed as follows:

$$\mathbf{F}^{\text{intEXC}} = \int_{\Omega^{\text{exc}}} \mathbf{B}^{\text{T}} \boldsymbol{\sigma}^{\text{tot}} \ \mathrm{d} \cdot \left\{ \begin{array}{l} LTF(t) \\ 0, \text{ if no unloading function is given} \end{array} \right\}$$

where the integration is carried out over the excavated domain. Each excavated element is associated with a load function which can be used to control progressive unloading.

1) before the excavation:

$$\mathbf{F}^{\text{int}\,EXC} = \int \mathbf{B}^{T} \sigma d\Omega_{EXV}$$

$$\mathbf{F}^{\text{int}\,REM} = -\mathbf{F}^{\text{int}\,EXC}$$

$$\mathbf{F}^{\text{int}\,REM} = \int \mathbf{B}^{T} \sigma d\Omega_{REM}$$

2.a) after the excavation, **no progressive unloading**:

$$\mathbf{F}^{\text{int}\,REM}$$

2.b) after the excavation, **with progressive unloading**:

$$LTF(t) \cdot \mathbf{F}^{\text{int}\,EXC}$$

$$\mathbf{F}^{\text{int}\,REM}$$

3) final equilibrium state after excavation:

$$\mathbf{F}^{\text{int}\,REM} = \mathbf{0}$$
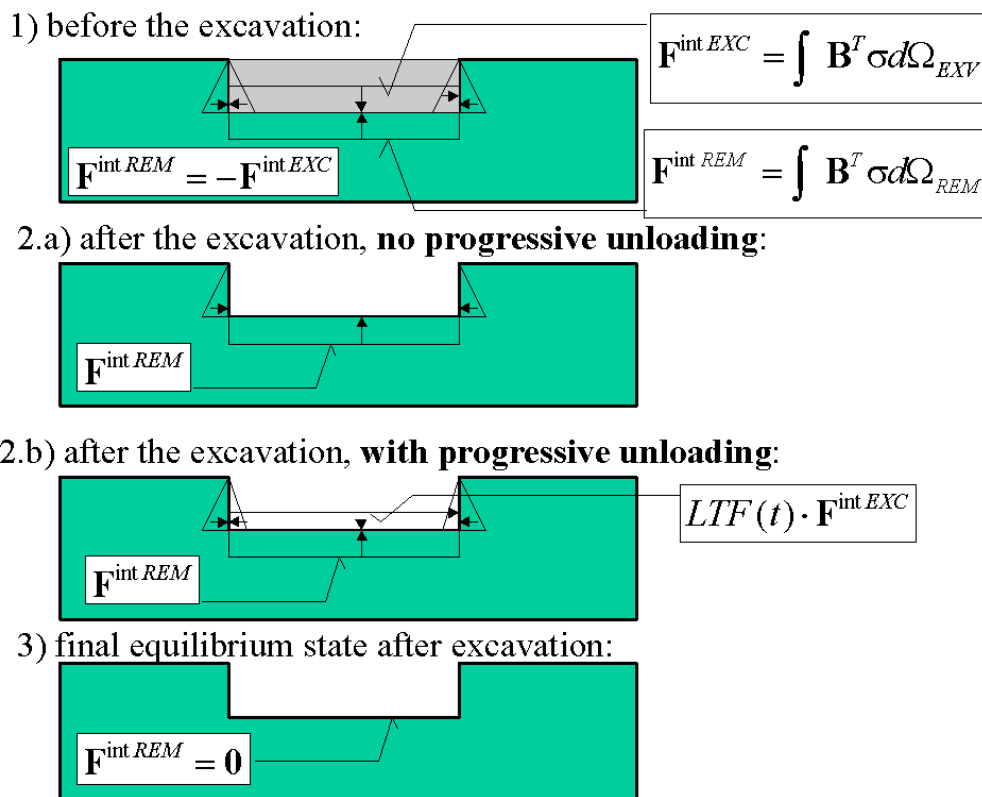
Simulation of excavation. Events sequence

If no LTF (unloading function) is specified for excavated elements, interaction forces from excavated media will vanish immediately at the moment of excavation (situation 2a in the above figure). Forces $\mathbf{F}^{intREM}$ will act as a load in a first step after the excavation. If compressive stresses dominated in the

area before the excavation then $\mathbf{F}^{intREM}$ will generate tensile load around newly created boundary. In the case of elasto-plastic media this may cause difficulties in obtaining converged solution. In that case **progressive unloading after excavation** (situation 2b in the above figure) will deminish destabilizing effect of $\mathbf{F}^{intREM}$ and helps to redistribute stresses in the surroundings of the excavated domain, and in consequence to obtain convergent solution of the new equilibrium state, (situation 3 in the above figure). The excavation data should include existence function and, if needed, unloading function. Both are shown in the below figure

existence function for excavated elements

shape of unloading function for excavated elements
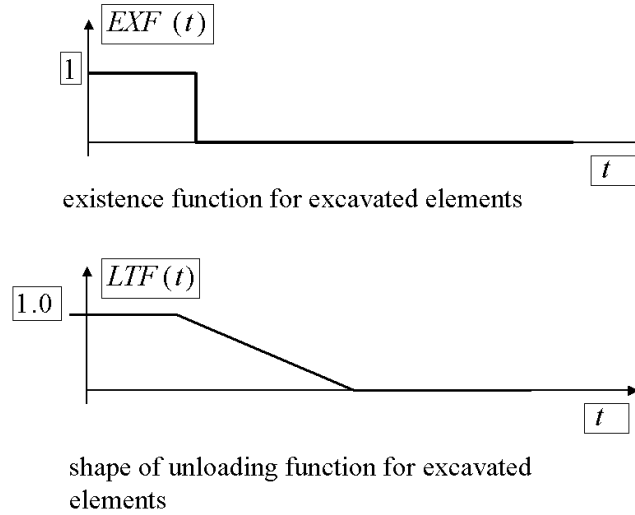
Functions controlling excavation process

Above numerical procedure, despite being useful in obtaining solution, corresponds to technical measures normally undertaken at the construction site in order to prevent failure of a soil mass during the excavation, like temporary supports or spacers.

Index